DOCTOR OF PHILOSOPHY

Development and evaluation of anti-biofouling nano-composite coatings

Su, Xueju

Award date:
2013

DOCTOR OF PHILOSOPHY

Development and Evaluation of Anti-Biofouling Nano-composite Coatings

Xueju Su

2013

University of Dundee

Mechanical Engineering and Mechatronics
School of Engineering, Physics and Mathematics

Development and Evaluation of Anti-Biofouling Nano-composite Coatings

Xueju Su

A Thesis Submitted to University of Dundee, in Fulfilment of the Requirements for the Degree of Doctor of Philosophy (Ph.D.)

December 2012

CONTENTS

DECLARATION

I hereby declare that the following thesis is of my own composition, that it is a true record of work completed by myself and that it has not previously been accepted for a higher degree at this University or any other institution of learning.

……..

Xueju Su

CERTIFICATE

I certify that Xueju Su has performed the research described in this thesis under my supervision and has fulfilled the conditions of the relevant Ordinance and Regulations of the University of Dundee, so that she is qualified to submit for the Degree of Doctor of Philosophy.

……

Dr. Qi Zhao

Division of Mechanical & Mechatronics Engineering

ACKNOWLEDGMENTS

First of all, I would like to express my deepest gratitude to my supervisors Dr. Qi Zhao and Prof Eric Abel for their kind guidance, encouragement, invaluable suggestions and financial support throughout my research work. I would like to thank the financial supports for my project from CSO (CZB/4/441), EU FP7 (BioSurf 232172) and UK Department of Health (B09-07).

I would like to thank to Laurent Akesso, Xiaoling Zhang, Parnia Navabpour, Dennis Teer, Teer Coatings Ltd, UK for preparing Si-N-DLC coatings and SiOx-like coatings. I would like to thank to Dr Avi Bendavid, CSIRO Materials Science and Engineering, Sydney for preparing F-doped DLC coatings. I would like to thank to Tecvac Ltd, UK for preparing B-DLC coatings and Ti-DLC coatings. I would like to thank to N. Noormofidi, E. Kreutzwiesener and C. Slugovc, Institute for Chemistry and Technology of Materials, Graz University of Technology, Austria for providing a range of biocide polymers for me to prepare novel Ni-P-PTFE-biocide polymer nanocomposite coatings. Thanks to David Perrett and Nanda Nayuni, Barts and London School of Medicine, London for the adhesion assays with brain homogenate. Thanks to Dory Cwikel and Abraham Marmur, Department of Chemical Engineering, Technion, Israel Institute of Technology for most stable contact angle analysis.

I would like to thank to the technicians in the Division of Mechanical Engineering at the University of Dundee for helping me cutting the sample, modifying the chamber and maintenance of laboratory instruments, and to Mr. Ernie Kuperus and Dr. Gary Callon for their kind support in my research work. And thanks to the members of my supervisor's research group, including Qian Li and Yingwei Qu et al for their help in bacterial adhesion assays during my PhD study.

Finally, I would like to express my sincere gratitude to my family for their support and encouragement during my PhD study in UK.

Xueju SU

ABSTRACT

The rapid development of the global offshore industry and of amphibious chemical, steel and power plants leads to more intensive use of natural water resources (sea, river and lake water) as a cooling medium. However, heat exchangers using the water as a coolant suffer from biofouling problem, which reduces heat transfer performance significantly. The cost of cleaning and lost output can be extremely high. The high incidence of infections caused by the biofilm formation on the surfaces of medical devices and implants, including catheters and bone fracture fixation pins etc. has a severe impact on human health and health care costs. An approach to reduce biofouling or infection rate is the application of a range of different coatings to the surfaces of equipment. So far the most promising coatings include Ni–P–PTFE coatings and modified diamond like carbon (DLC) coatings etc. However these coatings need to be futher improved and optimised in order to get the best anti-biofouling performance.

In this study, a range of novel Ni–P–PTFE-biocide polymer nanocomposite coatings and modified DLC coatings with B, F, N, Si and Ti were designed and produced using electroless plating, magnetron sputter ion-plating and plasma enhanced chemical vapour deposition techniques. The surface properties of the coatings were characterized using surface analysis facilities, including AFM, EDX, OCA-20, SEM and XPS. These nano-composite coatings and nano-structured surfaces were evaluated with bacterial strains that frequently cause heat exchanger biofouling or medical devices-related infections. The experimental results showed that new Ni–P–PTFE-biocide polymer nanocomposite coatings reduced bacterial adhesion by 70% and 94% respectively, compared with Ni–P–PTFE and stainless steel. The experimental results showed that both type and content of the doped elements in DLC coatings had significant influence on bacterial adhesion. The new doped DLC coatings, including Si-N-DLC, F-DLC, B-DLC and Ti-DLC coatings as well as new SiOx-like coatings reduced bacterial adhesion by 60-90% compared with pure DLC and stainless steel. B and Ti-doped DLC coatings also reduced residual protein adhesion by 88-95% compared with pure DLC coatings and stainless steel. In general bacterial adhesion decreased with decreasing total surface energy or with increasing γ^- surface energy of the coatings. The bacterial adhesion mechanism of the coatings was explained with extended DLVO theory.

NOMENCLATURE

Latin Letters

A	Hamaker constant, surface area
A_{131}	Hamaker constant between particles 1 across medium 3
A_{132}	Hamaker constant between particle 1 and surface 2 across medium 3
E	Voltage, interaction energy
h	Coating thickness
H	Distance
H_0	Minimum equilibrium distance of interaction = 0.157 nm
k	Constant
k_B	Boltzmann constant
r	Coating rate
R	Microbial radius
t	Coating time
T	Temperature
U	Fluid velocity
V	Volume
W	Weight

Greek letters

β	Constant in Equation of state approach
γ^{AB}	Polar or acid-base component of surface energy
γ^{d}	Apolar component of surface energy
γ^{LW}	Lifshitz-van der Waals component of surface energy
γ^{p}	Polar component of surface energy
γ_s	Solid surface energy
γ_{sl}	Solid-liquid interfacial energy
γ^{-}	Electron-donating parameter of the acid-base component
γ^{+}	Electron-accepting parameter of the acid-base component
ε	Permittivity, 6.95×10^{-10}
ε_0	Permittivity of vacuum, 8.85×10^{-12}

ε_r	Relative permittivity or dielectric constant
θ	Contact angle
κ^{-1}	Double layer thickness
λ	Correction length of molecules in a liquid
ζ	Zeta potential
ρ	Fluid or solid density
μ	Fluid viscosity

Abbreviation

AFM	Atomic Force Microscope
CFU	Colony Forming Units
DLVO	Derjaguin – Landau – Verwey – Overbeek
EDXS	Energy Dispersive X-ray Spectroscopy
E. coli	*Escherichia coli*
Ni-P-PTFE	Nickel-Phosphorus-Polytetrafluoroethylene
P.Aeruginosa	*Pseudomonas Aeruginosa*
PBS	Phosphate Buffered Saline
PTFE	Polytetrafluoroethylene
rpm	revolutions per minute
SEM	Scanning Electron Microscope
S.aureus	*Staphylococcus aureus*
S.epidermidis	*Staphylococcus epidermidis*
Ti	Titanium
TSA	Tryptone Soya Agar
TSB	Tryptone Soya Broth
XPS	X-ray Photoelectron Spectroscopy

LIST OF TABLES

LIST OF FIGURES

CHAPTER 1

INTRODUCTION

1.1 Biofouling Problems in Heat Exchangers

Fouling is generally defined as the accumulation of unwanted materials on the surfaces of processing equipment (Garret-Price et al 1985). It has been recognised as a nearly universal problem in design and operation and affects the operation of equipment in three ways:

1) The fouling layer has a low thermal conductivity. This increases the resistance to heat transfer and reduces effectiveness of heat exchangers.
2) As deposition occurs, the cross-sectional flow area is reduced, which causes an increase in the pressure drop across the apparatus. This requires additional pumping or fan power to maintain the same throughput.
3) Fouling can cause substrate corrosion and erosion, especially in the case of sea water fouling.

The economic penalty for fouling due to oversized plant, decreased thermal efficiency, increased pressure drop, additional maintenance and loss of production has been estimated as about U.S. $\$1.5 \times 10^9$ per year for the U.K., and U.S. $\$5 \times 10^{10}$ per year for the total industrialised world (Garret-Price et al 1985; Müller-Steinhagen and Zhao, 1997). It was reported that total heat exchanger fouling costs for highly industrialised countries such as the US and the UK were about 0.25% of the countries' gross national

product (GNP) (Garrett-Price *et al.*1985; Pritchard 1987; Müller-Steinhagen 2013). For New Zealand, Steinhagen *et al.* (1990) found that the fouling costs were 0.15% of the New Zealand GNP and for China, Xu *et al.* (2007) reported that the the fouling costs were 0.169% GDP of China.

The heat exchanger is a device which directs the flow paths in such a way that the two streams (cold and hot) are brought into thermal contact through a conducting wall while being kept physically separate. Heat exchangers are designed for heat transfer duties in which all kinds of natural water resources (sea, river and lake water) are used as cooling medium.

Biofouling is widespread phenomena in sea water cooling systems. Biofouling is usually divided into macro-biofouling and microbiofouling (Epstein, 1983):

1) Macrobiofouling: settlement of mussels, tube worms etc. primarily in the unheated intake system. This is not normally a problem within the heat exchanger itself, apart from indirect effect such as tube blockage by mussel shells detached from the intake. Macrobiofouling is a major problem of water-intake structures, equipment and power-plant piping.
2) Microbiofouling: bacterial biofim is a major problem of heat exchangers.

As micro-biofouling has been recognized as a widespread problem in the design and operation of processing equipment, especially in heat exchangers, one aim of this study is to investigate the methods for the control of micro-biofouling or biofouling in heat exchangers.

1.2 Biofilm Problems in Medical Devices and Implants

The high incidence of infections caused by the use of implanted biomedical devices, including catheters (Plowman et al, 2001), bone fracture fixation pins (Wassall et al, 1997) and heart valves (Tozzi et al, 2001; Cook et al, 2000) etc. has a severe impact on human health and health care costs. Current estimates suggest that in the UK nosocomial infections cost the UK £1.0 billion per year (Plowman R *et al.* 1999) and medical devices and implant-associated infections cost the UK £11 million per year

(Darouiche 2004). In the United States, nosocomial infections cost the USA $11 billion per year and at least half of the 2 million cases of nosocomial infections are medical devices-related infections (Darouiche 2004, 2007, Richards *et al.* 1999; Jarvis 1996, McGowan 2001, Schierholz *et al.* 1998, 2002). As the use of medicals devices and implants has increased, the device-related infections become a major concern. Another aim of this study is to investigate the methods for the control of biofilm formation in medical devices and implants.

1.3 Control of Biofilm Formation

Since bacterial adhesion on the surfaces is a prerequisite for biofouling formation in heat exchangers or for medical device infection, prevention of bacterial adhesion on the surfaces will have a major impact in preventing heat exchanger biofouling or medical devices-related infections. An effective and desired approach to reduce biofouling is to alter the surface properties of heat exchangers or medical devices by surface coating techniques and to make it less attractive for the biofouling components, so that they can be removed easily from the surfaces by flowing fluids.

The most effective method of biofouling control in industrial heat exchangers until now is the application of anti-biofouling coatings containing biocides such as cuprous oxide and organo-tin compounds, with properties toxic to biofouling organisms (Ghanem et al, 1982; Kjaer, 1992). The mechanism of surface protection by these coatings or paints depends upon controlled leaching of the poisonous ingredients. The main disadvantage is the pollution to the environment. Due to the world-wide legislation, one can assume that toxic antifouling coatings will eventually disappear completely from the market. Therefore, non-toxic coatings have attracted more attention. Many attempts have also been made to reduce biofouling by coating surfaces with silicone or PTFE due to their non-stick properties. However, the poor thermal conductivity of these polymer coatings currently inhibits their commercial use for heat exchangers (Müller-Steinhagen and Zhao, 1997).

An approach to reduce medical devices-related infections is the application of a range of different coatings to the surfaces of the medical devices and implants, including biocidal coatings, polymeric coatings based on hydrogels and silicone. In view of increasing

bacterial resistance to antibiotics and antiseptics, silver coating may be an effective strategy to prevent catheter and other medical devices-related infections (Schierholz et al 1998). However, numerous clinical studies show that the use of silver-coated devices resulted in non-significant reduction in medical devices-related infections as bacteria (dead and alive) strongly stick to the silver-coated surfaces (Lai and Fontecchio, 2002; Thibon et al 2000; Morris et al 1997; Leone *et al.*, 2004). The silver-coated medical devices are not recommended for widespread use (Thibon et al 2000).

In this study, three new types of anti-biofouling coatings (Ni-P-PTFE-biocide polymers, doped diamond-like carbon and SiOx-like coatings) with good thermal conductivity and biocompatibility have been developed and evaluated for the potential applications of heat exchangers and medical devices/implants.

CHAPTER 2

LITERATURE SURVEY AND BACKGROUND

2.1 Biofouling in Heat Exchangers

The rapid development of the global offshore industry and of amphibious chemical, steel and power plants leads to more intensive use of natural water resources (sea, river and lake water) as a cooling medium. However, heat exchangers using water as a coolant suffer from biofouling in the form of biofilm (Koh *et al*. 1991; Lucas *et al.* 1996; Eguia et al. 2007). Biofouling can lead to bio-corrosion of metal, which increases safety hazards from conventional and nuclear power plants (DiCinto and DeCarolis, 1993; Mussalli and Tsou, 1989). In the US approximately 4% of the failures of power stations with a capacity >600 MW are caused by biofouling in condensers (Bott 1995). Because a biofilm is highly hydrated, consisting of 98-99% water, its conductivity is similar to that of stationary water, but much lower than that of metals (Characklis, 1983). It therefore acts as an insulator, increasing heat transfer resistance, especially in heat exchangers. Very thin micro-biofouling films can have a significant impact on the thermal performance of OTEC (Ocean Thermal Energy Conversion) heat exchangers (Aftring *et al.* 1978; Berger *et al.* 1979; Kinelski, 1978; Little and Lavoie 1979). Biofouling in condenser tubes of power plants alone costs the USA over US$1 billion annually (Chow 1987; Strauss 1989). The presence of a biofilm on transfer surfaces of heat exchangers cooled by water reduces the heat transfer rate by 20 to 50% and incurs

a global expenditure of over $15 billion per annum to control the problem (Azis et al, 2001). Biofouling not only reduces heat transfer performance significantly, but also causes considerable pressure drop, calling for higher pumping requirements. For example, biofouling on a 20- centimetre carbon steel pipe reduced the cross-sectional area by 52% in 2.5 years (Gaffoglio, 1987). The cost of cleaning and lost output can be extremely high (Zhao et al, 2005; 2009).

2.1.1 Effect of Main Parameters on Biofouling

2.1.1.1 Effect of Temperature

The temperature at the interface of the water and the surface of the heat exchanger is the main parameter that affects biofouling. Biological growths have definite temperature ranges within which they can survive. For marine system, seawater temperature can change in the range from -2 °C to 28 °C (Yebra *et al.* 2004). The water temperature has significant influence on biofouling formation (Kukulka and Devgun 2007 and Butterworth 2002). In general, the marine biofilm growth rate increases with seawater temperature increasing until it reaches a maximum value. Experiments by L.Novak (1981; 1982) were carried out with the Rhine river water in Ludwigshafen, Germany, and with seawater of the Öresund in Landskorona, Sweden. The biofouling rate reached a maximum at a mean temperature of approximately 32^{o}C for Rhine water and at approximately 35-37 ^{o}C for sea water. Mott (1991) investigated the effect of cooling water temperature on biofilm formation and reported that by raising temperature from 30 °C to 35 °C the thickness of biofouling deposit increased by 80%. Melo and Bott (1997) reported that the optimum temperature for maximum growth of the most bacteria in cooling water systems was about 40 °C. Ritter and Suitor (1975) showed that biofouling was severe at temperatures below about 49°C, but became insignificant at elevated temperatures. Operation in seawater at surface temperatures above 49^{o}C would be abnormal. Ritter and Suitor (1976) conducted a test at 66^{o}C to determine an upper limit to biofouling. The result showed that there was no biofouling at the surface temperature of 66^{o}C. The tests by Ritter and Suitor (1976) further indicated that the increase in surface temperature of titanium heat exchangers from 38°C to 66^{o}C resulted in a decrease in biofouling.

2.1.1.2 Effect of Flow Velocity

The velocity of the water has a significant influence on biofouling formation. If water flow velocity is very slow or in stagnant water, biological growths would probably die of lack of oxygen and nutrients, so a slight velocity is essential for biofouling growth. But at higher velocities, biological deposits can either be sheared off or they are unable to attach themselves to the surfaces.

Fouling is usually most widespread in warm conditions and in low velocity (< 1 m/s) sea water. Above 1 m/s, most fouling organisms have difficulty attaching themselves to surfaces unless already secured (Powell, 1994). Bott and Miller (2008) showed the maximum biofilm development occurred at the flow velocities around 1m/s in aluminium tubes and biofilm growth was faster even in the low nutrient condition. Titanium and its alloys are non toxic to fouling organisms in seawater and foul heavily in water flowing at less than 0.22 m/s. Tsai (2005) reported that the biofilm biomass did not change when flow velocity was increased from 0.2 to 0.4 m/s, but when flow velocity was further increased to 0.6 m/s, biofilm biomass was reduced significantly due to shearing stress increasing. Melo and Bott (1997) showed that when the velocity increased from 0.13 m/s to 0.54 m/s, the density of the dry *Pseudomonas fluorescens* biofilm increased from 26 kg/m^3 to 76 kg/m^3 (dry mass/wet volume). When flow velocity was over 1 – 1.8 m/s, biofouling deposition in the heat exchanger tubes decreased with velocity increasing (Nebot *et al*. 2007). Biofouling did not occur at ship's speeds higher than 3m/s (Yebra *et al*. 2004). In general, biofilm thickness increases to maximum when flow velocity is around 0.5~1 m/s). When flow velocity is over 1 m/s, biofilm thickness decreases with velocity increasing. However the pumping costs and shearing stress to the pipes also increase significantly when flow velocity increases. The water velocity is dictated by both biofouling considerations and by the cost of pumping the water through the heat exchangers. In general the flow velocity in heat exchanger tubes is around 1 – 3 m/s (Kinelski, 1985).

2.1.1.3 Effect of Materials

Marine organisms attach themselves to some metals and alloys more readily than they do to others. Some metals and alloys containing copper, nickel, zinc or silver are toxic

to microorganisms (Fang 2002; Gibert, 1972, 1978, 1982, Griffin, 1978). It has been demonstrated that the Cu/Ni alloys reduced biofouling growth significantly (Albaugh 1984; Straight *et al.* 1988; Powell 1994; Mathiyarasu *et al.* 2002). Copper-based alloys, including copper-nickel, have very good resistance to biofouling, and this property is used to advantage. In the case of copper-nickel, it is used to minimise biofouling on intake screens, sea water pipe work, water boxes, and cladding of pilings and mesh cages in fish farming and heat exchangers. There was little to distinguish between the 90-10 and 70-30 alloys (Efird 1976; Powell 1985). Copper alloys have good resistance to micro-biofouling, but they are not totally immune to it. They only remain effective in heat exchanger for about 3 – 4 months (Powell 1985; Tuthill, 1987). Another problem for the use of copper-alloys is that they are readily corroded in sea water.

Some metals or alloys (e.g. stainless steel) are not toxic, so biofouling forms on these surfaces easily (Videla 1994; Sleigh 1987; Greenberg and Itzhak 2005; Palraj and Venkatachari 2008; Vishwakarma *et al.* 2009). Titanium can successfully cope with sea water corrosion, but it tends to be expensive and has poor anti-biofouling properties.

It has also been demonstrated that poly (ethylene glycol) (PEG) was able to resist bioadhesion (Preiser *et al.* 1984; Kingshott and Griesser 1999; Kenausis *et al.* 2000; Roosjen *et al.* 2004; Vladkova 2007). Recently the development of antibacterial polymers with minimal bacterial adhesion has been focused on siloxanes, fluoropolymer and fluorosiloxanes because they have low surface free energy (Brady and Singer, 2000; Vladkova 2007). Polymers may have anti-biofouling or fouling-release properties but they may not be suitable for the applications in heat exchangers due to their low thermal conductivity.

Currently most scientists are focuing on the development of anti-biofouling coatings on stainless steels and titanium substratates, but no significant progress has been made.

2.1.1.4 Effect of Surface Morphology

The effect of surface roughness on biofouling adhesion is complex. Some researchers found that biofouling adhesion was less on smooth surfaces. Bollen *et al.* (1997) found

that the adhesion of micoorganisms increased with surface roughness *Ra* values increasing, but if $Ra \leq 0.2$ μm it had a negligible effect on microbial adherence. Taylor *et al.* (1998) found that bacterial attachement increased with increasing *Ra* values for *Ra* in the range of 0.04~1.24μm. When *Ra* was in the range of 1.86~7.89μm, it had no significant effect in bacterial adhesion. Kerr (2000) reported that reducing surface roughness should reduce biofouling build-up. Pasmore *et al.* (2001) found that biofilm coverage of *P. aeruginosa* increased slighly with surface roughness increasing for *Ra* in the range of 0.3 ~ 3.8 μm. Katsikogianni and Missirlis (2004) explained that a rough surface has a greater surface area and the depressions in the roughened surfaces provide more favourable sites for colonization. Medilanski et al. (2002) showed that bacterial adhesion on bare stainless steel was minimal at an average roughness (Ra) of 0.16 μm, whereas smoother and rougher surfaces led to more retention.

However, some studies showed that the surface roughness had no significant influence on biofouling (McGuire and Swartzel,1987; Yoon and Lund 1994; Hahnel *et al.* 2009). McGuire and Swartzel (1987) tested fouling adhesion on polished stainless steel , rough stainless steel, teflon and aluminosilicate with corroesponding *Ra* values of 0.04, 0.41, 1.93 and 2.31μm respectively. They did not find any correlation between fouling adhesion and *Ra* values. Yoon and Lund (1994) evaluated fouling adhesion on the surfaces of teflon, polysiloxane, stainless steel, polished stainless steel and titanium with *Ra* values in the range from 0.07~0.60 μm, and did not find any any correlation between fouling adhesion and *Ra* values.

A specific micro-topography which decreased the contact area between the material surface and the microorganism reduced the level of adhesion (Allion et al., 2006; Kesel and Liedert 2007; Carmen et al. 2006; Bers and Wahl 2004; Scardino et al. 2009; Baum et al. 2002). A surface with fewer attachment points may reduce the shear force required for biofouling removal. Unfortunately, the surface pattern techniques are not suitable for large scale heat exchanger plates and tubes.

2.1.1.5 Effect of Surface Energy

An effective and desired approach to reduce biofouling is to alter the surface properties

of the equipment and to make it less attractive for the fouling components, so that they can be removed easily from the surfaces by flowing water (Zhao et al, 2005). The surface energy of a solid surface gives a direct measure of intermolecular or interfacial attractive forces. van Oss et al (1986, 1988, 1994) proposed to divide the total surface energy of a material (γ_i^{TOT}) into 3 independent components, Lifshitz-van der Waals apolar (γ_i^{LW}), the electron acceptor (γ_i^+) and the electron donor (γ_i^-): $\gamma_i^{TOT} = \gamma_i^{LW} + 2\sqrt{\gamma_i^+ \gamma_i^-}$. Over the past three decades, fouling adhesion to surfaces with different surface energies has been investigated with the frequent conclusion that fouling adhesion is less to low energy surfaces and easier to clean because of weaker binding at the interface (Dexter et al., 1975; van Dijk *et al.* 1987; Quirynen and Bollen 1995; Hamza et al., 1997; Swain 1998; Tsibouklis *et al.* 1999; 2000; Forster and Bohnet 1999, 2000). Dexter et al. (1975; 1979) demonstrated the low number of marine bacteria associated with low-energy substrates and high numbers on high-energy substrates. Milne and Callow (1985) and Callow et al (2005) also reported fewer bacteria adhering to a low surface energy material compared to a high surface energy material. Tsou and Mussalli (1988) evaluated 30 nontoxic coatings and their results indicated that silicon-based coatings performed satisfactorily. Although these coatings with low surface energy fouled, the fouling growth was easily removed from them. Hardy and Moss (1979) reported that biofouling deposits weakly attached to Teflon (PTFE) with low surface enegy were, compared with those produced on higher surface energy surfaces. Sipahi *et al.* (2001) and Aronov *et al.* (2008) reported that biofouling adhesion strength increased with the surface energy of the coatings increasing.

However, there are also a number of contrary findings, i.e. that high energy surfaces have a smaller biofouling tendency than low energy surfaces (Fletcher and Marshall, 1982; Fletcher and Pringle 1985; Brink et al., 1993; Busscher 1992; Pasmore *et al.* 2001).

Baier et al. (1980, 1981, 1983) first gave a relationship between surface energy and relative bacterial adhesion. Fig. 2.1, known as the Baier curve, shows this relationship, and can partially explain the above inconsistent conclusion on the effects of surface energy on bacterial adhesion. Clearly, there exists an optimum value of the surface energy (about 25mJ/m^2) for which bacterial adhesion is minimal.

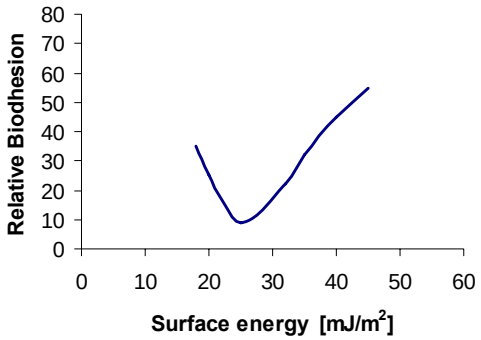

Fig. 2.1 Relative bacterial adhesion *vs* surface energy (Baier, 1980)

In addition to biofouling, numerous studies have also demonstrated the existence of the optimal total surface energy for other type of fouling, such as milk protein fouling (see Figure 2.2; McGuire and Swartzel,1987) and crystalline fouling (Zhao et al. 2005).

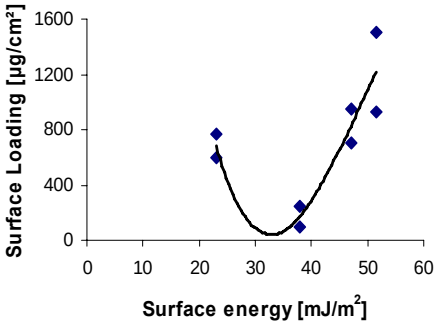

Fig. 2.2 Milk fouling *vs* surface energy (McGuire and Swartzel, 1987)

Zhao et al. (2002, 2004, 2005, 2007, 2009) explained this phenomena using extended DLVO theory. Baum et al. (2002) have shown that the pilot whale skin has both hydrophobic and hydrophilic surfaces. Recently, Zhao et al. (2007) presented an extended Baier Curve, as shown in Figure 2.3. For the superhydrophobic surface with extreme low surface energy, a thin layer of air could remain on the surface that inhibits bacteria reaching the surface; while for the super-hydrophilic surface with extreme high surface free energy, a thin layer of water remains attached on the surface that also inhibits bacteria to reach the surface. Zhao et al. (2007) performed bacterial adhesion experiments and obtained the results similar to the extended Baier Curve (Figure 2.4).

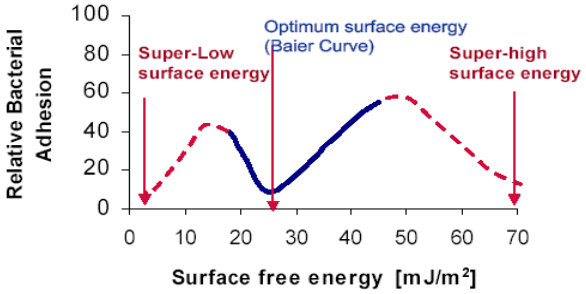

Fig. 2.3 Extended Baier curve

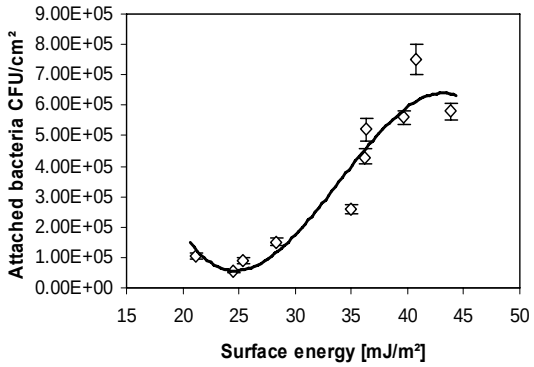

Fig. 2.4 Attached bacteria vs surface energy (Zhao et al., 2007)

2.1.2 Biofouling Control and Removal Techniques

There are many ways to reduce biofouling both mechanically and chemically. So far no single countermeasure has been identified to completely control biofouling (Lira et al, 1985, 1990). Over the past 50 years, various measures have been taken to combat the problem marine biofouling in heat exchangers. These have included careful screening of sea inlets to prevent larger objects being drawn in and the injection of chlorine and hypochlorite to either discourage biofouling settlement and growth or remove existing fouling. If possible, the seawater should be allowed to heat up by an extra 15-25 °C (i.e. to not less than 40 °C) from time to time thereby killing the offending organisms. Chemical additives often offer an effective anti-biofouling means; however, processing changes, mechanical modifications of equipment and other methods available to the plant should not be overlooked. The application of the techniques mainly depend on the following factors: 1) accessibility, 2) nature of the microorganisms, 3) hydraulic-thermal

conditions of the process, 4) costs of the treatment, 5) safety standards and 6) environmental impact (Sriyutha Murthy *et al.* 2004; Eguia *et al.* 2008).

2.1.2.1 Chemical Techniques

Chlorination

Chlorination of cooling water has been the most widely used process to control condenser biofouling. Chlorine injection is the normal method of chemical dosing. It may be either intermittent (shock dosing), or continuous, or a combination of both, depending upon the type of biofouling which can be expected.

It is common practice nowadays for chlorination to be effected by a chlorine generator so as to avoid the potential risks associated with storage of substantial quantities of liquid or gaseous chlorine (Fuller, 1976, 1979; Boyer and Malherbe, 1979). Large modern plants generally chlorinate at regular intervals 2-4 times per day for period of 15-30 min/application (Burton, 1979; Lira et al, 1976, 1979). From the experience gathered, it is believed that an electrochlorination system, capable of producing 0.5 ppm chlorine, will maintain seawater cooling systems free of fouling, as shown in Figure 2.5 and Figure 2.6 (Shone and Grim, 1986).

In general a chlorination cell consists essentially of two electrodes with seawater passing between them. Part of the contained salt is converted into sodium hypochlorite and the resulting solution is metered into the cooling system it is protecting (Campbell et al, 1979). A titanium heat exchanger complete with a chlorination cell (Figure 2.7) was installed and seawater pumped through the heat exchanger for four months. Examination of the heat exchanger after four months showed the heat exchanger to be as installed, i.e. no fouling. Another test was conducted on the heat exchanger, without chlorination. Severe fouling was observed after a relatively short period, as shown in Figure 2.8 (Campbell et al, 1979).

Fig. 2.5 Condenser inlet free from fouling by electrochlorination
(Shone and Grim, 1986).

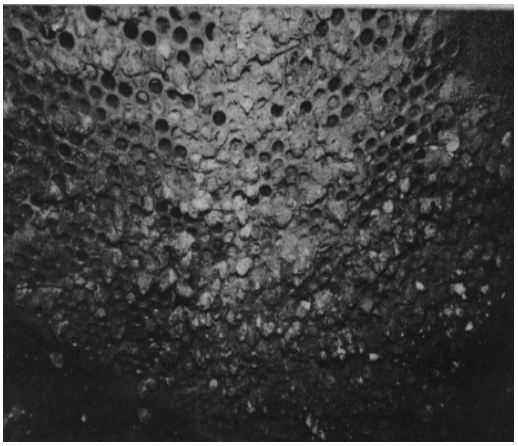

Fig. 2.6 Condenser heavily fouled after failure of electrochlorination
(Shone and Grim, 1986).

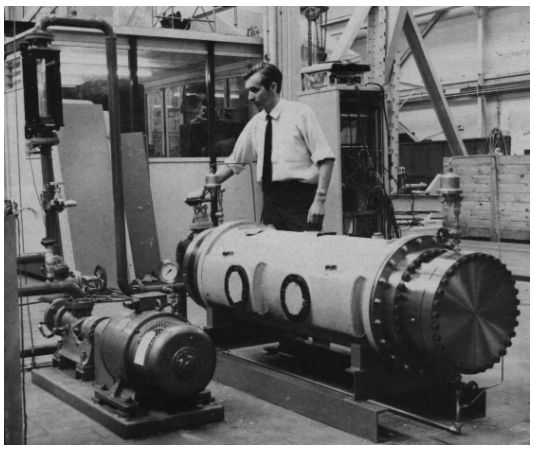

Fig. 2.7 Titanium Heat Exchanger (Campbell et al, 1979)

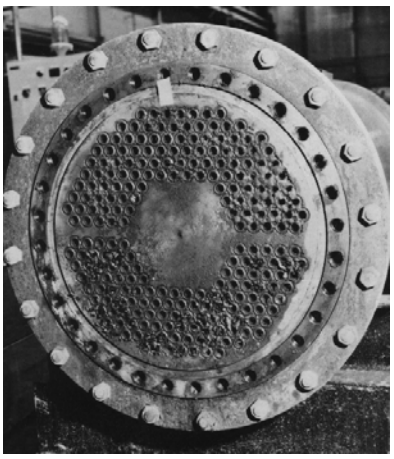

Fig. 2.8 Titanium Heat Exchanger without Chlorination Exchanger
(Campbell et al, 1979)

Continuous chlorination of cooling water with concentration about 0.5 – 1.5 mg/litre as Cl_2 has been the most widely used process to control biofouling (Allonier et al., 1999; Jenner et al., 1997; Rajagopal et al., 2003; Venugopalan *et al.* 1997; Eguia *et al.* 2007). Direct cooled fossil fuel and nuclear power stations on the coast typically use 30 and 45 m^3/s of seawater per 1000 MW (megawatt), respectively (Jenner et al., 1997). The generation and use of such large amounts of chlorine lead to pollution to the environment and the formation of halogenated by-products (Allonier et al., 1999). While trihalomethanes (THMs), which are suspected carcinogens, are the major compounds formed, other by-products are of concern due to their potential toxicity

towards aquatic organisms. Any non-chemical method or less use of chemicals for inhibiting biofouling will reduce marine pollution significantly (Zhao et al, 2005; 2009).

Other Biocides/Inhibitors

Bacteria can be chemically killed by application of bactericidal compounds termed biocides at lethal doses. To-date, many kinds of biocides are used to control biofouling in industrial water systems (Azis *et al.* 2003; Eguia *et al.* 2007). For different kinds of bacteria, it is essential to apply the correct biocides and dosages at the correct frequency. Denyer (1990) listed the antimicrobial effects of selected water treatment biocides. The use of biocides is expensive and could lead to pollution of the environment.

Biocides avalable are of the principal types (Denyer, 1990 ; Kaiga et al 1989; Azis *et al.* 2003; Eguia *et al.* 2007) :

1) Oxidising agents - the halogens and potassium permanganate:
    - chlorine
    - chlorine dioxide
    - ozone
    - bromine
    - bromine chloride
    - hydrogen-peroxide
    - iodine
    - potassium permanganate
2) Non-Oxidizing biocides
    - acrolen
    - arsenates and arsenites
    - ammonia and amines
    - cyano compounds
    - metals- salts
    - chlorinated phenolics
    - organometals
    - organo-tin ammonium salts
    - phenols-chlorinated and phenylated
    - proprietary formulations
    - surfactants
3) Hydrolysing agents - acids and alkalis.

4) Cell poisons - heavy metals.
5) Protein coagulants- mercury and phenol
6) Surfactants - cationic detergents.

Of the above, types 4, 5 and 6 can be ruled out for an open circuits. Phenol and heavy metals are forbidden by anti-pollution rules, and the surfactants cause foams. Type 3 would involve such concentrations as to upset pH and promote corrosion in the circuit. Of the oxidising agents, permanganate is sometimes used in closed fresh water circuits, but would be too expensive in open circuit.

2.1.2.2 Mechanical Techniques

Micro-mesh filters

The most effective water treatment is to filter out the eggs and larvae of the organisms to reduce their attachment and settlement in the cooling-water-system piping. Test results using a 50-micro roundwire filter with backwash capability by water and air indicated reduced fouling (Mussalli and Tsou, 1989; Torbin and Mussalli, 1979). The filter may be used to treat small flow systems that can withstand a pressure drop.

Sponge rubber balls

Biofilms in pipelines can be removed by a hard sponge bullet or rotary ball which is placed inside of a pipe and is propelled through the system in the direction of flow (Bell et all, 1985). Due to the high water pressure building up behind it, it rotates while moving, scrubbing off the attached material on its way. A major disadvantage is that the balls can jam the pipe (Shone and Grim, 1986; Nosetani *et al*. 1981, 1987, 1988, 1989; Melo and Bott, 1997)

Tube Inserts

A tube insert is a mechanical device which prevents fouling inside the tubes of heat exchangers. When the insert rotates due to fluid flow, it scrubs the surface of the tube to remove fouling (Carlos, 1981)

Robots

Several remotely operated underwater robots, developed by Mitsubishi Heavy Industries of Japan, have been used in Japanese power plants for cleaning water channels and intake structures. (Mussalli and Tsou, 1989; Torbin and Mussalli, 1979; Tsou and Mussalli, 1988).

Hydroblasting

Hydroblasting is used in cases where chemical cleaning is unsatisfactory. The advantage of hydroblasting is that the equipment can be easily inspected after the cleaning operation is completed to verify that the deposits have been removed. The main disadvantage of hydroblasting is the time and the cost of pulling and reinstalling the exchanger bundles. For hydroblasting, high-pressure water or a water-sand slurry is often effective (Eguia *et al.* 2008). In general, increasing the water velocity to approximately 3m/s could eliminate "dead" zones and then impede the attachment of marine and vegetable organisms, as well as more sophisticated organism such as molluscs.

2.1.2.3 Physical Techniques

Electromagnetic Method

Kvajic (1978) studied electromagnetic water treatment and fouling of heat exchangers. However, most systematic investigations of magnetic fouling reduction have not produced any consistent results.

Ultraviolet Light

This method can be used to treat small volumes of water. Ultraviolet light is very effective in controlling bacteria. But it is not an effective way to control biofouling caused by such organisms as mussels and barnacles because they are protected by their shells. The water must be clear so that ultraviolet rays can penetrate it, and there must be no dissolved iron, even in trace quantities, since it will absorb ultraviolet light. Preliminary results have shown that seawater bacteria are significantly different from the well-documented human bacteria and that the associated kill rates are not as high as anticipated (Seki et al, 1985, 1986). Initial results have also shown that ultraviolet

irradiation subdues marine microbiological growth in the early stages by as much as 95.5 % (Seki et al, 1986).

Acoustic Techniques

The acoustic technique works on the principle of creating an inhospitable environment in which the species finds it unacceptable to settle and live. Experiments indicate that asonics (20-60 Hz) and ultrasonics (>20K Hz) can retard biofouling (Tsou and Mussalli, 1988). Work in Hawaii on OTEC heat exchangers showed that ultrasonics retarded biofouling, but neither killed nor stunned the bacteria in seawater, and the surviving bacteria eventually attached and colonized in heat exchangers (Takahoshi, 1990).

Thermal Treatment

Thermal recirculation, or heat treatment is a highly effective method of controlling macrofouling in conduit systems (Mussalli and Tsou, 1989). It does not affect condenser slime but does control most species of mussels and barnacles (Boyer and Malherbe, 1979).

Ice Nucleation

Biofilms in heat exchangers can be removed by a process known as ice nucleation where the heat exchanger is frozen, and ice crystals form between the metal surface and the attached material (Patent: US4419248). The biofilm is physically dislodged from the surface. This process is usually repeated more than once to obtain satisfactory results.

2.2 Medical Devices-Related Infections

The high incidence of infections caused by the use of implanted biomedical devices, including catheters (Plowman er al, 2001), bone fracture fixation pins (Wassall et al, 1997) and heart valves (Tozzi et al, 2001; Cook et al, 2000) etc. has a severe impact on human health and health care costs. Current estimates suggest that in the UK nosocomial infections cost the UK £1.0 billion per year (Plowman R *et al.* 1999) and medical devices and implant-associated infections cost the UK £11 million per year (Darouiche 2004). In the United States, nosocomial infections cost the USA $11 billion per year and at least half of the 2 million cases of nosocomial infections are medical

devices-related infections (Darouiche 2004, 2007, Richards *et al.* 1999; Jarvis 1996, McGowan 2001, Schierholz *et al.* 1998, 2002). As the use of medicals devices and implants has increased, the device-related infections become a major concern.

2.2.1 Catheter-associated Infections

Intravascular catheters and urinary catheters are essential components of modern medical care. Intravascular catheters or central venous catheters are used to deliver life-sustaining fluids, such as antimicrobial agents, parenteral nutrition, and blood or blood products. Urinary catheters are used to drain the bladder. Catheter-related infection remains a leading cause of nosocomial infection, especially in intensive care units and is associated with significant patient morbidity and mortality (Brun-Buisson *et al*., 1987; Blot *et al*., 1999; Kite *et al*., 1999; Sherertz *et al*., 2000; Öncü *et al.,* 2003).

Central venous catheter-related infection rate is high, accounting for 34% - 40% of nosocomial infections (Bambauer *et al.,* 1982, 1994; Veenstra *et al*., 1999). It is estimated that about 5 million and 200,000 central venous catheters are inserted annually in the US and UK, respectively. About 3% - 8% of central venous catheters cause bloodstream infections with the mortality of 12% -25% (Pearson 1996; Darouiche, 2001; O'Grady *et al*., 2002; Elliott *et al*., 1992). It is estimated that approximately 80,000 -400,000 cases of catheter-related bloodstream infections occurs in US each year, leading to between 2,400 and 20,000 deaths (Mermel, 2000; Raad *et al*., 1996, 2002).

Catheter-associated urinary tract infection is the most common nosocomial infection in medical intensive care units, with infection rate about 31% - 40% (Richards MJ *et al*., 1999; Lai KK *et al*., 2002). There are more than 30 million bladder catheters used each year in US, about 7.6 infections per 1000 catheter-days (Darouiche, 2001; Maki *et al*., 2001; Saint, 2000). In the UK, catheter-associated urinary tract infections alone account for up to one third of all hospital-acquired infections and cost the UK health service £177 million in 798,000 extended bed days each year and result in increased morbidity and mortality (Plowman er al, 1999, 2001). Long-term catheterisation (more than 30 days) is usually used for the treatment of permanent urinary incontinence (Morris et al, 1997). The risk of catheter-associated infections increases with increasing catheterisation time and over 90% of patients will develop bacteriuria and infection

within 28 days of catheterisation (Choong et al, 2001). Urinary tract infections can lead to life-threatening conditions (e.g. septicaemia) with an increase in mortality (Lai and Fontecchio, 2002). Encrustation of catheters is another common complication in the care of many patients undergoing long-term indwelling bladder catheterisation (Morris et al, 1997). Under the alkaline conditions, struvite (magnesium ammonium phosphate) and calcium phosphate crystals precipitate from the urine and agglomerate onto the catheter surface and its biofilm, forming crystalline biofilm (Jones et al, 2005). These crystalline deposits are hard and can cause trauma to the urethra and bladder mucosa during catheter removal (Jones et al, 2005).

2.2.2 Pin Tract Infection

A bone fracture is a medical condition in which a bone is cracked or broken. The basic goal of fracture fixation is to stabilize the fractured bone, to enable fast healing of the injured bone, and to return early mobility and full function of the injured extremity. There are two main types' surgical techniques of fracture fixation: external and internal (Pfahler M *et al.* 1996). External fixation uses a combination of pins, wires, clamps, and bars or rings to set bone fractures (Karunaker MA *et al.* 2001; Taljanovic MS *et al.* 2003, Hunter TB *et al*. 2001). The internal fixation consists of wires, pins and screws, plates and intramedullary nails or rods. The majority of internal fixation implants are currently made of stainless steel and titanium.

External and internal fixations are widely used in patients with skeletal fixation, where the pins and wires travel through skin and soft tissue into bone. Pin tract infection is common nosocomial infection. Many means are used to avoid these infections including accurate nursing care, antiseptic baths, frequent skin cleaning, frequent dressings and use of ointments and antibiotics. In spite of these preventive methods the results are not satisfactory and pin tract infections still occur in approximately one third of patients (Wassall et al 1997; Clasper et al 2001; Darouiche 2001). The rates of pin site infection range from 11% to 56% were reported (Ahlborg and Josefsson 1999; Antich-Adrover *et al* 1997; Gregory *et al* 1996; Hedin *et al* 2003; Johnson *et al* 1990; Mahan J *et al.,* 1991; Mason *et al* 2005; Masse A *et al.,* 2000; Maueret *et al* 2000; McGraw and Lim 1998; Mostafavi *et al.* 1997; Parameswaran *et al* 2003; Patterson 2005; Sims M *et al.,* 2000;

Wheelwright and Court-Brown 1992; Yokoyama *et al* 1998). In the UK, pin tract infection rates around 37% in external fixation have been reported (Clifford et al 1987; Gopal et al 2000; Keating et al 1991).

Failure to treat a pin site infection in a timely manner may lead to deeper infection, loosening of the pin, loss of fixation, or stability of the external fixator and osteomyelitis. In cases of infection the pin/wire must be removed and at worst the fixator as well. The pin tract infection phenomena can be classified into three grades: 1) Irritation or inflammation of the soft tissues and skin; 2) True soft tissue infections; 3) Bone infection and pin loosening, which can result in persisting osteomyelitis.

2.2.3 Surgical Instruments-Related Infections

An epidemic of a new variant Creutzfeldt-Jakob disease (vCJD) was first described in the United Kingdom (UK) in 1996 (Will et al, 1996). It was eventually shown that this epidemic resulted from eating beef from cows infected with Bovine Spongiform Encephalopathy (BSE) (Collinge et al, 1996). It is now generally believed that these diseases are caused by an infectious protein called a "prion". 117 patients in the UK and 10 patients in other countries who are dying from vCJD have been reported (Deslys et al, 1997; La et al, 2002). BSE has been reported in cow herds in every country in the European Union except Sweden, it has also been reported in Switzerland, the Ukraine, Slovakia, Slovenia, the Azores, Canada, the Czech Republic, Oman, Poland, Israel and Japan (Bosque et al, 2002). Due to the extremely long incubation periods of these diseases in humans, it remains entirely possible that a substantial worldwide epidemic of vCJD will occur over the coming years (Ghani et al, 1999, 2000; Hilton et al, 1998, 2002; Prusiner et al 1990). In the meantime we are faced with the possibility that significant numbers in other human populations and animal herds may be incubating prion diseases.

It has been known for a long time that prion disease can be transmitted by surgical instruments and that cross-infection may occur despite the use of current sterilisation protocols (Gibbs et al, 1968, 1994; Frosh et al, 2001; Bernoulli et al 1977). It has already been demonstrated that stainless steel is capable of transmitting prion disease (Zobeley et al 1999; Flechsig et al 2001). Stainless steel is used in the majority of

surgical instruments and there is clear evidence from case reports in humans and animal models that prion diseases can be transmitted via stainless steel surgical instruments (Laurenson et al 1999).

The most effective generic approach to prevent vCJD transmission via surgical instruments is to remove all traces of prions at the washing phase of the decontamination process. Unfortunately it is very difficult to remove prions completely from stainless steel surfaces as they are readily and tightly bound to the surfaces (Zobeley et al 1999). Prions also exhibit unusual resistance to conventional chemical and physical decontamination methods, and cannot readily be destroyed by conventional disinfection and sterilization methods (Brown et al 1982, 2000; Ernst and Race 1993). It has been shown that stainless steel instruments can retain CJD infectivity even after formaldehyde or sodium hydroxide treatment, and extended periods of autoclaving have also been shown to be unreliable (Taylor et al 1994; 1996). Surgical instruments are reused often, and their time in service often exceeds 10 years (Frosh et al, 2001). Each set of instruments over its lifetime will have come into contact with many patients, significantly increasing the risk of contamination (Laurenson et al 1999).

2.2.4 Other Devices Related Infections

In addition to the catheter, pins and surgical instruments, prosthetic heart valves, total artificial hearts, joint replacement or other orthopaedic devices, and dental implants etc. also have infection problems. For example, prosthetic valve endocarditis remains one of the most dangerous and life-threatening complications following heart valve replacement, there are more than 100,000 artificial heart valves are implanted per year in the US, and the number is increasing (Fang G *et al*., 1993). Mortality rates of prosthetic valve endocarditis as high as 75% have been reported (Illingworth BL *et al*., 2000). Over 12,000 infections related to joint prostheses per year in the US (Darouiche RO, 2004).

2.2.5 Pathogenesis of Medical Devices and Implants Related Infections

As these devices are made of inert biomaterials, they are also highly susceptible to bacterial contamination. Generally, bacteria come from patient's skin and air or from

somewhere in the patient's body (Gillespie WJ, 1990; Maderazo EG *et al*., 1988). Bos R *et al.* (1999) described the initial steps in the formation of a complex, multispecies biofilm, as shown in Figure 2.9

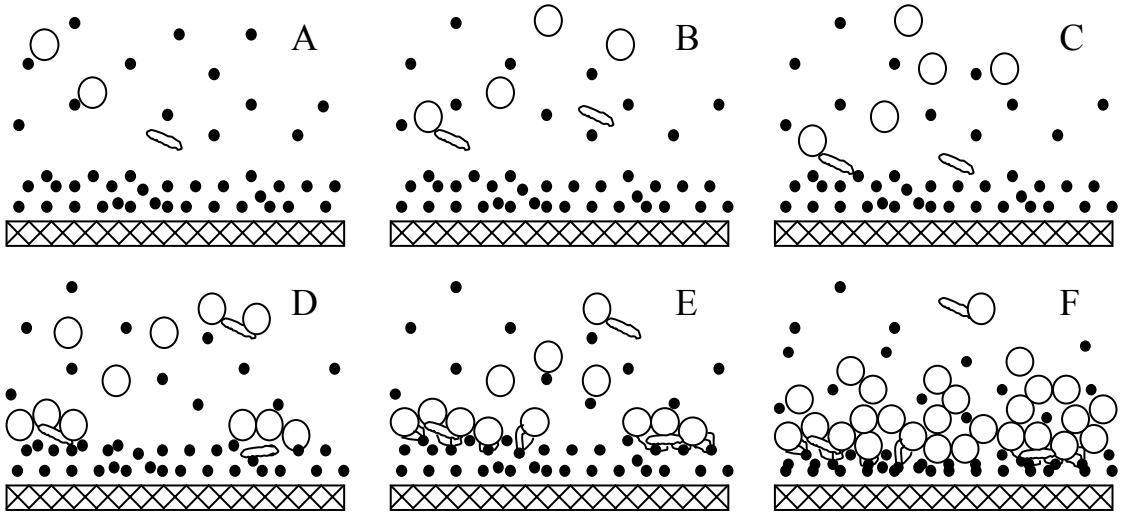

Fig.2.9 Initial steps in biofilm formation

A: Adsorption of conditioning film components; B: microbial transport and coaggregation; C: reversible adhesion of single organisms and of microbial coaggregates; D: co-adhesion between microbial pairs; E. anchoring or the establishment of firm, irreversible adhesion through exopolymer production; F: growth (Reproduced from Bos R *et al.*, 1999)

The initiation of biofilms on the inert surfaces always begins with the attachment of a small number of bacterial cells which, under favourable conditions, multiply to form a biofilm (Gristina, 1987). The initial bacterial adhesion is called reversible adhesion and it is governed by physico-chemical interactions. It has been demonstrated that the surface properties of the biomaterials have significantly influence on bacterial adhesion, such as surface energy and surface chemistry etc. This stage or reversible adhesion is soon followed by a physical binding of the bacterial cells to the inert surface (irreversible adhesion) through exopolysaccharides produced by the bacteria. The multiplication of these adhered cells would lead to the formation of microcolonies and the development of a mature biofilm, which is resistant to the host's defence mechanisms, antibiotics and antiseptic treatments, leading to infection (Bos et al 1999; Pereni et al 2006). Biofilm formation on the surfaces of medical devices and implants is

the pathogenesis of the devices-related infections (An *et al*., 1996, 2000; Fitzgerald 1989; von Eiff *et al*., 2005).

The devices-related infections cause increased morbidity and mortality (Cook G *et al.* 2000; Lai KK *et al.* 2002). For example, for bacteria to cause pin tract infection, they must first attach and colonize at the skin-device interface, and then advance along the surface of the pin, causing deep pin tract infection and even posteomyelitis (Wassall et al 1997; Darouiche 2001). As the "inert" pin surfaces are not well protected by host defences and by antibiotics treatment, they provide a focal point for infecting pathogens (Darouiche 2001; Bosetti et al 2002). Therefore prevention of bacterial attachment and colonization on the device surfaces will have a major impact in reducing the rate of infections (Darouiche 2001; Bosetti et al 2002). Although the initial adhesion process is thermodynamically influenced by the characteristics of the bacteria, the inert surface and the interaction medium, in practice it is only the device surface that can be modified in order to reduce the bacterial adhesion and infection.

CHAPTER 3

AIMS AND OBJECTIVES

3.1 Anti-biofouling Coating Techniques

An effective and desired approach to reduce biofouling is to alter the surface properties of heat exchangers or medical devices by surface coating techniques and to make it less attractive for the biofouling components, so that they can be removed easily from the surfaces by flowing fluids. So far many toxic coatings and non-toxic coatings have been developed for the control of biofouling using a range of coating techniques, including chemical plating, physical vapour deposition (PVD) and chemical vapour deposition (CVD) etc.

3.1.1 Toxic Anti-biofouling Coatings

The most important biocides are cuprous oxide and organo-tin compounds (Kjaer, 1992). These toxic ingredients must leach out or release slowly in the surrounding water. Although the antifouling coatings offer the "best" solution of the biofouling problem, a number of disadvantages exist of which three are most important. First, its antifouling formulations have limited time of effective performance, estimated at 12 months for copper coatings and 18-30 months for organotin coatings (Kjaer, 1992; Lindner, 1988). The second disadvantage is the pollution to the environment. This in turn creates

pollution problems affecting fish and other living inhabitants of the marine environment. Environmental concerns are also expressed related to the effects of organotin compounds from human consumption of contaminated animals. Therefore since 1990, many countries, including UK, USA, Canada, Japan, Australia and New Zealand have legislated restrictions on the use of organotin-based antifouling coatings (Kjaer, 1992). The third disadvantage is the poor thermal conductivity and poor abrasion of the coatings that inhibit their commercial use in heat exchangers.

In view of increasing bacterial resistance to antibiotics and antiseptics, silver coating may be an effective strategy to prevent medical devices-related infections (Schierholz et al 1998). However, numerous clinical studies show that the use of silver-coated devices resulted in non-significant reduction in medical devices-related infections as bacteria (dead and alive) strongly stick to the silver-coated surfaces (Thibon et al 2000; Leone *et al.*, 2004; Cook et al 2000). As a result, the silver-coated sewing cuff (Silzone valve) was withdrawn from the market on January 2000 (Tozzi et al 2001). The silver-coated medical devices are not recommended for widespread use (Thibon et al 2000).

3.1.2 Non-Toxic Anti-biofouling Coatings

Due to the world-wide legislation, one can assume that toxic antifouling coatings will eventually disappear completely from the market. Therefore, non-toxic coatings have attracted more attention.

Polymer and Metal Nanocomposite Coatings

Many attempts have also been made to reduce fouling by coating surfaces with polymers (e.g. silicone, PTFE) due to their non-stick properties. However, the poor thermal conductivity, poor abrasion resistance and poor adhesion to metal substrate of these polymer coatings currently inhibit their commercial use (Müller-Steinhagen and Zhao, 1997). In order to overcome the disadvantages of polymer coatings, Zhao et al (2002, 2004, 2005, 2007) have developed polymer-metal nanocomposite coatings using electroless plating technique for the control of fouling. Because the electroless Ni–P–PTFE coatings are metal-based, their thermal conductivity, anti-abrasive property, mechanical strength and adhesion strength to the substrate are superior to standard

PTFE coatings. Zhao et al (2002, 2004) found that Ni–P–PTFE coatings reduced significantly bacterial adhesion, compared with stainless steel.

Diamond-like carbon coatings

Diamond-like carbon (DLC) coatings have attracted great interest due to their excellent properties such as excellent thermal conductivity similar to metals, low friction, extremely smooth surface, hardness, wear resistance and corrosion resistance (Grill, 1993). DLC is also an excellent base coating to be alloyed with different elements. The amorphous nature of DLC opens the possibility of introducing additional elements, such as Si, F, N, O and their combinations, into the coating whilst still maintaining the amorphous phase of the coating (Hauert, 2003). Recently, the incorporation of selective elements into DLC has been shown to be an effective method to enhance the anti-fouling and other properties of DLC coatings. The modified DLC coatings are usually produced by magnetron sputtering techniques or by plasma enhanced chemical vapour deposition (PECVD) techniques. Zhao et al. (2007, 2010) explored initial bacterial attachment on silicon-doped DLC coatings and showed that the silicon-doped DLC coatings reduced bacterial attachment. Numerous studies demonstrated that the heat transfer surfaces coated with DLC reduced scale adhesion and subsequent scale formation, compared with untreated titanium and stainless steel surfaces (Müller-Steinhagen and Zhao, 2000; Bornhorst et al, 1999; Santos et al. 2004). Zhao and Wang (2005) demonstrated that the fluorinated DLC coatings further significantly reduced scale adhesion and subsequent scale formation, compared with DLC coatings. Hasebe et al. (2007) showed that the fluorinated DLC coatings inhibit protein adsorption and platelet activation. Ishihara et al. (2006) demonstrated that the antibacterial performance of the pure DLC coatings was improved significantly by the incorporation of fluorine with *Escherichia coli*.

3.2 Aims and Objectives

3.2.1 Development of Novel Anti-bacterial Nanocoatings

Ni–P–PTFE coatings seem the one of the best coating techniques for controlling biofouling. However their anti-biofouling properties could be futher improved by incorperating biocide polymer nanoparticles into the Ni–P–PTFE coatings. The

modified DLC coatings with selected elements have great potential for controlling biofouling in heat exchangers and for controlling biofilm formation in medical devices and implants. Howevever the deoped elements and their contents in the DLC coatings should be optimised in order to get best anti-biofouling formance.

In this study, the electroless plating technique was used to develop novel anti-biofouling Ni–P–PTFE-Biocide Polymer nanocomposite coatings; Magnetron sputtering and plasma enhanced chemical vapour deposition (PECVD) techniques were used to develop new anti-bacterial modified DLC coatings, including Si-N-DLC coatings, B-DLC coatings, Ti-DLC coatings. A range of new SiOx-like coatings was also developed and evaluated. A series of coatings with different surface properties such as surface chemistries and surface energies were designed and produced. The surface properties of the coatings were characterized using surface analysis facilities, such as AFM, SEM, XPS and OCA 20 etc.

3.2.2 Evaluation of the Nanocoatings

The nanocomposite coatings were evaluated with bacterial strains that frequently cause heat exchanger biofouling and medical devices-related infections. Viable plate count and microscope techniques were used for bacterial adhesion assays.

3.2.3 Investigation of Anti-bacterial Mechanisms

In this study both a thermodynamic approach and the extended DLVO theory were used to explain the bacterial adhesion mechanism and the bacterial adhesion results on the nanocomposite coatings.

CHAPTER 4

PREPARATION OF Ni–P–POLYMERS AND MODIFIED DLC NANOCOATINGS

4.1 Electroless Plating Ni-P-Polymers Coatings

4.1.1 Electroless Plating Ni-P Coatings

Electroless plating is a process of electrochemical reaction, in which metal ions are reduced to a metallic coating by reducing agent in solution. Since plating takes place only on suitable catalytic surfaces without external current source required, it is also known as autocatalytic plating. The first bright metallic deposits of nickel-phosphorus (Ni-P) alloys were obtained in 1911 by Breteau (1911). Later Roux (1916) developed an electroless nickel plating bath. Paal (1931) and Scholder (1931) studied this reaction in details. In 1946, Brenner and Riddell further developed Ni-P plating process by using reducing agent hypophosphite, which was patented in 1950 in USA. In 1953, General Application Transport Company in USA made the first industry line of electroless plating Ni-P with improved electroless nickel process, which was licensed to some 25 other companies during the 1960's and early 1970's (Duncan, 1995).

The advantages of electroless plating Ni-P technique include (Totlani, 1992):

1) Coating thickness is very uniform;
2) No external current are required;
3) Almost any metallic or non-metallic, non-conducting surfaces, including polymers (plastics), ceramics, glasses can be plated at low temperature (< 90°C). Those materials which are not catalytic to the reaction can be made catalytic by suitable sensitizing and nucleation treatments;
4) Coatings have unique chemical, mechanical and physical properties, such as good hardness, excellent corrosion resistance, electrical conductivity, good wear and abrasion resistance, low coefficient of friction.

Due to the unique properties of electroless plating Ni-P coatings, they have been applied in many industries, including chemical, mechanical, food processing and electronic industries etc. (Bates, 1998; Chitty *et al*., 1997; Staia *et al*., 1996). Bates (1998) gave the ratio of electroless plating Ni-P coating application in industry, as shown in Fig. 4.1

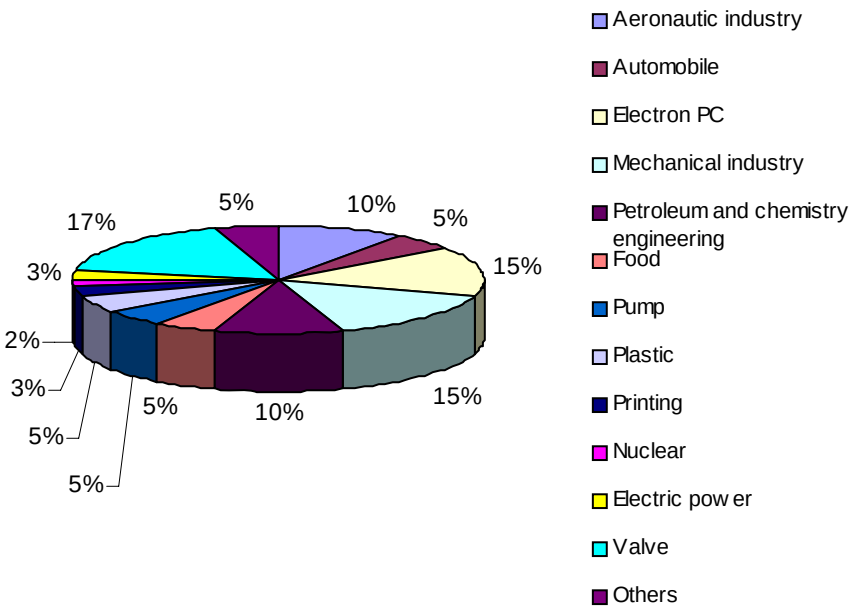

Fig. 4.1 The distribution of electroless nickel coating application in industry

The electroless Ni-P is usually deposited by the catalytic reduction of nickel ions with sodium hypophosphite in acidic or alkaline baths. The phosphorus content in the Ni-P coating has significant influence on its chemical and physical properties. For example, the corrosion resistance of the Ni-P coatings increases with increasing P contents in the

coatings (Ploof 2008; Armyanov *et al*., 1999; Tachev *et al*., 2001; Martyak *et al.*, 1993). The hardness of electroless plating Ni-P is generally around 450~600 HV (Vickers Hardness). The hardness increases to 1000 HV after heat treatment at 300°C - 400°C, which is much higher than stainless steel (220 HV) or electroplating Cr (800~900 HV) (Kumar *et al.*, 1996).

4.1.2 Electroless Plating Ni-P-PTFE Coatings

Although electroless nickel coating has been used in many industries, future modification is required in order to meet special requirements by the incorporation of solid particles into Ni-P coatings to form Ni-P based nano- or micro-composite coatings. These composite coatings combine the advantages of the metal matrix and the included particles (Losiewicz *et al.*, 1999; Shuji *et al.*, 1996). The particles include SiC, WC, Al_2O_3, TiO_2, Si_3N_4, MoS_2 and PTFE etc (Kerr *et al.*, 2000; Feldstein, 1998; Moonir-Vaghefi *et al.*, 1997; Nishira *et al.*, 1994; Zhao et al 2002). For example, the incorporation of SiC particles into Ni-P coating significantly increases the hardness of the Ni-P coating, i.e. the hardness of the Ni-P-SiC composite coatings is much higher than that of Ni-P coatings (Apachitei, *et al*., 1998; Grosjean *et al*., 1997).

The first composite coating of electroless Ni-P-PTFE was introduced by Tulsi *et al.* in 1981 (Tulsi *et al.* 1982, 1983). The incorporation of PTFE particles into the Ni-P matrix can take advantage of the different properties of Ni-P alloy and PTFE (polytetrafluoroethylene). PTFE is also known as Teflon with chemical formula as shown in Fig. 4.2, which was developed by Roy Plunkett of Kinetic Chemicals in New Jersey in 1938 and registered with the Teflon trademark in 1945 (Plunkett).

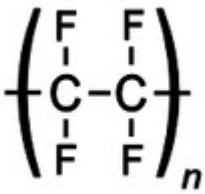

Fig 4.2 Chemical structural formula of PTFE

PTFE is chemically very inert and has a relatively high melting point (325 °C). Its coefficient of friction is lower than that of almost any other polymers. Because of its extremely low surface energy (18.6 mJ/m^2), PTFE has excellent non-stick properties (Hadley and Harland 1987). The resulting properties of electroless Ni-P-PTFE coatings, such as non-stick, non-galling, anti-adhesive, higher dry lubricity, lower friction, good wear and good corrosion resistance, have been used successfully in many industries, automotives, pump, oil pipes, dished valve, shaft bearing, gear, electronics, synthetics, textile, pneumatics, pharmaceutics and food (Pietsch 2009). A concise review of the field of Ni-P-PTFE and highlights the importance of process control in obtaining critical deposit characteristics for a variety of demanding industrial applications were given by Roberto (1988), Kerrr *et al* (2000) and Helle and Walsh (1997).

Zhao et al first demonstrated that Ni-P-PTFE coatings have anti-fouling properties, including water scaling (Zhao etal 2002, 2005) and biofouling (Zhao et al 2004, 2005, 2006). Because electroless Ni-P-PTFE coatings are metal-based, their thermal conductivity, anti-abrasive property and mechanical strength are superior to standard PTFE coatings.

PTFE particles readily coagulate and precipitate in the plating solution since PTFE is a water-repellent material. Due to this agglomerate formation it is difficult to obtain a uniform dispersion of PTFE particles in a plating bath. This will not only reduce the PTFE content in the coatings, but also increase the surface roughness as larger PTFE particles are incorporated (Matsuda *et al*., 1995; Nishira *et al*., 1996; Zhao et al 2002). To produce a better electroless Ni-P-PTFE coating, the PTFE particles must be uniformly suspended in a plating solution using surfactants (Ger *et al.*, 2002) or mechanical agitation (Nishira *et al*., 1996) or ultrasonic agitation (Higahitani *et al*., 1993; Nishira *et al*., 1996) during the electroless plating Ni-P-PTFE process. If the PTFE particles are not uniformly suspended in a plating solution, they will not able to uniformly distribute throughout the Ni-P matrix. Areas where less PTFE is incorporated do not have the same physical and mechanical properties as areas where the PTFE content is higher (Zhao et al 2002). This influences the mechanical and tribological (friction, lubrication, bearing and hydrodynamic) properties of the coating, and is a main problem in many electroless Ni-P-PTFE coatings. Nishira *et al.* (1996) studied the effects of agitation methods on the particle size distribution of PTFE aggregates in a

plating solution. One of their findings was that an ultrasonic homogenizer was more effective than mechanical agitation. It would be very desirable if the PTFE particles in the plating solution could be dispersed uniformly by using surfactants alone (Zhao et al 2002). A surfactant is a chemical whose molecules have a hydrophilic section (water soluble) and a hydrophobic section (water insoluble), see Fig. 4.3a.

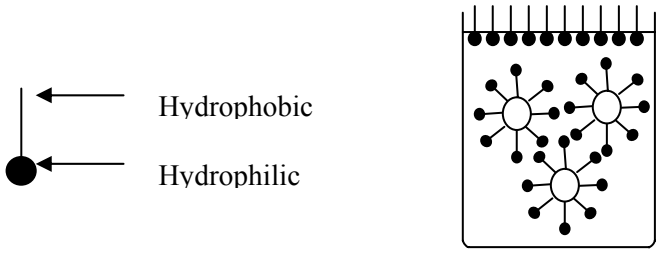

Fig. 4.3 Typical surfactant molecule

A hydrophobic section of surfactant will absorb onto the PTFE surface. A hydrophilic section of surfactant will solubilize in aqueous solution and then prohibit PTFE coagulation and precipitate (Fig. 4.3b). Surfactants usually are classified into cationic, non-ionic and anionic surfactants. The functions of surfactants used in Ni-P-PTFE plating solutions include: 1) to make PTFE particles hydrophilic and to suspend them uniformly in the plating solution; 2) to make the PTFE particles to be charged so that the particles can move to the substrate and then co-deposit onto the substrate together with Ni-P (Liu and Zhao 2003). Zhao and Liu (2003) investigated the effect of different types of surfactants on the suspension of PTFE micro-particles and found that a cationic surfactant $C_{20}H_{20}F_{23}N_2O_4I$ (FC-4) performed best.

4.1.3 Electroless Plating Ni-P-Biocide Polymer Coatings

Ni–P–PTFE coatings seem the one of the best coating techniques for controlling biofouling in heat exchangers and pipelines. However their anti-biofouling properties could be futher improved by incorperation biocide polymer nanoparticles into the Ni–P–PTFE coatings. In this study, an electroless plating technique is used to develop novel anti-biofouling Ni–P–Biocide Polymer and Ni–P–PTFE-Biocide Polymer nanocomposite coatings.

4.1.3.1 Biocide Polymers

As mentioned above, the conventional toxic anti-biofouling coatings contain anti-microbial agents and they must release slowly in the surrounding water. The disadvantages of the toxic coatings include poor durability and the pollution to the environment.

Recently the Graz University of Technology, Austria has developed a range of new contact biocide polymers using the Ring Opening Metathesis Polymerisation (ROMP) synthesis technique (Kreutzwiesner et al, 2010; Ilker et al. 2004). Compared to such conventional antimicrobial agents, contact biocide polymers have the advantages to be non-volatile, chemically stable and do not leak degradation products of low molecular weight into the surrounding. The anti-microbial mechanism of the new contact biocide polymers is not based on the slow release of biocide into the surrounding, the polymers are real contact biocides, i.e. they have "contact kill" function (Kreutzwiesner et al, 2010). In this study, the anti-microbial efficiency of 13 different types of biocide polymers from Graz University of Technology was evaluated with *Escherichia coli* and *Staphylococcus aureus*. It was found that two biocide polymers SM14 and SM20 perform best against bacterial attachment. The chemical structures of SM14 and SM20 are shown in Fig. 4.4 (Su et al, 2011). As a result, four new anti-biofouling Ni-P-biocide polymers nanocomposite coatings: Ni-P-SM14, Ni-P-PTFE-SM14, Ni-P-SM20 and Ni-P-PTFE-SM20 were developed. A patent has been filed in 2012 (Su et al 2012).

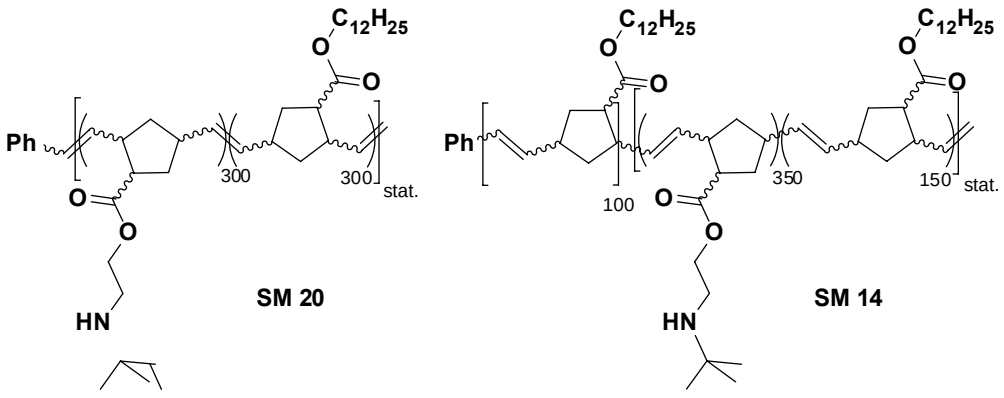

Fig. 4.4 Chemical structures of SM14 and SM20

4.1.3.2 Mechanism of Electroless Plating Ni-P-Polymers

Agarwala *et al.* (2006) suggested that the mechanisms of electroless plating Ni-P could be due to chemical bonding. Chemical bonding mechanism is divided into electrochemical bonding mechanism and atomic hydrogen mechanism. The electrochemical mechanism supposed that hypophosphite ion is catalytically oxidized and nickel and hydrogen ions are reduced at the catalytic surface (Gutzeit and Crehan 1954; Agarwala *et al.* 2006). The atomic hydrogen mechanism involves following reactions (Brenner A *et al*., 1946; Goldie 1968; Mallory 1979; Agarwala *et al.* 2006):

(1) Atomic hydrogen generation: The atomic hydrogen, generated by the reaction of water with hypophosphite, is absorbed at the catalytic surface:

$$H_2PO_2^- + H_2O \xrightarrow{catalytic} HPO_3^{2-} + H^+ + 2\,[H] \qquad (4.1)$$

(2) Nickel ions reduction: The absorbed atomic hydrogen reduces nickel ions at the catalytic surface:

$$Ni^{2+} + 2[H] \rightarrow Ni^0 + 2H^+ \qquad (4.2)$$

The evolution of hydrogen gas, which always accompanies catalytic nickel reduction, was ascribed to the recombination of two atomic hydrogen atoms:

$$2\,[H] \rightarrow H_2 \qquad (4.3)$$

(3) Phosphorus generation: A secondary reaction between hypophosphite and atomic hydrogen results in the formation of elemental phosphorus:

$$H_2PO_2^- + [H] \rightarrow H_2O + OH^- + P^0 \qquad (4.4)$$

(4) Nickel and phosphorus codeposition: Nickel and phosphorus codeposit on substrate materials to form Ni-P coatings.

$$Ni + P \rightarrow Ni\text{-}P \qquad (4.5)$$

(5) Nickel, phosphorus and polymer nanoparticles codeposition:

$$Ni + P + Polymers\ (PTFE,\ SM14\ or\ SM20) \rightarrow Ni\text{-}P\text{-}Polymers \qquad (4.6)$$

4.1.3.3 Pretreatment Procedures of Steel Substrate

In this study, Ni-P-Polymers (Ni-P, Ni-P-PTFE, Ni-P-SM14, Ni-P-SM20, Ni-P-PTFE-SM14, Ni-P-PTFE-SM20) were coated on AISI 316 stainless steel sheets of 25mm × 25mm × 1mm containing Fe 69%, Cr 18%, Ni 10%, Mo 3% with density of 7.96 g/cm^3 (Goodfellow Company, UK) at the Biological and Nanomaterials Lab, University of Dundee. The pre-treatment and coating procedures are listed in Table 4.1.

Table 4.1 Pretreatment of steel substrates for electroless plating Ni-P-Polymers

Procedures	Bath composition and operating conditions
Alkaline cleaning	NaOH: 20 ~ 35 g/l; Na_3PO_4: 25 ~ 35 g/l; Na_2CO_3: 25 ~ 30 g/l; Na_2SiO_3: 5 ~ 10 g/l; 60 ~ 80 °C; 5 ~ 10 min.
Rinsing	H_2O; room temperature
Electrocleaning	NaOH : 20 ~ 35 g/l; Na_3PO_4: 25 ~ 35 g/l; Na_2CO_3: 25 ~ 30 g/l; Na_2SiO_3: 5 ~ 10 g/l; room temperature; 2 ~ 3 min; voltage: 5 ~ 7 V.
Rinsing	H_2O; room temperature
Pickling	HCl(30%):H_2O=1:1; room temperature, 0.5 ~ 1 min.
Activation	$NiCl_2 \cdot 6H_2O$: 200 ~ 400 g/l; HCl (30%): 75 ~ 200 ml/l; anode plates: Ni; current density: 2~3 A/dm^2; room temperature; 1~3 min.

Alkaline Cleaning

Alkaline cleaning is to remove oil from substrate surfaces. The composition of alkaline cleaning solution used in this investigation is given in Table 4.1. After alkaline cleaning, the samples are rinsed after cleaning in deionised water at room temperature.

Eletrocleaning

The composition of cathodic electrocleaning solution is the same as alkaline cleaning solution. The samples to be cleaned act as anode and two stainless steel plates act as cathodes, as shown in Fig 4.5. The cleaning is usually performed under the direct current voltage: 5 ~ 7 V at room temperature. After cleaning, the samples are rinsed in deionised water at room temperature. The electrocleaning time is about 5~10 min depending on the degree of contamination and substrate materials (Zhao et al 2002).

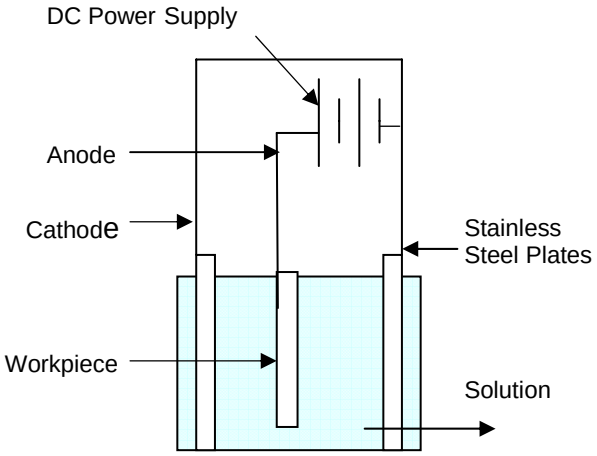

Fig 4.5 Schematic drawing of eletrocleaning device

Pickling

Pickling is used to remove oxidized film or rust from the substrate surfaces. The common pickling solution consists of hydrochloric acid (HCl). In this study, the pickling solution with HCl 30%: H_2O (1:1 in volume) were used. Picking time is important. If pickling time is too short, oxidized film or rust cannot be removed completely leading to poor coating quality; if pickling time is too long, the substrates are subjected to over etching. Pickling time for the stainless steel 316 in this study was 1 min.

Activation

As stainless steel is an inert metal, it is not easy to react with other chemicals. Therefore, activation is required to make the substrate active, that is, to coat a thin sub-layer of nickel on the stainless steel substrate using electro plating process with power supply (Zhao et al 2002). The composition of activation solution used in this investigation is shown in Table 4.1. The activation was performed under direct current density 2~3 A/dm^2 at room temperature for 1~3 min. Two nickel plates and the sample (workpiece) act as anodes and cathode, respectively as shown in Fig 4.6. After activation, the sample was rinsed with deionised water at room temperature and then transferred into Ni-P plating solution immediately for Ni-P-Polymers coatings.

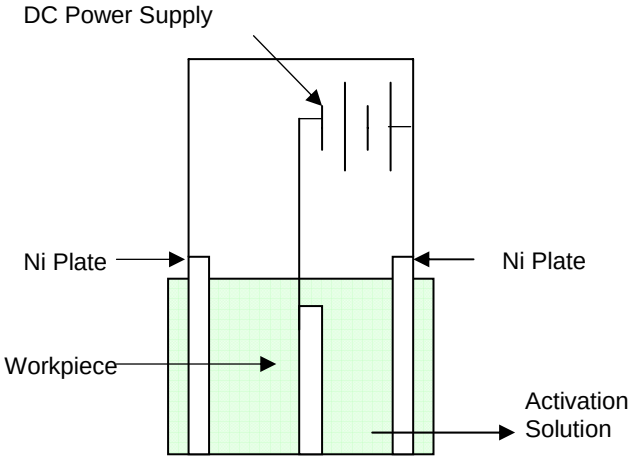

Fig 4.6 Schematic drawing of activation device

4.1.3.4 Bath Composition of Electroless Plating Ni-P-Polymers

The composition and the electroless plating Ni-P and Ni-P-Polymers conditions used in this investigation are listed in Table 4.2.

The chemical compositions of electroless plating Ni-P-Polymers solution under acidic conditions consist of nickel salts, reducing agent, complexing agent and stabilizer, buffering agent and polymer particles (PTFE, SM14 or SM20).

Nickel Salts

Nickel sulfate ($NiSO_4 \cdot 6H_2O$) is the most widely used for producing high quality Ni-P based coatings (Zhao et al 2002). $NiSO_4 \cdot 6H_2O$ with the molecular mass 262.86 g/mol was used in this research. In addition, other nickel salts are also available for producing nickel ions, such as nickel chloride, nickel sulfamate, nickel acetate and nickel hypophosphite.

Reducing Agent

The reducing agent widely used in Ni-P based plating is sodium hypophosphite ($NaH_2PO_2 \cdot H_2O$). In this research, sodium hypophosphite was also used.

Table 4.2 Bath composition and operating conditions for electroless Ni-P and Ni-P-Polymers nano-composite coating

Composition	Ni-P	Ni-P-PTFE	Ni-P-SM14 Ni-P-SM20	Ni-P-PTFE-SM14 Ni-P-PTFE-SM20
$NiSO_4.6H_2O$ (g/l)	15~35	15~35	15~35	15~35
$NaH_2PO_2.H_2O$ (g/l)	20~40	20~40	20~40	20~40
$Na_3C_6H_5O7.2H_2O$ (g/l)	10~30	10~30	10~30	10~30
$(NH2)_2CS$ (ppm=mg/l)	0~3	0~3	0~3	0~3
CH_3COONa (g/l)	15	15	15	15
PTFE (60 wt. %) (ml/l)		0~15		0~15
SM14 or SM20 (g/l)			0~2	0~2
Surfactant (g/l)		0~0.8	0~0.8	0~0.8
Temperature (°C)	80~95	80~95	80~95	80~95
pH	4.5~6.0	4.5~6.0	4.5~6.0	4.5~6.0
Stir			60rpm	60rpm

Complexing Agent

In this study, sodium citrate ($Na_3C_6H_5O_7 \cdot 2H_2O$) was used as complexing agent. There are three principal functions that complexing agents perform in the electroless plating Ni-P solutions: 1) To exert a buffering action that prevents the pH of the solution from decreasing too fast; 2) To prevent the precipitation of nickel salts, e.g., basic salts or phosphates; 3) To reduce the concentration of free nickel ions. In Ni-P plating process, Ni-P could precipitate in the bath bottom. If this happens, the surface quality of coating deteriorates resulting in rough and dark coatings. Moreover, the nickel ion concentration in the solution also decreases and the bath gets on to the verge of total decomposition. Complexing agent maintains the nickel in a stable complex until it's needed for plating (Agarwala *et al.* 2006).

Stabilizers

After a period of the electroless nickel plating under normal operating conditions, the bath solution could decompose spontaneously leading to precipitate which consists of nickel particles and nickel phosphate. Stabilizers are used to control the plating reaction by absorbing the active precipitates that trigger the subsequent random decomposition

of the entire plating bath. Thiourea and Pb are widely used as stabilizers. In this research, thiourea $(NH_2)_2CS$ was used as a stabilizer. The stabilizer concentration in the plating bath is critical. Generally, the range of stabilizer for thiourea is 1-2 mg/l (ppm). In many cases, when the concentration of thiourea is over 3 ppm, the plating reaction can be completely inhibited and the quality of coating will be poor such as voids, pits or skip plating, especially around sharp edges.

Buffering Agents

As hydrogen ion generates in the plating bath during electroless plating Ni-P process, PH value will decrease with increasing plating time. Buffers are used to minimize pH change in the plating bath and to keep the solution pH stable. In this study, sodium acetate (CH_3COONa) was used as buffering agent. However if PH decreases to the correct value, a neutralizer such as ammonia or sodium hydroxide must added to keep the PH of plating solution to the correct value.

Polymer Particles

A 60% PTFE emulsion from Aldrich with the particle size in the range 0.05 - 0.5 μm, and particles of SM14 and SM20 (0.2μm) from the Graz University of Technology, Austria were used. In order to suspend the polymer particles the FC-4 cationic surfactant ($C_{20}H_{20}F_{23}N_2O_4I$) was used. In order to get nano-composite Ni-P-Polymers coatings, PTFE emulsion was passed through a filter of the pore size 0.2 μm before the use. Total coating time was about 1 hr with the average coating thickness around 12 μm.

In order to improve adhesion force of Ni-P-Polymers coatings to substrate, a 2 μm Ni-P sublayer was coated on the stainless steel substrates to form Ni-P/Ni-P-Polymers multi-layer nanocomposite coatings.

4.1.3.5 Deposition Rate

The deposition rate is defined as the coating thickness, h (μm) divided by coating time t (hour):

$$\gamma = \frac{h}{t} \tag{4.7}$$

Generally, several parameters affect the deposition rate of Ni-P-Polymers coatings,

including the chemical compositions and concentrations of plating bath, pH, operating temperature etc.

4.1.4 Electroless Plating Ni-P-Polymer System

The elcetroless plating system at the Biological and Nanomaterials Lab, University of Dundee for preparing Ni-P-Polymers coatings is shown in Fig 4.7.

Fig. 4.7 Elcetroless plating system

The elcetroless plating system consists of the following equipment:

SUB 14 water bath (Grant, UK) was used to maintain a constant water temperature (5 ~ 99 °C) with stability ±0.2 °C. It consists of a stainless steel tank with capacity 14 litres, heaters and temperature sensors mounted underneath the tank. A water bath was used to keep a stable temperature for electroless plating.

The vacuum filtration system (Millipore Company) consists of a 300ml glass funnel, a membrane filter, a 1 litre flask and a vacuum pump. The funnel and filter are held by clamp. The filter is made of PTFE with diameter 47mm and pore size 0.2μm. In this study it was used to remove impurities and large polymer particles from plating solutions.

SevenEsay pH Meter S20 (Fisher, UK) was used for pH measurements of the electroless plating solution by immersing its probe into the test solution. The pH range is 0~14, the temperature is in the range from -5.0 ºC to 105 ºC and the accuracy is 0.01. The buffers correct can be used three point calibrations to improved accuracy.

ISO-TECH IPS-3610D power supply was used for electrocleaning and activation of substrates before electroless Ni-P plating. The direct current range is up to 10A and voltage range is up to 36V, depending on the requirement.

Barnstead EASYpure RoDi laboratory water purification system was used in this study. For coating preparation, pure water is required. Tap water contains impurities such as trace amount of ions Ca, Mg, Ni, Cu and Fe etc, which may led to plating solution decomposition or may have significant adverse effect on coating quality. It combines Easypure UV and Easypure RO into a single unit with a 6.5 litre internal reservoir. The flow rate is 800 ml/min. The pure water for bacterial adhesion assays was also produced using this system.

4.2 Doped Diamond-like Carbon Coatings

4.2.1 An Overview of the DLC Coatings

Diamond-like carbon (DLC) coatings have attracted great interest because of their properties such as excellent thermal conductivity similar to metals, low friction, extremely smooth surface, hardness, wear resistance and corrosion resistance (Grill, 1993), which make them suitable for heat exchanger applications. DLC coatings also have excellent biocompatibility, which are very suitable for the applications in medical devices and implants (Grill A, 1993; Butter RS *et al.*, 1995; Singh A *et al.*, 2003).

DLC itself does not have particularly good non-stick properties due to its high surface energy. The amorphous nature of DLC opens the possibility of introducing additional elements, such as Si, F, N, O and their combinations, into the coating whilst still maintaining the amorphous phase of the coating (Hauert 2003). A number of researchers have reported that the incorporation of silicon or nitrogen improves the properties of DLC coatings (Robertson 2002). It has been demonstrated that the incorporation of silicon in DLC coatings greatly improved the thermal stability of DLC

coatings (Gangophadhyay et al. 1997; Wu and Hon 1999). It was also reported that silicon-doped DLC coatings had a low friction coefficient (Kim et al. 1999; Lee et al. 1997). Franceschini et al. (1992) showed that the nitrogen-doped DLC coatings reduced internal stress. Grischke et al (1998) found that the doped DLC coatings with silicon and oxygen had significant influence on the surface energy of the DLC coatings. Zhao et al. (2007) showed that the surface energy of DLC coatings reduced significantly by doping F or Si into DLC coatings. Recently the incorporation of selective elements into DLC has been shown to be an effective method to alter the surface energy of the DLC coatings and to enhance the antibiofouling and other properties of DLC coatings. Si-doped DLC on stainless steel has been used as a protective coating for biocompatible implants (Okpalugo et al, 2001). Zhao et al. (2007, 2010) showed that the silicon-doped DLC coatings reduced bacterial attachment significantly compared with pure DLC coatings. Numerous studies demonstrated that the heat transfer surfaces coated with fluorine-doped DLC coatings reduced scale adhesion and subsequent scale formation, compared with DLC coatings, untreated titanium and stainless steel surfaces (Müller-Steinhagen and Zhao, 2000; Bornhorst et al, 1999; Santos et al. 2004; Zhao and Wang 2005). Hasebe et al. (2007) showed that the fluorinated DLC coatings inhibit protein adsorption and platelet activation. Ishihara et al. (2006) demonstrated that the antibacterial performance of the pure DLC coatings was improved significantly by the incorporation of fluorine with *Escherichia coli*.

However the optimal contents of the doped elements on bacterial adhesion have not been investigated yet. There are no studies that explore bacterial adhesion and removal with boron doped DLC coatings and titanium-doped DLC coatings. There are no studies that explore removal properties of bacteria and proteins from the doped DLC coatings with these elements.

In the present study, B, F, N, Si and Ti-doped DLC coatings with a range of proportion of the doping elements were produced by plasma-enhanced chemical vapour deposition (PECVD) or by magnetron sputtering in order to investigate the effect of the doped element contents on the adhesion and removal of bacteria and proteins. DLC coating manufacture is well established, however there are no standard manufacturing processes for producing doped DLC coatings and it is still at the experimental stage. The selection of the doped elements were based on our previous experience on producing non-stick

doped DLC coatings and on the ability of manufacturers to produce the coatings with consistent quality after a period of experimentation and development using a PECVD process, which is feasible for application to heat exchangers and medical devices. In this study the doped DLC coatings were prepared by Teer Coatings Ltd. UK, Commonwealth Scientific and Industrial Research Organisation (CSIRO) Australia and Tecvac Ltd. UK, respectively.

4.2.2 Si-N-Doped DLC Coatings Prepared by Teer Coatings Ltd

Si-doped DLC coatings were deposited on stainless steel substrates at Teer Coatings Ltd, using their patented unbalanced magnetron sputter ion-plating system combined with plasma-enhanced chemical vapour deposition (PECVD) as shown in Figure 4.8 (Zhao et al 2009). The apparatus consists of a vacuum chamber with three magnetrons and a radio frequency (RF) electrode. The samples are placed vertically in the substrate holder which undergoes one- or two-axis rotation depending on the complexity of the sample and is pulsed-DC biased. Stainless steel plates (76 x 26 x 1 mm) were cleaned in an ultrasonic bath containing acetone for 10 min before being placed in the coating chamber. The substrates were further ion cleaned prior to deposition. A silicon layer was first deposited by pulsed direct current (DC) magnetron sputtering using argon as the working gas, followed by a silicon carbide layer by the addition of butane (C_4H_{10}) and sputtered carbon. Finally, a Si doped DLC layer was deposited using a pulsed DC bias and an electrode with a 13.56-MHz RF generator. The substrates are biased using pulsed DC rather than conventional RF. Some of the advantages offered are improved reliability, a reduction in cost and elimination of load volume limitations associated with RF-biased systems, enabling the coating of industrially relevant dimensions and geometries. The equipment also uses a low-power ancillary RF electrode to assist the dissociation of the butane precursor, thereby allowing independent control of the substrate bias voltage and substrate ion current. It is possible to control and optimise the properties of the coatings with this system. Both carbon target and butane are used as the carbon sources during the deposition. The Si content in the DLC coatings was altered by changing the sputtering current on the Si target. Three Si-doped DLC coatings with Si contents of 1%, 2% and 3.8% were prepared. The thickness of Si-doped diamond-like carbon coatings was about 1 μm.

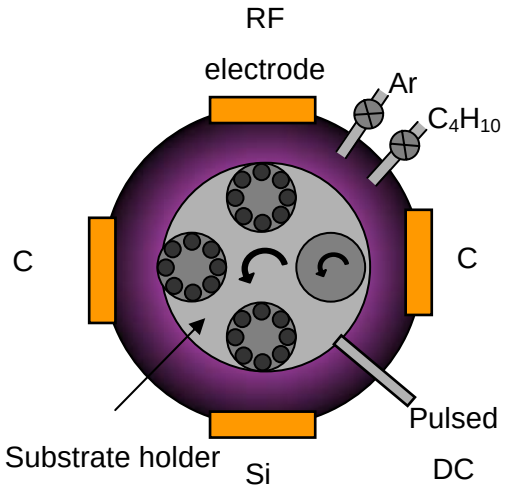

Fig 4.8 Schematic diagram of the apparatus used to deposit Si-doped DLC coatings showing the two carbon targets (C), Si target (Si), RF electrode, the sample holder, pulsed-DC bias and two flow control valves for argon (Ar) and butane (C_4H_{10}) gases.

In order to investigate the effect of DLC coatings doped with both silicon and nitrogen on bacterial adhesion and removal, the Si-N-doped DLC coatings at first time were deposited on stainless steel plates (76 x26 x 1 mm) by radio frequency (13.56 MHz) PECVD at Teer Coatings Ltd. The deposition system consisted of a plasma reactor equipped with rotary and turbo molecular pumps with controlled gas supply and pumping. Acetylene (C_2H_2), tetramethylsilane ($Si(CH_3)_4$), argon (Ar) and nitrogen (N), were used as process gases. The plates were cleaned in an ultrasonic bath containing acetone for 10 min. before being placed in the coating chamber. The substrates were further ion cleaned prior to deposition in argon plasma for 5 min. The Si-N-doped DLC coatings were deposited using a mixture of C_2H_2 , $Si(CH_3)_4$ and N_2 as precursors. Four Si-N-doped DLC coatings with 0.5%Si-2.2%N; 3.7%Si-2.1%N; 9%Si-2.3%N and 20%Si-2%N were prepared. The coatings compositions are given by atomic percentages. Table 4.3 lists the name and chemistry of the Si-N-doped DLC coatings produced by Teer Coatings Ltd.

Table 4.3 Si-N-doped DLC coatings by Teer Coatings Ltd.

Name	Chemistry
DLC1	1%Si-DLC
DLC2	2%Si-DLC
DLC3	3.8%Si-DLC
DLC4	0.5%Si-2.2N%-DLC
DLC5	3.7%Si-2.1N%-DLC
DLC6	9.0%Si-2.3N%-DLC
DLC7	20%Si-2.0N%-DLC

4.2.3 F-Doped DLC Coatings Prepared by CSIRO

In order to investigate the effect of fluorine (F) contents in DLC coatings on bacterial adhesion and removal, the F-doped DLC coatings with a wide range of F contents were prepared on stainless steel plates by CSIRO Materials Science and Engineering, Australia (Su et al 2010).

The diamond like carbon (DLC) and fluorinated DLC (F-DLC) coatings were deposited onto stainless steel 316L plates by radio frequency plasma-enhanced chemical vapour deposition (rf-PECVD). The deposition system consisted of a plasma reactor equipped with rotary and turbo molecular pumps with controlled gas supply and pumping system. A base pressure of $1x10^{-3}$ Pa was attained in the chamber prior to deposition. Acetylene (C_2H_2), carbon tetrafluoride (CF_4) and argon (Ar) were used as process gases. The gases were introduced into the system through a gas distributor using mass flow controllers. The total pressure could be set independently of the gas flow by adjusting a throttle valve. Prior to deposition, the substrates were sputter-cleaned in-situ for 5 mins in argon plasma operated at 3.3 Pa with the argon flow rate set at 10 sccm (standard cubic centimeters per minute) at 200 W power. A thin layer of hydrogenated amorphous silicon carbide (a-SiC:H) was first deposited onto the substrate using tetramethylsilane (TMS or $Si(CH_3)_4$)) as precursor to improve the adhesion. The interlayer deposition was performed at 3.3 Pa with the TMS flow rate set at 17 sccm at 200W power for 2 mins (approximately 50 nm thickness). The F-DLC coatings were deposited using a mixture of C_2H_2 and CF_4 as precursors. The flow rate of C_2H_2 was kept constant at 60 sccm and

the flow rate of CF_4 was varied between 0 and 90 sccm in order to obtain different fluorine contents in the films. Three F-doped DLC coatings with F contents of 6.5% , 20.7% and 39.2% were prepared. The films compositions were given by atomic percentages. Table 4.4 lists the name and chemistry of the F-doped DLC coatings produced by CSIRO.

Table 4.4 F -doped DLC coatings by CSIRO.

Name	Chemistry
DLC 8	DLC
DLC 9	6.5F%F-DLC
DLC 10	20.7%F-DLC
DLC 11	39.2%F-DLC

4.2.4 B and Ti-Doped DLC Coatings Prepared by Tecvac Ltd

The B (boron) doped DLC coatings were prepared by Tecvac Ltd, UK, using their plasma-enhanced chemical vapour deposition (PECVD) system. The Ti (titanium) doped DLC coatings were also prepared by a magnetron sputter system consisting of a Ti target combined with plasma-enhanced chemical vapour deposition (PECVD). These coatings were mainly used to investigate the protein removal from surgical steels, supported by UK Department of Health, in addition to bacterial adhesion and removal. There are serious concerns about the levels of residual protein contamination on surgical and dental instruments after they have been through the standard cleaning processes, and the risk of disease transmission (e.g. variant Creutzfeldt-Jakob disease or vCJD) due to poor cleaning.

Table 4.5 lists the name and chemistry of the B and Ti-doped DLC coatings produced by Tecvac Ltd.

Table 4.5 B and Ti-doped DLC coatings by Tecvac Ltd

Name	Chemistry
DLC 12	DLC
DLC 13	4.9% B-DLC
DLC 14	7.6%B-DLC
DLC 15	9.5%B-DLC
DLC 16	1.3%Ti-DLC
DLC 17	1.8%Ti-DLC
DLC 18	3.2%Ti-DLC

4.3 SiO_x-Like Coatings

4.3.1 An Overview of SiO_x-Like Coatings

Nanocomposite siloxane films containing high concentrations of SiO_x have been employed in various ways in the thin film industry due to their good abrasion and corrosion resistance, electrical insulation and high thermal stability (Akesso et al, 2009). Rosmaninho et al (2006) demonstrated that silicon dioxide (SiO_2) coatings have potential to reduce milk protein adhesion. However there are no studies that explore the potential use of SiO_2 or SiO_x-like coatings in controlling the initial bacterial attachment and removal. Plasma enhanced chemical vapour deposition, either at low or atmospheric pressure is a versatile method for depositing such films on a wide range of substrates and at low temperatures. Unlike SiO_2 coatings, the surface chemistry and physical properties of SiO_x-like coatings such as surface energy and topology can be varied in a wide range, depending on the method of deposition and process parameters: these properties, especially surface energy are well known to influence the adhesion of bacteria (Zhao et al, 2007). Teer Coatings Ltd. and University of Dundee first investigated the potential for such coatings in the control of bacterial adhesion and removal (Akesso et al, 2009; Navabpour et al, 2010).

SiO_x-like coatings are deposited from a mixture of oxygen and hexamethyldisiloxane (HMDSO or $O[Si(CH_3)_3]_2$). At low HMDSO to oxygen ratios, the coatings are more

silicon-oxide (SiO_2) like with higher surface energy and hardness but with lower potential for anti-biofouling. At high HMDSO to oxygen ratios, however, the coatings are more SiO_x-like with high carbon content and low surface energy and good anti-biofouling properties. Although better for their anti-biofouling properties, the latter suffer from poor adhesion to the substrate and have inadequate mechanical properties to render them useful for many industrial applications. Teer Coatings Ltd. has developed a hybrid method that can be used for the deposition of coating which involves simultaneous sputtering from a target and plasma polymerisation of HMDSO/oxygen mixture (Navabpour et al, 2010). Using this hybrid method, a range of SiO_x-like coatings with improved mechanical properties while maintaining the anti-biofouling properties are produced. In this work, the potential of such hybrid coatings using silicon as the sputtered material has been investigated. These SiO_x-like coatings with improved performance have potential for use as coatings in the control of biofouling in applications such as heat exchangers.

4.3.2 SiO_x-Like Coatings Prepared by Teer Coatings Ltd.

HMDSO (≥ 98 %) was supplied by Sigma-Aldrich, acetone (99.5 %) by Hammond Chemicals Ltd. Oxygen and argon (both 99.999%) were supplied by BOC Edwards.

First group of SiO_x-like coatings (see Table 4.6, S1 –S7, S7-1 – S7-3) were deposited using a Teer Coatings Ltd PECVD deposition system (Akesso et al, 2009). The steel substrates were ion cleaned in the chamber in order to prepare them for the coating deposition. The chamber was evacuated to 5.5 x 10^{-5} mbar prior to commencing coating deposition. The reactive gas, at a pressure of 1.8 x 10^{-1} mbar, comprised O_2 and HMDSO. Plasma was induced by application of 200 W of power to electrode A and 125 W to electrode B. The duration of plasma deposition was varied between 20 and 45 min. At the end of the coating process, the chamber was evacuated to a pressure of 5 x 10^{-5} mbar before being returned to atmospheric pressure with ambient air. Table 4.6 shows the reactive gas composition and times for the coatings prepared. Samples S1-S7 have the same ion cleaning times (5 min), but different monomer ratios and S7 to S7-1 – S7-3 have the same monomer ratios, but different ion cleaning times (5, 10, 20 and 30 min, respectively).

Table 4.6 Parameters used for the deposition of SiO_x-like coatings

Coatings	Si current (A)	O_2 (sccm or ml/min)	HMDSO (sccm or ml/min)	Deposition time (min)	Ion cleaning time (min)
S1	-	90	8	45	5
S2	-	65	8	30	5
S3	-	65	14	30	5
S4	-	65	23	30	5
S5	-	65	29	30	5
S6	-	65	41	20	5
S7	-	65	48	20	5
S7-1	-	65	48	20	10
S7-2	-	65	48	20	20
S7-3	-	65	48	20	30
TCL40bt	-	50	36	20	30
TCL40C1	-	19	16	100	30
TCL40C2	3	19	16	40	30
TCL40C3	3	23	12	50	30
TCL40C4	3	27	8	100	30

Second group of SiOx-like coatings (see Table 4.6, TCL40bt, TCL40C1-C4) were deposited using a Teer Coatings Ltd hybrid unbalanced magnetron sputter ion-plating PECVD deposition system (Navabpour et al, 2010).

CHAPTER 5

CHARACTERISATION OF COATINGS

5.1 Morphology of Coatings

5.1.1 Atomic Force Microscopy

Atomic Force Microscopy (AFM) is a very high-resolution type of scanning probe microscope, which provides measurements of surface roughness, grain size and grain size distribution. A Dimension 3000 Atomic Force Microscope (Nanoscope III) in the Electronic Engineering and Physics Division, University of Dundee was used to obtain topographic and three-dimensional imaging of surfaces with a lateral resolution of 1~2 nm and a vertical resolution of 0.01 nm. The equipment was operated in contact mode in air.

Fig. 5.1 shows the typical AFM images of Si-doped DLC films with Si contents of 1%, 2% and 3.8%, respectively (Zhao et al, 2007b). These Si-doped coatings were prepared by Teer Coatings Ltd and were used for bacterial adhesion and removal in this study. The surface roughness for the different samples was measured over 2μm × 2μm area by the AFM. Fig 5.1 and Table 5.1 indicate that the surface roughness increases slightly with increasing Si content in the DLC films (Zhao et al, 2007b).

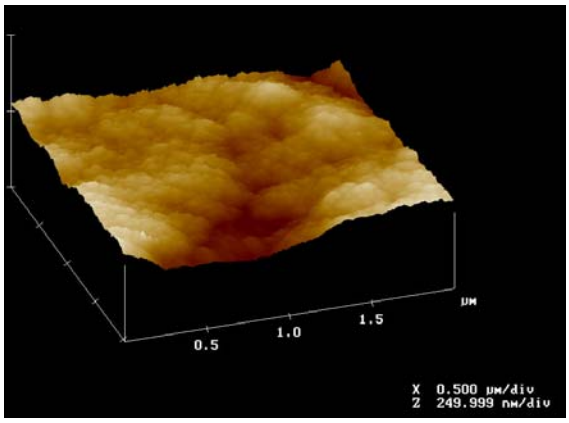

(a)

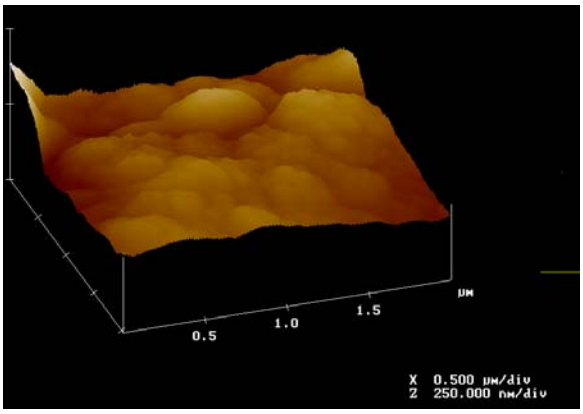

(b)

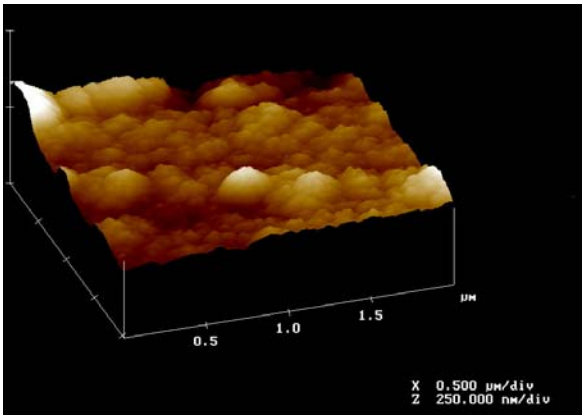

(c)

Fig. 5.1 AFM image of Si-doped DLC (a) Si:1%; (b)Si:2%; (c) Si:3.8%

Table 5.1 Si content, the ratio of sp^2/sp^3 and roughness *Ra*

Materials	sp^2 content	*Ra* by AFM (nm)
Si-doped DLC with 1% Si	67.1%	16.0
Si-doped DLC with 2% Si	34.2%	17.7
Si-doped DLC with 3.8% Si	25.0%	27.8

The AFM images indicated that for most doped DLC coatings and SOx-like coatings used in this study, their surface roughness values (Ra) were in the range of 15(±3) ~ 50(±7) nm, while the Ra for Ni-P-polymers coatings were about 170(±8) ~200 (±11) nm. The AFM images indicated that the Ni-P coating had a very similar *Ra* with stainless steel, about 50(±7) nm. The Ni-P-polymers coatings become rougher due to the incorporation of PTFE and biocide polymer nano-particles with diameter 50~200 nm.

5.1.2 Scanning Electron Microscope

The scanning electron microscope (SEM) is a type of electron microscope capable of producing high resolution images of a sample surface. As the primary electrons strike the surface they are inelastically scattered by atoms in the sample. Through these scattering events, the primary electron beam effectively spreads and fills a teardrop-shaped volume, known as the interaction volume, extending from less than 100 nm to around 5 μm into the surface. Interactions in this region lead to the subsequent emission of electrons which are then detected to produce an image. SEM images have a characteristic three dimensional appearances and are useful for judging the surface structure of the sample (O'Connor DJ *et al*.1992).

In this study, the Philips XL 30 Scanning Electron Microscope (SEM) in the Life Science College, University of Dundee was used for observing the surface morphology and the particles distribution in the Ni-P-polymers coating. Samples were examined in an atmosphere of up to 10^{-2} Pa of nitrogen carbon dioxide gas. Resolution at 30KV is 3.5 nm. The magnification is in the range from 20X to approximately 30,000X with high resolution of 50 to 100 nm. Figure 5.2 shows a typical morphology of Ni-P-

Polymers nanocomposite coating. Clearly, PTFE polymer nano-particles (black dots) were uniformly distributed into the coatings. The particles sizes were in the range of 50 nm~200 nm.

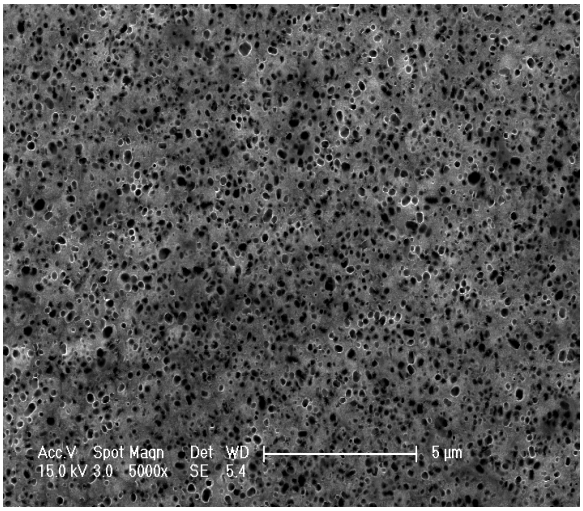

Fig. 5.2 Typical SEM image of Ni-P-Polymers nanocomposite coating

5.2 Composition of Coatings

5.2.1 Energy-dispersive X-ray spectroscopy

SEM is also capable of performing analyses of selected point locations on the samples, which are especially useful in quantitatively or semi-quantitatively determining chemical compositions of the coatings using energy-dispersive X-ray spectroscopy (EDX). In this study, the EDX in the Life Science College, University of Dundee was used for the measurement of element content in the Ni-P-Polymers nanocomposite coatings. In general, if the thickness of coatings is over 1 μm and the substrates are conductive, the EDX method is acceptable.

The chemical compositions of typical Ni-P based coatings (Ni-P, Ni-P-PTFE and Ni-P-PTFE-biocide polymer) are given in Table 5.2. The PTFE content was calculated based on F element content in the coating.

Table 5.2 Chemical compositions and content (wt. %) of coatings by EDX

Coatings	C	O	F	P	Fe	Ni	PTPE content (wt. %)
Ni-P	3.6	1.9	-	10.7	0.5	83.4	-
Ni-P-PTFE	4.2	10.0	3.9	9.0	1.4	71.5	5.1
Ni-P-PTFE-SM14	6.8	10.2	5.5	9.9	1.0	66.6	7.2
Ni-P- PTFE-SM20	11.3	9.7	8.0	9.0	0.9	61.1	10.5

5.2.2 X-ray Photoelectron Spectroscopy

X-ray Photoelectron Spectroscopy (XPS) is used to determine quantitive atomic composition and chemistry. It is a surface analysis technique with a sampling volume that extends from the surface to a depth of approximately 50-70 angstroms. Alternatively, XPS can be utilized for sputter depth profiling to characterize thin films by quantifying matrix-level elements as a function of depth. XPS is an elemental analysis technique that is unique in providing chemical state information of the detected elements. The process works by irradiating a sample with monochromatic x-rays, resulting in the emission of photoelectrons whose energies are characteristic of the elements within the sampling volume. In this study the percentage of doped elements in the DLC coatings was determined with XPS using a Speces 150 SAGE instrument operated with MgK_{α} X-ray source with anode voltage 10kV and emission current 10 mA (Su et al, 2010). The results are shown in Tables 4.3, 4.4 and 4.5 respectively. XPS measurements were also performed on the SiO_x-like coatings in Table 5.6 with a VG Scientific Microlab 310F instrument using Mg K_{α} radiation at 1253.6 eV with anode voltage × emission current = 12.5 kV × 16 mA = 200W power (Akesso et al, 2009; Navabpour et al, 2010). The results are given in Table 5.3

5.3 Coating Thickness

In this study a Digital Micrometer (Brown and Sharpe TESA, Swiss) was used for coating thickness measurement of Ni-P-polymers coatings with accuracy ± 1 μm. The

coating thickness of these coatings was in the range of 10 – 15 μm, depending on deposition time and bath composition.

The coating thickness of doped DLC coatings and SiO_x-like coatings was measured using a Cambridge Stereoscan 200 SEM. Coated samples were fractured and coated with a thin layer of gold in order to obtain conductive samples. The cross-section of the resulting samples was analysed using SEM. Thickness was measured in five different places and mean and standard deviation were obtained. For the doped DLC coatings, the average coating thickness was about 1 μm. The coating thickness of the SiO_x-like coatings is given in Table 5.3 (Akesso et al, 2009; Navabpour et al, 2010).

Table 5.3 Atomic composition and thickness of SiO_x-like coatings

Coatings	C (Atom %)	O (Atom %)	Si (Atom %)	Film Thickness (nm)
S1	1 ±0	64 ±6	35 ±4	400 ±20
S2	0 ±0	60 ±5	40 ±4	400 ±20
S3	4 ±1	57 ±5	39 ±4	920 ±80
S4	9 ±1	52 ±5	39 ±4	1000 ±60
S5	10 ±1	50 ±4	40 ±4	1120 ±80
S6	14 ±2	51 ±4	35 ±3	840 ±40
S7	16 ±2	41 ±4	43 ±4	1000 ±50
S7-1	17 ±2	44 ±4	39 ±4	1240 ±40
S7-2	16 ±2	46 ±5	38 ±4	970 ±30
S7-3	25 ±3	39 ±4	36 ±4	1030 ±30
TCL40bt	27 ±2	37 ±4	36 ±3	730 ±100
TCL40C1	32 ±3	32 ±3	36 ±4	1030 ±100
TCL40C2	31 ±3	37 ±3	32 ±3	1070 ±80
TCL40C3	22 ±1	43 ±4	35 ±3	1060 ±80
TCL40C4	2.0 ±0.5	58 ±5	40 ±3	890 ±40

5.4 Contact Angle and Surface Energy

5.4.1 Contact Angle Measurement

Surface energy is probably the most important physico-chemical property of a solid surface. The environment of particles (ion, atom, or molecule) on the surface of a solid differs from that in its interior. In the interior, a particle is evenly acted on by forces exerted by the particles around it. On the surface, there is a tendency for the particle on the surface to be pulled into the main body where an unsaturated force field exists, in order to reduce the surface area to a minimum, so that surface free energy is produced, as shown in Fig.5.3 (Liu, YL 2005). The stronger the interaction between particles, the higher the surface energy. For metals, the bonding is strong, so usually metal surface possesses high surface energy (Liu, YL 2005).

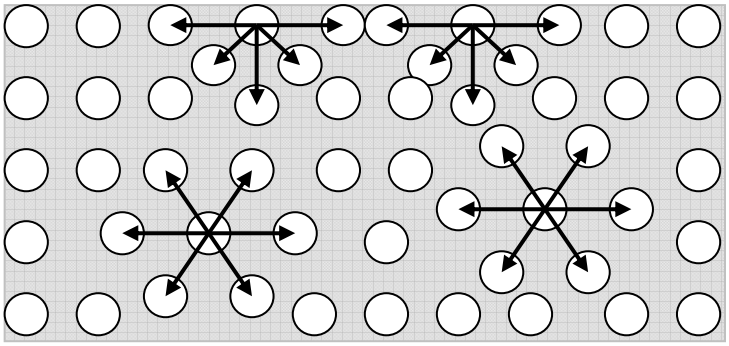

Fig. 5.3 Force between atoms or molecules inside and at the phase boundary

The surface energy (γ_s) of a solid is defined as the change of the total surface energy (G) per surface area (A) at constant temperature (*T*), pressure (*P*) and moles (*n*) (Chaudhury MK, 1996; Good RJ, 1992):

$$\gamma_S = (dG/dA)_{T,P,n} \qquad (5.1)$$

One way to quantify surface energy of a solid is to measure the contact angle of a drop of liquid placed on the surface of an object. The contact angle, θ, is the angle formed by a liquid drop at the three phase boundary where a liquid, air and solid intersect, as shown in Figure 5.4. The contact angle is a quantitative measure of the wetting of a

solid by a liquid. If a liquid drop rests on a solid surface, the drop is in equilibrium by balancing three forces, namely, the interfacial tensions between solid and liquid, γ_{SL}; between liquid and vapor, γ_{LV} (or γ_L); and between solid and vapor, γ_{SV} (or γ_S).

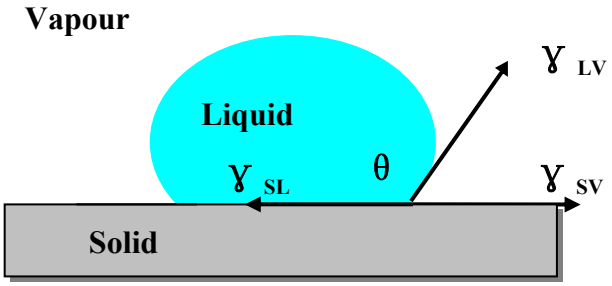

Figure 5.4 Contact angle on solid surface

Low values of θ indicate a strong liquid-solid interaction such that the liquid tends to spread on the solid, while high θ values indicate weak interaction. If the angle θ is less than 90°, then the liquid is said to wet the solid; a zero contact angle represents complete wetting; if the θ is greater than 90°, then it is said to be non-wetting.

In this study the contact angles on the coatings were obtained using a sessile drop method with a Dataphysics OCA-20 contact angle analyser (Figure 5.5) at the Biological and Nanomaterials Lab, University of Dundee. This instrument consists of a CCD video camera with a resolution of 768×576 pixel and up to 50 images per second, multiple dosing/micro-syringe units and a temperature controlled environmental chamber. The drop image was processed by an image analysis system, which calculated both the left- and right contact angles from the shape of the drop with an accuracy of ± 0.1°. Three test liquids were used as a probe for surface free energy calculations: distilled water, diiodomethane (Sigma) and ethylene glycol (Sigma). The data for surface tension components of the test liquids are given in Table 5.4 (van Oss et al 1988; Good RJ 1992). All measurements were made at 25 °C. The samples were ultrasonically cleaned in acetone, ethanol and deionized water in sequence for 5 minutes before contact angle measurement.

The contact angle of bacterial cells was measured on the lawns of bacteria deposited on membrane filters with a pore diameter of 0.45μm. Prior to contact angle measurement,

the bacterial lawns were dried in the air to a certain state, indicated by stable water contact angles. Usually this state of drying of a microbial lawn lasts 30-60 minutes and indicated that only bound water is present on the surface (Liu and Zhao, 2005).

Figure 5.5 Dataphysics OCA-20 Contact Angle Analyzer

Table 5.4 Test liquids and their surface tension components

Surface tension data (mJ/m²)	γ_L	γ_L^{LW}	γ_L^{AB}	γ_L^+	γ_L^-
Water (W), H_2O	72.8	21.8	51.0	25.5	25.5
Diiodomethane (D), CH_2I_2	50.8	50.8	0	0	0
Ethylene glycol (E), $C_2H_6O_2$	48.0	29.0	19.0	1.92	47.0

5.4.2 Calculation of Surface Energy

The theory of the contact angle of pure liquids on a solid was developed over 200 years ago in terms of the Young equation (Young T, 1805):

$$\gamma_{LV}\cos\theta = \gamma_{SV} - \gamma_{SL} \tag{5.2}$$

If the spreading pressure is neglected, the Young equation is modified as (Girifalco LA *et al.*, 1957):

$$\gamma_L \cos\theta = \gamma_S - \gamma_{SL} \quad (5.3)$$

Where γ_L is the experimentally determined surface tension of the liquid, θ is the contact angle, γ_S is the surface energy of the solid and γ_{SL} is the solid/liquid interfacial energy. γ_L (Table 5.4) and θ are usually known. In order to obtain the solid surface energy γ_S an estimate of γ_{SL} has to be obtained.

In 1962 Fowkes pioneered a surface energy component approach (Fowkes FM, 1962; Fowkes FM, 1964). He divided the total surface energy in 2 parts: dispersive part and non-dispersive (or polar) part. The first part results from the molecular interaction due to London forces and the second part is due to all the non-London forces:

$$\gamma_i = \gamma_i^d + \gamma_i^p \quad (5.4)$$

He proposed the following relation for solid-liquid interaction by only dispersion force interaction:

$$\gamma_{SL} = \gamma_S + \gamma_L - 2\sqrt{\gamma_S^d \cdot \gamma_L^d} \quad (5.5)$$

Combining with Young equation (5.3), it follows that

$$\gamma_L(1+\cos\theta) = 2\sqrt{\gamma_S^d \gamma_L^d} \quad (5.6)$$

Since only dispersive interactions are taken into account, the application of the method is quite restricted. Later the improved approaches (e.g. Owens-Wendt, Wu, van Oss approach and equation of state) for the estimation of γ_{SL} are widely used (Zhao et al 2004c).

5.4.2.1 Owens and Wendt Geometric Mean Approach

In 1969, Owens and Wendt proposed the division of the total surface energy of a solid or liquid in two components-dispersion force component and hydrogen bonding

component ($\gamma_L = \gamma_L^d + \gamma_L^p$ and $\gamma_S = \gamma_S^d + \gamma_S^p$). The interaction energy of the non-dispersive forces at the interface was quantified and included as geometric mean of the non-dispersive components of solid and liquid. They extended the Fowkes equation and used geometric mean to combine the dispersion force and hydrogen bonding components:

$$\gamma_{SL} = \gamma_S + \gamma_L - 2\sqrt{\gamma_S^d \cdot \gamma_L^d} - 2\sqrt{\gamma_S^p \cdot \gamma_L^p} \tag{5.7}$$

Combining the Young equation (5.3), the following expression is obtained:

$$\gamma_L(1+\cos\theta) = 2\sqrt{\gamma_S^d \gamma_L^d} + 2\sqrt{\gamma_S^p \gamma_L^p} \tag{5.8}$$

To obtain γ_S^d and γ_S^p of a solid, the contact angle of at least two liquids with known surface tension components ($\gamma_L, \gamma_L^d, \gamma_L^p$) on the solid must be determined.

5.4.2.2 Wu Harmonic Mean Approach

Wu (1971) proposed the harmonic mean approach to combine the polar and dispersion components of the solid and liquid surface energies in 1971:

$$\gamma_{SL} = \gamma_S + \gamma_L - \frac{4\gamma_S^d \gamma_L^d}{\gamma_S^d + \gamma_L^d} - \frac{4\gamma_S^p \gamma_L^p}{\gamma_S^p + \gamma_L^p} \tag{5.9}$$

Combining the equation (5.9) with the Eq. (5.3), the following equation is obtained:

$$\gamma_L(1+\cos\theta) = \frac{4\gamma_S^d \gamma_L^d}{\gamma_S^d + \gamma_L^d} + \frac{4\gamma_S^p \gamma_L^p}{\gamma_S^p + \gamma_L^p} \tag{5.10}$$

Similar to the Geometric mean approach, the contact angle data with two liquids with known surface tension components ($\gamma_L, \gamma_L^d, \gamma_L^p$) are required in order to obtain the γ_S^d and γ_S^p components of the solid. At least one of the test liquids must have a polar part.

5.4.2.3 van Oss Acid-Base Approach

van Oss *et al*. proposed the division of the total surface energy of a solid into two components, Lifshitz-van der Waals apolar component γ_i^{LW} (corresponding to γ_i^d) and Lewis acid/base polar component γ_i^{AB} (corresponding to γ_i^p) in 1986 (van Oss CJ *et al*., 1986):

$$\gamma_i = \gamma_i^{LW} + \gamma_i^{AB} \tag{5.11}$$

The acid-base polar component γ_i^{AB} can be further subdivided by using specific terms for an electron donor (γ_i^-) and an electron acceptor (γ_i^+) subcomponent:

$$\gamma_i^{AB} = 2\sqrt{\gamma_i^+ \gamma_i^-} \tag{5.12}$$

The solid/liquid interfacial energy is then given by:

$$\gamma_{SL} = \gamma_S + \gamma_L - 2(\sqrt{\gamma_S^{LW} \cdot \gamma_L^{LW}} + \sqrt{\gamma_S^+ \cdot \gamma_L^-} + \sqrt{\gamma_S^- \cdot \gamma_L^+}) \tag{5.13}$$

Combining this with Eq. (5.3), a relation between the measured contact angle and the solid and liquid surface energy terms can be obtained:

$$\gamma_L \cdot (1 + \cos\theta) = 2(\sqrt{\gamma_S^{LW} \cdot \gamma_L^{LW}} + \sqrt{\gamma_S^+ \cdot \gamma_L^-} + \sqrt{\gamma_S^- \cdot \gamma_L^+}) \tag{5.14}$$

In order to determine the surface free energy components (γ_S^{LW}) and parameters γ_S^+ and γ_S^- of a solid, the contact angle of at least three liquids with known surface tension components ($\gamma_L^{LW}, \gamma_L^+, \gamma_L^-$), two of which must be polar, has to be determined.

5.4.2.4 Equation of State Approach

Equation of state approach is based on one principle, i.e. the solid-liquid interfacial tension is a unique function of liquid and solid surface tensions, $\gamma_{SL} = f(\gamma_{L,}\gamma_S)$.

Neumann *et al*. developed the first equation of state for calculation of solid/liquid interfacial energy (Neumann AW *et al*., 1974):

$$\gamma_{SL} = \frac{\left(\sqrt{\gamma_S} - \sqrt{\gamma_L}\right)^2}{1 - 0.015\sqrt{\gamma_S \gamma_L}} \tag{5.15}$$

Combining this to Eq. (5.3), the following equation is obtained:

$$\cos\theta = \frac{\left(0.015\gamma_S - 2.00\right)\sqrt{\gamma_S + \gamma_L} + \gamma_L}{\gamma_L\left(0.015\sqrt{\gamma_S \gamma_L} - 1\right)} \tag{5.16}$$

Li and Neumann gave another form of equation of state for solid-liquid interfacial surface energy in 1990 (Li D *et al*., 1990):

$$\gamma_{SL} = \gamma_S + \gamma_L - 2\sqrt{\gamma_S \cdot \gamma_L} \cdot e^{-\beta(\gamma_L - \gamma_S)^2} \tag{5.17}$$

Combining this with Eq. (5.3), the following equation is obtained

$$\gamma_L \cdot (\cos\theta + 1) = 2\sqrt{\gamma_S \cdot \gamma_L} \cdot e^{-\beta(\gamma_L - \gamma_S)^2} \tag{5.18}$$

where β =0.0001247 $(m/mN)^2$ was obtained by fitting equation (5.18) to accurate contact angle data obtained on polymeric solids.

Kwok and Neumann (1990; 2000) modified the equation (5.17) and derived an equation of state for solid-liquid interfacial surface energy:

$$\gamma_{SL} = \gamma_S + \gamma_L - 2\sqrt{\gamma_S \cdot \gamma_L} \cdot [1 - \beta_1(\gamma_S - \gamma_L)^2] \tag{5.19}$$

In conjunction with the Young equation (5.3), the current form of the equation of state is as follows:

$$\gamma_L \cdot (1+\cos\theta) = 2\sqrt{\gamma_S \cdot \gamma_L} \cdot [1-\beta_1(\gamma_S-\gamma_L)^2] \qquad (5.20)$$

where β_1 =0.0001057 $(m/mN)^2$. Equation (5.20) enables the evaluation of the surface energy of a solid γ_S from a single measurement of contact angle of a liquid with a known surface tension γ_L, but neither the dispersion nor the polar component can be evaluated.

5.5 Surface Energy of Coatings

The total surface energy values of the coatings obtained from the different methods are not similar and are statistically significant different (p-value <0.05) (Zhao et al, 2005). Currently van Oss acid-base approach is recommended to determine the surface energy and its components as it contains three independent surface energy components which are used in the extended DLVO theory (Sharma et al, 2002). In this study, the contact angles of the coatings were measured with a Dataphysics OCA-20 contact angle analyser and calculated the surface energy components of the coatings using van Oss acid-base approach.

Tables 5.5-5.9 show the data of contact angle and surface energy components of the coatings. Table 5.5 indicates that for the Ni-P-polymers coatings, the water contact angle was generally larger than that of stainless steel. The γ^{TOT} values for Ni-P-biocide polymers were in the range of 28~30 mJ/m^2 and the γ^{TOT} values for Ni-P-PTFE or Ni-P-PTFE-biocide polymers were in the range of 23~25 mJ/m^2.

Table 5.6 indicates that for Si-doped DLC coatings, the water contact angle decreased with increasing Si content. The γ^- values of the Si-doped DLC coatings increased significantly with increasing Si content while the γ^{TOT} values were almost similar. For Si-N-doped DLC coatings, the water contact angle increased with increasing Si content, while the γ^{TOT} values decreased from 52mJ/m^2 to 41 mJ/m^2.

Table 5.7 shows that the γ^{TOT} values of F-doped DLC coatings decreased with increasing F content.

Table 5.5 Contact angle and surface energy components of Ni-P-polymers coatings

Coatings	Contact Angle θ [°]			Surface Energy Components [mJ/m^2]				
	θ^W	θ^{Di}	θ^{EG}	γ^{LW}	γ^+	γ^-	γ^{AB}	γ^{TOT}
Stainless steel	77.9±1.1	35.4±0.3	47.5±0.8	41.84	0.08	6.00	1.39	43.23
Ni-P	81.3±0.7	51.3±0.5	58.1±0.6	33.55	0.07	7.21	1.42	34.97
Ni-P-SM14	78.3±0.7	65.4±0.5	63.8±0.3	25.47	0.12	13.41	2.54	28.01
Ni-P-SM20	84.5±0.5	59.7±0.3	65.5±0.6	28.75	0.03	7.61	0.96	29.71
Ni-P-PTFE	91.8±1.6	69.6±2.0	88.1±0.7	23.00	0.00	11.36	0.00	23.00
Ni-P-PTFE-SM14	88.8±0.9	69.5±0.7	74.2±1.0	23.15	0.11	7.85	1.86	25.01
Ni-P-PTFE-SM20	90.1±1.1	69.2±0.9	73.3±0.7	23.32	0.04	6.39	1.01	24.33

Table 5.6 Contact angle and surface energy components of Si-N-doped DLC coatings

Coatings		Contact Angle θ [°]			Surface Energy Components [mJ/m^2]				
Name	Chemistry	θ^W	θ^{Di}	θ^{EG}	γ^{LW}	γ^+	γ^-	γ^{AB}	γ^{TOT}
DLC1	1%Si-DLC	72.2±1.2	19.4±0.8	45.3±0.3	46.78	5.21	1.52	5.63	52.41
DLC2	2%Si-DLC	69.4±0.4	16.9±0.4	34.8±0.6	47.43	0.96	8.05	5.56	52.99
DLC3	3.8%Si-DLC	61.4±0.7	16.3±0.4	30.6±0.7	47.58	0.57	16.11	6.06	53.64
DLC4	0.5%Si-2.2N%-DLC	69.1±0.7	25.7±0.7	45.8±0.3	44.77	2.10	6.68	7.50	52.27
DLC5	3.7%Si-2.1N%-DLC	69.2±0.3	27.3±0.2	45.2±0.9	44.18	1.90	7.21	7.41	51.59
DLC6	9.0%Si-2.3N%-DLC	73.6±0.2	31.6±0.1	46.0±0.4	42.47	1.02	6.90	5.31	47.78
DLC7	20%Si-2.0N%-DLC	80.2±0.8	39.0±0.5	50.5±0.8	39.12	0.12	7.20	1.86	41.00

Table 5.7 Contact angle and surface energy components of F doped DLC coatings

Coatings		Contact Angle θ [°]			Surface Energy Components [mJ/m^2]				
Name	Chemistry	θ^W	θ^{Di}	θ^{EG}	γ^{LW}	γ^+	γ^-	γ^{AB}	γ^{TOT}
DLC 8	DLC	70.0±0.6	21.4±0.5	47.0±0.5	46.35	0.00	11.08	0.00	46.35
DLC 9	6.5F%F-DLC	69.9±0.1	26.5±0.3	44.8±0.7	45.52	0.00	11.86	0.00	45.52
DLC 10	20.7%F-DLC	73.6±0.4	36.7±0.3	47.6±0.9	41.23	0.04	9.73	1.25	42.48
DLC 11	39.2%F-DLC	81.3±0.3	59.6±0.3	57.3±0.4	28.81	0.40	7.33	3.42	32.23

Table 5.8 shows that the γ^{TOT} values for these doped DLC coatings were changed in the range of 29~46 mJ/m^2, depending on the doped elements and their contents in the DLC coatings. For B-doped DLC coatings, with increasing B content the water contact angle increased, while the γ^{TOT} values decreased. For Ti-doped DLC coatings, with increasing Ti content the water contact angle decreased, while the γ^- values increased.

Table 5.8 Contact angle and surface energy components of B and Ti-doped DLC coatings

Coatings		**Contact Angle θ [°]**			**Surface Energy Components [mJ/m^2]**				
Name	**Chemistry**	θ^W	θ^{Di}	θ^{EG}	γ^{LW}	γ^+	γ^-	γ^{AB}	γ^{TOT}
DLC 12	DLC	77.2±3.0	31.6±1.5	39.5±1.5	43.56	0.35	4.47	2.50	46.06
DLC 13	4.9% B-DLC	74.1±3.2	40.5±1.9	41.6±1.3	39.36	0.40	7.55	3.48	42.84
DLC 14	7.6%B-DLC	92.3±3.5	47.2±2.0	72.1±0.9	33.94	0.00	2.03	0.00	33.94
DLC 15	9.5%B-DLC	90.3±3.8	58.8±1.5	71.3±2.5	28.99	0.00	4.73	0.00	28.99
DLC 16	1.3%Ti-DLC	78.9±1.9	27.1±1.0	54.6±0.2	44.11	0.00	5.72	0.00	44.11
DLC 17	1.8%Ti-DLC	75.2±0.3	29.6±2.9	47.4±0.3	44.39	0.00	7.97	0.00	44.39
DLC 18	3.2%Ti-DLC	72.8±0.3	27.4±0.2	50.0±0.9	44.40	0.00	9.83	0.00	44.40

So far there are no standard manufacturing processes for producing doped DLC coatings and it is still at the experimental stage. The selection of the doped elements was based on previous experience on producing non-stick doped DLC coatings and on the ability of manufacturers to produce the coatings. For example, initially we asked a manufacture to prepare Ti-doped DLC coatings with Ti content of 3%, 6% and 12%, but the manufacture produced the Ti-doped DLC coatings with Ti content of 1.3%, 1.8% and 3.2%, respectively after XPS analysis. Similar problems existed for other doped DLC coatings. As the coatings were costly, we did not ask the manufacturers to do the coatings again.

Table 5.9 shows that the γ^{TOT} and γ^- values for these SiO_x-like coatings were changed in the wide range: 23.1~45.7 mJ/m^2 and 1.5~39.5 mJ/m^2, respectively.

Table 5.9 Contact angle and surface energy components of SiO_x-like coatings

Coatings	Contact Angle θ [°]			Surface Free Energy Components [mJ/m^2]				
	θ^W	θ^{Di}	θ^{EG}	γ^{LW}	γ^+	γ^-	γ^{AB}	γ^{TOT}
S1	47.4 ± 0.6	57.6 ± 0.3	27.4 ± 1.3	29.96	1.24	34.95	13.17	43.13
S2	41.6 ± 0.7	58.2 ± 0.3	18.2± 0.5	29.60	1.64	39.50	16.10	45.70
S3	75.6 ± 1.5	67.7 ± 0.3	65.3 ± 0.4	24.17	0.06	17.66	2.06	26.23
S4	80.5 ± 0.5	66.4 ± 0.4	62.7 ± 0.4	24.90	0.28	10.60	3.45	28.35
S5	85.0± 0.5	67.5 ± 0.3	67.2 ± 0.1	24.30	0.16	8.30	2.30	26.60
S6	88.8 ± 0.3	69.5 ± 0.5	74.2 ± 0.4	23.15	0.11	7.85	1.86	25.01
S7	90.1 ± 0.4	69.2± 0.7	73.3 ± 0.3	23.30	0.04	6.40	1.01	24.31
S7-1	92.3 ± 0.9	70.5 ± 0.2	76.8 ± 0.8	22.59	0.00	6.02	0.00	22.59
S7-2	94.3 ± 0.7	70.4 ± 0.4	77.4 ± 0.2	22.60	0.01	4.70	0.43	23.03
S7-3	90.2 ± 0.6	70.1 ± 0.8	75.7 ± 0.3	22.82	0.00	7.28	0.00	22.82
TCL40bt	97.6 ± 0.5	72.0 ± 0.9	74.6 ± 0.3	21.76	0.22	2.17	1.38	23.14
TCL40C1	99.9 ± 0.7	69.1± 0.4	76.5 ± 0.6	23.38	0.07	1.5	0.65	24.03
TCL40C2	96.9 ± 0.4	65.1 ± 0.9	71.5 ± 0.2	25.65	0.14	1.65	0.96	26.61
TCL40C3	97.7 ± 0.2	66.3 ± 0.3	71.2 ± 0.4	34.96	0.02	1.33	0.33	26.05
TCL40C4	71.7 ± 1.0	61.7 ± 0.3	49.9 ± 0.8	27.60	0.76	14	6.52	34.13

It was found that for most coatings, including Ni-P-Polymers coatings, doped DLC coatings and SiO_x-like coatings, their γ^+ values were almost zero, leading to γ^{AB} values were very small and γ^{LW} values were almost similar to the γ^{TOT} of the coatings.

CHAPTER 6

ADHESION ASSAYS OF BACTERIA AND PROTEINS

6.1 Bacterial Culture

6.1.1 Types of Bacteria

In this study, the assays of bacterial adhesion and removal were performed at the Biological and Nanomaterials Lab, University of Dundee. The bacteria including *Pseudomonas fluorescens (CHAO), Escherichia coli WT (F1693), Pseudomonas aeruginosa (ATCC 33347), Staphylococcus aureus (F1557)* and *Staphylococcus epidermidis (F1661)* from Institute of Infection and Immunity, Nottingham University, UK were used for the investigation of bacterial adhesion and removal. *Pseudomonas fluorescens* is a common gram-negative, rod-shaped bacterium, which is usually found in water and frequently causes biofouling in piping system, heat exchangers and membrane filters (Bott, 2001). It can also cause bloodstream infections. The size of *P. fluorescens* is around 0.6 μm and its growth temperature is 25~30 ºC. In laboratory, the growth medium for *P. fluorescens* is Tryptone Soya Broth (TSB), which contains casein peptone 10 g/l, soya peptone 3.0 g/l, NaCl 5.0 g/l, K_2PO_4H 2.5 g/l and glucose 2.5 g/l.

E. coli, *P. aeruginosa, S. aureus and S. epidermidis* are microorganism representative that frequently cause medical devices and implants-related infections. The strains

belonged to an original collection of clinical isolates and then stored in laboratory. The details of the bacterial culture method were described by Zhao et al. (2008). In brief, the strains were subcultured and preserved in 15% glycerol in TSB (Tryptone Soya Broth, Oxoid®, UK) as frozen stock at −80 °C. For all adhesion tests, TSA (Tryptone Soya Agar) plates were streaked out with a loop from the frozen stock and grown overnight at 37 °C. A single colony was inoculated in 10 ml TSB and grown statically overnight at 37 °C. Five hundred microlitres from this culture were further inoculated into 100 ml TSB in a conical flask and grown in a shaker-incubator at 37 °C and 250 rpm. The culture was grown to mid-exponential phase. The strains were harvested by centrifuging at 4500 rpm for 5 min at −4 °C, washed once in sterile distilled water and resuspended PBS (Phosphate Buffered Saline) in the medium (pre-warmed to 37 °C) at a 10^7 CFU/ml concentration. The components of TSB, TSA and PBS are given in Table 6.1.

Table 6.1 Components of TSB, TSA and PBS

	Components	**Quantity (g/l)**
TSB	Pancreatic digest of casein	17
	Papaic digest of soybean meal	3
	Sodium chloride	5
	Di-basic potassium phosphate	2.5
	Glucose	2.5
TSA	Tryptone	15
	Soya peptone	5
	Sodium chloride	5
	Agar	15
PBS	Sodium chloride	8
	Potassium chloride	0.2
	Di-sodium hydrogen phosphate	1.15

6.1.2 Growth Curve of Bacteria

Bacterial growth means an increase in cellular constituents that may result in an increase in cell size, an increase in cell number, or both. The growth curve is usually analyzed in a closed system called a batch culture; usually plotted as the logarithm of cell number versus the incubation time.

Bacteria that exhibit characteristic growth can be divided into the four distinct growth phases as shown in Figure 6.1.

1) Lag Phase: Cells in a new inoculum adjust to the medium. Increases occur in enzyme production and cell size. There is no cell division and therefore no increase in numbers. Metabolically active but no increase in number. The lag phase may last for 1 hour to several days, depending on the type of bacteria and other conditions.

2) Exponential or logarithmic (log) phase: Cells and cell mass double at a constant rate. Thus there is a rapid exponential increase in population, which doubles regularly until a maximum number of cells are reached. Most bacteria reproduce by binary fission. One cell roughly doubles in volume, contents, and divides into 2 cells. As bacteria in log phase is more active, the bacteria in log phase are usually used for bacterial adhesion and removal assays.

3) Stationary Phase: The number of cells undergoing division is equal to the number of cells that are dying. Therefore there is no further increase in cell number and the population is maintained at its maximum level for a period of time.

4) Death or Decline phase: Death rate is greater than growth rate. Cell lysis may occur. During the death phase, the number of viable cells decreases exponentially.

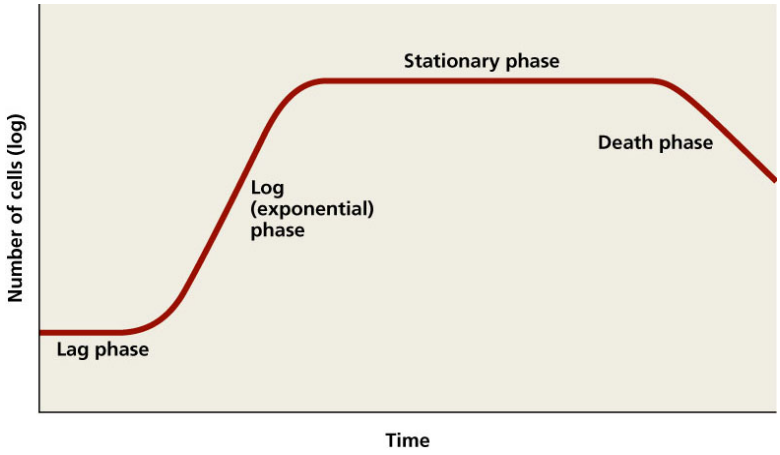

Fig. 6.1 Bacterial growth curve

6.1.3 Growth Curve Measurement

After the frozen bacteria stock had been defrosted, they were cultured in TSA plates in an incubator (Gallenkamp plus II Incubator) overnight at 28 °C for *P. fluorescens* and at 37 °C for *P. aeruginosa, S. aureus, S. epidermidis* and *E. coli*. A species bacterial colony from agar was taken with a loop and was put into a conical flask containing 10 ml medium to grow statically in a shaker-incubator (Stuart Oribital Incubator SI50) at 150 rpm overnight at 28 °C for *P. fluorescens* and at 37°C for other bacteria. Then the 500 µl of a bacterial suspension was transferred into 100 ml medium in a conical flask and cultured in the shaker-incubator at 150 rpm. The optical density (OD) value of bacterial suspension was recorded by a cell density meter (Biowave CO8000 Cell Density Meter) at set intervals, at which the number of cells were counted using viable plate count method.

Figure 6.2(a) ~ 6.6(a) show the growth curves (Log Phases) of five bacteria (*P. fluorescens*, *E. coli, P. aeruginosa, S. aureus and S. epidermidis*) respectively. Clearly, the log number of cells increased along the growth time. The correlations between OD_{600} of culture solution and log CFU/ml during the exponential phases for the five bacteria are shown in Figure 6.2(b) ~ 6.6(b), respectively. The required concentration of each bacterial suspension was calculated using the OD value and corresponding equations in Figure 6.2(b) ~ 6.6(b).

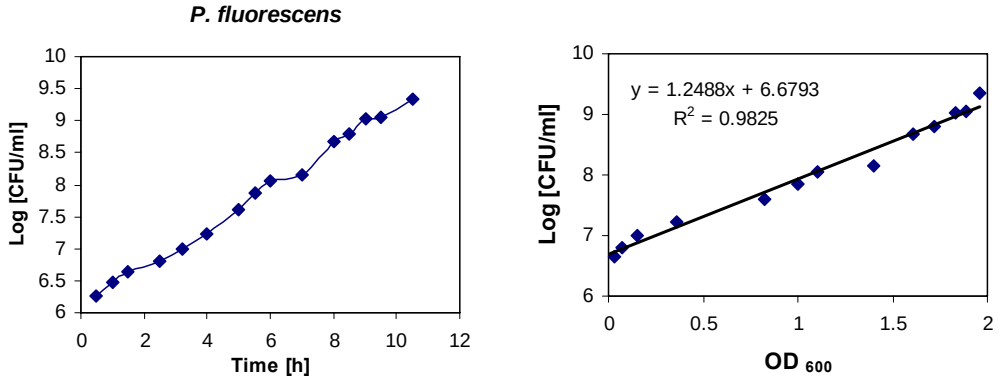

(a) (b)

Figure 6.2 (a) *P. fluorescens* growth curve; (b) Log (CFU/ml) vs OD_{600}

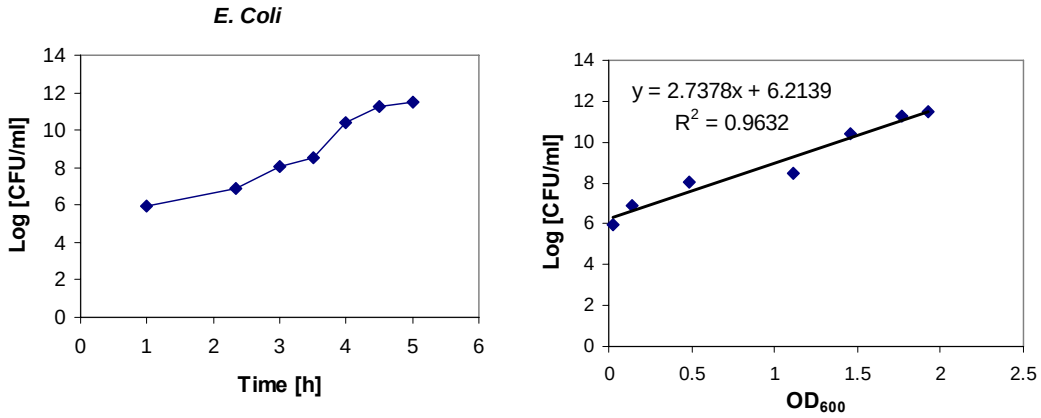

(a) (b)

Figure 6.3 (a) *E. coli* growth curve; (b) Log (CFU/ml) vs OD_{600}

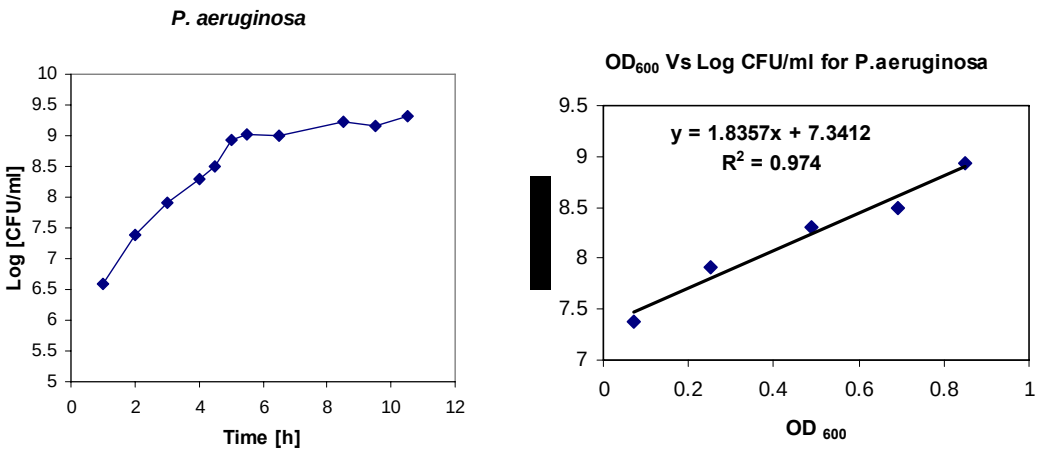

(a) (b)

Figure 6.4 (a) *P. aeruginosa* growth curve; (b) Log (CFU/ml) vs OD_{600}

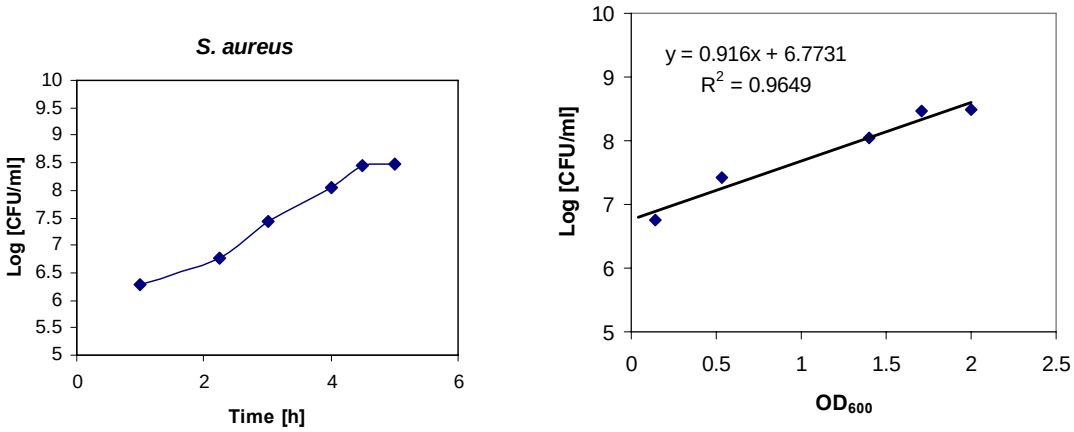

(a) (b)

Figure 6.5 (a) *S. aureus* growth curve; (b) Log (CFU/ml) vs OD_{600}

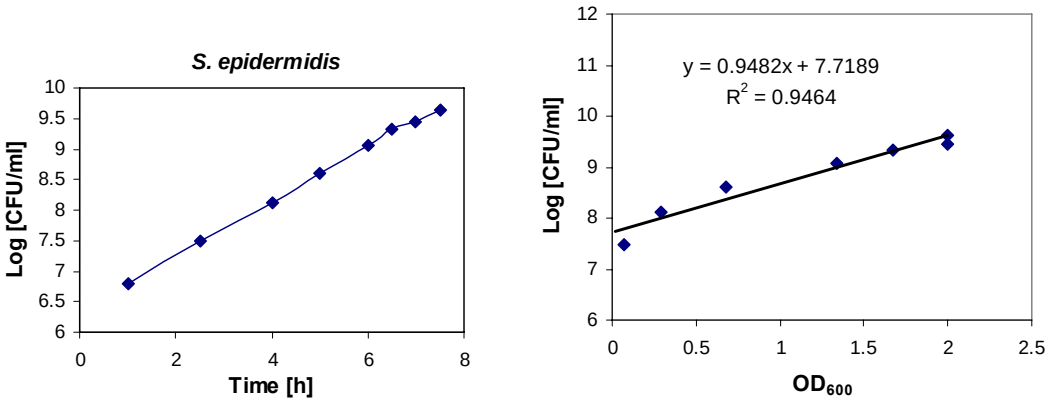

(a) (b)

Figure 6.6 (a) *S. epidermidis* growth curve; (b) Log (CFU/ml) vs OD_{600}

6.1.4 Contact angle and Surface Energy of Bacteria

The contact angle of bacterial cells was measured on the lawns of bacteria deposited on membrane filters with pore diameter of 0.45μm. Prior to contact angle measurement, the bacterial lawns were dried in the air to a certain state, indicated by stable water contact angles. Usually this state of drying of a microbial lawn lasts 30-60 minutes and indicated that only bound water is present on the surface. The static contact angles of the three test liquids: distilled water (θ_w), diiodomethane (θ_D) and ethylene glycol (θ_E) on the bacterial membrane filters at room temperature are given in Table 6.2. The value of each contact angle is the average of three measurements and the standard deviation value is 0.3-1.2°. Table 6.2 shows the contact angle values and the surface free energy of the different bacteria strains, which were calculated using van Oss acid-base approach (Liu, 2008; Wang 2008).

Table 6.2 Contact Angle and Surface Energy Components of Bacteria

Bacteria	**Contact Angle θ [°]**			**Surface Free Energy Components [mJ/m^2]**				
	θ^W	θ^{Di}	θ^{EG}	γ^{LW}	γ^+	γ^-	γ^{AB}	γ^{TOT}
Pseudomonas fluorescens	17.9	61.7	18.6	27.62	1.08	66.79	16.96	44.58
Escherichia coli	16.5	47.6	22.9	35.60	0.14	67.68	6.16	41.76
Pseudomonas aeruginosa	78.0	55.4	72.4	31.10	0.00	17.60	0.00	31.10
Staphylococcus aureus	16.6	54.8	22.3	31.56	0.43	68.32	10.84	42.40
Staphylococcus epidermidis	31.0	48.2	50.1	32.91	0.00	63.15	0.00	32.91

6.2 Bacterial Adhesion and Removal

6.2.1 Bacterial Adhesion

In this study, the bacterial suspension with a 10^6 CFU/ml concentration for each type of 5 bacteria was prepared. Five replicate samples of each coating were immersed vertically in a glass tank containing 500 ml of a bacterial suspension and were incubated on a shaker at 20 rpm for 1, 5 or 18 hour at 28˚C for *P. fluorescens* or at 37˚C for *E. coli, P. aeruginosa, S. aureus* or *S. epidermidis*. After that, each coating plate was taken out from the tank using sterile forceps and was dipped twice vertically in sterile distilled

water with a custom-made automated dipper apparatus under a constant speed of 0.03 m s^{-1} in order to remove loosely attached bacteria. Then the total number of bacteria on the plate was counted either by viable plate count method or by fluorescence microscope.

For viable plate count method the plate was immersed in the 25ml sterile water beaker and sonicated for 5 min to remove adhered bacteria from the surface of sample thoroughly. Then 100 µl of sonicated suspension, 10^{-1}, 10^{-2} and 10^{-3} dilutions were plated out on TSA plates and incubated overnight at 28 °C or at 37 °C. The colonies were counted out. Five parallel coating plate of each type were used to obtain the average number of adherent bacteria of each coating. The adhered bacteria to each substrate were the average of 5×4 measurements (maximum) by the viable plating count method. For fluorescence microscope method, the number of bacteria on the plate was counted directly using *Image-Pro Plus* software. For each plate 6 areas were counted. Five replicate samples of each coating were used to obtain the average number of adherent bacteria of each coating. The adhered bacteria to each substrate were the average of 5×6 measurements (maximum) by the fluorescence microscope method.

6.2.2 Bacterial Removal

In order to investigate bacterial adhesion strength, a home-made dipping device (Figure 6.7) was designed by Zhao *et al.* (2008). It is designed to remove 10% ~ 90% bacteria from surfaces through moving the sample up and down into the water at constant speed (0.03 m/s) controlled by a motor. This process is identical to water flowing over the surface of the sample and the whole area of samples is flushed with water at constant shear stress. Therefore, the bacteria that adhered weakly to the surfaces can be removed into the water tank. Finally, bacterial adhesion strength and removal percentage can be determined (Zhao et al 2008; Liu 2011).

Figure 6.7 Dipping Device

To assess the adhesion strength of the attached bacteria, each sample was dipped 20 times vertically in a glass tank (A) containing 130 ml sterile distilled water at 28˚C (or at 37 ˚C) at a constant 0.03 m/s speed (or a constant shear stress of 0.014 N m^{-2}, see equation 6.4) to remove 10-90% adhered bacteria using a dipping device. Each test sample was transferred to a second glass tank (B) with 25 ml sterile distilled water and sonicated in an ultrasonic bath to remove all the remaining attached bacteria thoroughly. The number of bacteria in the tank (A) was defined as $B_{A,}$ while the number of bacteria in the tank (B) was B_B. The total number of bacteria attached to the sample B_{TOT} is the sum of the bacteria in tank (A), B_A and the bacteria in tank (B), B_B, as described in equation (6.1). The percentage removal of bacteria from the sample was calculated using equation (6.2):

$$B_{TOT} = B_A + B_B \quad (6.1)$$

$$\text{Removal (\%)} = B_A / B_{TOT} \times 100 \quad (6.2)$$

The values of B_A and B_B were determined using a standard plating method for viable counts. For vessel (A), 100 µl of bacterial suspension from 130 ml tank (A) as well as 10^{-1} and 10^{-2} dilutions were plated out onto TSA plates, respectively. The agar plates were incubated for 24 h at 28˚C (or 37˚C) for viable cell counts. The number of bacteria in 100 µl of bacterial suspension was obtained using the appropriate concentration from

original, 10^{-1} dilution or 10^{-2} dilution. Then the total number of bacteria in 130 ml in vessel (A) was calculated. The number of bacteria in 25 ml from tank B was determined using the same method. The total number of bacteria, as colony-forming units (CFU) attached to the coating and the percentage removal from the coating was the mean of maximum 15 measurements, 3 from each of 5 replicate samples.

For water flows over a flat plate with width b and length L with velocity U, the drag force can be calculated using the following equation:

$$F_d = 0.646b\sqrt{\rho\mu LU^3} \tag{6.3}$$

where ρ and μ are water density and viscosity, respectively. The corresponding shear stress τ_w is defined as:

$$\tau_w = \frac{F_d}{b \times L} = 0.646\sqrt{\frac{\rho\mu U^3}{L}} \tag{6.4}$$

The equation (6.4) is also suitable for the calculation of shear stress using the dipping device. In this case, U is the dipping speed (0.03 m/s) and L is the height of water in tank (0.075 m) (Zhao et al 2008).

6.3 Methods of Cell Counting

6.3.1 Viable Plate Counts Method

Plate counts is one of the most common methods of determining bacterial number, and it is also a gratifying method to enumerating surface bacteria calls for the investigator to detach the bacteria and count the number of colony forming units (CFU) recovered from the detachment procedure. The plate counts method consists of diluting a sample until the bacteria are dilute enough to count accurately. That is, the final plates in the series should have between 30 and 300 colonies. Fewer than 30 colonies are not acceptable for statistical reasons, and more than 300 colonies on a plate are likely to produce colonies

too close to each other to be distinguished as distinct CFU (Prescott LM *et al.*, 2005). The general procedure for the plate count method includes:

1) Plate out 100 µl from the obtained suspension and its dilutions (10^{-1}, 10^{-2}, 10^{-3}, and 10^{-4}) on an agar plate (TSA)
2) Incubate at 28-37˚C the plates overnight, depending of the strains.
3) Count the colonies by a Digital Colony Counter next day

The main disadvantages of plate count method include:

1) It is very time-consuming and it takes about 1-2 days to get the results
2) It can only count viable bacteria.

6.3.2 Microscope Method

In general microorganisms cannot be observed in naked eye. If they are stained with fluorescent dyes they can be seen with the fluorescence microscope. The main advantages of this technique include:

1) It is very quick, compared with plate count method, making it especially suitable for large sets of samples;
2) It can count both alive and dead bacteria;

In this study, the LIVE/DEAD *BacLight* bacterial viability kit was used for the enumeration of bacteria on the coatings. The kit consists of two nucleic acid stains: SYTO 9, which penetrates most membranes freely, and propidium iodide, which is highly charged and normally does not permeate cells but does penetrate damaged membrane. Simultaneous application of both dyes therefore results in green fluorescence of viable cell with an intact membrane, whereas dead cells, because of a compromised membrane, show intense red fluorescence. The procedures are shown as follows (Wang, 2008):

1) Concentrate 10 mL of the bacterial suspension by centrifugation for 10 minutes.
2) Remove the supernatant and resuspend the pellet in 2 mL of 0.85% NaCl.

3) Add 1 mL of this suspension to each of two 30–40 mL centrifuge tubes containing either 20 mL 0.85% NaCl (for live bacteria) or 20 mL of 70% isopropyl alcohol (for killed bacteria).
4) Incubate both samples at room temperature for 1 hour, mixing every 15 minutes.
5) Pellet both samples by centrifugation for 10minutes.
6) Resuspend the pellets in 20 mL 0.85% NaCl and centrifuge again as in step 5.
7) Resuspend both pellets in separate tubes with 10 mL of 0.85% NaCl each.
8) Determine the optical density at 670 nm (OD670) of a 3 mL aliquot of the bacterial suspensions in glass (1 cm pathlength).
9) Selection of Optical Filters (The fluorescence from both live and dead bacteria may be viewed simultaneously with any standard fluorescein longpassfilter set. Alternatively, the live (green fluorescent) and dead (red fluorescent) cells may be viewed separately with fluoresceinn and Texas Red bandpass filter sets).
10) Staining Bacteria in Suspension with LIVE/DEAD BacLight stain. (Mix thoroughly and incubate at room temperature in the dark for 15 minutes).
11) Trap 5 µL of the stained bacterial suspension between a slide and an 18 mm square coverslip.
12) Observe in a fluorescence microscope equipped with filters. Prepare 3 slides for each sample and record 10 fields.
13) Data analysis by image pro plus software.

In this study, a BX41 Olympus Fluorescence Microscope with QICAM High-Performance Digital CCD Camera and *Image-Pro Plus* software was used for counting bacteria on the coatings, as shown in Figure 6.8. The number of bacteria can be accurately counted manually or automatically using image analysis by *Image Pro Plus*, as shown in Figure 6.9. The green colour shows alive bacteria while the red colour shows dead bacteria.

Figure 6.8 BX41 Olympus Fluorescence Microscope

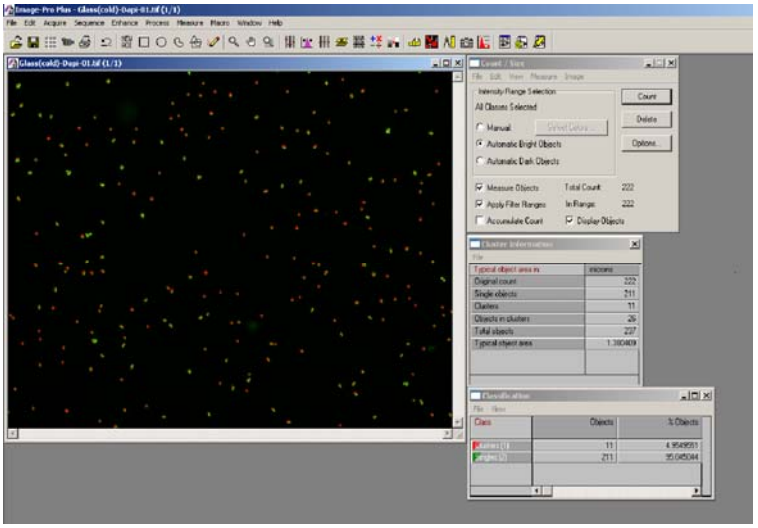

Figure 6.9 Image Analysis by Image *Pro Plus* Software

6.4 Protein Removal Assays

So far there are no studies that explore protein removal properties from the doped DLC coatings with selected elements. The exact mechanisms of how individual doping elements affect surface properties with respect to protein adhesion are not known and are complex. In the present study, B and Ti-doped DLC coatings with a range of proportion of the doping elements were produced by Tecvac Ltd in order to investigate their effectiveness in enabling protein removal using two established cleaning methods, one with a chemical detergent, the other with an enzymatic agent. All the coatings were

treated with 100 µg/ml brain homogenate and dried for 24 hours in the room temperature. Then they were subsequently cleaned using a detergent- Decon. The quantity of protein remaining after cleaning was determined by looking at the fluorescence produced with OPA/NAC and comparing this to positive and negative controls. The protein removal assays were performed at Barts and London School of Medicine.

CHAPTER 7

EXPERIMENTAL RESULTS

In this chapter, the adhesion and removal of bacteria and protein were investigated using a range of nano-composite coatings including Ni-P-polymers coatings, doped DLC coatings and SiO_x-like coatings. The bacteria used included *P. fluorescens, E. coli, P. aeruginosa, S. aureus* and *S. epidermidis.* The protein was brain homogenate. The effect of surface energy, doped elements and their contents in the coatings on the adhesion and removal of bacteria and protein were investigated.

7.1 Ni-P-Biocide Polymer Nanocomposite Coatings

7.1.1 Selection of Biocide Polymers

According to the literature search, Ni–P–PTFE coatings seem the one of the best coating techniques for controlling biofouling in heat exchangers and pipelines. However their anti-biofouling and anti-corrosion properties could be futher improved by incorperation biocide polymer nanoparticles into the Ni–P–PTFE coatings.

In this study, the anti-microbial efficiency of 13 different types of biocide polymers from Graz University of Technology were evaluated with *Escherichia coli* and *Staphylococcus aureus*. The detailed procedures of bacterial adhesion and removal are described in Section 6.2: Bacterial Adhesion and Removal. In brief, the biocide polymer

samples were put into a beaker containing 500ml bacterial suspension with 1×10^6 CFU/ml concentration and then the beaker was put in a shaker incubator (Stuart Scientific, UK) at 37°C for 1h under a gentle stirring at 20rpm. In order to observe the number of cells microscopically, the bacteria on the samples was stained using LIVE/DEAD BacLight Kit L 13152 for 15 minutes and then observed under a fluorescence microscope (OLYMPUS BX 41, Japan) and counted using Image Pro Plus software (Media Cybernetics, USA).

Figure 7.1 shows that all the biocide polymers have strong antimicrobial properties with respect to the bacterium *Escherichia coli*, compared to the control polymer without additives (355.09.012). The polymers 355.09.004; 355.09.006; SK13; SM14 and SM20 perform better than others against bacterial attachment. Figure 7.2 shows bacterial adhesion strength or bacterial removal rate. All these polymers have similar bacterial removal rate except for SK13.

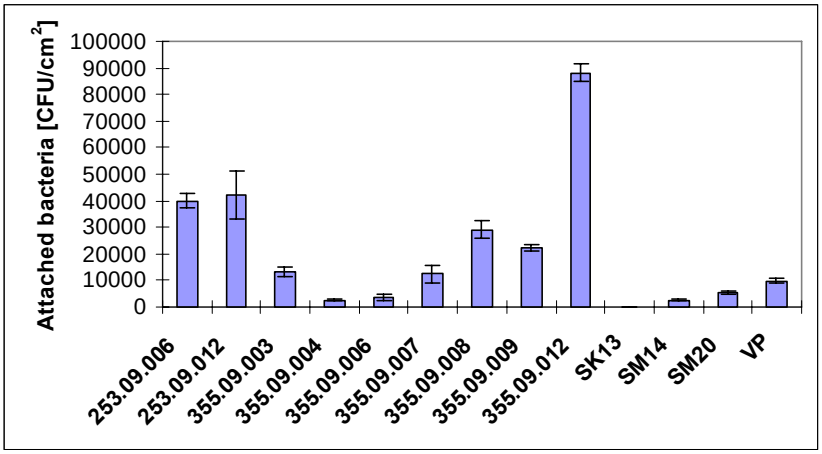

Figure 7.1 Bacterial attachment with *Escherichia coli*

Figure 7.3 shows that the biocide polymers have strong antimicrobial properties with respect to the bacterium *Staphylococcus aureus*, compared to the control polymer without additives (355.09.012). Again the polymers 355.09.004; 355.09.006; SK13; SM14 and SM20 perform best against bacterial attachment. Figure 7.4 shows bacterial adhesion strength or bacterial removal rate. SM14 and SM20 have higher bacterial removal rate than the polymers 355.09.004; 355.09.006; SK13.

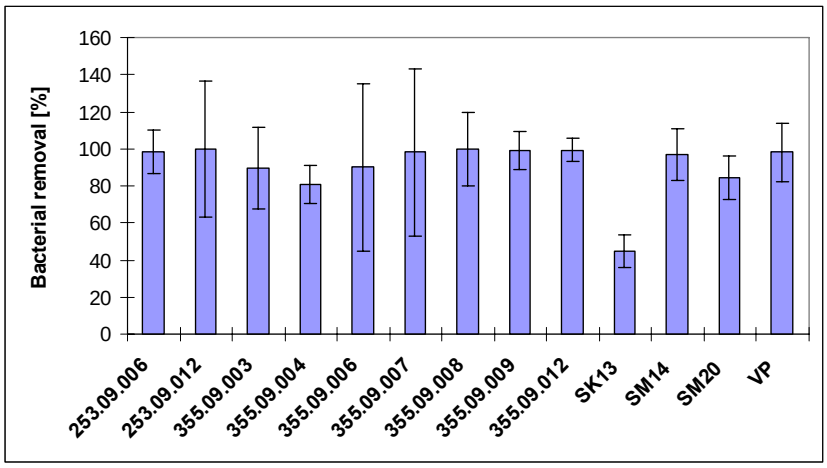

Figure 7.2 Bacterial removal with *Escherichia coli*

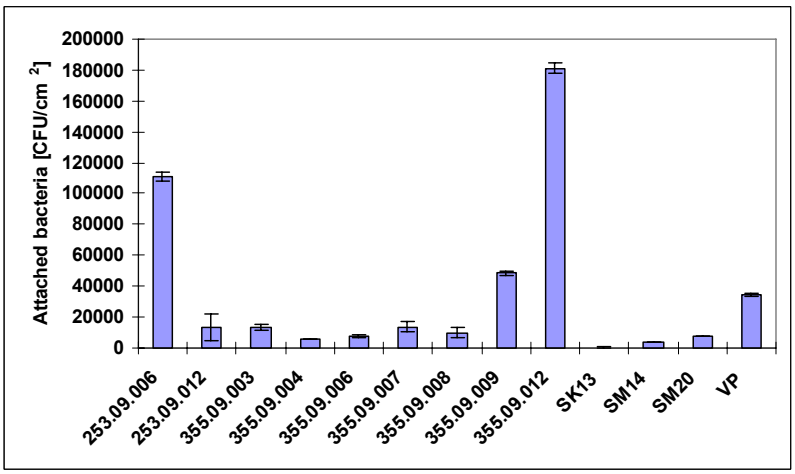

Figure 7.3 Bacterial attachment with *Staphylococcus aureus*

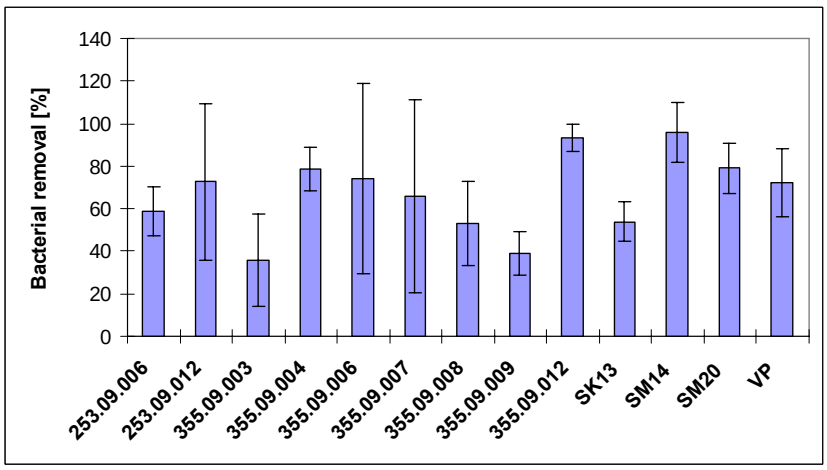

Figure 7.4 Bacterial removal with *Staphylococcus aureus*

7.1.2 Ni-P-Biocide Polymers Coatings

Figures 7.1-7.4 indicate that the two biocide polymers SM14 and SM20 perform best against bacterial attachment and removal. The chemical structures of SM14 and SM20 are shown in Fig. 4.4. As a result, four new anti-biofouling Ni-P-biocide polymers nanocomposite coatings: Ni-P-SM14, Ni-P-PTFE-SM14, Ni-P-SM20 and Ni-P-PTFE-SM20 were developed.

Figure 7.5 shows *Escherichia coli* adhesion on the coatings. Stainless steel and Ni-P coatings were used as control. Overall all the coatings with biocide polymers and PTFE performed much better than stainless steel and Ni-P coatings. The coatings with biocide polymers (Ni-P-SM14 and Ni-P-SM20) performed much better than Ni-P coatings, and the coatings with PTFE (Ni-P-PTFE-SM14 and Ni-P-PTFE-SM20) performed better than the coatings without PTFE (Ni-P-SM14 and Ni-P-SM20). Ni-P-PTFE-SM14 and Ni-P-PTFE-SM20 performed best, which reduced bacterial attachment by 94% and 70% respectively as compared with stainless steel and Ni-P-PTFE. Figure 7.6 shows bacterial removal with *Escherichia coli.* Overall the removal rate for the coatings with biocide polymers and PTFE was much better than stainless steel and Ni-P coatings. As PTFE has non-stick property, the coatings with PTFE (Ni-P-PTFE, Ni-P-PTFE-SM14 and Ni-P-PTFE-SM20) have highest bacterial removal rate.

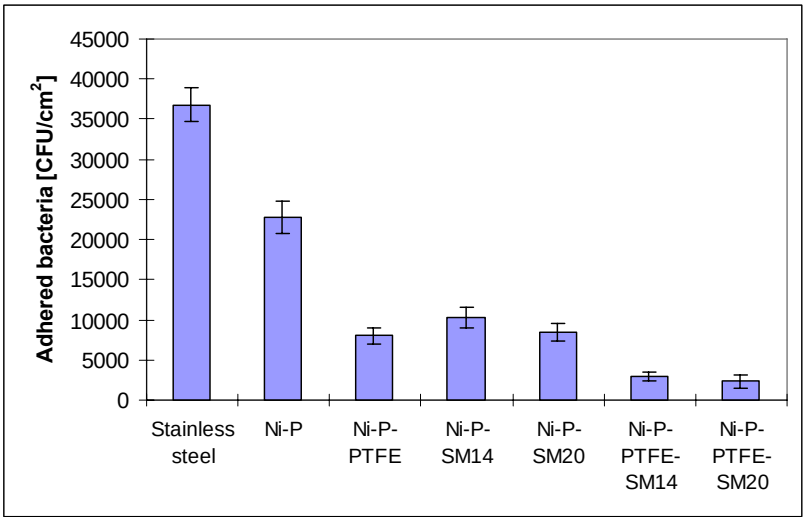

Figure 7.5 Attachment of *E. coli* on Ni-P-Polymer coatings

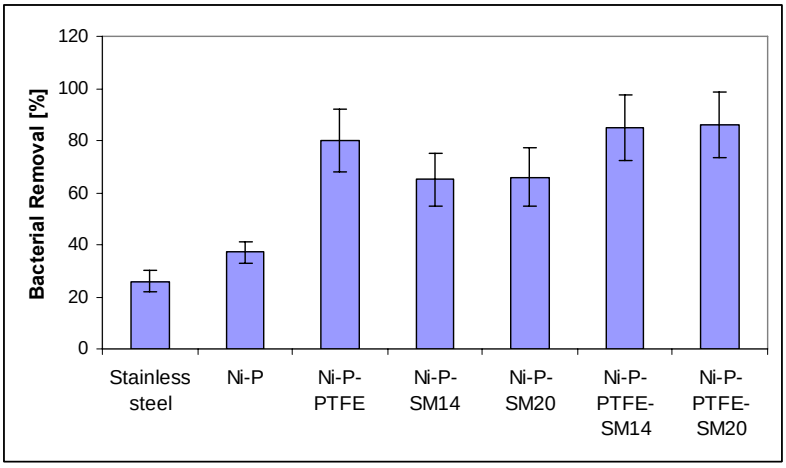

Figure 7.6 Removal of *E. coli* from Ni-P-Polymer coatings

Figure 7.7 shows *Staphylococcus aureus* adhesion on the coatings. Similar results were obtained. Ni-P-PTFE-SM14 and Ni-P-PTFE-SM20 performed best, which reduced bacterial attachment by 87% and 53% respectively, as compared with stainless steel and Ni-P-PTFE. Figure 7.8 shows bacterial removal with *Staphylococcus aureus.* The removal rate for the coatings with biocide polymers and PTFE was much better than stainless steel and Ni-P coatings. The coatings with PTFE (Ni-P-PTFE, Ni-P-PTFE-SM14 and Ni-P-PTFE-SM20) have highest bacterial removal rate.

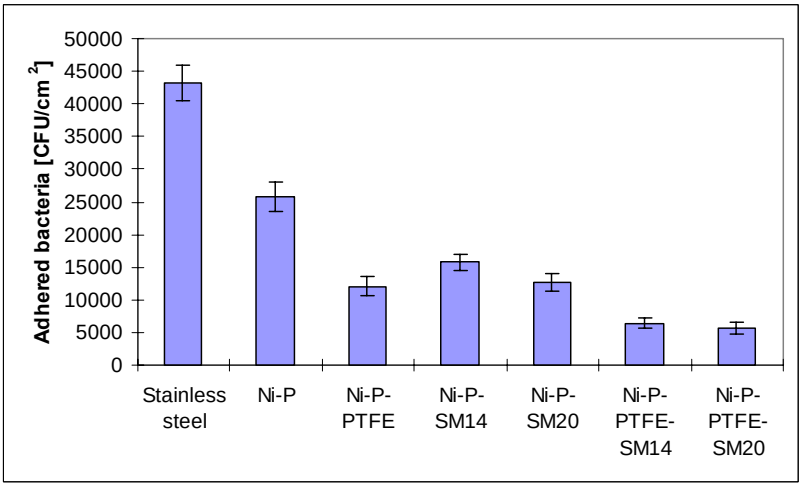

Figure 7.7 Attachment of *S. aureus* on Ni-P-Polymer coatings

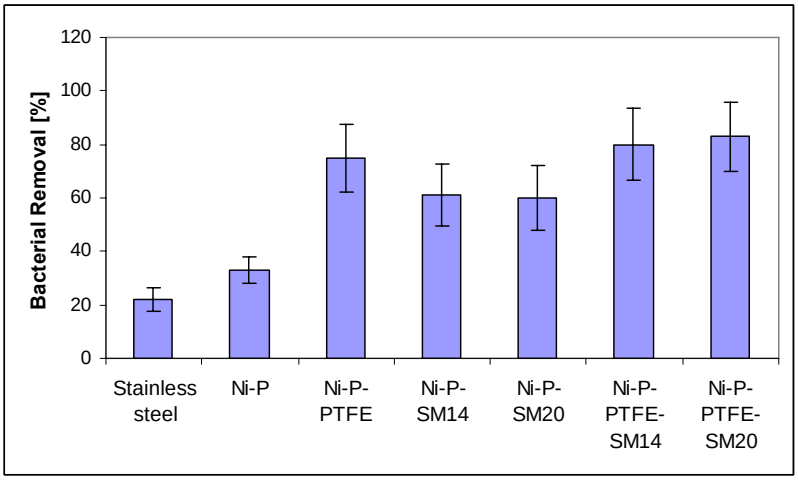

Figure 7.8 Removal of *S. aureus* from Ni-P-Polymer coatings

Figure 7.9 shows the effect of surface energy of coatings on bacterial attachment. In general, the number of adhered bacteria decreased with surface energy decreasing for both *S. aureus* and *E. coli.* The experimental data in Figure 7.9 also indicates that when the surface energy of the coatings was about 25 mJ/m^2, the number of adhered bacteria was least.

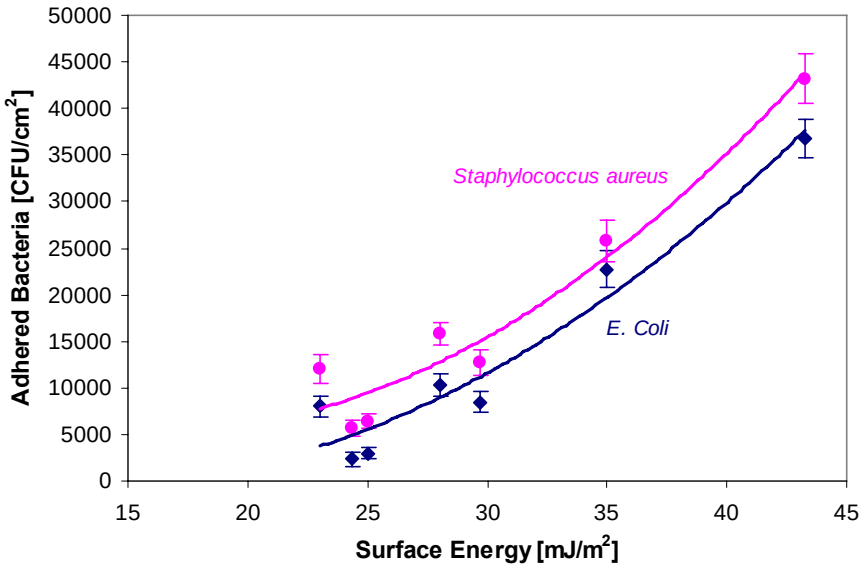

Figure 7.9 Effect of surface energy of coatings on bacterial adhesion

Summary and discussion:

For Ni-P-PTFE coating, its anti-bacterial mechanism is due to the inherent non-stick property of PTFE. For Ni-P-SM14 or Ni-P-SM20, their anti-bacterial mechanism is due to the biocidal property of the biocide polymers SM14 and SM20. For Ni-P-PTFE-SM14 and Ni-P-PTFE-SM20, their anti-bacterial mechanisms are due to the non-stick property of PTFE and biocidal property of the biocide polymer SM14 or SM20. In addition, the total surface energy of Ni-P-PTFE-SM14 and Ni-P-PTFE-SM20 was controlled for the optimum value, about 25mJ/m^2 (see Table 5.5). As a result, Ni-P-PTFE-SM14 and Ni-P-PTFE-SM20 performed best against bacterial attachment and had highest bacterial removal rate. Some of research work was presented in Euro-Thermo Heat Exchanger Fouling and Cleaning Conference - June 05-10, 2011, Crete, Greece and included in the refereed conference proceedings (Su et al 2011). An EU patent was filed on 1 June 2012 (Su et al 2012).

7.2 Doped Diamond-Like Carbon Coatings

7.2.1 Si-N-Doped DLC Coatings

In the present study, a range of silicon- and nitrogen-doped DLC coatings with different Si and N contents were produced in order to investigate microbial attachment and release properties of the coatings i.e. the strength of attachment of cells, for a number of applications where the control of biological fouling is critical e.g. heat exchangers, pipelines and biomedical devices. The detailed procedure for preparing the Si- and N-doped DLC coatings is given in Section 4.2.2. The chemical composition, contact angle and surface energy components of Si-N-doped DLC coatings are given in Table 5.6.

These coatings were evaluated for attachment and removal of *Pseudomonas fluorescens*, which is one of the most common bacteria that form biofilms on the surface of heat exchangers in freshwater cooling water systems (Bott 2001). The detailed procedures of bacterial adhesion and removal are described in Section 6.2: Bacterial Adhesion and Removal. In brief, for bacterial attachment assays, five replicate samples of each

coating were immersed in a glass tank containing 500 ml of a suspension of *P. fluorescens* (10^6 cells ml^{-1}), incubated on a shaker (20 rpm) at 28˚C for 1 h. To assess the adhesion strength of the attached bacteria, each sample was dipped a further 20 times vertically in a glass vessel containing 130 ml sterile distilled water at 28˚C at a constant shear stress of 0.014 N m^{-2}.

Initial attachment of *Pseudomonas fluorescens* on the Si-and Si-N-doped DLC coatings (DLC1 - DLC7) is shown in Figure 7.10. The incorporation of 2%N into the Si-doped DLC coatings (DLC4, DLC5, DLC6, DLC7) significantly reduced bacterial attachment (p=0.05), compared with pure Si-DLC coatings (DLC1, DLC2, DLC3) and the standard, Silastic® T2. Silicone coatings based on polydimethylsiloxane are being investigated as fouling-release coatings for various applications including ship hulls. However, the poor thermal conductivity, poor abrasion resistance and poor adhesion to metal substrates of silicone elastomers currently inhibit their commercial use in heat exchangers (Müller-Steinhagen and Zhao 1997). Figure 7.10 indicates that the Si-N-doped DLC coatings performed better than silicone coatings against bacterial attachment.

The incorporation of 2%N into the Si-doped DLC coatings also increased bacterial removal. Figure 7.11 indicates that for the first 3 Si-doped DLC coatings (DLC1, DLC2, DLC3), percent bacterial removal increased with increasing Si content in the DLC coatings i.e. adhesion strength decreased with increasing Si content in the DLC coatings. DLC1 (1%Si-DLC) was significantly different (p=0.05) to DLC2 (2%Si-DLC) and DLC3 (3.8%Si-DLC). Figure 7.11 also indicates that for the four Si-N-doped DLC coatings (DLC4, DLC5, DLC6, DLC7), percent bacterial removal increased significantly with increasing Si content in the DLC coatings.

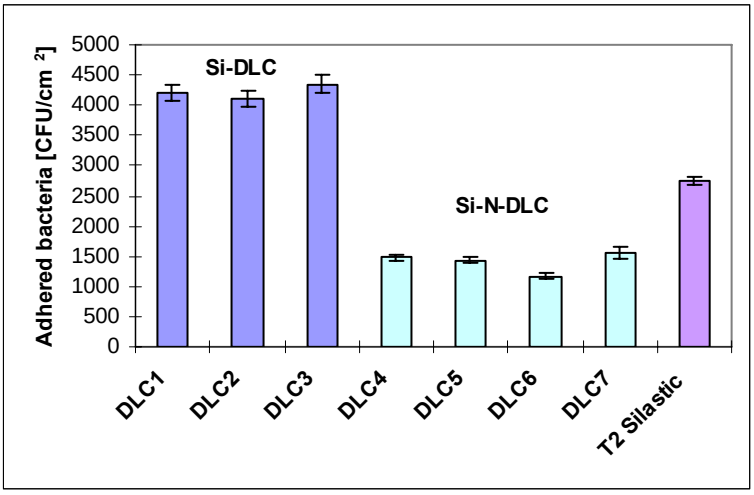

Figure 7.10: Comparison of formation of *pseudomonas fluorescens* cells on Si-N-DLC coatings and on T2 silastic. N = 15, error bars are 2× Standard Error.

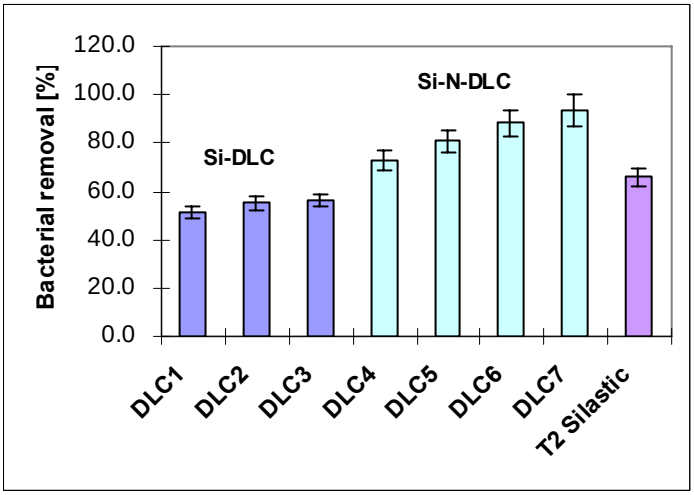

Figure 7.11: Comparison of removal of *pseudomonas fluorescens* cells on Si-N-DLC coatings and on T2 silastic. N = 15, error bars are 2× Standard Error.

Figure 7.12 shows that percent bacterial removal strongly correlated with the surface energy components electron acceptor γ_S^+ and electron donor γ_S^- of the DLC coatings. *Pseudomonas fluorescens* had high value of γ_B^- component (66.79 mN/m, see Table 6.2) and low value of γ_B^+ component (1.08 mN/m, see Table 6.2), and would be negatively charged with the zeta potential of -16.1 mV (Azeredo et al. 2003). Chibowski et al. (1994) investigated the changes in zeta potential and surface energy components of

calcium carbonate due to exposure to radiofrequency electric field. They observed that zeta potential decreased with an increase in the electron donor component γ_S^- of the surface energy. The observed changes in zeta potential and surface energy components were believed to result from changes in the surface charge of calcium carbonate (Chibowski et al. 1994). These observations may explain why bacterial removal decreased with increasing electron acceptor γ_S^+ values of the DLC coatings (Fig 7.12a, b) and increased with increasing electron donor γ_S^- values of DLC coatings (Fig. 7.12c, d).

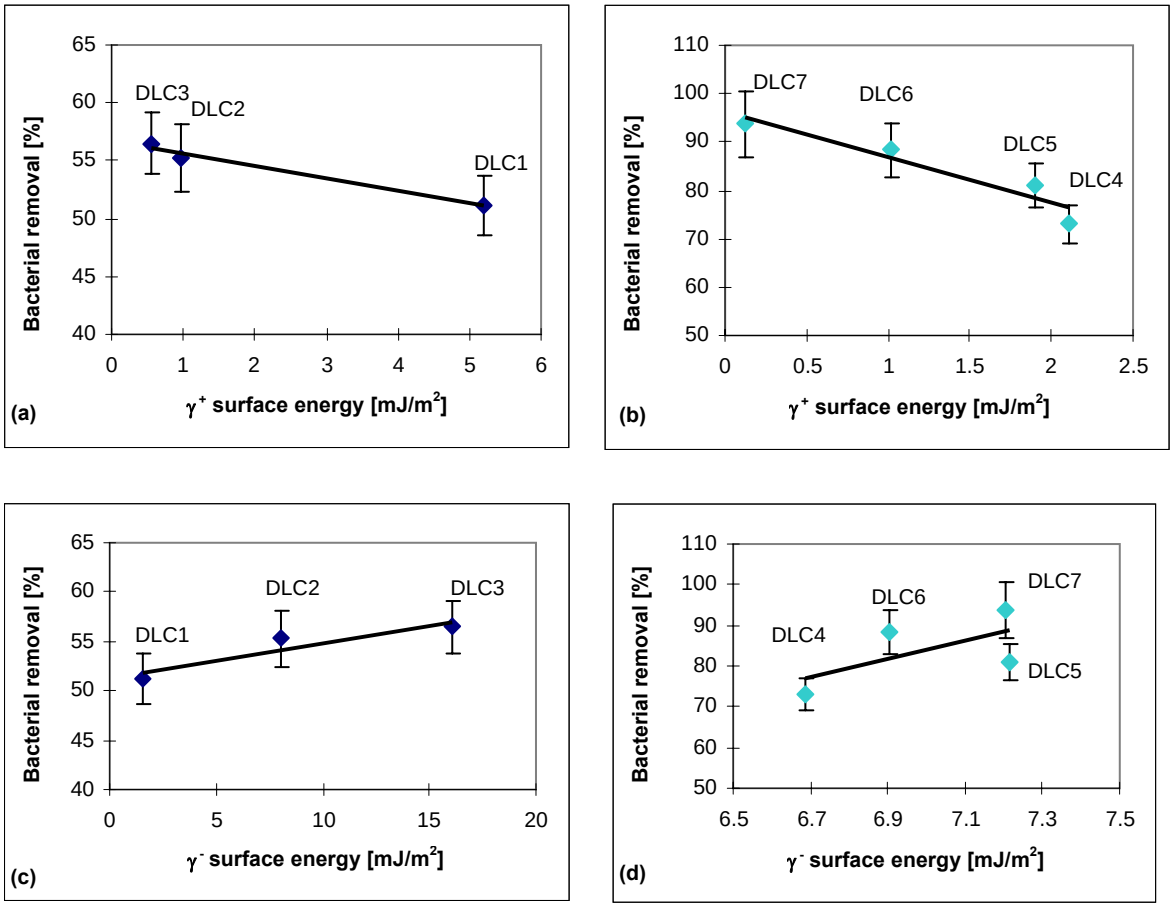

Figure 7.12 (a) Electron acceptor γ_S^+ vs bacterial removal for Si-doped DLC coatings; (b) Electron acceptor γ_S^+ vs bacterial removal for Si-N-doped DLC coatings; (c) electron donor γ_S^- vs bacterial removal for Si-doped DLC coatings; (d) electron donor γ_S^- vs bacterial removal for Si-N-doped DLC coatings. N = 15, error bars are 2× Standard Error.

Summary and discussion:

In this investigation two types of the DLC coatings were produced. The Si-doped DLC coatings (DLC1 - DLC3) were produced by an unbalanced magnetron sputter ion-plating combined with PECVD. The Si in the DLC coatings was achieved by sputtering a solid Si target, while the Si-N-doped DLC coatings (DLC4 – DLC7) were produced by radio frequency PECVD and the Si in the DLC coatings was from the $Si(CH_3)_4$ gas. The experimental results showed that the Si-N-doped DLC coatings performed more efficiently than Si-doped DLC coatings both in reducing bacterial attachment and in removal by shear stress. Clearly the incorporation of 2%N into the Si-doped DLC coatings considerably improved the performance of the coatings. As well as the addition of 2%N, the PECVD coating method and the Si source from $Si(CH_3)_4$ gas may also lead to the improvement in performance of Si-N-doped DLC coatings. Some of the research results were published in <*Biofouling*> (Zhao and Su et al, 2009).

Diamond-like carbon (DLC) coatings have favourable properties, such as excellent thermal conductivity similar to metals, low friction, extremely smooth surface, hardness, wear resistance and corrosion resistance, which are very suitable for heat exchanger applications. It has already been demonstrated that DLC coatings reduce the formation of hard mineral scale on heat transfer surfaces and have potential for heat exchanger application (Förster and Bohnet 1999; Zhao and Wang 2005). This investigation further demonstrates that the modified DLC coatings have the potential to reduce biofouling in heat exchangers. As both DLC coatings and modified DLC coatings with Si and N are biocompatible, they also have potential to reduce bacterial adhesion in biomedical devices and implants.

7.2.2 F-Doped DLC Coatings

In order to investigate the effect of fluorine contents in DLC coatings on bacterial adhesion and removal, the F-doped DLC coatings with a wide range of F contents were prepared on stainless steel plates by CSIRO Materials Science and Engineering, Australia. The detailed procedure for preparing F-doped DLC coatings is given in Section 4.2.3. The chemical composition, contact angle and surface energy components of F-doped DLC coatings are given in Table 5.7.

These coatings were evaluated for attachment and removal with *Pseudomonas fluorescens* and *Staphylococcus aureus,* respectively. The detailed procedures of bacterial adhesion and removal are described in Section 6.2: Bacterial Adhesion and Removal. In brief, for bacterial attachment assays, five replicate samples of each coating were immersed in a glass tank containing 500 ml of a suspension of *P. fluorescens* or *S. aureus* (10^6 cells ml^{-1}), incubated on a shaker (20 rpm) at 28 ˚C or 37 ˚C for 1 h. To assess the adhesion strength of the attached bacteria or bacterial removal rate, each sample was dipped a further 20 times vertically in a glass vessel containing 130 ml sterile distilled water at 28 ˚C or 37 ˚C at a constant shear stress of 0.014 N m^{-2}.

Initial attachment of *Pseudomonas fluorescens* on the fluorinated DLC coatings is shown in Figure 7.13. The number of adhered bacteria decreases with increasing F contents in the F-DLC coatings. The F-DLC coatings with higher F content (39.2 % at. %) reduced bacterial attachment by 49 %, compared with DLC coating.

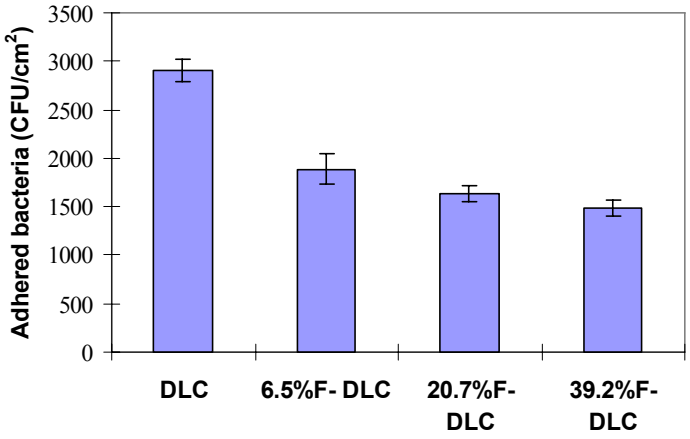

Figure 7.13: Comparison of formation of *Pseudomonas fluorescens* cells on F-DLC coatings and on DLC coatings. N = 15, error bars are 2× Standard Error.

Figure 7.14 indicates that percent bacterial removal increases significantly with increasing F content in the DLC coatings i.e. adhesion strength decreased with increasing F content in the DLC coatings. The F-DLC coatings with higher F content (39.2 at. %) increased removal by 90.2 %, compared with DLC coating.

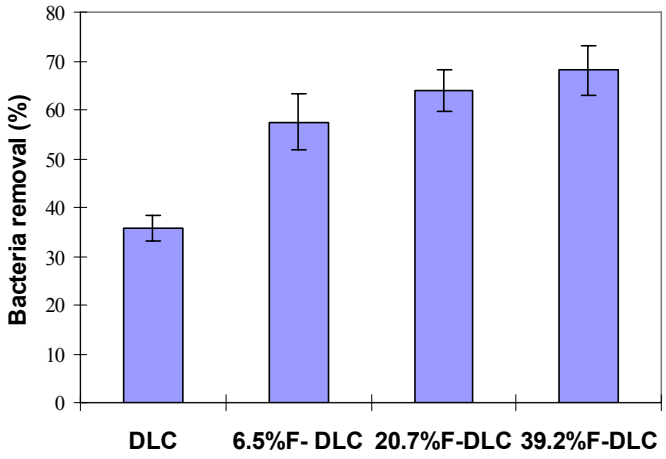

Figure 7.14: Comparison of removal of *Pseudomonas fluorescens* cells on F-DLC coatings and on DLC coatings. N = 15, error bars are 2× Standard Error.

The coatings were also stained with LIVE/DEAD BacLight Kit L 13152 for 15 minutes and then observed under a fluorescence microscope (OLYMPUS BX 41, Japan) and counted using Image Pro Plus software (Media Cybernetics, USA). The numbers of cells on the coatings observed microscopically were almost equal with that determined by the culture method. The effect of surface roughness on bacterial attachment and removal were investigated, but no correlation was found in this study.

Figure 7.15 shows that the initial attachment of *Pseudomonas fluorescens* strongly correlated with the total surface energy of the coatings. The number of adhered bacteria decreased with the total surface energy of the coatings decreasing. Figure 7.16 shows that percentage of bacterial removal strongly correlated with the total surface energy of the F-DLC coatings. The percentage of bacterial removal increased with the total surface energy of the F-DLC coatings decreasing.

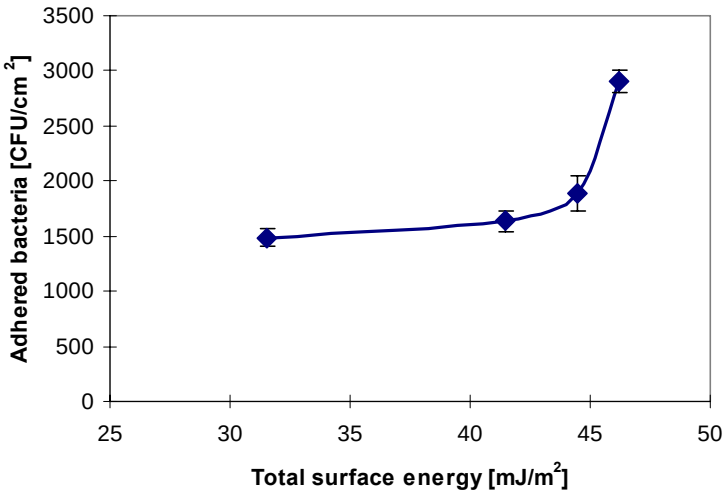

Figure 7.15 Effect of total surface energy of F-DLC coatings on adhesion of *Pseudomonas fluorescens* cells. N = 15, error bars are 2× Standard Error.

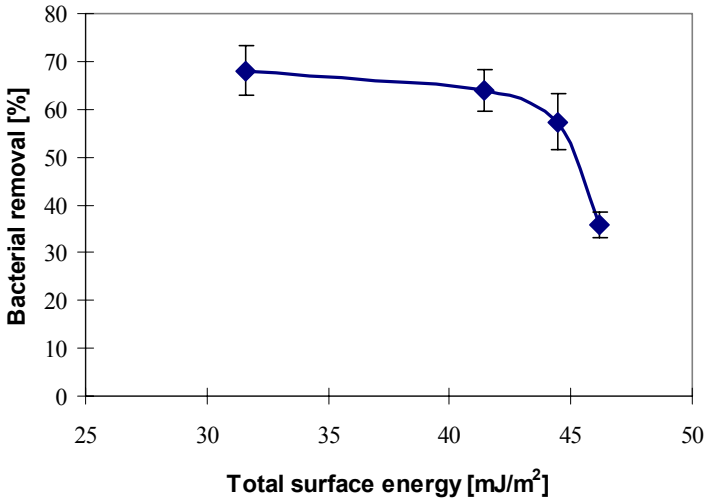

Figure 7.16: The effect of total surface energy of F-DLC coatings on removal of *Pseudomonas fluorescens* cells. N = 15, error bars are 2× Standard Error.

Figure 7.17 shows that the number of adhered *Staphylococcus aureus* decreased with increasing F contents in the F-DLC coatings. The F-DLC coatings with higher F content (39.2 at. %) reduced bacterial attachment by 67 %, compared with DLC coating.

Figure 7.18 indicates that percent bacterial removal increased significantly with increasing F content in the DLC coatings. The F-DLC coatings with the highest F content (39.2 at. %) increased removal rate 32 %, compared with DLC coating.

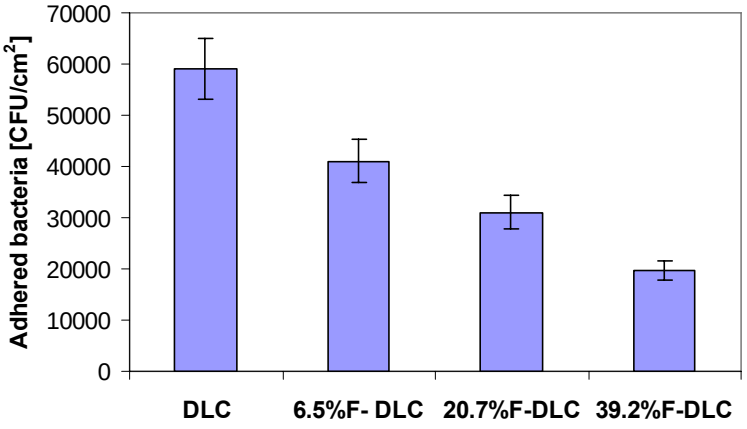

Figure 7.17: Comparison of formation of *Staphylococcus aureus* cells on F-DLC coatings and on DLC coatings. N = 15, error bars are 2× Standard Error.

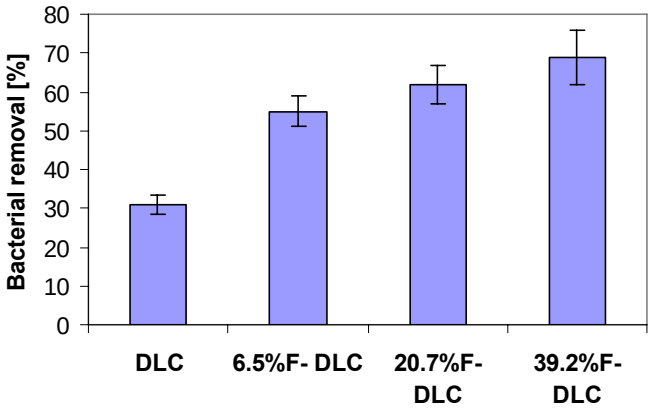

Figure 7.18: Comparison of removal of *Staphylococcus aureus* cells on F-DLC coatings and on DLC coatings. N = 15, error bars are 2× Standard Error.

Figure 7.19 shows that the number of adhered *Staphylococcus aureus* decreased with the total surface energy of the coatings decreasing.

Figure 7.20 shows that percentage of bacterial removal strongly correlated with the total surface energy of the F-DLC coatings. The percentage of bacterial removal increased with the total surface energy of the F-DLC coatings decreasing.

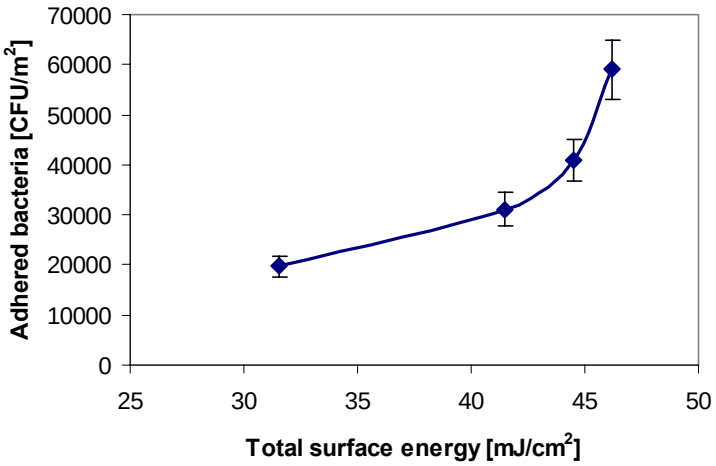

Figure 7.19 Effect of total surface energy of F-DLC coatings on adhesion of *Staphylococcus aureus* cells. N = 15, error bars are 2× Standard Error.

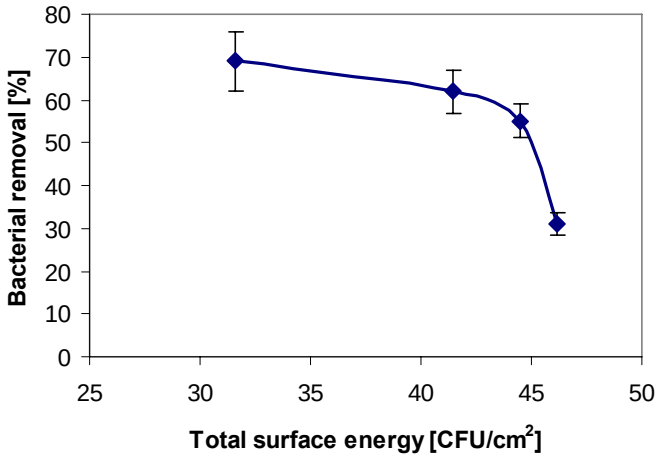

Figure 7.20: The effect of total surface energy of F-DLC coatings on removal of *Staphylococcus aureus* cells. N = 15, error bars are 2× Standard Error.

Summary and discussion:

The DLC and F-DLC coatings were prepared onto stainless steel substrates by radio frequency plasma-enhanced chemical vapour deposition. The surface energy of the F-DLC coatings decreased with increasing F content in the coatings. The incorporation of fluorine into the DLC coatings reduced significantly bacterial attachment and increased bacterial removal. The F-DLC coatings with higher F content (39.0 at. %) reduced bacterial attachment by 49-67 % and increased removal 32 %, compared with pure DLC coating. Both the initial bacterial attachment and the percent bacterial removal strongly correlated with the total surface energy of the coatings. Some of the research results were published in <*Surface & Coatings Technology*> (Su et al, 2009).

From the point of view of surface science, the bacterial adhesion on the coatings may be considered as an interaction between the bacteria and the coatings. In general, maximum adhesion occurs in systems undergoing a maximum decrease in surface energy and weakest fouling adhesion should occur on materials that have low surface energies. Therefore, it may be concluded that the prerequisite condition for a surface to possess low biofouling behaviour is that the surface should have a low surface energy.

F-doped diamond-like carbon coatings have favorable properties, such as excellent thermal conductivity similar to metals, low friction, extremely smooth surface, hardness, wear resistance and corrosion resistance, which are very suitable for heat exchanger applications. As the F-doped DLC coatings are biocompatible, they also have potential to reduce bacterial adhesion in biomedical devices and implants.

7.2.3 B-Doped DLC Coatings

The detailed procedure for preparing B-doped DLC coatings is given in Section 4.2.4. The chemical composition, contact angle and surface energy components of B-doped DLC coatings are given in Table 5.8.

These coatings were evaluated for attachment and removal with *Pseudomonas aeruginosa* and *Staphylococcus epidermidis,* respectively. The detailed procedures of bacterial adhesion and removal are described in Section 6.2: Bacterial Adhesion and

Removal. In brief, for bacterial attachment assays, five replicate samples of each coating were immersed in a glass tank containing 500 ml of a suspension of *P. aeruginosa* or *S. epidermidis* (10^6 cells ml^{-1}), incubated on a shaker (20 rpm) at 37 ˚C for different contact time, 1 h, 5h and 18h, respectively. To assess the adhesion strength of the attached bacteria or bacterial removal rate, each sample was dipped a further 20 times vertically in a glass vessel containing 130 ml sterile distilled water at 37 ˚C at a constant shear stress of 0.014 N m^{-2}.

To count the number of bacteria on coatings, the coatings were stained with LIVE/DEAD BacLight Kit L 13152 for 15 minutes and then observed under a fluorescence microscope (OLYMPUS BX 41, Japan) and counted using Image Pro Plus software (Media Cybernetics, USA). It was found that after the coatings were exposed to air for 15 minutes, some bacteria on the coatings were dead. Therefore the total bacteria on each coating are the sum of live bacteria (green colour) and dead bacteria (red colour) that were observed under the fluorescence microscope.

7.2.3.1 Contact time 1 h with *P. aeruginosa*

Figure 7.21 show typical images of live and dead *P. aeruginosa* cells on a DLC coating. For 4.9% B-DLC coatings, 7.6%B-DLC coatings and 9.5%B-DLC coatings, similar images were observed.

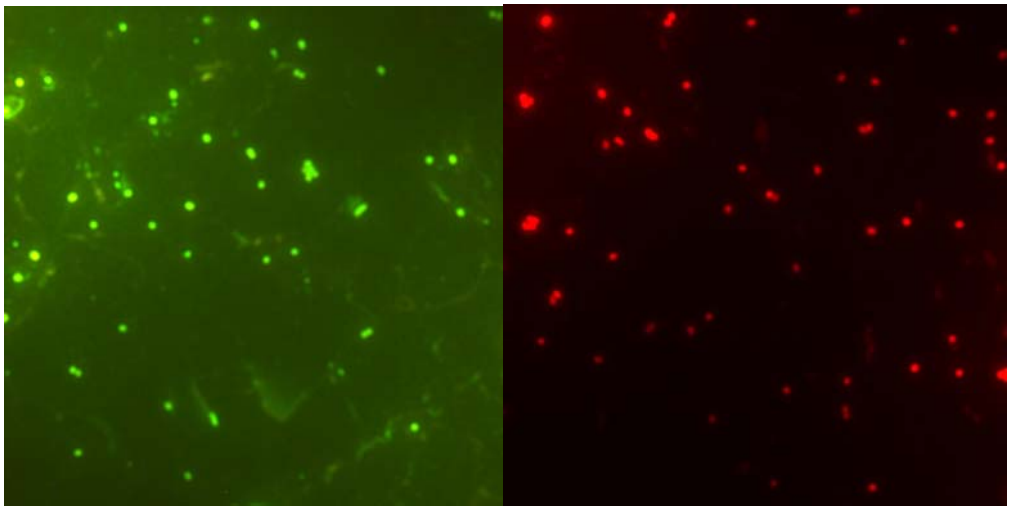

Figure 7.21 Live and dead *P. aeruginosa* cells on DLC coating
(Contact time: 1 h)

Figure 7.22 shows the attachment of *P. aeruginosa* cells on the B-DLC coatings for contact time 1 hour. After the coatings with bacteria were exposed to air for 15 minutes, some bacteria on the coatings were dead. Obviously all the B-DLC coatings performed much better than DLC coating against bacterial attachment. The number of adhered bacteria (live, dead and total bacteria) decreased with boron content increasing. The 9.5% B-DLC performed best, which reduced total bacterial adhesion by 70%, compared with pure DLC coating.

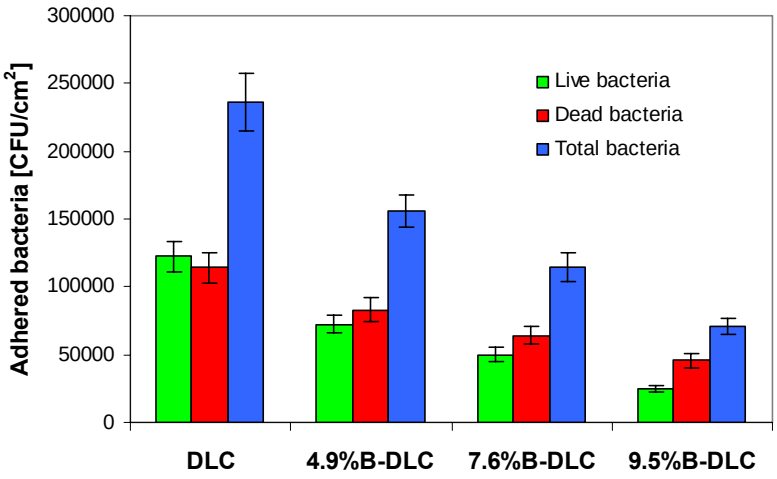

Figure 7.22 Attachment of *P. aeruginosa* cells on B-DLC coatings (Contact time: 1 h)

Figure 7.23 clearly shows that the live, dead and total *P. aeruginosa* cells on the B-DLC coatings decreased linearly with the boron content in the DLC coatings increasing.

Figure 7.24 shows that the live, dead and total *P. aeruginosa* cells on the B-DLC coatings decreased with the total surface energy of the B-DLC coatings decreasing. The results were consistent with previous results on the effect of total surface energy on bacterial adhesion. If the total surface energy approaches to 25 mJ/m^2, bacterial adhesion is minimal.

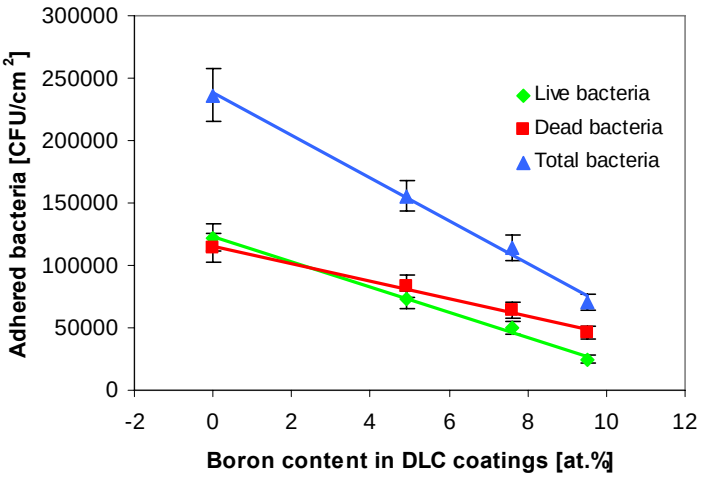

Figure 7.23 Effect of boron content on the number of live, dead and total *P. aeruginosa* cells on B-DLC coatings (Contact time: 1 h)

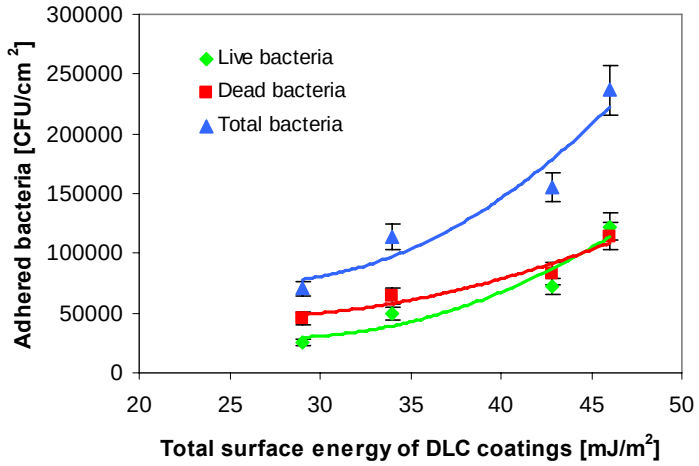

Figure 7.24 Effect of surface energy of B-DLC coatings on the attachment of live, dead and total *P. aeruginosa* cells (Contact time: 1 h)

In order to assess the adhesion strength of the attached bacteria, each sample with bacteria was dipped 20 times vertically in a glass vessel containing 130 ml sterile distilled water at 37 ˚C at a constant shear stress of 0.014 N m^{-2}. During the dipping process, some bacteria were removed from the coatings. The remaining bacteria on the coatings were observed under the fluorescence microscope (OLYMPUS BX 41, Japan) and counted using Image Pro Plus software (Media Cybernetics, USA).

Figure 7.25 shows the remaining *P. aeruginosa* cells on the B-DLC coatings after dipping process. The numbers of remaining bacteria (live, dead and total bacteria) decreased with boron content increasing. The remaining bacteria (live, dead and total bacteria) on the 9.5% B-DLC coatings were reduced by 87%, 77% and 83% respectively, compared with pure DLC coating.

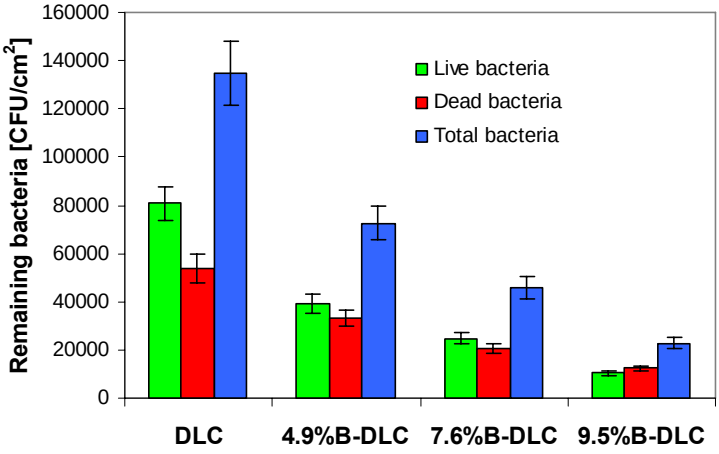

Figure 7.25 Remaining *P. aeruginosa* cells on B-DLC coatings after dipping process(Contact time: 1 h)

Figure 7.26 clearly shows that the remaining *P. aeruginosa* cells (live, dead and total bacteria) decreased linearly with boron content increasing.

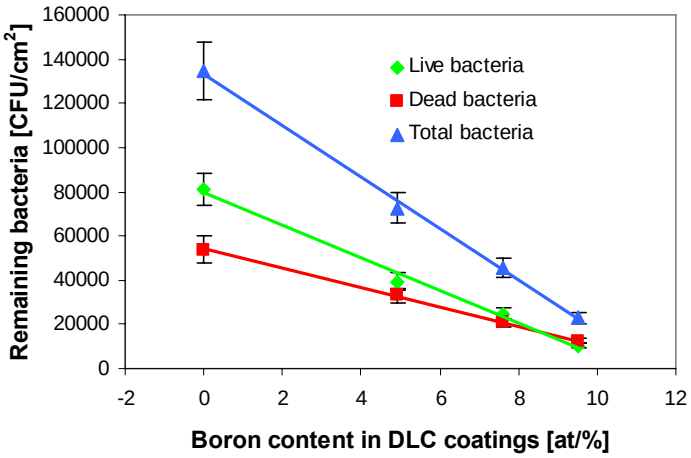

Figure 7.26 Effect of Boron content in DLC coatings on the remaining *P. aeruginosa* cells (Contact time: 1 h)

Figure 7.27 shows that the remaining *P. aeruginosa* cells (live, dead and total bacteria) on the B-DLC coatings decreased with the total surface energy of the B-DLC coatings decreasing. Again if the surface energy approaches 25mJ/m^2, the number of the remaining bacteria is minimal.

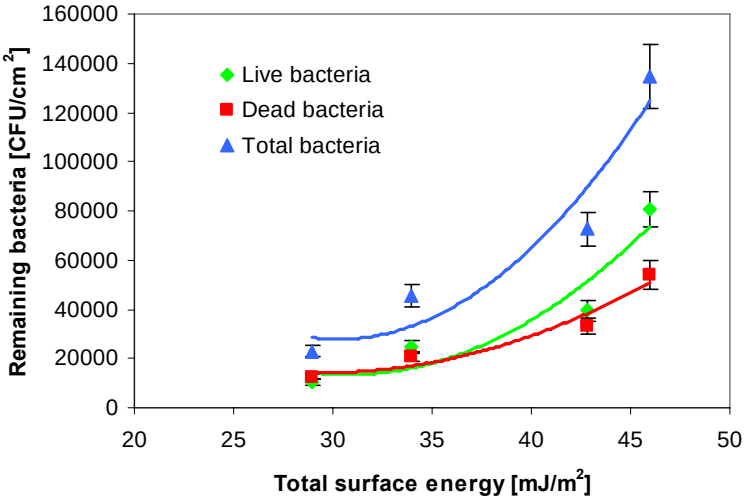

Figure 7.27 Effect of surface energy of B-DLC coatings on the remaining *P. aeruginosa* cells (Contact time: 1 h)

Figure 7.28 shows the removal percentage of *P. aeruginosa* cells from the B-DLC coatings after dipping process. The removal percentage of live, dead and total bacteria increased with boron content in the DLC coating increasing. The removal percentage of live, dead and total bacteria on the 9.5% B-DLC coatings was 58%, 73% and 68% respectively; while the removal percentage on the pure DLC coatings was only 34%, 53% and 43%. Figure 7.28 also indicates that the removal percentage of dead bacteria was higher than that of live bacteria. This means the dead bacteria were more easily removed than the live bacteria.

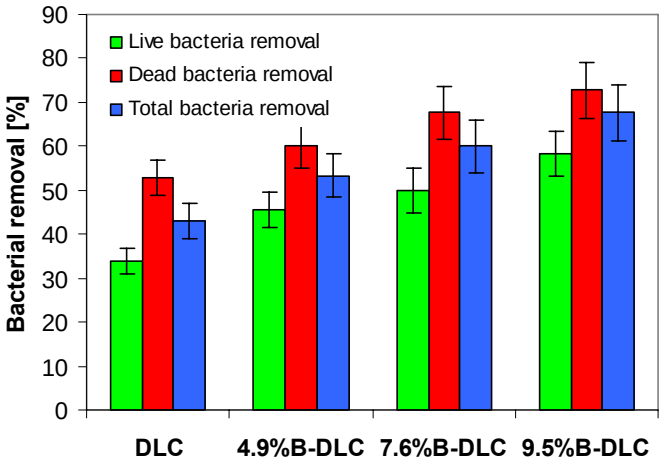

Figure 7.28 Removal percentage of *P. aeruginosa* cells from B-DLC coatings after dipping process (Contact time: 1 h)

7.2.3.2 Contact time 5 h with *P. aeruginosa*

Figure 7.29 shows the attachment of *P. aeruginosa* cells on the B-DLC coatings for a contact time of 5 hours. After the coatings with bacteria were exposed to air for 15 minutes, some bacteria on the coatings were dead. Obviously all the B-DLC coatings performed much better than DLC coating against bacterial attachment. The number of adhered bacteria (live, dead and total bacteria) decreased with boron content increasing. The 9.5% B-DLC performed best, which reduced bacterial adhesion (live, dead and total bacteria) by 43%, 46% and 44% respectively, compared with pure DLC coating.

Figure 7.30 clearly shows that the *P. aeruginosa* cells (live, dead and total) on the B-DLC coatings decreased linearly with the boron content in the DLC coatings increasing.

Figure 7.31 shows that the live, dead and total *P. aeruginosa* cells on the B-DLC coatings decreased with the total surface energy of the B-DLC coatings decreasing. The results were consistent with previous results on the effect of total surface energy on bacterial adhesion.

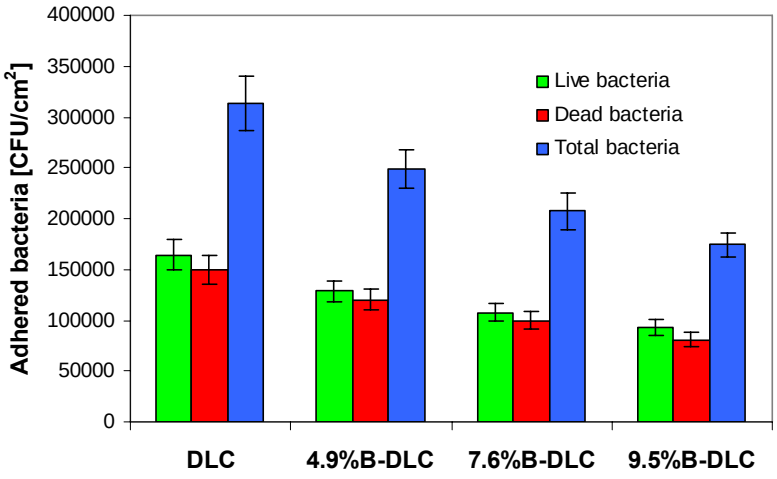

Figure 7.29 Attachment of *P. aeruginosa* cells on B-DLC coatings (Contact time: 5 h)

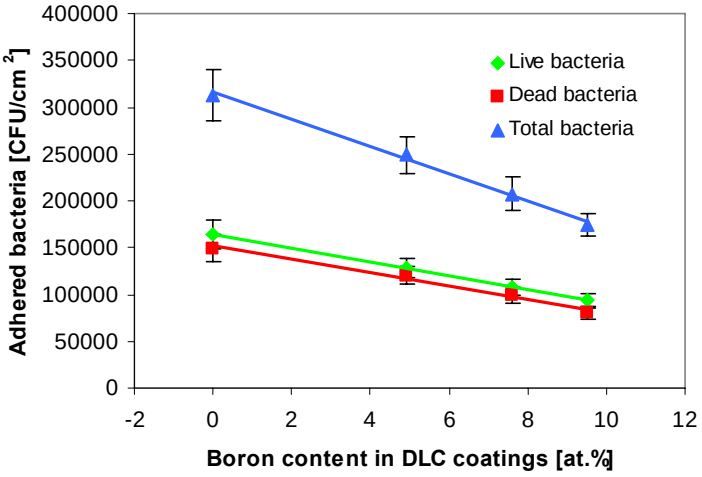

Figure 7.30 Effect of boron content on the number of live, dead and total *P. aeruginosa* cells on B-DLC coatings (Contact time: 5 h)

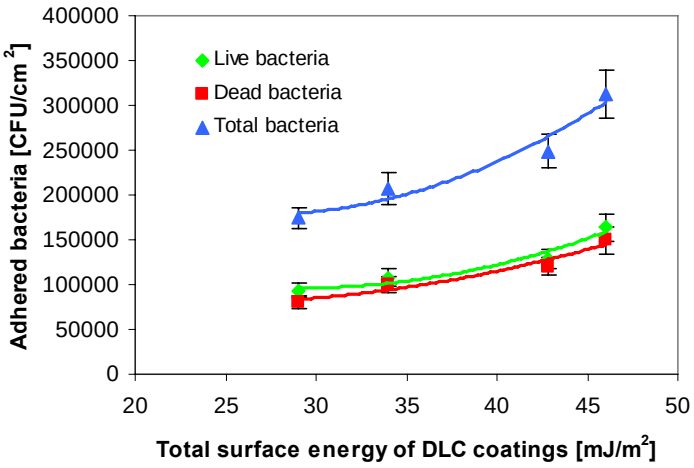

Figure 7.31 Effect of surface energy of B-DLC coatings
on the attachment of *P. aeruginosa* cells (Contact time: 5 h)

In order to assess the adhesion strength of the attached bacteria, each sample with bacteria was dipped 20 times vertically in a glass vessel containing 130 ml sterile distilled water at 37 ˚C at a constant shear stress of 0.014 N m^{-2}. During the dipping process, some bacteria were removed from the coatings. Figure 7.32 shows the remaining *P. aeruginosa* cells on the B-DLC coatings after dipping process. The numbers of remaining bacteria decreased with boron content increasing. The remaining bacteria (live, dead and total bacteria) on the 9.5% B-DLC coatings were reduced by 61%, 67% and 63% respectively, compared with pure DLC coating.

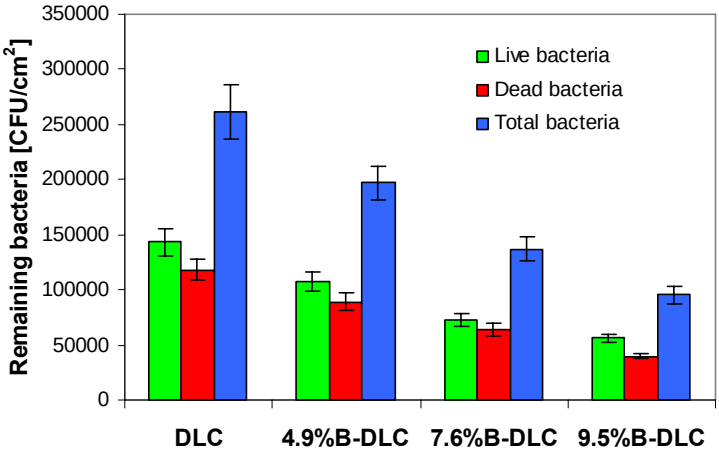

Figure 7.32 Remaining *P. aeruginosa* cells on B-DLC coatings after dipping process

Figure 7.33 clearly shows that the remaining *P. aeruginosa* cells (live, dead and total bacteria) decreased linearly with boron content increasing.

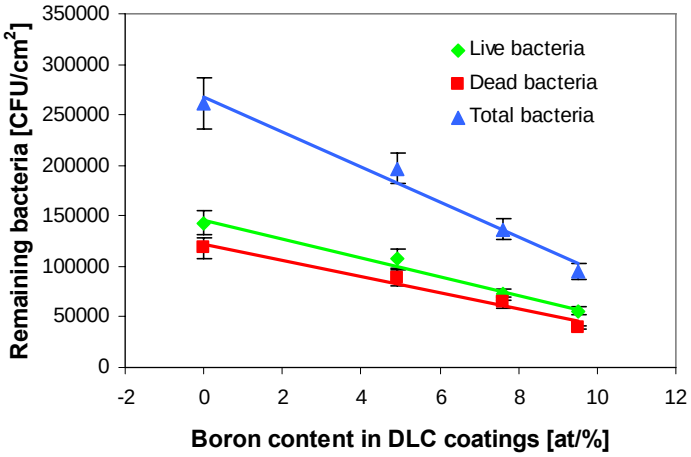

Figure 7.33 Effect of Boron content in DLC coatings on the remaining *P. aeruginosa* cells (Contact time: 5 h)

Figure 7.34 shows that the remaining *P. aeruginosa* cells (live, dead and total bacteria) on the B-DLC coatings decreased with the total surface energy of the B-DLC coatings decreasing.

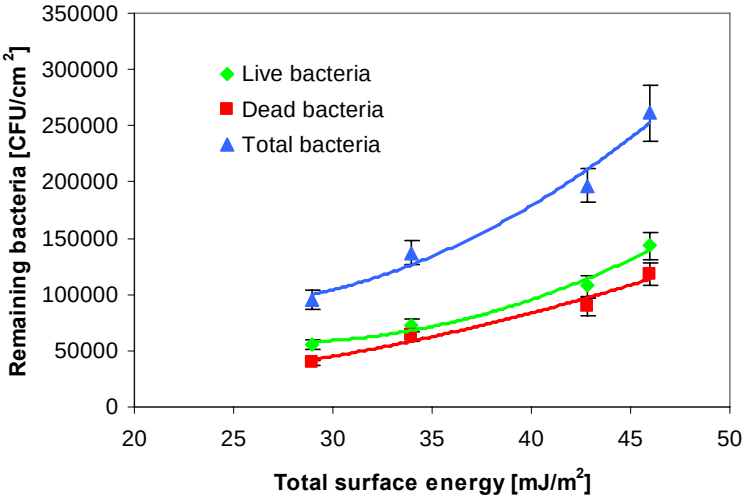

Figure 7.34 Effect of surface energy of B-DLC coatings on the remaining *P. aeruginosa* cells (Contact time: 5 h)

Figure 7.35 shows the removal percentage of *P. aeruginosa* cells from the B-DLC coatings after dipping process. The removal percentage of live, dead and total bacteria increased with boron content in the DLC coating increasing. The removal percentage of live, dead and total bacteria on the pure DLC coatings was only 13%, 21% and 17% , respectively; while the removal percentage of live, dead and total bacteria on the 9.5%B- DLC coatings was increased to 40%, 51% and 45% , respectively. Figure 7.35 also indicates that the removal percentage of dead bacteria was higher than that of live bacteria. This means the dead bacteria were more easily removed than the live bacteria.

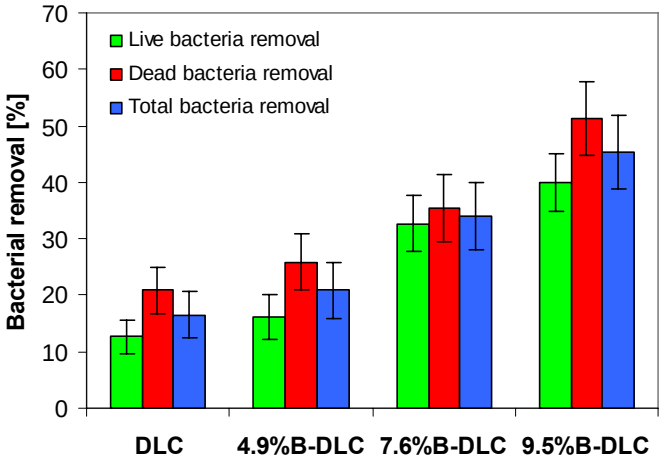

Figure 7.35 Removal percentage of *P. aeruginosa* cells from B-DLC coatings after dipping process (Contact time: 5 h)

7.2.3.3 Contact time 18 h with *P. aeruginosa*

Figure 7.36 shows the attachment of *P. aeruginosa* cells on the B-DLC coatings for a contact time of 18 hours. After the coatings with bacteria were exposed to air for 15 minutes, some bacteria on the coatings were dead. All the B-DLC coatings performed much better than DLC coating against bacterial attachment. The number of adhered bacteria (live, dead and total bacteria) decreased with boron content increasing. The 9.5% B-DLC performed best, which reduced bacterial adhesion (live, dead and total bacteria) by 52%, 47% and 50% respectively, compared with pure DLC coating.

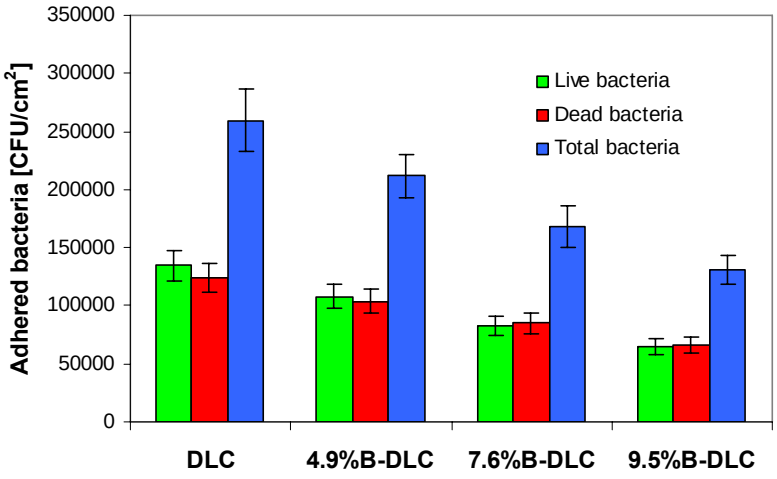

Figure 7.36 Attachment of *P. aeruginosa* cells on B-DLC coatings (Contact time: 18 h)

Figure 7.37 clearly shows that the *P. aeruginosa* cells (live, dead and total) on the B-DLC coatings decreased linearly with the boron content in the DLC coatings increasing.

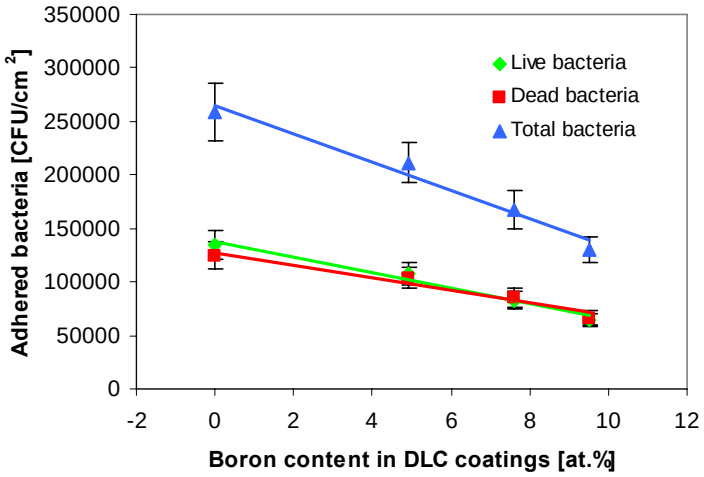

Figure 7.37 Effect of boron content on the number of live, dead and total *P. aeruginosa* cells on B-DLC coatings (Contact time: 18 h)

Figure 7.38 shows that the live, dead and total *P. aeruginosa* cells on the B-DLC coatings decreased with the total surface energy of the B-DLC coatings decreasing. The results were consistent with previous results on the effect of total surface energy on bacterial adhesion.

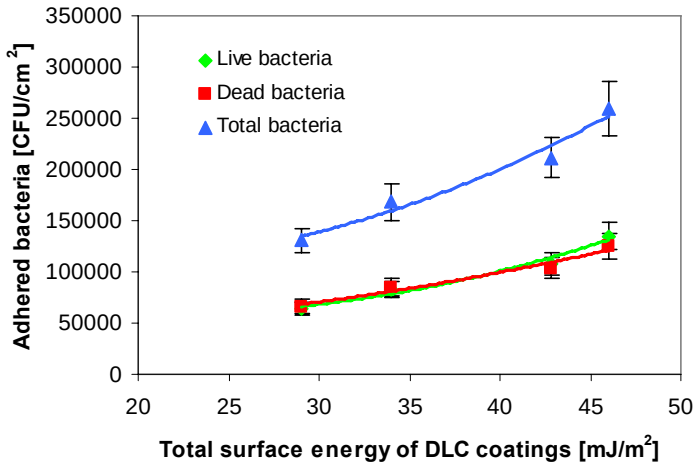

Figure 7.38 Effect of surface energy of B-DLC coatings
on the attachment of *P. aeruginosa* cells (Contact time: 18 h)

In order to assess the adhesion strength of the attached bacteria, each sample with bacteria was dipped 20 times vertically in a glass vessel containing 130 ml sterile distilled water at 37 ˚C at a constant shear stress of 0.014 N m^{-2}. During the dipping process, some bacteria were removed from the coatings. The remaining bacteria on the coatings were observed under the fluorescence microscope and counted using Image Pro Plus software.

Figure 7.39 shows the remaining *P. aeruginosa* cells on the B-DLC coatings after dipping process. The numbers of remaining bacteria (live, dead and total bacteria) decreased with boron content increasing. The remaining bacteria (live, dead and total bacteria) on the 9.5% B-DLC coatings were reduced by 63%, 58% and 61% respectively, compared with pure DLC coating.

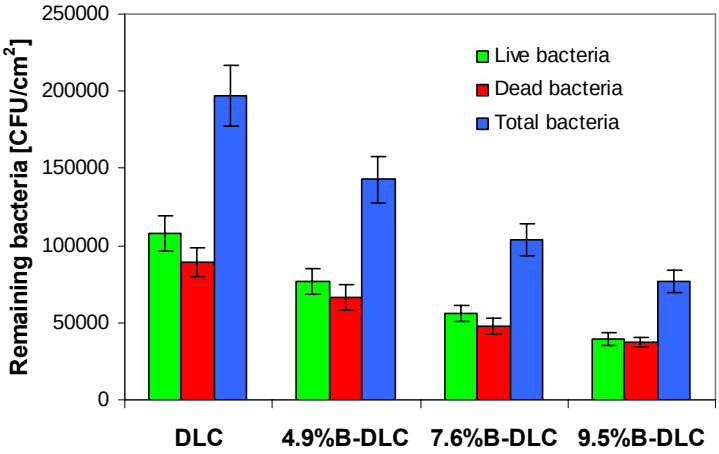

Figure 7.39 Remaining *P. aeruginosa* cells on B-DLC coatings after dipping process (Contact time: 18 h).

Figure 7.40 clearly shows that the remaining *P. aeruginosa* cells (live, dead and total bacteria) decreased linearly with boron content increasing.

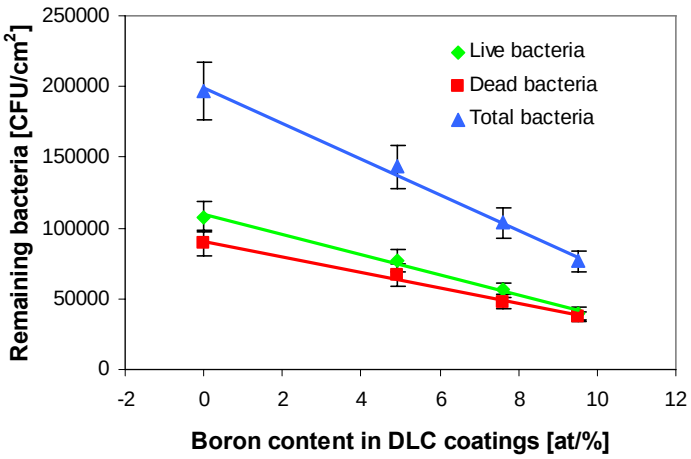

Figure 7.40 Effect of Boron content in DLC coatings on the remaining *P. aeruginosa* cells (Contact time: 18 h)

Figure 7.41 shows that the remaining *P. aeruginosa* cells (live, dead and total bacteria) on the B-DLC coatings decreased with the total surface energy of the B-DLC coatings decreasing.

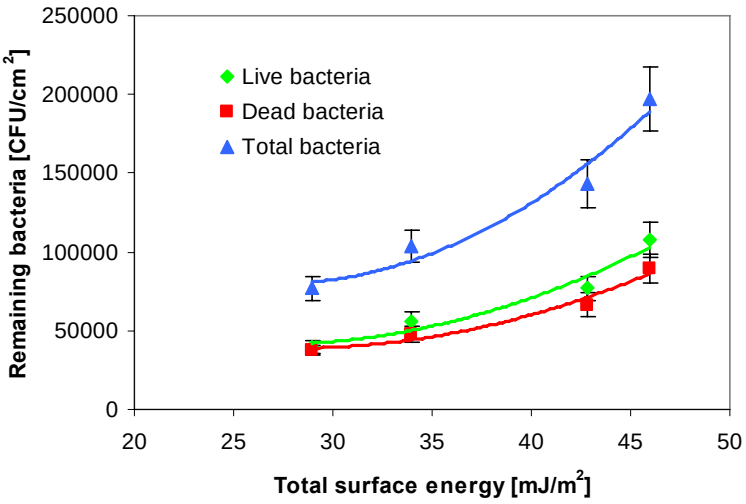

Figure 7.41 Effect of surface energy of B-DLC coatings on the remaining *P. aeruginosa* cells (Contact time: 18 h).

Figure 7.42 shows the removal percentage of *P. aeruginosa* cells from the B-DLC coatings after dipping process. The bacterial removal percentage increased with boron content in the DLC coating increasing. The removal percentage of live, dead and total bacteria on the pure DLC coatings was only 20%, 28% and 24%, respectively; while the removal percentage of live, dead and total bacteria on the 9.5%B- DLC coatings was increased to 39%, 44% and 41%, respectively. The removal percentage of dead bacteria was higher than that of live bacteria.

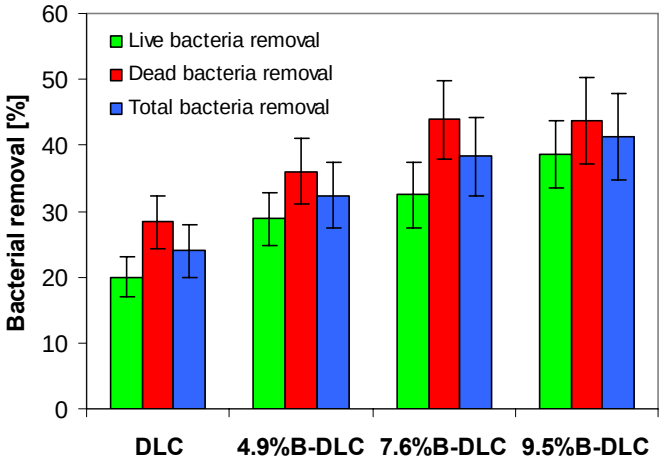

Figure 7.42 Removal percentage of *P. aeruginosa* cells from the B-DLC coatings after dipping process (Contact time: 18 h).

7.2.3.4 Effect of Contact Time on *P. aeruginosa* Adhesion

Figure 7.43 shows the effect of contact time (1 hour, 5 hour and 18 hours) on the attachment of live, dead and total *P. aeruginosa* cells on the B-DLC coatings. When contact time increased to 5 hours from 1 hour more bacteria attached to each type of the coatings. However when contact time increased to 18 hours from 5 hour the number of adhered bacteria on the coatings decreased. Due to lack of nutrients, the number of dead *P. aeruginosa* cells in bacterial suspension and on the coatings increased with time increasing. As a result, less bacteria attached to the coatings and some adhered bacteria were also detached from the coatings (Zhao et al 2007, 2008).

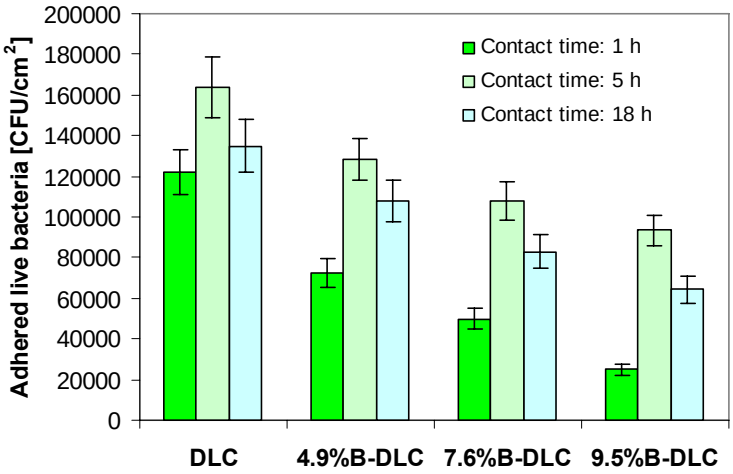

(a)

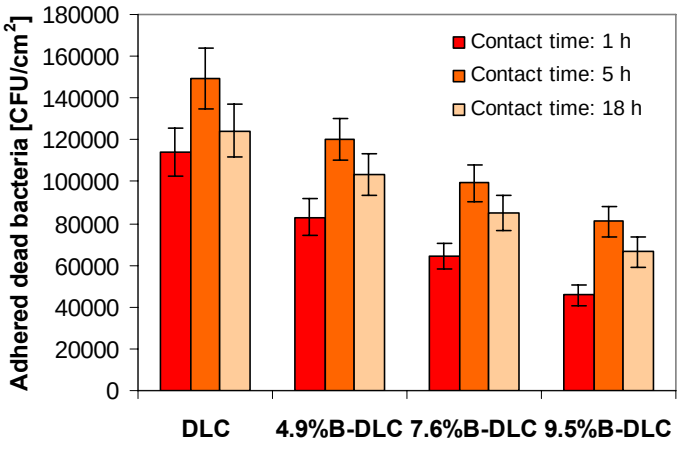

(b)

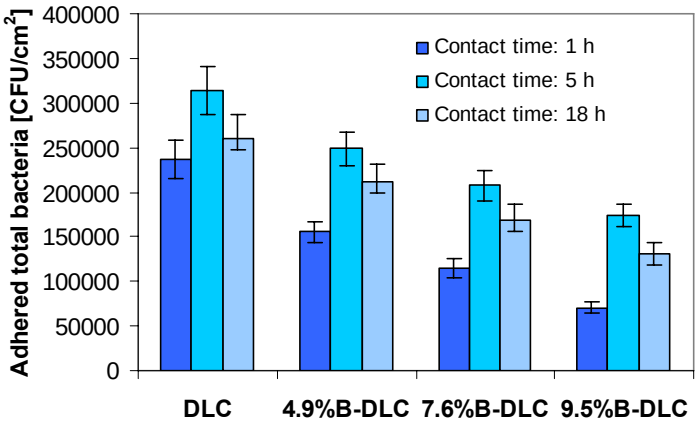

(c)

Figure 7.43 Effect of contact time on the attachment of live (a), dead (b) and total (c) *P. aeruginosa* cells on B-DLC coatings

Figure 7.44 shows the effect of contact time (1 hour, 5 hour and 18 hours) on the removal of live, dead and total *P. aeruginosa* cells on the B-DLC coatings. For contact time 1 hour, the bacterial removal percentage was much higher than those for contact time 5 h and 18 h. For contact time 1 h, the initial bacterial adhesion to the coatings was weak. However when contact time increased to 5 h or 18 h, the bacterial adhesion strength increased significantly as live bacteria on the coatings started producing sticky exopolymer (Bos R *et al.*, 1999). This explains Figure 7.44a why the bacterial removal percentage for contact time 1 hour was higher than that for contact time 5 h or 18 h. For Figure 7.44b, most bacteria on the coatings had produced exopolymer after 5 or 18 h contact before they were dead, so the dead bacterial adhesion strength was higher than the dead bacteria for contact time 1 h.

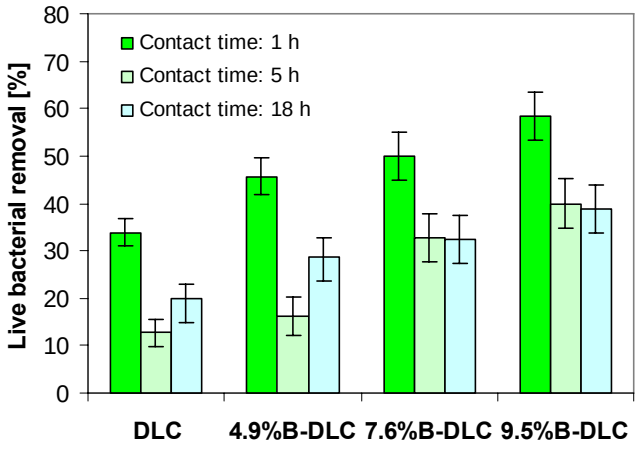

(a)

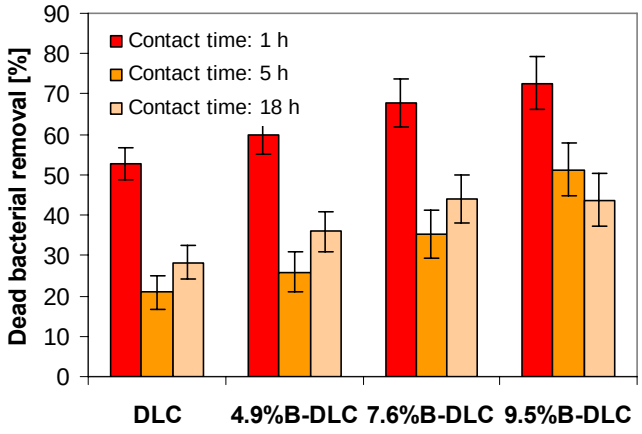

(b)

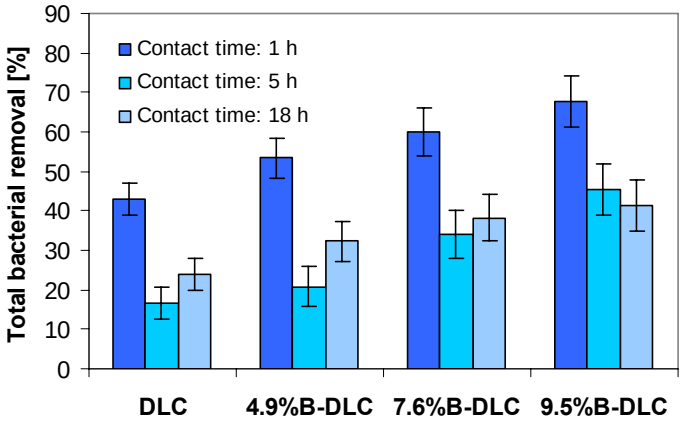

(c)

Figure 7.44 Effect of contact time on the removal of live (a), dead (b) and total (c) *P. aeruginosa* cells on B-DLC coatings

7.2.3.5 Contact time 1 h with *S. epidermidis*

The B-DLC coatings were evaluated with *S. epidermidis* and very similar results to *P. aeruginosa* were obtained. The number of adhered *S. epidermidis* cells (live, dead and total bacteria) decreased linearly with boron content increasing (Figure 7.45), but decreased with the total surface energy of the B-DLC coatings decreasing (Figure 7.46). The 9.5% B-DLC performed best, which reduced total bacterial adhesion by 57%, compared with pure DLC coating.

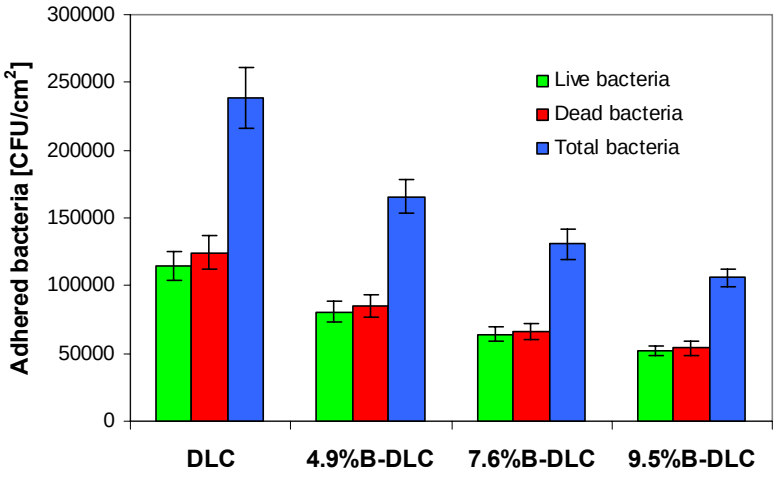

Figure 7.45 Attachment of *S. epidermidis* cells on the B-DLC coatings (Contact time: 1 h)

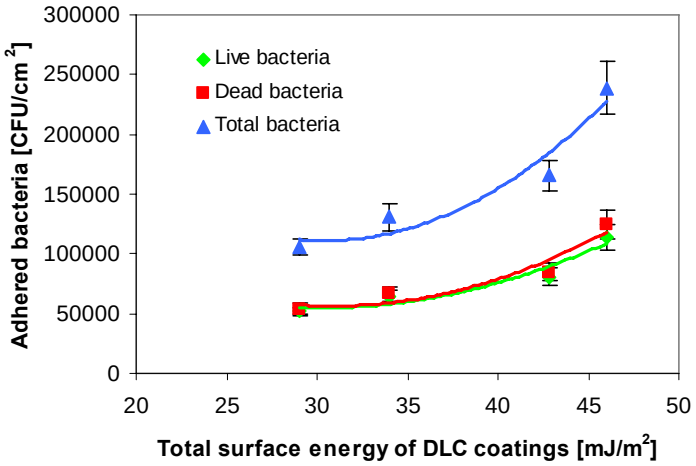

Figure 7.46 Effect of surface energy of B-DLC coatings on the attachment of live, dead and total *S. epidermidis* cells (Contact time: 1 h)

The remaining *S. epidermidis* cells on the B-DLC coatings after dipping process also decreased with boron content increasing (Figure 7.47), but decreased with the total surface energy of the B-DLC coatings decreasing (Figure 7.48).

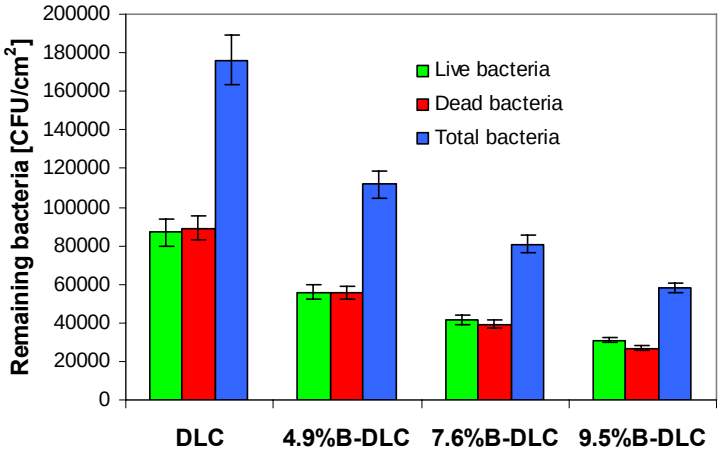

Figure 7.47 Remaining *S. epidermidis* cells on the B-DLC coatings after dipping process(Contact time: 1 h)

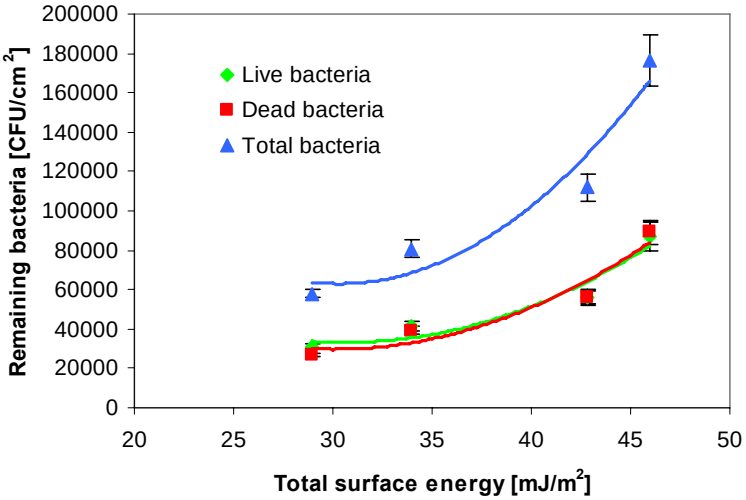

Figure 7.48 Effect of surface energy of B-DLC coatings on the remaining *S. epidermidis* cells (Contact time: 1 h)

The removal percentage of *S. epidermidis* cells from the B-DLC coatings after dipping process increased with boron content in the DLC coating increasing, as shown in Figure 7.49. The removal percentage of live, dead and total bacteria on the 9.5% B-DLC coatings was 40%, 50% and 45% respectively; while the removal percentage on the pure DLC coatings was only 24%, 28% and 26%.

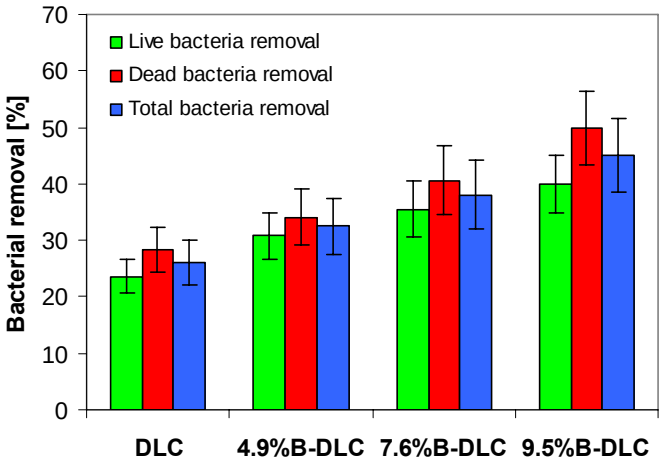

Figure 7.49 Removal percentage of *S. epidermidis* cells from the B-DLC coatings after dipping process (Contact time: 1 h)

7.2.3.6 Contact time 5 h with *S. epidermidis*

The results for contact time 5 h show that the number of adhered *S. epidermidis* cells (live, dead and total bacteria) decreased linearly with boron content increasing (Figure 7.50), but decreased with the total surface energy of the B-DLC coatings decreasing (Figure 7.51). The 9.5% B-DLC performed best, which reduced bacterial adhesion (live, dead and total bacteria) by 41%, 46% and 44% respectively, compared with pure DLC coating.

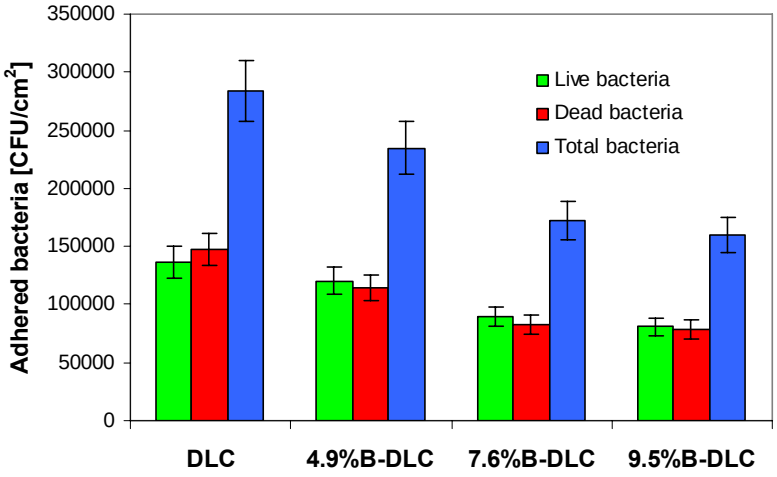

Figure 7.50 Attachment of *S. epidermidis* cells on the B-DLC coatings (Contact time: 5 h)

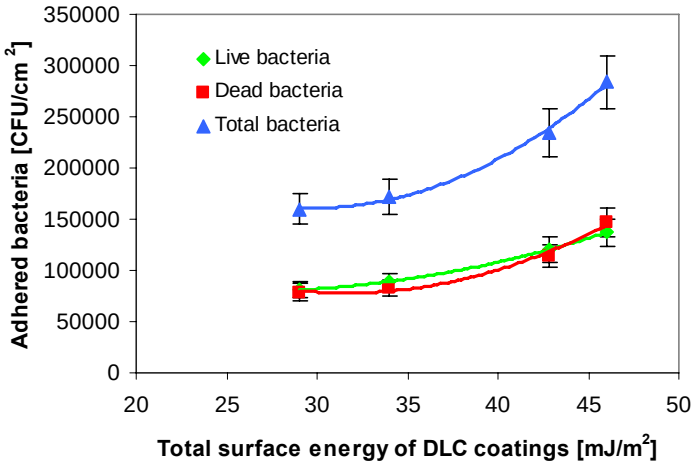

Figure 7.51 Effect of surface energy of B-DLC coatings on the attachment of *S. epidermidis* cells (Contact time: 5 h)

The remaining *S. epidermidis* cells on the B-DLC coatings after dipping process decreased with boron content increasing (Figure 7.52), but decreased with the total surface energy of the B-DLC coatings decreasing (Figure 7.53). The remaining bacteria (live, dead and total bacteria) on the 9.5% B-DLC coatings were reduced by 55%, 60% and 58% respectively, compared with pure DLC coating.

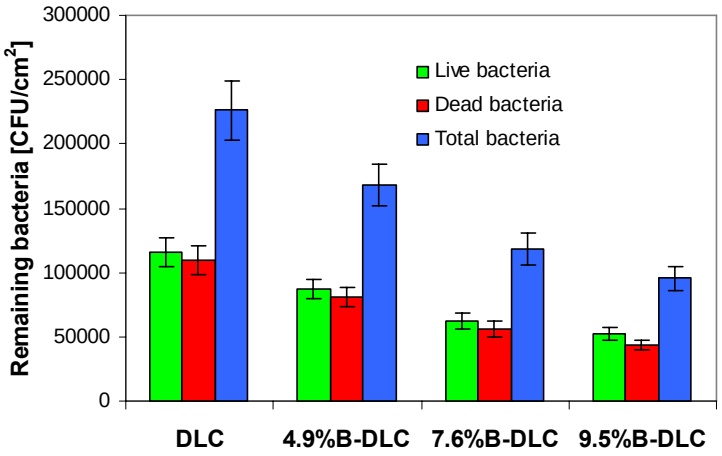

Figure 7.52 Remaining *S. epidermidis* cells on the B-DLC coatings after dipping process (Contact time: 5 h)

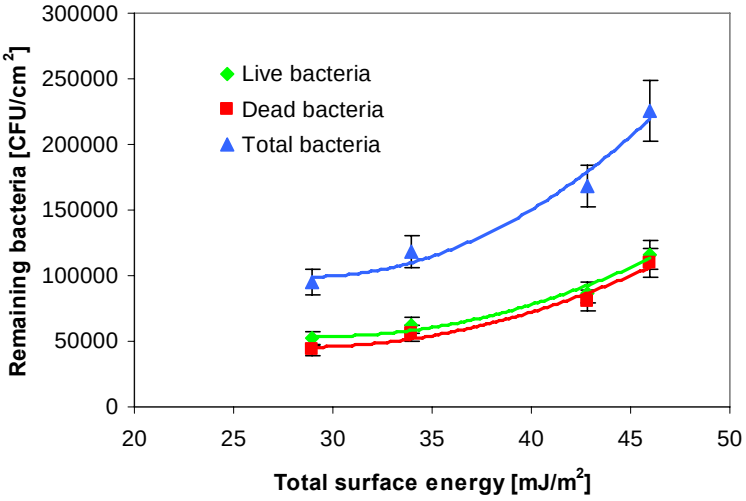

Figure 7.53 Effect of surface energy of B-DLC coatings on the remaining *S. epidermidis* cells (Contact time: 5 h)

Figure 7.54 shows the removal percentage of *S. epidermidis* cells from the B-DLC coatings after dipping process. The removal percentage of live, dead and total bacteria increased with boron content in the DLC coating increasing. The removal percentage of

live, dead and total bacteria on the pure DLC coatings was only 15%, 25% and 20% , respectively; while the removal percentage of live, dead and total bacteria on the 9.5%B- DLC coatings was increased to 36%, 45% and 40% , respectively. Figure 7.54 also indicates that the removal percentage of dead bacteria was higher than that of live bacteria. This means the dead bacteria were more easily removed than the live bacteria.

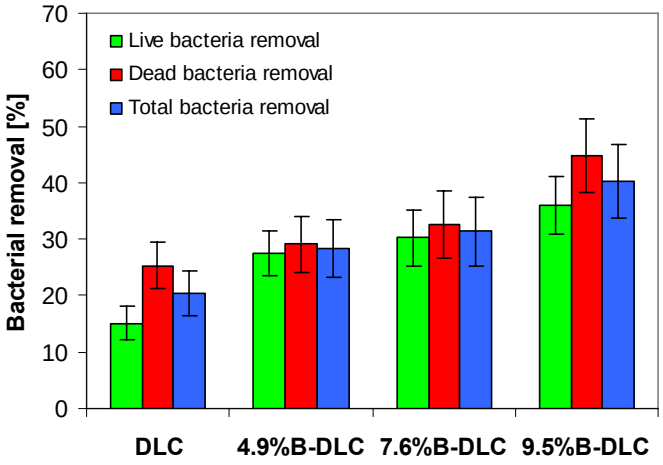

Figure 7.54 Removal percentage of *S. epidermidis* cells from the B-DLC coatings after dipping process (Contact time: 5 h)

7.2.3.7 Contact time 18 h with *S. epidermidis*

For contact time 18 h the number of adhered *S. epidermidis* cells (live, dead and total bacteria) decreased linearly with boron content increasing (Figure 7.55), but decreased with the total surface energy of the B-DLC coatings decreasing (Figure 7.56). The 9.5% B-DLC performed best, which reduced bacterial adhesion (live, dead and total bacteria) by 44%, 49% and 46% respectively, compared with pure DLC coating.

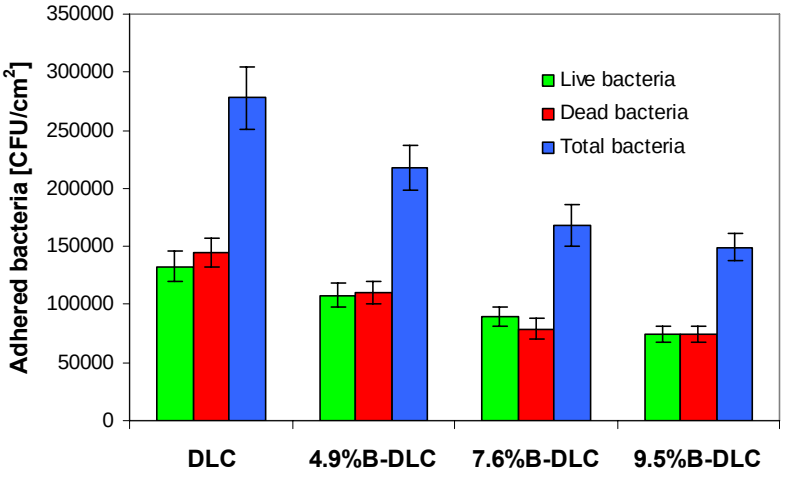

Figure 7.55 Attachment of *S. epidermidis* cells on the B-DLC coatings (Contact time: 18 h)

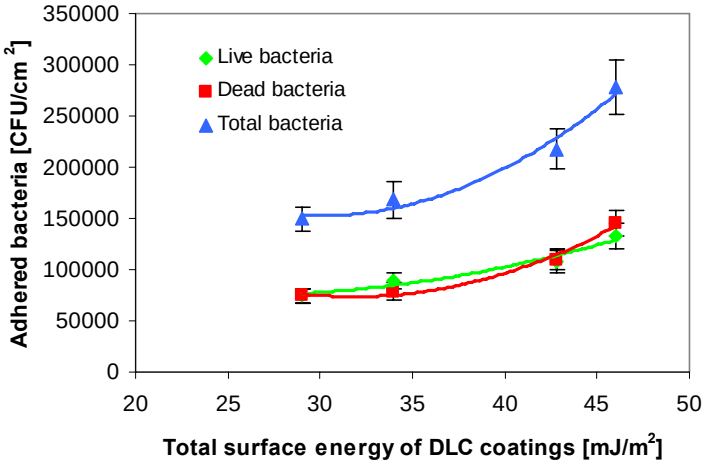

Figure 7.56 Effect of surface energy of B-DLC coatings on the attachment of *S. epidermidis* cells (Contact time: 18 h)

After dipping process the numbers of remaining *S. epidermidis* cells (live, dead and total bacteria) decreased linearly with boron content increasing (Figure 7.57), but decreased with the total surface energy of the B-DLC coatings decreasing (Figure 7.58). The remaining bacteria (live, dead and total bacteria) on the 9.5% B-DLC coatings were reduced by 58%, 61% and 59% respectively, compared with pure DLC coating.

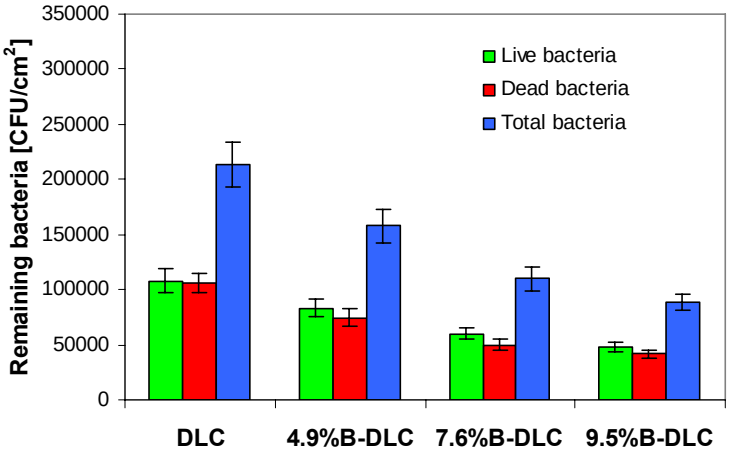

Figure 7.57 Remaining *S. epidermidis* cells on the B-DLC coatings after dipping process (Contact time: 18 h).

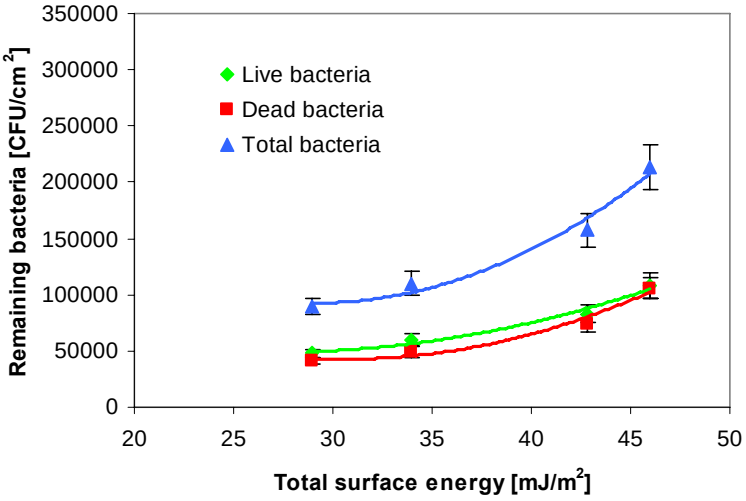

Figure 7.58 Effect of surface energy of B-DLC coatings on the remaining *S. epidermidis* cells (Contact time: 18 h).

Figure 7.59 shows the removal percentage of *S. epidermidis* cells from the B-DLC coatings after dipping process. The bacterial removal percentage increased with boron content in the DLC coating increasing. The removal percentage of live, dead and total bacteria on the pure DLC coatings was only 19%, 27% and 23%, respectively; while the removal percentage of live, dead and total bacteria on the 9.5%B- DLC coatings was increased to 39%, 44% and 42%, respectively. The removal percentage of dead bacteria was higher than that of live bacteria.

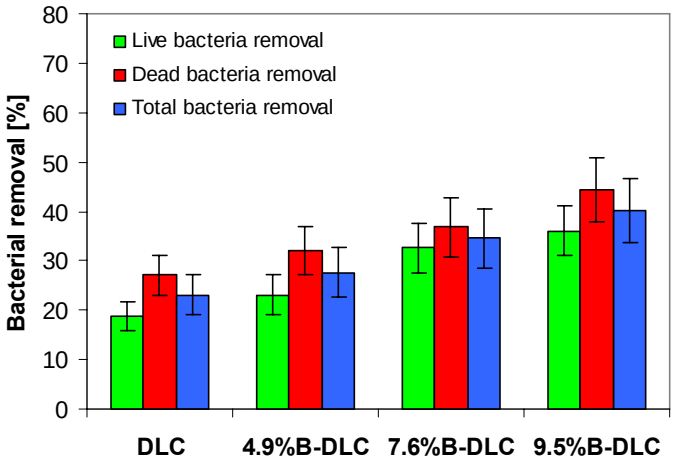

Figure 7.59 Removal percentage of *S. epidermidis* cells from the B-DLC coatings after dipping process (Contact time: 18 h).

7.2.3.8 Effect of Contact Time on *S. epidermidis* Adhesion

Figure 7.60 shows the effect of contact time (1 hour, 5 hour and 18 hours) on the attachment of total *S. epidermidis* cells on the B-DLC coatings. Initially the number of adhered bacteria increased with contact time increasing until 5 h. However due to lack of nutrients, some *S. epidermidis* cells were dead, leading to the number of adhered bacteria at 18 h was slightly lower than that at 5 h.

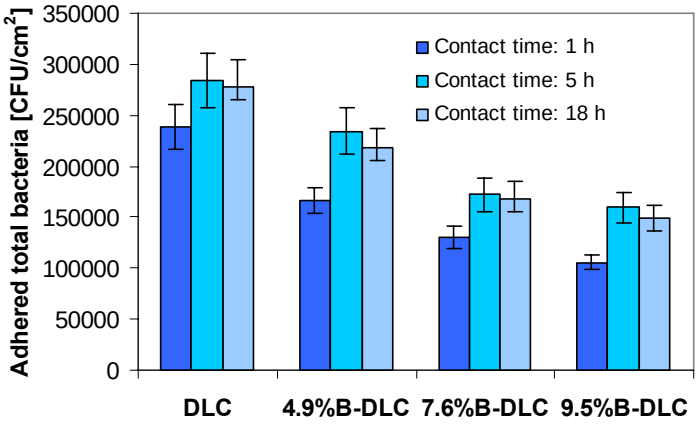

Figure 7.60 Effect of contact time on the attachment of *S. epidermidis* cells on B-DLC coatings

Figure 7.61 shows the effect of contact time (1 hour, 5 hour and 18 hours) on the removal of total *S. epidermidis* cells on the B-DLC coatings. For contact time 1 hour, the bacterial removal percentage was much higher than those for contact time 5 h and 18 h. For contact time 1 h, the initial bacterial adhesion to the coatings was weak. However when contact time increased to over 5 h, the bacterial adhesion strength increased significantly as bacteria on the coatings started producing sticky exopolymer (Bos R *et al.*, 1999).

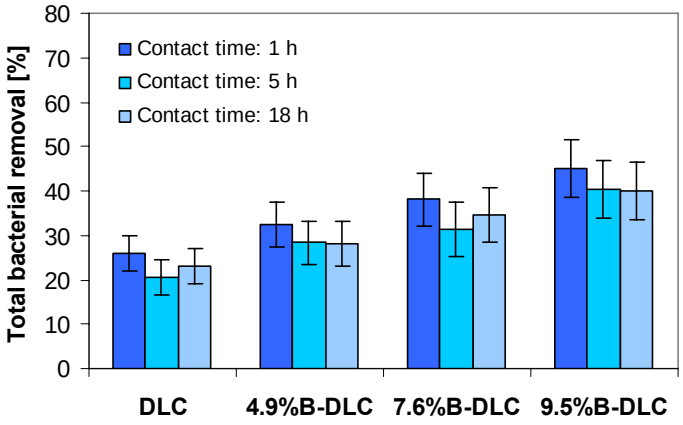

Figure 7.61 Effect of contact time on the removal of *S. epidermidis* cells on B-DLC coatings

Summary and discussion:

The experimental results showed that the surface energy of the B-DLC coatings decreased with increasing B content in the coatings. The incorporation of Boron into the DLC coatings reduced significantly bacterial attachment and increased bacterial removal.

It was observed that after the coatings with bacteria were exposed to air for 15 minutes, some bacteria on the coatings were dead. The numbers of adhered bacteria (live, dead and total *P. aeruginosa* and *S. epidermidis*) decreased with boron content increasing or with the total surface energy of the B-DLC coatings decreasing. The 9.5% B-DLC performed best, which reduced total bacterial adhesion by up to 70%, compared with pure DLC coating.

In order to assess the adhesion strength of the attached bacteria, some bacteria on the coatings were removed through the dipping process. The numbers of remaining bacteria (live, dead and total *P. aeruginosa* and *S. epidermidis*) also decreased with boron content increasing or with the total surface energy of the B-DLC coatings decreasing. The remaining bacteria (live, dead and total bacteria) on the 9.5% B-DLC coatings were reduced by up to 87%, 77% and 83% respectively, compared with pure DLC coating.

The removal percentage of the bacteria (live, dead and total *P. aeruginosa* and *S. epidermidis*) increased with boron content increasing or with the total surface energy of the B-DLC coatings decreasing. The removal percentage of live, dead and total bacteria on the 9.5% B-DLC coatings increased by up to 207%, 142% and 164% respectively, compared with pure DLC coatings. The dead bacteria were more easily removed than the live bacteria.

In this study the contact time (1 hour, 5 hour and 18 hours) had significant influence on the attachment of live, dead and total *P. aeruginosa* and *S. epidermidis* cells on the B-DLC coatings. In general, the numbers of adhered bacteria increased with contact time increasing. However when contact time increased to 18 hours the number of adhered bacteria on the coatings decreased due to lack of nutrients for bacteria to survive. The contact time also had significant influence on the bacterial removal. For contact time 1 hour, the bacterial removal percentage was much higher than those for contact time 5 h and 18 h as bacteria on the coatings started producing sticky exopolymer with contact time increasing.

7.2.4 Ti-Doped DLC Coatings

The detailed procedure for preparing titanium-doped DLC coatings is given in Section 4.2.4. The chemical composition, contact angle and surface energy components of Ti-doped DLC coatings are given in Table 5.8.

These coatings were evaluated for attachment and removal with *E. coli* for contact time 1 h and 5h. The detailed procedures of bacterial adhesion and removal are described in

Section 6.2: Bacterial Adhesion and Removal. The numbers of bacteria on the coatings were observed under a fluorescence microscope and counted using Image Pro Plus software as described previously.

7.2.4.1 Contact time 1 h with *E. coli*

Figures 7.62 and 7.63 show the attachment of *E. coli* cells on the Ti-DLC coatings for contact time 1 hour. After the coatings with bacteria were exposed to air for 15 minutes, some bacteria on the coatings were dead. Both pure DLC coating and the Ti-DLC coatings performed much better than stainless steel against bacterial attachment. The number of adhered bacteria (live, dead and total bacteria) decreased linearly with Ti content increasing (Figure 7.63). The 3.2% Ti-DLC performed best, which reduced total bacterial adhesion by 75% and 66% respectively, compared with stainless steel and pure DLC coating.

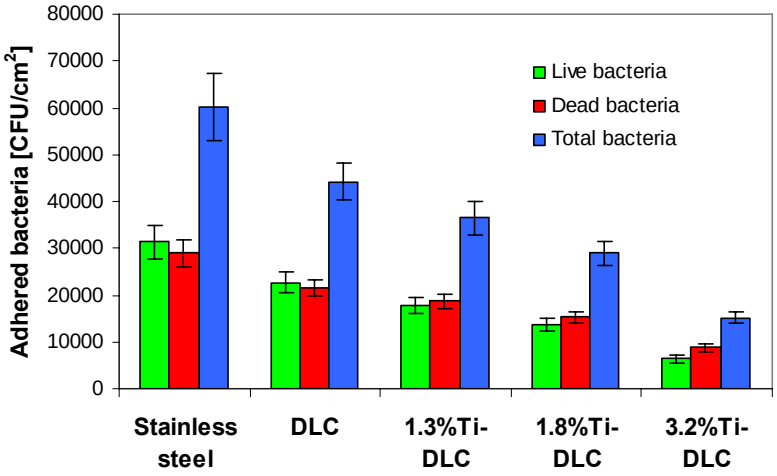

Figure 7.62 Attachment of *E. coli* cells on Ti-DLC coatings
(Contact time: 1 h)

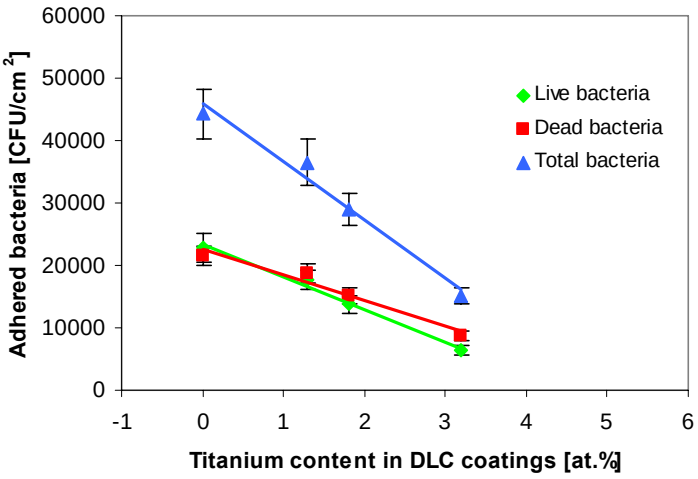

Figure 7.63 Effect of Titanium content on the attachment of *E. coli* cells on Ti-DLC coatings (Contact time: 1 h)

The improved anti-bacterial properties of Ti-DLC coatings with Ti content increasing could be due to electron donor γ^- increasing and titanium oxide (e.g. TiOx or TiO_2) increasing.

Table 5.8 indicates that the γ^- surface energy component of Ti-DLC coatings increased with Ti content increasing. In general bacteria are negatively charged. It was reported that the larger the electron donor component γ^- of a surface, the more negatively charged the surface (Chibowski et al. 1994). Therefore bacterial adhesion should decrease with increasing electron donor γ^- values of the coatings if other parameters that affect bacterial adhesion are identical. In this study the total surface energies of Ti-DLC coatings were almost same, about 44 mJ/m^2, but γ^- values were changed in the range of 4.47- 9.83 mJ/m^2 (see Table 5.8).

Figure 7.64 shows that the live, dead and total *E. coli* cells on the Ti-DLC coatings decreased linearly with the γ^- surface energy of the Ti-DLC coatings increasing.

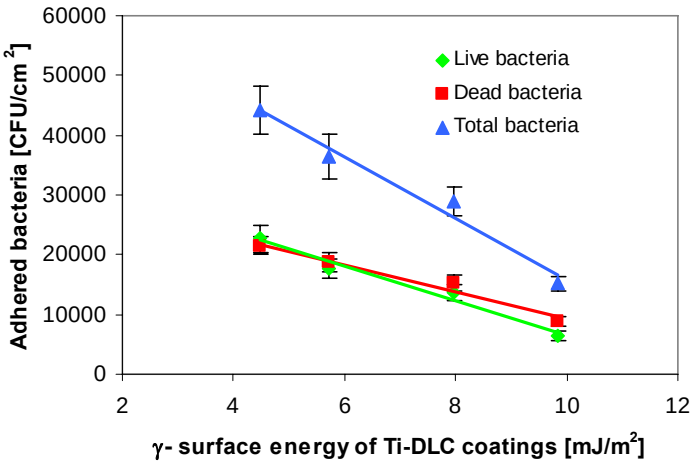

Figure 7.64 Effect of γ^- surface energy of Ti-DLC coatings on the attachment of *E. coli* cells (Contact time: 1 h)

The microbiocidal effect of TiO_2 photocatalytic reactions was first reported by Matsunaga et al (1985). The microbiocidal mechanisms of TiO_2 photocatalysts have been investigated in details by Huang et al (2000) and Wang et al (2000). It is suggested that TiO_2 photocatalysts generate strong oxidizing power when illuminated with UV light with wave-lengths of less than 385 nm. The initial oxidative damage takes place on the cell wall when contact with the TiO_2 photocatalytic surface. Then the further oxidative damage takes place on the underlying cytoplasmic membrane, leading to cell death. Kikuchi *et al.* (1997) showed that TiO_2 films coated on different substrates such as glass, tiles and stainless steel possessed antibacterial functions under weak ultraviolet light in living areas and the viable number of *Escherichia coli* significantly decreased on the illuminated TiO_2 film. Li and Logan (2005) reported that bacterial adhesion on TiO_2 coated surfaces reduced significantly after exposed UV light. In this study all the Ti-DLC coatings had been treated with UV light for 1 hour before they were tested with bacteria.

Figure 7.65 shows that the ratio of dead *E. coli* cells to total *E. coli* cells on the coatings increased slightly with Ti content increasing after they had been immerged in bacterial suspension for 1 h and then exposed to air for 15 minutes.

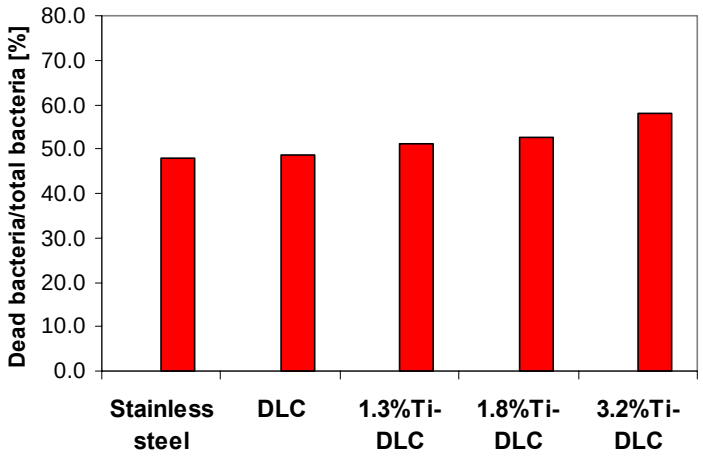

Figure 7.65 Effect of Ti content on the ratio of dead/total *E. coli* cells (contact time: 1 hour)

In order to assess the adhesion strength of the attached bacteria, each sample with bacteria was dipped 20 times vertically in a glass vessel containing 130 ml sterile distilled water at 37 ˚C at a constant shear stress of 0.014 N m^{-2}. During the dipping process, some bacteria were removed from the coatings. Figure 7.66 and Figure 7.67 show that the numbers of remaining bacteria (live, dead and total bacteria) decreased linearly with Ti content increasing.

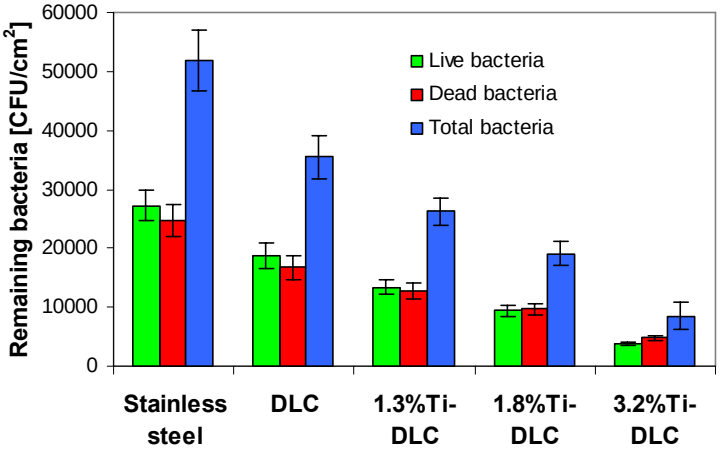

Figure 7.66 Remaining *E. coli* cells on Ti-DLC coatings after dipping process (Contact time: 1 h)

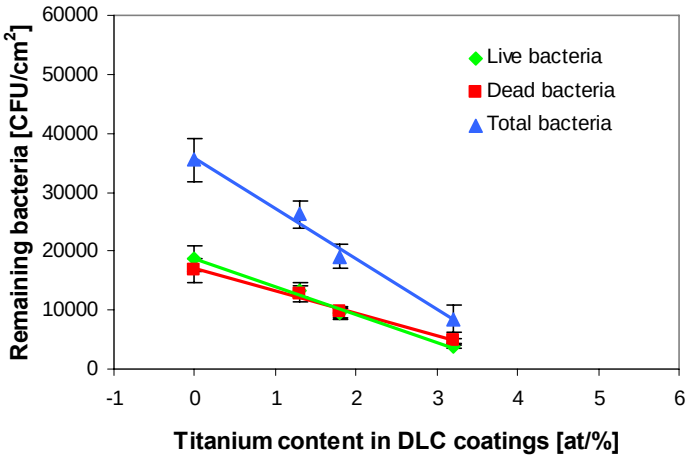

Figure 7.67 Effect of Ti content in DLC coatings on the remaining *E. coli* cells (Contact time: 1 h)

Figure 7.68 shows that the remaining *E. coli* cells (live, dead and total bacteria) on the Ti-DLC coatings decreased linearly with the γ^- surface energy of the Ti-DLC coatings increasing.

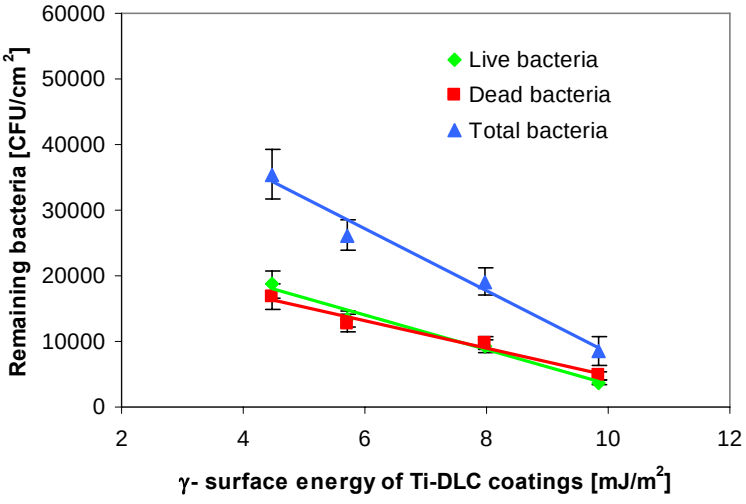

Figure 7.68 Effect of γ^- surface energy of Ti-DLC coatings on the remaining *E. coli* cells (Contact time: 1 h)

Figure 7.69 shows that the removal percentage of *E. coli* cells from the Ti-DLC coatings after dipping process increased with Ti content in the DLC coating increasing. The removal percentages of live, dead and total bacteria on the 3.2% Ti-DLC coatings increased by 215%, 206% and 214% respectively, compared with stainless steel.

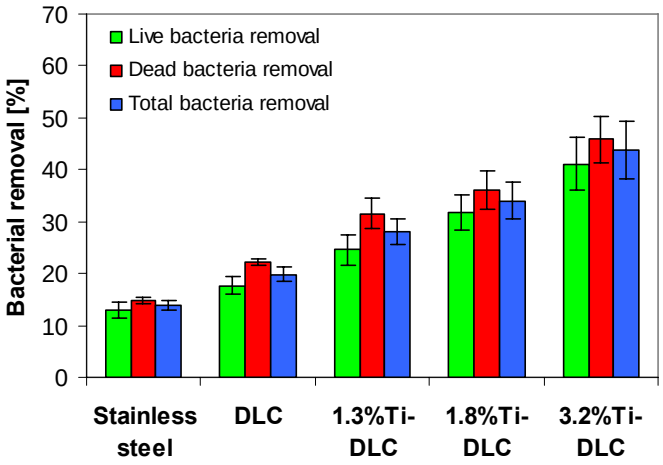

Figure 7.69 Removal percentage of *E. coli* cells from Ti-DLC coatings after dipping process (Contact time: 1 h)

7.2.4.2 Contact time 5 h with *E. coli*

Figures 7.70 and 7.71 show the attachment of *E. coli* cells on the Ti-DLC coatings for contact time 5 hour. The number of adhered bacteria (live, dead and total bacteria) decreased linearly with Ti content increasing. The 3.2% Ti-DLC performed best, which reduced bacterial adhesion (live, dead and total bacteria) by 75%, 66% and 71% respectively, compared with stainless steel.

Figure 7.72 shows that the live, dead and total *E. coli* cells on the Ti-DLC coatings decreased with the γ^- surface energy of the Ti-DLC coatings increasing. The results were consistent with previous results on the effect of surface energy on bacterial adhesion.

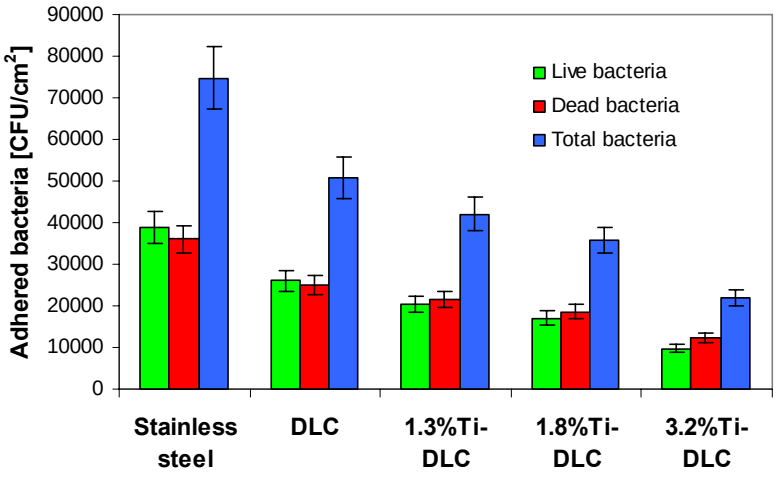

Figure 7.70 Attachment of *E. coli* cells on Ti-DLC coatings (Contact time: 5 h)

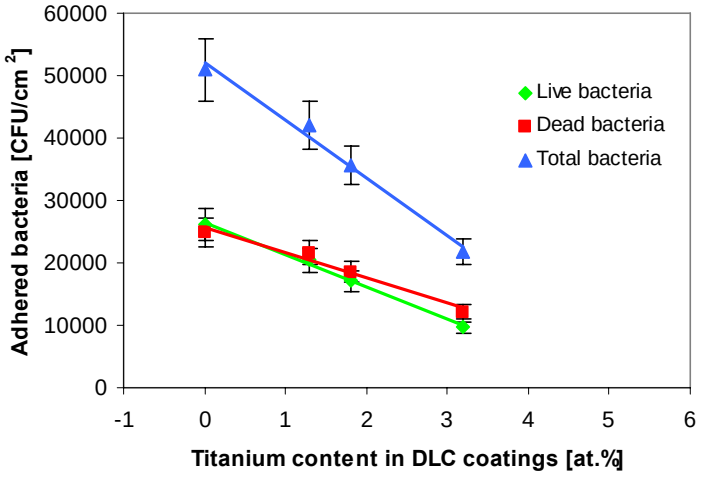

Figure 7.71 Effect of Ti content on the attachment of *E. coli* cells on Ti-DLC coatings (Contact time: 5 h)

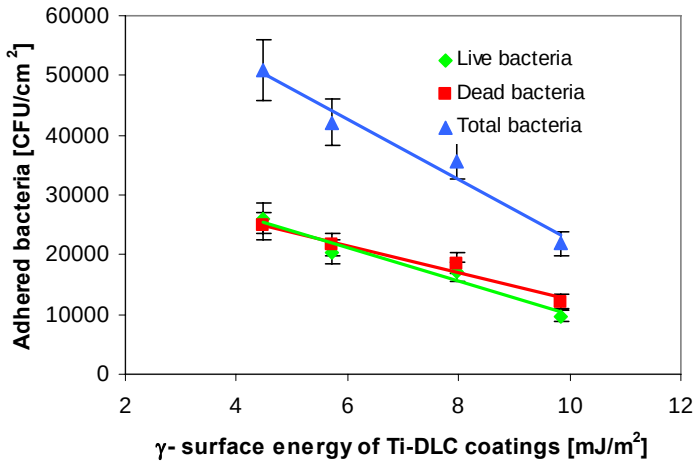

Figure 7.72 Effect of γ^- surface energy of Ti-DLC coatings on the attachment of *E. coli* cells (Contact time: 5 h)

Figure 7.73 shows that the ratio of dead *E. coli* cells to total *E. coli* cells increased slightly with Ti content increasing after they had been immerged in bacterial suspension for 5 h and then exposed to air for 15 minutes.

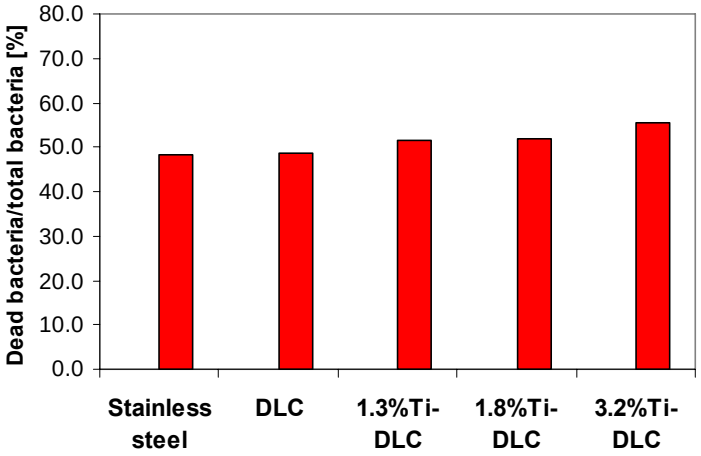

Figure 7.73 Effect of Ti content on the ratio of dead/total *E. coli* cells (contact time: 5 hours)

Figure 7.74 and Figure 7.75 show the remaining *E. coli* cells on the Ti-DLC coatings after dipping process. The numbers of remaining bacteria decreased with Ti content increasing. The remaining bacteria (live, dead and total bacteria) on the 3.2% Ti-DLC coatings were reduced by 82%, 92% and 80% respectively, compared with stainless steel.

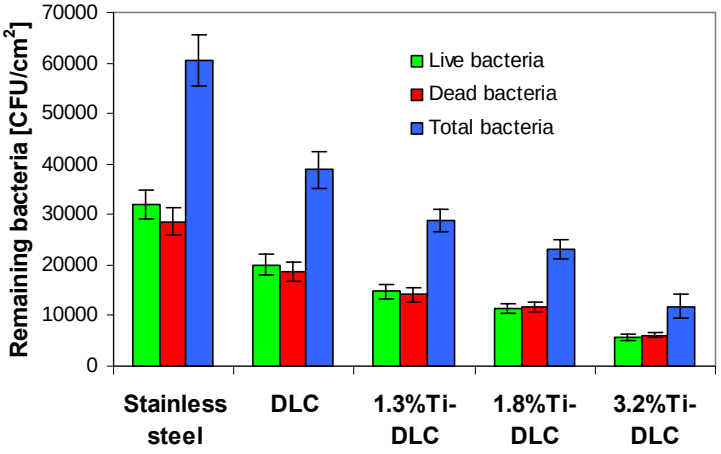

Figure 7.74 Remaining *E. coli* cells on Ti-DLC coatings after dipping process (contact time: 5 hour)

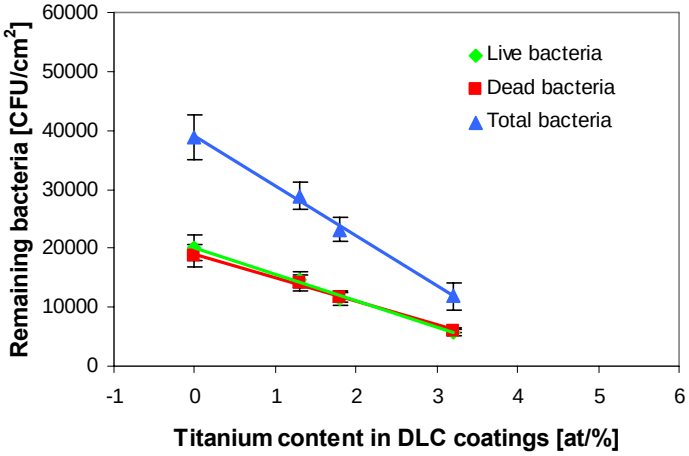

Figure 7.75 Effect of Ti content in DLC coatings on the remaining *E. coli* cells (Contact time: 5 h)

Figure 7.76 shows that the remaining *E. coli* cells (live, dead and total bacteria) on the Ti-DLC coatings decreased with the γ^- surface energy of the Ti-DLC coatings increasing.

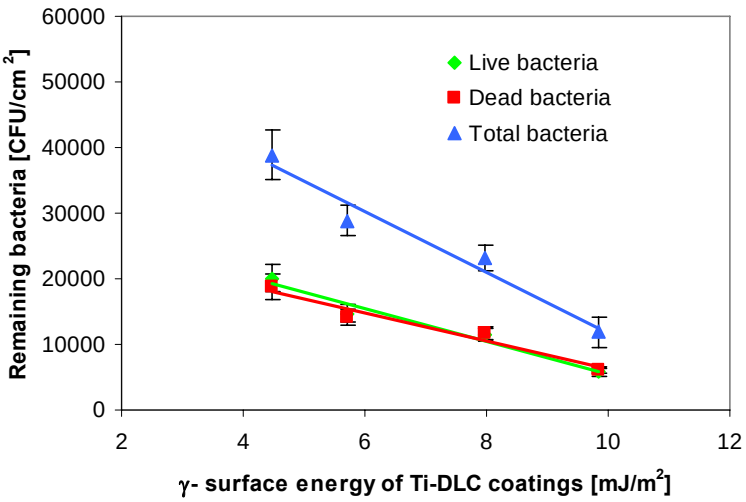

Figure 7.76 Effect of γ^- surface energy of Ti-DLC coatings on the remaining *E. coli* cells (Contact time: 5 h)

Figure 7.77 shows the removal percentage of *E. coli* cells from the Ti-DLC coatings after dipping process. The removal percentage of live, dead and total bacteria increased with Ti content in the DLC coating increasing. The removal percentage of live, dead and total bacteria on the 3.2%Ti-DLC coatings was increased by 127%, 150% and 142% respectively, compared with stainless steel. Figure 7.77 also indicates that the removal percentage of dead bacteria was higher than that of live bacteria. This means the dead bacteria were more easily removed than the live bacteria.

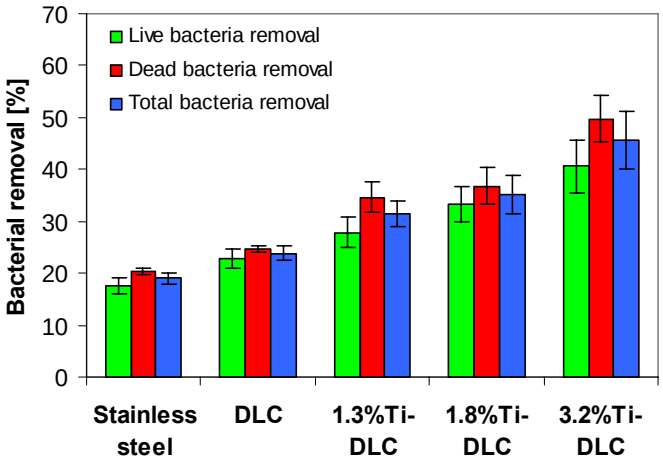

Figure 7.77 Removal percentage of *E. coli* cells from Ti-DLC coatings after dipping process (Contact time: 5 h)

7.2.4.3 Effect of Contact Time on *E. coli* Adhesion

Figure 7.78 shows the effect of contact time (1 hour, 5 hour) on the attachment of live, dead and total *E. coli* cells on the Ti-DLC coatings. As expected, when contact time increased to 5 hours from 1 hour more bacteria attached to each type of the coatings.

Figure 7.79 shows the effect of contact time (1 hour, 5 hour) on the removal of live, dead and total *E. coli* cells on the Ti-DLC coatings. The bacterial removal percentage at contact time 5 hour was higher than that at contact time 1 h. The results were not consistent to the B-DLC coatings. In general, when contact time increased to 5 h the bacterial adhesion strength increased as live bacteria on the coatings started producing sticky exopolymer. However as the Ti-DLC coatings may be toxic to the bacteria, the bacterial adhesion may decrease with contact time increasing. This may explain why the bacterial removal percentage for contact time 5 hour was slightly higher than that for contact time 1 h.

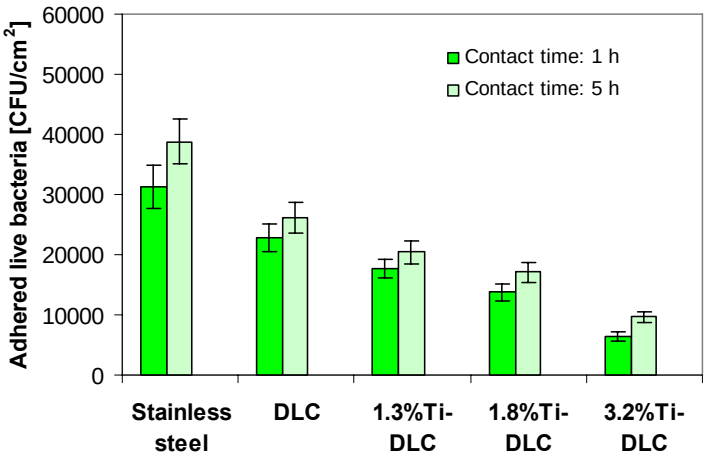

(a)

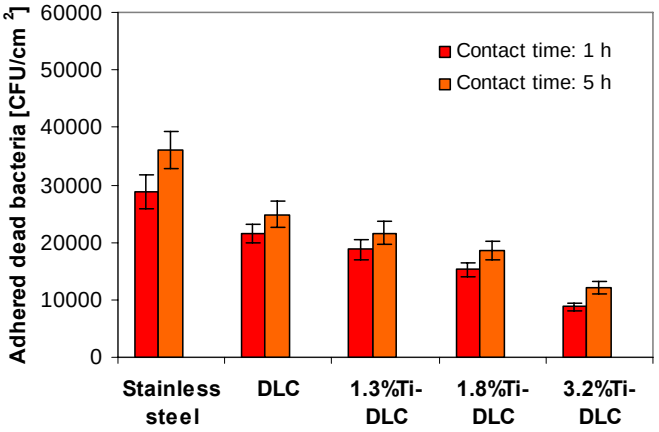

(b)

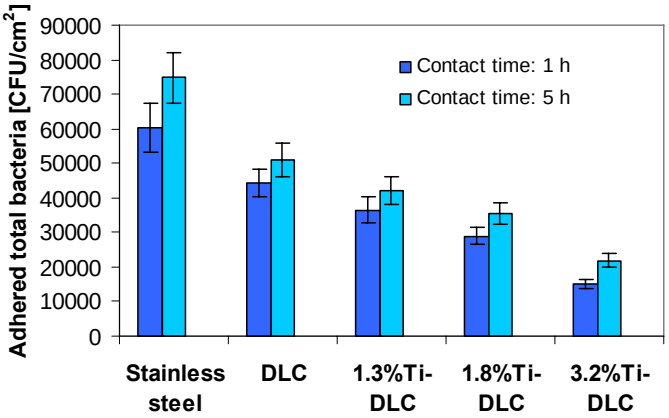

(c)

Figure 7.78 Effect of contact time on the attachment of live (a), dead (b) and total (c) *E. coli* cells on Ti-DLC coatings

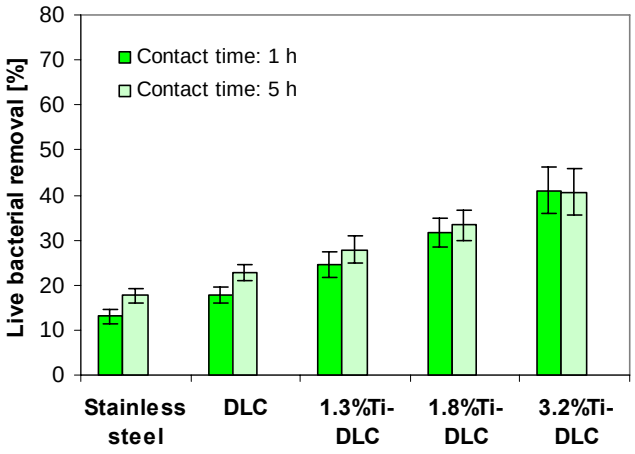

(a)

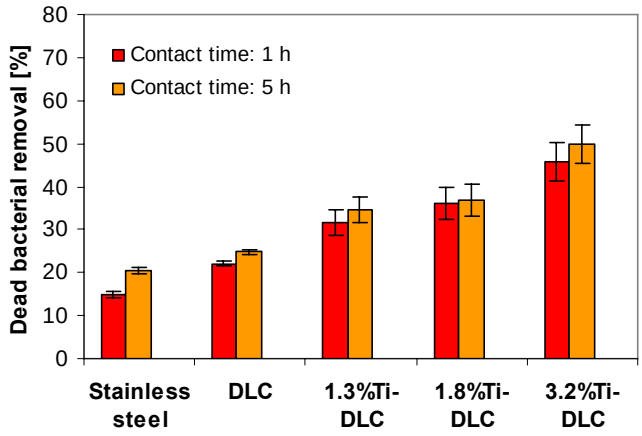

(b)

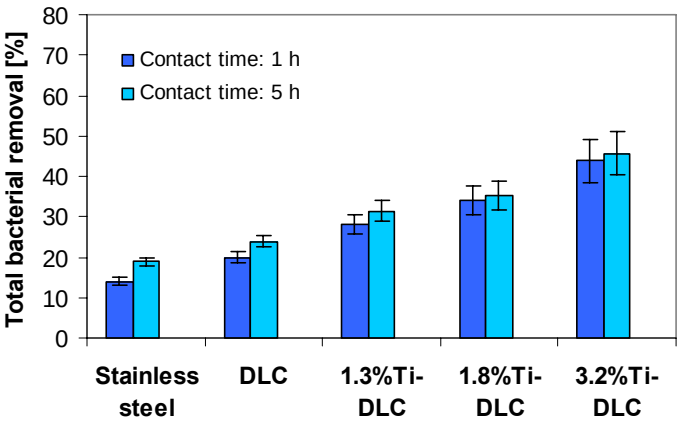

(c)

Figure 7.79 Effect of contact time on the removal of live (a), dead (b) and total (c) *E. coli* cells on Ti-DLC coatings

Summary and discussion:

The experimental results showed that the total surface energies of Ti-DLC coatings were almost same, about 44 mJ/m^2, but γ^- values were changed in the range of 4.47-9.83 mJ/m^2 (see Table 5.8).

It was observed that after the coatings with bacteria were exposed to air for 15 minutes, some bacteria on the coatings were dead. The numbers of adhered bacteria (live, dead and total *E. coli* cells) decreased with Ti content or γ^- values increasing. The 3.2% Ti-DLC performed best, which reduced total bacterial adhesion by 75% and 66% respectively, compared with stainless steel and pure DLC coating.

The removal percentage of the bacteria (live, dead and total *E. coli* cells) increased with Ti content or γ^- values increasing. The removal percentage of live, dead and total bacteria on the 3.2%Ti-DLC coatings was increased by 127%, 150% and 142% respectively, compared with stainless steel. The dead bacteria were more easily removed than the live bacteria.

In this study the contact time (1 hour, 5 hour) had significant influence on the attachment of *E. coli* cells on the Ti-DLC coatings. In general, the numbers of adhered bacteria increased with contact time increasing. The Ti-DLC coatings may be toxic to bacteria due to the formation TiOx or TiO_2. Further study is required to confirm the existence of TiOx or TiO_2 in the Ti-DLC coatings.

7.3 SiOx-like Coatings

The detailed procedure for preparing SiOx-like coatings is given in Section 4.3. The chemical composition, contact angle and surface energy components of the SiOx-like coatings are given in Table 5.9.

These coatings were evaluated for attachment and removal with *P. fluorescens* for contact time 1 h. The detailed procedures of bacterial adhesion and removal are described in Section 6.2: Bacterial Adhesion and Removal.

First group of SiOx-like coatings:

Figure 7.80 shows the initial attachment of *P. fluorescens* cells on the first group of SiOx-like coatings (see Table 5.9). S7-1, S7-2 and S7-3 with lower surface energy (23 mJ/m^2) performed best against bacterial attachment. Figure 7.81 shows that the number of adhered bacteria increased with increasing total surface energy of the coatings.

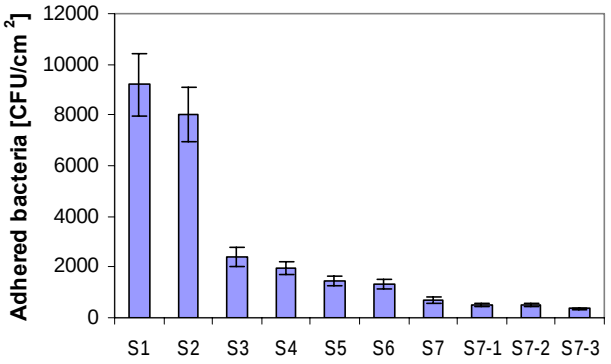

Figure 7.80 Initial attachment of *P. fluorescens* cells on SiOx-like coatings

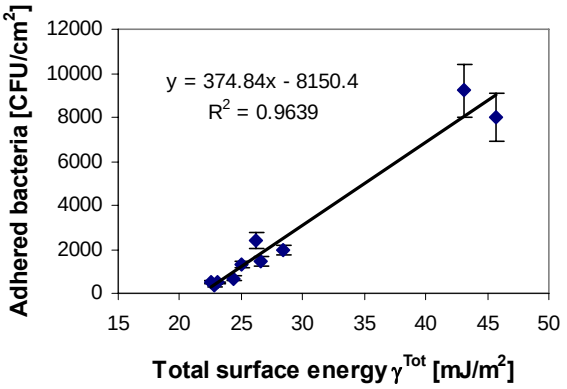

Figure 7.81: Effect of total surface energy of SiOx-like coatings on the attachment of *P. fluorescens*

Figure 7.82 shows the removal of *P. fluorescens* cells from the SiOx-like coatings. S2 with the highest surface energy (45.7 mJ/m^2) had the lowest bacterial removal rate (7.5% cells removed). Figure 7.83 shows that the bacterial removal rate decreased with increasing total surface energy of the SiOx-like coatings.

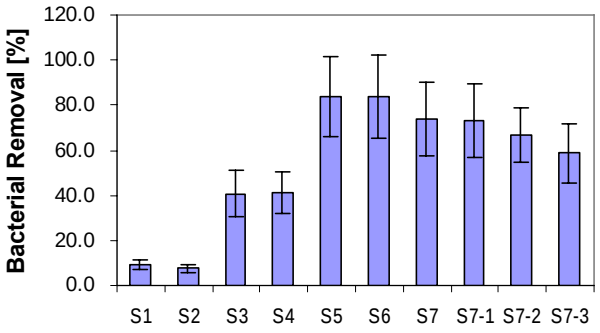

Figure 7.82 Removal of *P. fluorescens* cells from SiOx-like coatings

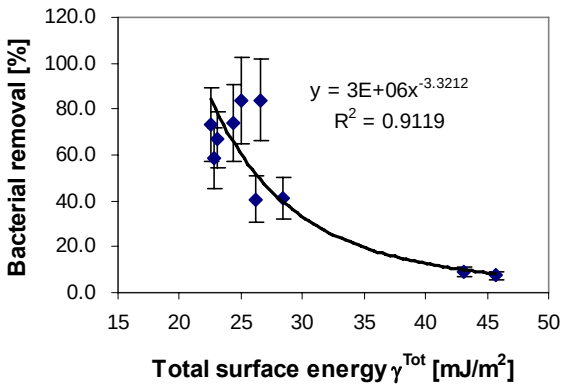

Figure 7.83: Effect of total surface energy of SiOx-like coatings on removal of biofilm of *P. fluorescens* cells

Second group of SiOx-like coatings:

Figure 7.84 shows the initial attachment of *P. fluorescens* cells on the second group of SiOx-like coatings (see Table 5.9). TCL40bt with the lowest surface energy (23 mJ/m^2) performed best against bacterial attachment. Figure 7.85 shows that the number of adhered bacteria increased with total surface energy of the coatings increasing.

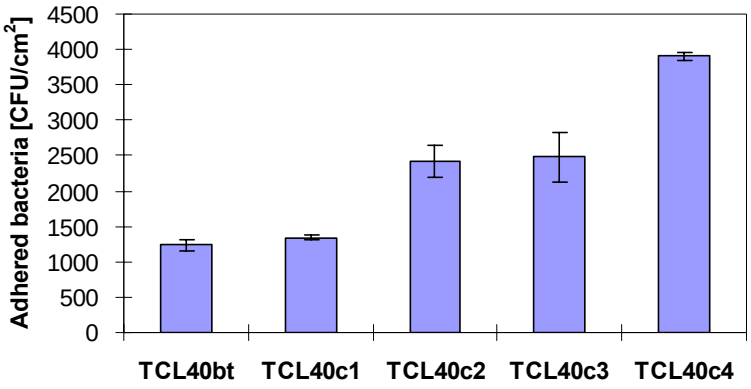

Figure 7.84 Initial attachment of *P. fluorescens* cells on SiOx-like coatings

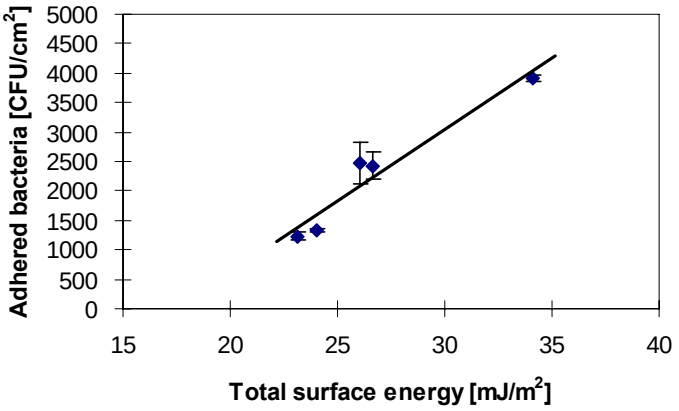

Figure 7.85: Effect of total surface energy of SiOx-like coatings on the attachment of *P. fluorescens*

Figure 7.86 shows the removal of *P. fluorescens* cells from the SiOx-like coatings. TCL40bt with the lowest surface energy (23 mJ/m^2) had the highest removal rate. Figure 7.87 shows that the bacterial removal rate decreased with increasing total surface energy.

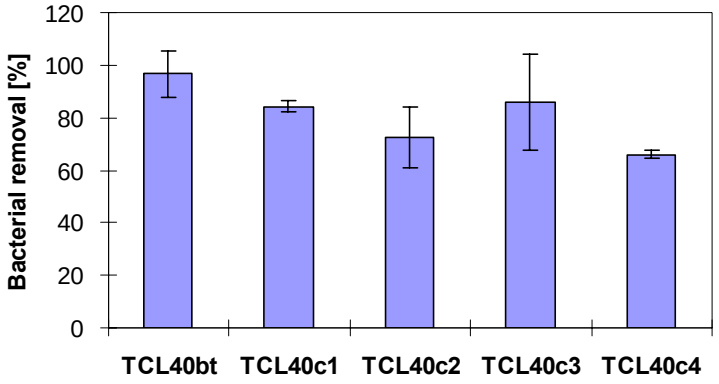

Figure 7.86 Removal of *P. fluorescens* cells from SiOx-like coatings

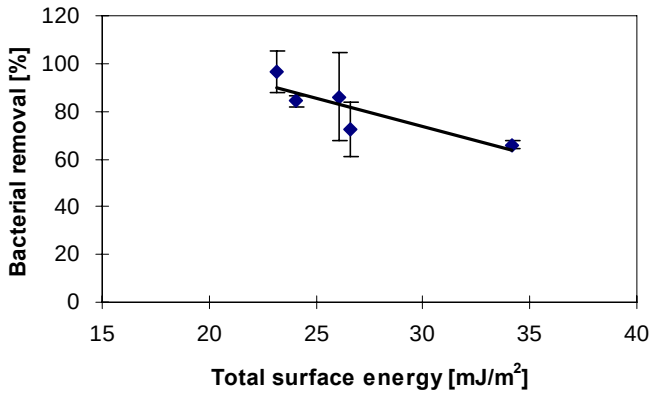

Figure 7.87: Effect of total surface energy of SiOx-like coatings on removal of biofilm of *P. fluorescens* cells

Summary and discussion:

Surface energy has a significant influence on bacterial adhesion. It can be seen that the number of adhered bacteria increased with increasing surface energy. When the surface energy of the coatings was 23 mN/m (S7-1, TCL40bt), the number of adhered bacteria was lowest. Zhao et al. (2004; 2007a) derived the optimum surface energy component

of a substrate, for which bacterial adhesion force is minimal, using the extended DLVO theory. According to the optimum surface energy equation, the theoretical value of surface energy of coatings to minimize the adhesion *P. fluorescens* is 21 mN/m. This value is also within the optimum range of the surface energy of a surface (20 - 30 mJ/m^2) to inhibit biofouling that Baier and Meyer (1992) recommend. Bacterial removal decreased with increasing surface energy, i.e. the adhesion strength increased with increasing surface energy. When the surface energy of the coatings was 23 mN/m (S7-1 or TCL40bt), the bacterial adhesion strength to the coatings was weakest. The results are consistent with the findings by Zhao et al. (2004; 2007a) on the optimum surface energy component of a substrate.

7.4 B- and Ti-DLC Coatings for Protein Removal

The detailed procedure for preparing B-DLC coatings and Ti-DLC coatings is given in Section 4.2.4. The chemical composition, contact angle and surface energy components of the coatings are given in Table 5.8. The detailed procedures of protein removal assays are described in Section 6.4: Protein Removal Assays. In brif, all the coatings were treated with 100 μg/ml brain homogenate and dried for 24 hours in the room temperature. Then they were subsequently cleaned using a detergent Decon. The quantity of protein remaining after cleaning was determined by a fluorescence technique. The protein removal assays were performed at Barts and London School of Medicine.

Figure 7.88 shows the protein remaining after cleaning with Decon. The 7.6%B-DLC and 9.5%B-DLC with lower surface energy performed better than others, which reduced protein adhesion by 88% and 78% respectively, compared with stainless steel and pure DLC coating.

Figure 7.89 shows that the protein remaining decreased with boron content increasing. Figure 7.90 shows that the protein remaining decreased with total surface energy of B-DLC coatings decreasing.

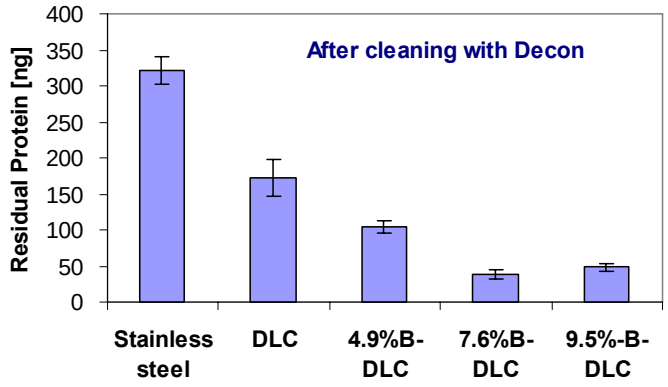

Figure 7.88 Protein remaining after cleaning with Decon

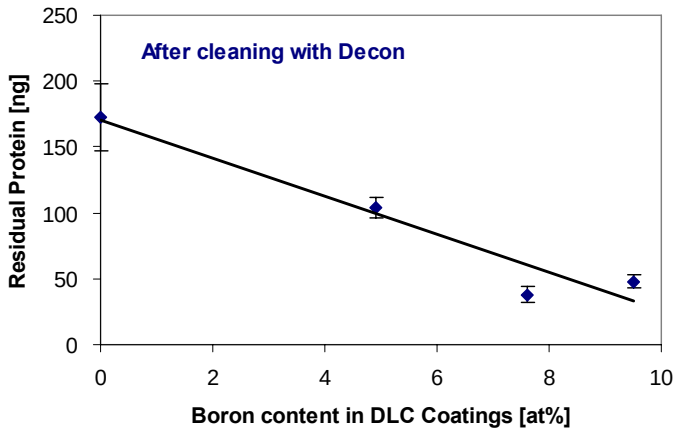

Figure 7.89 Effect of boron content in DLC coatings on protein remaining

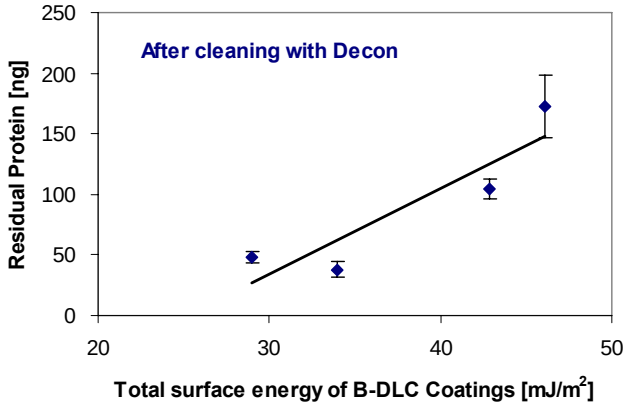

Figure 7.90 Effect of total surface energy of B-DLC coatings on protein remaining

Figure 7.91 shows the protein remaining after cleaning with Decon. The Ti-DLC coatings performed much better than stainless steel and pure DLC coating against protein adhesion. Figure 7.91 shows that the protein remaining decreased with Ti content increasing. The 3.2%Ti-DLC coatings performed best, which reduced protein adhesion by 95% and 91% respectively, compared with stainless steel and pure DLC coating. Figure 7.92 shows that the protein remaining decreased with γ^- surface energy of Ti-DLC coatings increasing.

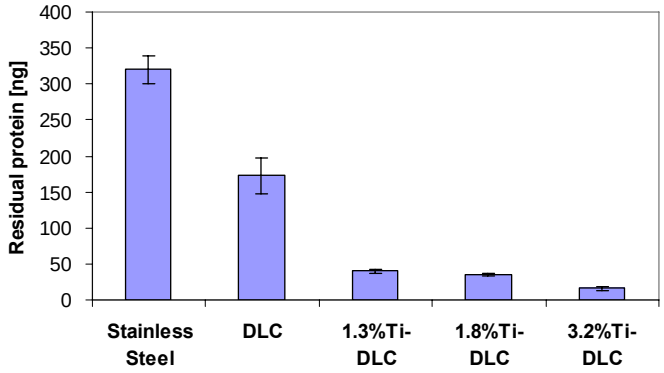

Figure 7.91 Protein remaining on Ti-DLC coatings

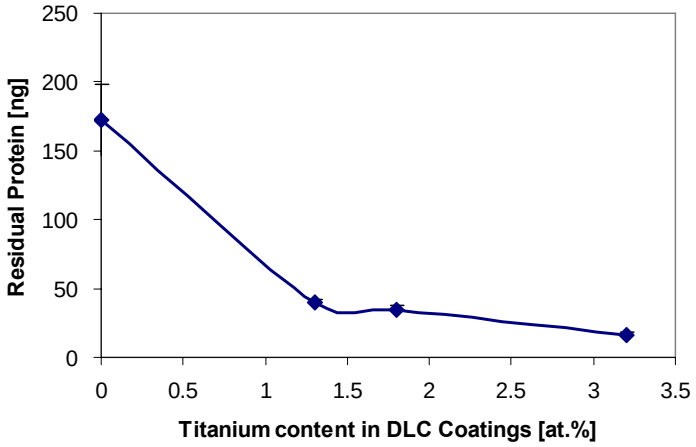

Figure 7.92 Effect of Ti content in DLC coatings on protein remaining

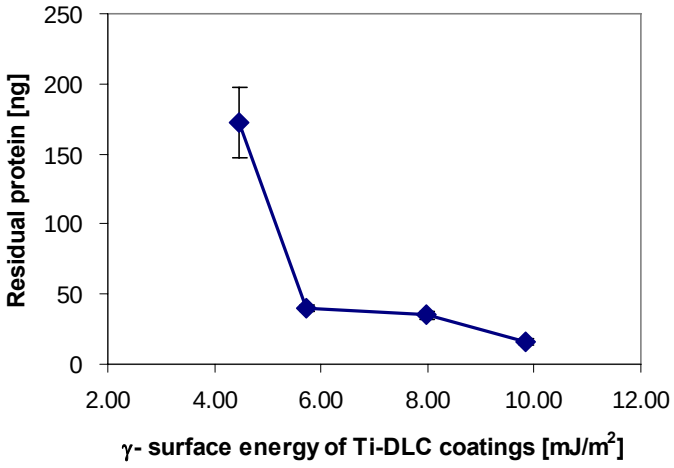

Figure 7.93 Effect of total surface energy of Ti-DLC coatings on protein remaining

Summary and discussion:

The experimental results showed that both type and content of the doped elements in DLC coatings had significant influence on the protein adhesion. The protein remaining decreased with boron or titanium content increasing. The protein remaining also decreased with total surface energy of B-DLC coatings decreasing or with γ^- surface energy of Ti-DLC coatings increasing. The best B and Ti doped DLC coatings reduced residual protein adhesion by 88% and 95%, respectively, compared with stainless steel.

CHAPTER 8

MODELLING OF INTERACTION ENERGIES

8.1 Thermodynamic Approach

A thermodynamic approach offers a useful tool to predict bacterial adhesion to solid substrates (Busscher HJ *et al.*, 1984). It is based on surface energies of the interacting surfaces and does not include an explicit role for electrostatic interactions. It is expressed in terms of work of adhesion as:

$$\Delta F_{adh} = \gamma_{SB} - \gamma_{SL} - \gamma_{BL} \qquad (8.1)$$

where ΔF_{adh} is the interfacial free energy of adhesion or work of adhesion, γ_{SB} is the solid-bacteria interfacial free energy, γ_{SL} is the solid-liquid interfacial free energy, and γ_{BL} is the bacteria-liquid interfacial free energy, whereas bacterial adhesion is energetically unfavourable if:

$$\Delta F_{adh} > 0 \qquad (8.2)$$

The interfacial free energies in Eq. (8.1) can be calculated from van Oss Acid-Base Approach.

In the Chapter 5.4.2.3 van Oss Acid-Base Approach, the interfacial free energy of adhesion of solid-liquid can be calculated by Eq. (5.13), with the same method, the solid-bacteria and bacteria-liquid interfacial free energies can be express as follows:

$$\gamma_{SB} = \gamma_S + \gamma_B - 2(\sqrt{\gamma_S^{LW} \cdot \gamma_B^{LW}} + \sqrt{\gamma_S^+ \cdot \gamma_B^-} + \sqrt{\gamma_S^- \cdot \gamma_B^+}) \tag{8.3}$$

$$\gamma_{BL} = \gamma_B + \gamma_L - 2(\sqrt{\gamma_B^{LW} \cdot \gamma_L^{LW}} + \sqrt{\gamma_B^+ \cdot \gamma_L^-} + \sqrt{\gamma_B^- \cdot \gamma_L^+}) \tag{8.4}$$

Combining Eq. (5.13), Eq. (8.1), Eq. (8.3) and Eq. (8.4), the work of adhesion ΔF_{adh} is obtained:

$$\begin{aligned}\Delta F_{adh} = 2(&\sqrt{\gamma_S^{LW}\gamma_L^{LW}} + \sqrt{\gamma_S^+\gamma_L^-} + \sqrt{\gamma_S^-\gamma_L^+} + \sqrt{\gamma_B^{LW}\gamma_L^{LW}} + \sqrt{\gamma_B^+\gamma_L^-} + \sqrt{\gamma_B^-\gamma_L^+} \\ &- \sqrt{\gamma_S^{LW}\gamma_B^{LW}} - \sqrt{\gamma_S^+\gamma_B^-} - \sqrt{\gamma_S^-\gamma_B^+} - \gamma_L)\end{aligned} \tag{8.5}$$

8.2 Extended DLVO Theory

Derjaguin – Landau – Verwey – Overbeek (DLVO) theory was the first theory to be used to explain microbial adhesion (Verwey and Overbeek 1955). It includes Lifshitz-Van de Waals force (LW) and electrostatic force (EL). Later, van Oss (1994) suggested an extended DLVO theory by including Lewis acid-base (AB) and Brownian motion interactions (Br). The Lewis acid-base interactions are based on electron-donating (γ^-) and electron-accepting (γ^+) interactions between polar moieties in aqueous solutions. The Brownian motion interactions are kinetic energy of onward motion by any molecule suspended in liquid. Therefore, microbial adhesion is described as a balance between attractive LW force, repulsive electrostatic force, AB interaction force and Br force (Sharma et al, 2002). The total interaction energy ΔE_{132}^{TOT} between a particle 1 and a solid surface 2 in liquid 3 can be written as the sum of these corresponding interaction terms:

$$\Delta E_{132}^{TOT} = \Delta E_{132}^{LW} + \Delta E_{132}^{EL} + \Delta E_{132}^{AB} + \Delta E^{Br} \qquad (8.6)$$

Later, Azeredo *et al.* (1999) and Oliveira (1997) suggested that the balance between all possible interactions determine whether or not the particle (or bacterium) prefer to attach on the surface: adhesion is unfavorable if

$$\Delta E_{132}^{TOT} > 0 \qquad (8.7)$$

8.2.1 Lifshitz-van der Waals Interaction

The Lifshitz-van der Waals (LW) interaction energy between a particle 1 and a solid surface 2 in liquid 3 can be calculated using the following equations:

$$\Delta E_{132}^{LW} = -\frac{A_{132} \cdot R}{6H} \qquad (8.8)$$

$$A_{132} = (\sqrt{A_{11}} - \sqrt{A_{33}})(\sqrt{A_{22}} - \sqrt{A_{33}}) \qquad (8.9)$$

where H is the distance of separation and A is the Hamaker constant related to the properties of the interacting materials. Recently van Oss presented a very simple method for the calculation of Hamaker constants based on the surface free energy of the interaction material:

$$A_{ii} = 24\pi H_0^2 \cdot \gamma_i^{LW} \qquad (8.10)$$

Where γ_i^{LW} is the LW apolar component of the surface energy and H_0 is the minimum equilibrium distance between the two interacting bodies, which has been found for a large range of materials to be equal to 0.157nm (van Oss CJ, 1994). In this study γ_i^{LW} values were measured for all the coatings and bacteria used.

Then the LW interaction component between a particle 1 and a solid surface 2 in liquid 3 can be expressed

$$\Delta E_{132}^{LW} = -\frac{24\pi H_0^2(\sqrt{\gamma_1^{LW}} - \sqrt{\gamma_3^{LW}})(\sqrt{\gamma_2^{LW}} - \sqrt{\gamma_3^{LW}}) \cdot R}{6H} \qquad (8.11)$$

8.2.2 Electrostatic Double-Layer Interaction

The electrostatic double layer interaction ΔE_{132}^{EL} for a particle 1 with radius R to a solid surface 2 in liquid 3 is given by (Bos R *et al.,* 1995):

$$\Delta E_{132}^{EL} = \pi \cdot \varepsilon \cdot R \cdot \left(\zeta_1^2 + \zeta_2^2\right) \cdot \left[\frac{2 \cdot \zeta_1 \cdot \zeta_2}{\zeta_1^2 + \zeta_2^2} \cdot \ln\frac{1 + \exp(-\kappa \cdot H)}{1 - \exp(-\kappa \cdot H)} + \ln\{1 - \exp(-2 \cdot \kappa \cdot H)\}\right] \quad (8.12)$$

where ε is the electrical permittivity of the solution; κ is the Debye-Hückel parameter ($1/\kappa$ =1.1nm). ζ is the zeta potential of the particle or the solid surface. ε (ε_0 ε_r) is permittivity. ε_0 is permittivity under vacuum 8.85×10^{-12} J m^{-1} V^{-2}, and ε_r is relative dielectric permittivity of water (78.54 for water).

8.2.3 Lewis Acid/Base Interaction

van Oss (1994) extended the DLVO theory by including the Lewis acid/base (AB) interaction ΔE_{132}^{AB} between the particle 1 and the surface 2 in medium 3 :

$$\Delta E_{132}^{AB} = 2\pi R\lambda \Delta E_{132(H_0)}^{AB} \exp\left(\frac{H_0 - H}{\lambda}\right) \qquad (8.13)$$

$$\Delta E_{132(H_0)}^{AB} = 2\left[\begin{array}{l}\sqrt{\gamma_3^+} \cdot \left(\sqrt{\gamma_1^-} + \sqrt{\gamma_2^-} - \sqrt{\gamma_3^-}\right) + \sqrt{\gamma_3^-} \cdot \left(\sqrt{\gamma_1^+} + \sqrt{\gamma_2^+} - \sqrt{\gamma_3^+}\right) \\ -\sqrt{\gamma_1^+ \cdot \gamma_2^-} - \sqrt{\gamma_1^- \gamma_2^+}\end{array}\right] \qquad (8.14)$$

where λ is the correlation length of the molecules of the liquid medium, which is in the range of 0.2~1.0 nm (Israelachvili 1985). For pure water, λ = 0.2 nm (Oliveira 1997). For water $\gamma_3^+ = \gamma_3^-$ =25.5 mJ/m^2; γ_1^+ , γ_1^- represent the acid and base polar components of the surface energy of bacteria, and γ_2^+ , γ_2^- represent the acid and base polar components of the surface energy of coatings.

8.2.4 Brownian Motion

A fundamental consequence of the kinetic theory is that, in the absence of external forces, all suspended particles, regardless of their size, have the same average translational kinetic energy. The average translational kinetic energy for any particle is 1½ *k*T, where *k* is Boltzmann's constant (1.381 × 10^{-23} J/K) and T the absolute temperature in degree K. Particles adhering to a surface have two instead of three degrees of freedom, as one perpendicular to the surface has been blocked by bonding. (for a system with two degrees of freedom) (van Oss CJ, 1994). Since Brownian motion comprises $\frac{1}{2}kT$ per degree of freedom, the corresponding free energy term ΔE^{Br} of a particle adhering to a surface equals *1 kT* = 0.414×10^{-20} J (300ºK).

$$\Delta E^{Br} = 0.414\times10^{-20} \text{ J} \qquad (8.15)$$

8.3 Work of Adhesion and Extended DLVO Theory

When $H=H_o$, the sum of ΔE_{132}^{LW} (Eq. 6.11) and ΔE_{132}^{AB} (Eq.8.14) is equal to the work of adhesion ΔF_{adh} in Eq. (8.5). This means the extended DLVO theory can be simplified to the work of adhesion approach if the electrostatic double layer interaction ΔE_{132}^{EL} and Brownian motion ΔE^{Br} are ignored and $H=H_o$. The extended DLVO theory is found to be more effective in predicting the adhesion behaviour than the expectations from the work of adhesion approach (Sharma et al, 2002, 2003). In this study the extended DLVO theory was used to predict bacterial adhesion.

8.4 Modelling Results

8.4.1 Effect of Surface Energy on Total Interaction Energy

According to the extended DLVO theory, the main parameters that affect ΔE_{132}^{TOT} value include λ, H, ζ and the surface energy components of bacteria, substrate and liquid. In the modeling, the 5 bacteria used in the bacterial adhesion assays were used, including *Pseudomonas fluorescens, Escherichia coli, Pseudomonas aeruginosa, Staphylococcus aureus* and *Staphylococcus epidermidis*. The surface energy components are given in Table 6.2. In the modeling, the surface energy components of substrates (γ_2^{LW}, γ_2^+ and γ_2^-) were assumed to be changed in the range 10 ~ 70 mJ/m², 0 ~1.6 mJ/m² and 10 ~ 70 mJ/m², respectively. The zeta potential for the all surfaces ζ_2 was assumed to be -25 mV (Liu and Zhao 2005). The λ value was taken 0.6 nm (Dávalos-Pantoja *et al.* 2000). The H value was assumed around 4nm depending on the coatings and the bacteria (Liu and Zhao 2005). The surface energy components of water are given in Table 5.4.

The total interaction energy ΔE_{132}^{TOT} between the 5 bacteria strains and the substrates with different surface energy components was modeled by extended DLVO theory. Figure 8.1 shows the effect of surface energy components on ΔE_{132}^{TOT}. The modeling results indicated that for given γ_2^- values, the ΔE_{132}^{TOT} values increased with decreasing γ_2^{LW}. In most case, the surface energy component γ_2^+ value is nearly equal to zero, leading to $\gamma_2^{LW} \approx \gamma_2^{TOT}$. Figure 8.1 also shows that for given γ_2^{LW} values, ΔE_{132}^{TOT} values increased with increasing γ_2^-. According to the DLVO theory, bacterial adhesion strength decreased with ΔE_{132}^{TOT} increasing. The modelling results give us a clear direction to design both anti-biofouling and biofouling-release coatings by decreasing γ_2^{LW} and by increasing γ_2^-. The modelling results explain the experimental results- why the number of adhered bacteria decreased with decreasing γ_2^{TOT} and with increasing γ_2^-; why bacterial removal rate increased with decreasing γ_2^{TOT} and with increasing γ_2^-.

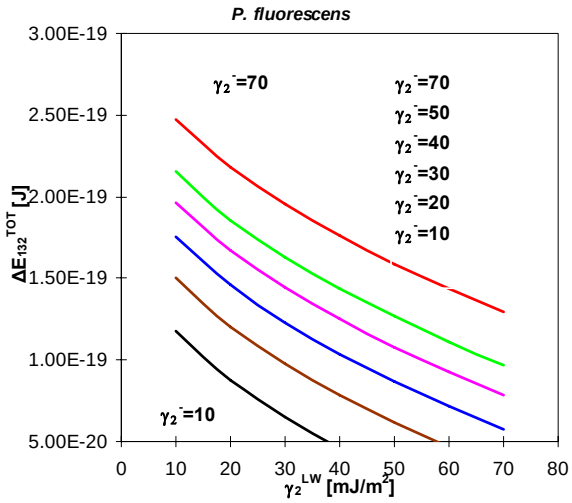
P. fluorescens
3.00E-19
2.50E-19
2.00E-19
1.50E-19
1.00E-19
5.00E-20
ΔE132 TOT [J]
γ2-=70
γ2-=70
γ2-=50
γ2-=40
γ2-=30
γ2-=20
γ2-=10
γ2-=10
0 10 20 30 40 50 60 70 80
γ2 LW [mJ/m2]

(a)

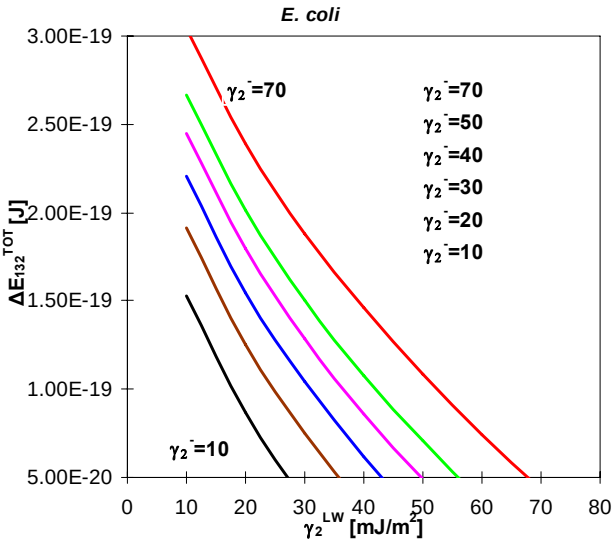
E. coli
3.00E-19
2.50E-19
2.00E-19
1.50E-19
1.00E-19
5.00E-20
ΔE132 TOT [J]
γ2-=70
γ2-=70
γ2-=50
γ2-=40
γ2-=30
γ2-=20
γ2-=10
γ2-=10
0 10 20 30 40 50 60 70 80
γ2 LW [mJ/m2]

(b)

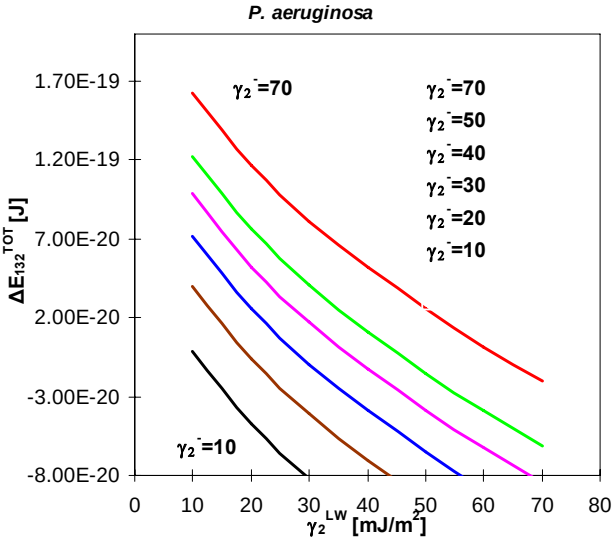
P. aeruginosa
1.70E-19
1.20E-19
7.00E-20
2.00E-20
-3.00E-20
-8.00E-20
ΔE132 TOT [J]
γ2-=70
γ2-=70
γ2-=50
γ2-=40
γ2-=30
γ2-=20
γ2-=10
γ2-=10
0 10 20 30 40 50 60 70 80
γ2 LW [mJ/m2]

(c)

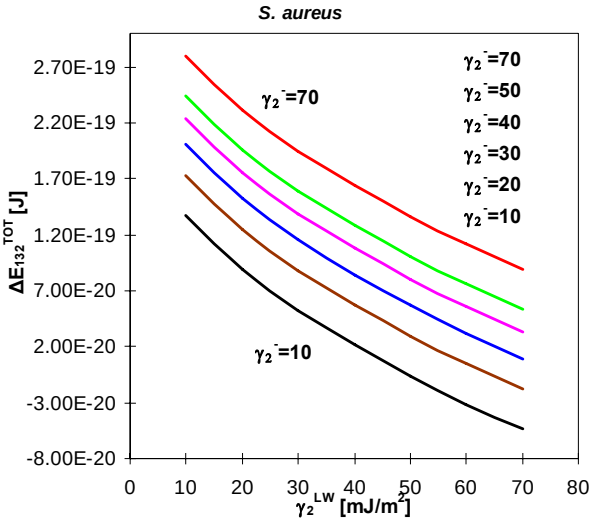

(d)

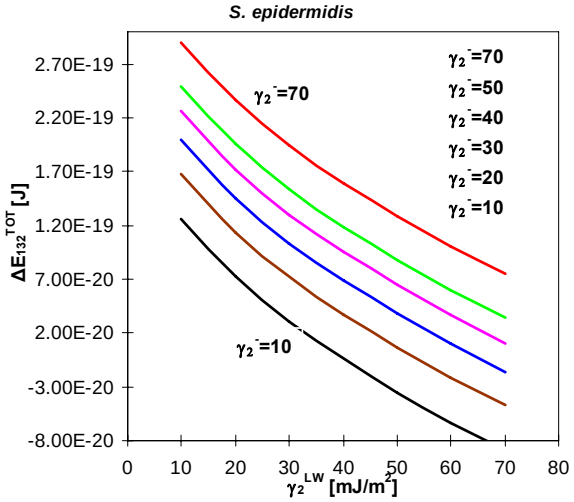

(e)

Figure 8.1 Effect of surface energy components of substrates on total interaction energy (a) *P. fluorescens,* (b) *E. coli,* (c) *P. aeruginosa,* (d) *S. aureus* and (e) *S. epidermidis*.

8.4.2 Case Study- Effect of Interaction Energy

In order to further validate the modelling results, the bacterial adhesion and removal on the coatings with different surface energy were investigated.

8.4.2.1 Ni-P-Biocide Polymer Nanocomposite Coatings

The total interaction energy ΔE_{132}^{TOT} between two types of bacteria (*E. coli* and *S. aureus*, see Table 6.2) and the substrates (stainless steel, Ni-P coating and 5 Ni-P-biocide polymer coatings, see Table 5.5) in water was calculated using the extended DLVO theory, as shown in Figure 8.2a and b. The results showed that the number of adhered bacteria decreased with increasing ΔE_{132}^{TOT} values, which is consistent with the DLVO theory, i.e. bacterial adhesion decreased with increasing ΔE_{132}^{TOT} values.

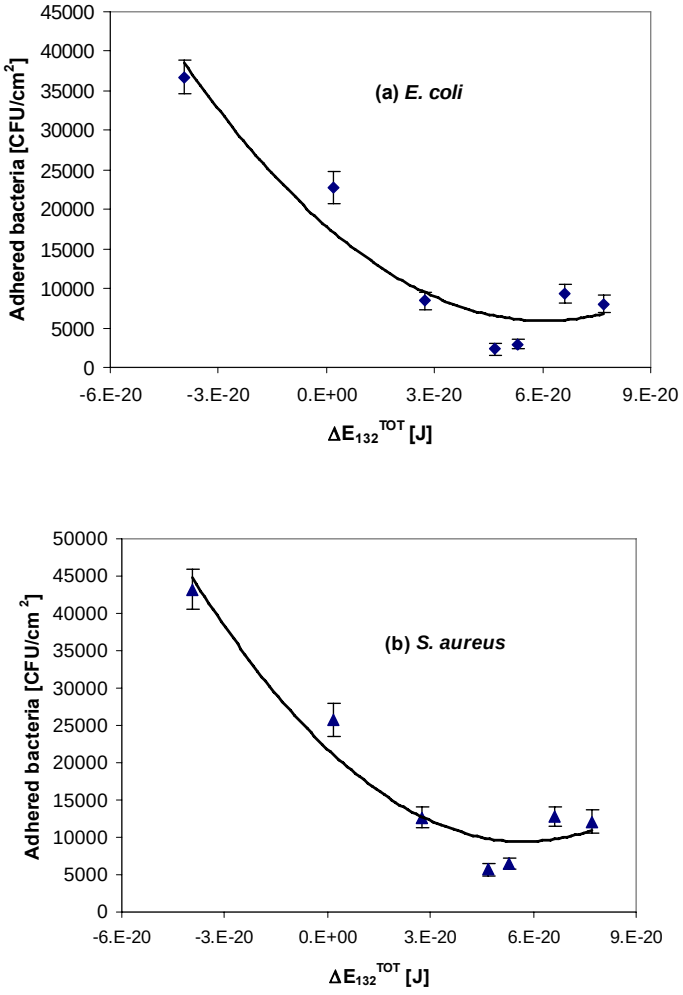

Figure 8.2 Effect of ΔE_{132}^{TOT} on the attachment of (a) *E. coli* (b) *S. aureus*

8.4.2.2 Si-N-doped DLC Coatings

The total interaction energy ΔE_{132}^{TOT} between *P. fluorescens* (see Table 6.2) and the 4 Si-N-DLC coatings (see Table 5.6) in water was calculated using the extended DLVO theory. Figure 8.3 shows that the bacterial removal percentage increased with increasing ΔE_{132}^{TOT} values, which is also consistent with the DLVO theory.

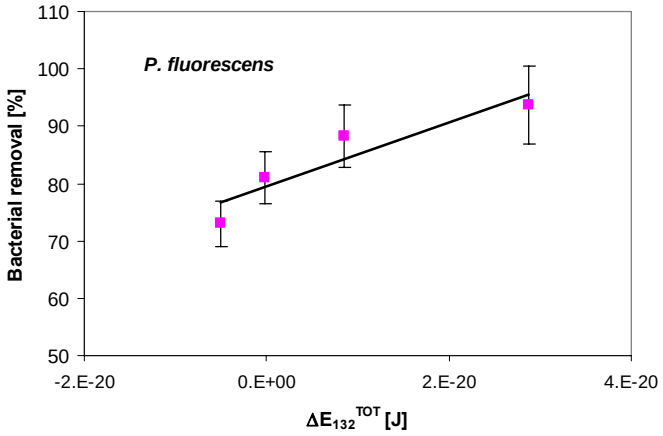

Figure 8.3 Effect of ΔE_{132}^{TOT} on the removal of *P. fluorescens*

8.4.2.3 F-doped DLC Coatings

The total interaction energy ΔE_{132}^{TOT} between *S. aureus* (see Table 6.2) and the F-DLC coatings (see Table 5.7) in water was calculated using the extended DLVO theory. Figure 8.4a shows that the number of adhered bacteria decreased with increasing ΔE_{132}^{TOT} values, which is consistent with the DLVO theory. Figure 8.4b shows that the bacterial removal percentage increased with increasing ΔE_{132}^{TOT} values, which is also consistent with the DLVO theory.

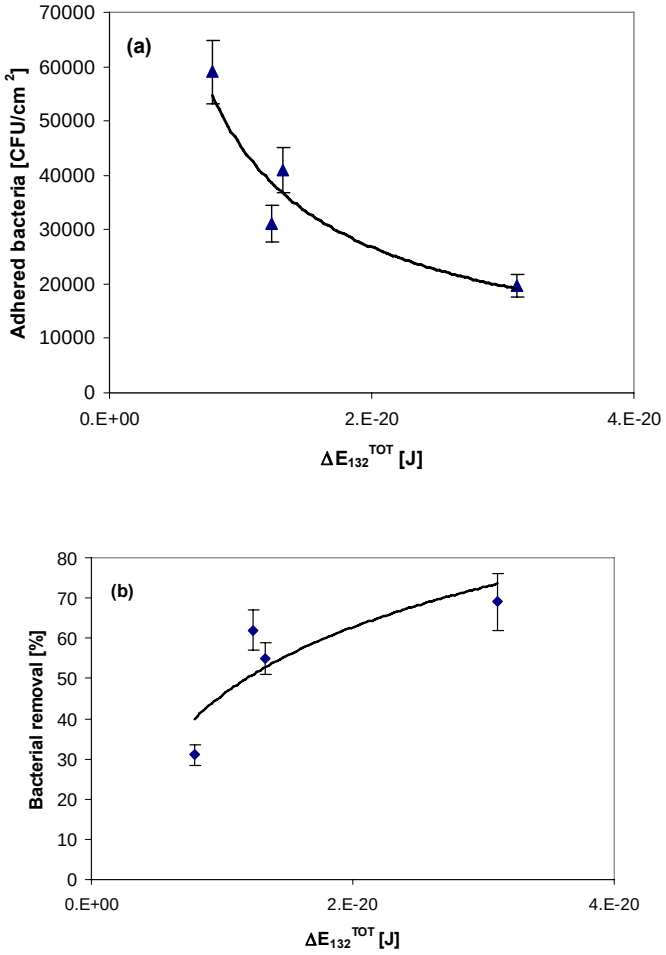

Figure 8.4 Effect of ΔE_{132}^{TOT} on the attachment (a) and removal (b) of *S. aureus*

8.4.2.4 B and Ti-doped DLC Coatings

The total interaction energy ΔE_{132}^{TOT} between *P. aeruginosa* and *S. epidermidis* (see Table 6.2) and the B-doped DLC coatings (see Table 5.8) in water was calculated using the extended DLVO theory. The total interaction energy ΔE_{132}^{TOT} between *E. coli* (see Table 6.2) and the Ti-doped DLC coatings (see Table 5.8) in water was also calculated using the extended DLVO theory. The results indicated that for B-DLC coatings the number of adhered bacteria decreased with increasing ΔE_{132}^{TOT} values for contact time 1h, 5h and 18h; and that the bacterial removal percentage increased with increasing ΔE_{132}^{TOT} values. The similar results were also obtained for the Ti-doped DLC coatings. Figure 8.5a and b

show typical modelling results on the effect of total interaction energy ΔE_{132}^{TOT} on the adhesion and removal of *S. epidermidis* cells from the B-doped DLC coatings for contact time 1 h.

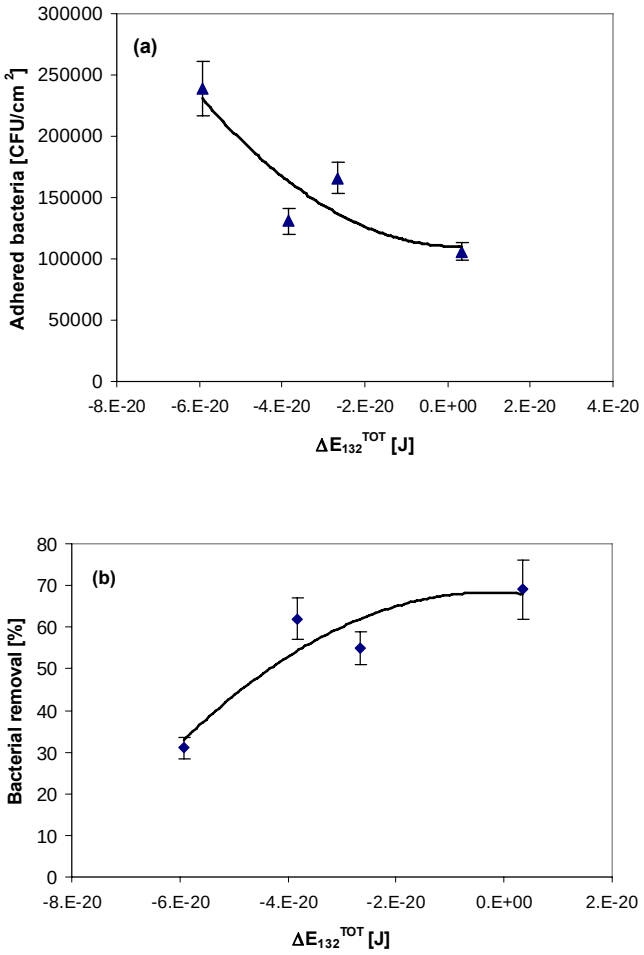

Figure 8.5 Effect of ΔE_{132}^{TOT} on the attachment (a) and removal (b) of *S. epidermidis*

CHAPTER 9

CONCLUSIONS

9.1 Ni-P-Biocide Polymers Noanocomposie Coatings

- A series of novel anti-bacterial Ni-P-Biocide polymers nanocomposite coatings was developed using electroless nanocoating technique.
- The novel electroless Ni-P-SM14, Ni-P-SM20, Ni-P-PTFE-SM14 and Ni-P-PTFE-SM20 composite coatings showed the excellent anti-microbial properties.
- Ni-P-PTFE-SM14 and Ni-P-PTFE-SM20 performed better than Ni-P-SM14 and Ni-P-SM20. For Ni-P-SM14 or Ni-P-SM20, their anti-bacterial mechanism is due to the biocidal property of the biocide polymers SM14 and SM20. For Ni-P-PTFE-SM14 and Ni-P-PTFE-SM20, their anti-bacterial mechanisms are due to the non-stick property of PTFE and biocidal property of the biocide polymer SM14 or SM20. Ni-P-PTFE-SM14 and Ni-P-PTFE-SM20 performed best, which reduced bacterial attachment by 94% and 70% respectively as compared with stainless steel and Ni-P-PTFE.
- In addition, the total surface energy of Ni-P-PTFE-SM14 and Ni-P-PTFE-SM20 was controlled in the optimum value, about 24.5 mJ/m^2(see Table 5.5). As a result, Ni-P-PTFE-SM14 and Ni-P-PTFE-SM20 performed best against bacterial attachment and had highest bacterial removal rate. An EU patent was filed on 1 June 2012.

9.2 Doped Diamond-like Carbon Coatings

9.2.1 Si-N-doped DLC Coatings

- A series of new Si-N-DLC coatings doped with different contents of silicon (1-3.8% Si) and nitrogen (2% N) were designed and produced in the collaboration with Teer Coatings Ltd using their PECVD technique.
- Previously we found that Si-DLC coatings with 1% -3.8% Si performed better than pure DLC coating and stainless steel against bacterial adhesion. In this study we found that the incorporation of 2%N into the Si-doped DLC coatings significantly reduced bacterial attachment, compared with Si-DLC coatings. The number of adhered bacteria decreased significantly with increasing Si content in the DLC coatings.
- The incorporation of 2%N into the Si-doped DLC coatings also increased bacterial removal. The bacterial removal percentage increased significantly with increasing Si content in the DLC coatings.

9.2.2 F-doped DLC Coatings

- A series of F-doped DLC coatings with different contents of fluorine (6.5 - 39.2%) were designed and produced on stainless steel substrates in the collaboration with CSIRO using their PECVD technique.
- The surface energy of the F-DLC coatings decreased with increasing F content in the coatings. The incorporation of fluorine into the DLC coatings reduced significantly bacterial attachment and increased bacterial removal. The F-DLC coatings with the highest F content (39.0 at. %) reduced bacterial attachment by 67 % and increased removal 32 %, compared with pure DLC coating. Both the initial bacterial attachment and the percent bacterial removal strongly correlated with the total surface energy of the coatings. The bacterial attachment decreased with decreasing surface energy of the F-DLC coatings; while the percent bacterial removal increased with decreasing surface energy of the F-DLC coatings.

9.2.3 B-doped DLC Coatings

- A series of new B-doped DLC coatings with different contents of boron (4.9 - 9.5%) were designed and produced on stainless steel substrates in the collaboration with Tecvac Ltd using their PECVD technique.
- The experimental results showed that the surface energy of the B-DLC coatings decreased with increasing B content in the coatings. The incorporation of boron into the DLC coatings reduced significantly bacterial attachment and increased bacterial removal.
- It was observed that after the coatings with bacteria were exposed to air for 15 minutes, some bacteria on the coatings were dead. The numbers of adhered bacteria (live, dead and total *P. aeruginosa* and *S. epidermidis*) decreased with boron content increasing or with the total surface energy of the B-DLC coatings decreasing. The 9.5% B-DLC performed best, which reduced total bacterial adhesion by up to 70%, compared with pure DLC coating.
- In order to assess the adhesion strength of the attached bacteria, some bacteria on the coatings were removed through the dipping process. The numbers of remaining bacteria (live, dead and total *P. aeruginosa* and *S. epidermidis*) also decreased with boron content increasing or with the total surface energy of the B-DLC coatings decreasing. The remaining bacteria (live, dead and total bacteria) on the 9.5% B-DLC coatings were reduced by up to 87%, 77% and 83% respectively, compared with pure DLC coating.
- The removal percentage of the bacteria (live, dead and total *P. aeruginosa* and *S. epidermidis*) increased with boron content increasing or with the total surface energy of the B-DLC coatings decreasing. The removal percentage of live, dead and total bacteria on the 9.5% B-DLC coatings increased by up to 207%, 142% and 164% respectively, compared with pure DLC coatings. The dead bacteria were more easily removed than the live bacteria.
- In this study the contact time (1 hour, 5 hour and 18 hours) had significant influence on the attachment of live, dead and total *P. aeruginosa* and *S. epidermidis* cells on the B-DLC coatings. In general, the numbers of adhered bacteria increased with contact time increasing. However when contact time increased to 18 hours the number of adhered bacteria on the coatings decreased due to lack of nutrients for bacteria to survive. The contact time also had

significant influence on the bacterial removal. For contact time 1 hour, the bacterial removal percentage was much higher than those for contact time 5 h and 18 h as bacteria on the coatings started producing sticky exopolymer with contact time increasing.

- The experimental results also showed that the B-DLC coatings reduced protein adhesion significantly. The protein remaining after cleaning decreased with boron content increasing. The protein remaining also decreased with total surface energy of B-DLC coatings decreasing. The best B doped DLC coatings reduced residual protein adhesion by 88%, compared with stainless steel.

9.2.4 Ti-doped DLC Coatings

- A series of new Ti-doped DLC coatings with different contents of titanium (1.3 -3.2%) were designed and produced on stainless steel substrates in the collaboration with Tecvac Ltd using their PECVD technique.
- The experimental results showed that the total surface energies of Ti-DLC coatings were almost same, about 44 mJ/m^2, but γ^- values were changed in the range of 4.47- 9.83 mJ/m^2 .
- It was observed that after the coatings with bacteria were exposed to air for 15 minutes, some bacteria on the coatings were dead. The numbers of adhered bacteria (live, dead and total *E. coli* cells) decreased with Ti content or γ^- values increasing. The 3.2% Ti-DLC performed best, which reduced total bacterial adhesion by 75% and 66% respectively, compared with stainless steel and pure DLC coating.
- The removal percentage of the bacteria (live, dead and total *E. coli* cells) increased with Ti content or γ^- values increasing. The removal percentage of live, dead and total bacteria on the 3.2%Ti-DLC coatings was increased by 127%, 150% and 142% respectively, compared with stainless steel. The dead bacteria were more easily removed than the live bacteria.
- In this study the contact time (1 hour, 5 hour) had significant influence on the attachment of *E. coli* cells on the Ti-DLC coatings. In general, the numbers of adhered bacteria increased with contact time increasing. The Ti-DLC coatings

may be toxic to bacteria due to the formation TiOx or TiO_2. Further study is required to confirm the existence of TiOx or TiO_2 in the Ti-DLC coatings.

- The experimental results also showed that the Ti-DLC coatings reduced protein adhesion significantly. The protein remaining decreased with titanium content increasing. The protein remaining also decreased with γ^- surface energy of Ti-DLC coatings increasing. The best Ti doped DLC coatings reduced residual protein adhesion by 95%, compared with stainless steel.

9.3 SiOx-like Coatings

- A series of new SiOx-like coatings with different surface energies (23 – 46 mJ/m^2) were designed and produced in the collaboration with Teer Coatings Ltd using their PECVD technique.
- Surface energy has a significant influence on bacterial adhesion. The number of adhered bacteria increased with increasing surface energy. When the surface energy of the coatings was 23 mN/m (S7-1, TCL40bt), the number of adhered bacteria was lowest.
- Bacterial removal decreased with increasing surface energy, i.e. the adhesion strength increased with increasing surface energy. When the surface energy of the coatings was 23 mN/m (S7-1 or TCL40bt), the bacterial adhesion strength to the coatings was weakest.

9.4 Bacterial Adhesion Mechanisms

- The total interaction energy ΔE_{132}^{TOT} between the different bacteria strains and the substrates with different surface energy components was modelled by extended DLVO theory. The modelling results indicated that for given γ_2^- values, the ΔE_{132}^{TOT} values increased with decreasing γ_2^{LW}. In most case, the surface energy component γ_2^+ value is nearly equal to zero, leading to $\gamma_2^{LW} \approx \gamma_2^{TOT}$. For given γ_2^{LW} values, ΔE_{132}^{TOT} values increased with increasing γ_2^-. According to the DLVO theory, bacterial adhesion strength decreased with ΔE_{132}^{TOT} increasing. The modelling results give us a clear

direction to design both anti-biofouling and biofouling-release coatings by decreasing γ_2^{LW} and by increasing γ_2^-. The modelling results explain the experimental results- why the number of adhered bacteria decreased with decreasing γ_2^{TOT} and with increasing γ_2^-; why bacterial removal rate increased with decreasing γ_2^{TOT} and with increasing γ_2^-.

CHAPTER 10

FUTURE WORK

10.1 Anti-biofouling Coatings

To further investigate the effect of B and Ti contents on bacterial adhesion by increasing B and Ti contents to 15 at%.

To further investigate the effect of two or more doped elements (Si-F; Si-B; B-Ti; etc) on bacterial adhesion.

10.2 Biofouling Adhesion Mechanisms

To further investigate the adhesion mechanisms of proteins if we know the surface energy of level 3 prion proteins.

10.3 Practical Applications of the New Coatings

To investigate the practical applications of the new anti-biofouling coatings for heat exchangers and medical devices in the collaboration with relevant industries.

REFERENCES

A

Aftring R.P., Capone D.C., Duguay L., Fell J., Master I.M. and Taylor B.F., 1978, Biofouling and site characterisation studies in the ocean thermal energy conversion (o.t.e.c.) experiment at st. croix, u.s. virgin islands, In Proceeding of The Fifth Ocean Thermal Energy Conversion Conference, Florida USA, pp. VIII-45-VIIII-73, Department Of Energy, Washington, USA

Agarwala R.C., Agarwala V., and Sharma R., 2006, Electroless Ni-P based nanocoating technology—a review, Synthesis and Reactivity in Inorganic, Metal-Organic, and Nano-Metal Chemistry, Volume 36, Issue 6, Pages 493–515

Ahlborg HG, Josefsson PO (1999), Pin-Tract Complications in External Fixation of Fractures of the Distal Radius, *Acta Orthop Scand*, Volume 70, pp.116-118

Akesso, L., Navabpour, P, Teer, D., Pettitt, ME., Callow, ME., Liu, C., **Su, XJ**., Wang, S., Zhao, Q., Donik, C., Kocijan, A., Jenko, M., Callow, JA., 2009a, Deposition parameters to improve the fouling-release properties of thin siloxane coatings prepared by PACVD. Applied Surface Science, Volume 255 (13-14):6508–6514

Akesso L, Pettitt M E, Callow J A, Callow M E, Stallard J, Teer D, Liu C, Wang S, Zhao Q, D'Souza F D, Willemsen P R, Donnelly G T, Donik C, Kocijan A, Jenko M, Jones L A, Guinaldo P C. 2009b. The potential of nanostructured silicon oxide type coatings deposited by PACVD for control of aquatic biofouling. Biofouling 25: 55-67.

Albaugh E.K., 1984, Copper-Nickel piping reduces costs, Biofouling Corrosion, World Oil, Volume 199, Issue 6, Pages 94-100

Allion A., Baron JP., Boulange-Petermann, L. (2006) Impact of surface energy and roughness on cell distribution and viability, Biofouling, 22(5): 269 – 278

Allonier, A.S., Khalanski, M., Camel, V., Bermond, A., (1999). Characterization of chlorination by –products in cooling effluents of coastal nuclear power stations. Marine Pollution Bulletin 38, 1232-1241.

An YH, Friedman RJ, Draughn RA (1995), Rapid Quantification of Staphylococci Adhered to Titanium Surfaces Using Image Analyzed Epifluorescence Microscopy, *J. Microbiol Meth.,* Volume 24, pp.29-40

An YH, Friedman RJ, Draughn RA, *et al*. (1996), Bacterial Adhesion to Biomaterial Surfaces. In: Wise DE, et al., ed. *Human Biomaterials Applications*. Humana Press, Totowa, New Jersey, pp.19-57

An YH, Friedman RJ (2000), Handbook of Bacterial Adhesion: Principles, Methods, and Applications, Humana Press, Totowa, New Jersey

An YH, Friedman RJ (1997), Laboratory methods for studies of bacterial adhesion, Journal Of Microbiological Methods, 30 (2):141-152

Antich-Adrover, Mari-Garin D, Murias-Alvarez J, Puente-Alonso CW (1997), External and Secondary Intramedullary Nailing of Open Tibial Fractures: A Randomized, Prospective Trial, *J Bone Joint Surg Br*; Volume 79B, pp.433-437

Apachitei I, Duszczyk J, Katgerman L, Overkamp PJB (1998a), Electroless Ni-P Composite Coatings: The Effect of Heat Treatment on the Microhardness of Substrate and Coating, *Scripta Mater*, Vol.38, No.9, pp.1347-1353

Apachitei I, Duszczyk J, Katgerman L, Overkamp P.J.B (1998b), Particles Co-Deposition by Electroless Nickel, *Scripta. Mater*. Vol. 38, No. 9, pp.1383-1389

Armyanov, S., Georgieva, J., Tachev, D., Valova, E., Nyagolova, N., Mehta, S., Leibman, D., Ruffini, A., (1999). Electroless deposition of Ni-Cu-P alloys in acidic solutions. Electrochemical and Solid State letters 2, 323-325.

Aronov D., Rosen R., Ron E.Z., and Rosenman G., 2008, Electron-induced surface modification of hydroxyapatite-coated implant, Surface and Coatings Technology, Volume 202, Issue 10, Pages 2093-2102

Azeredo J, Visser J, Oliveira R. (1999), Exopolymers in bacterial adhesion: interpretation in terms of DLVO and XDLVO theories, Colloid Surfaces B 14:141-148.

Azeredo J, Pacheco AP, Lopes I, Oliveira R, Vieira MJ. 2003. Monitoring cell detachment by surfactants in a parallel plate flow chamber. Water Science and Technology. 47:77-82.

AWWA, (1998). Standard Methods for the Examination of Water and Wastewater , 20th. Edition.

Azis, PKA, Al-Tisan, I., Sasikumar, N. (2001), Biofouling potential and environmental factors of seawater at a desalination plant intake, *Desalination,* 135:69-82.

Azis P. K. A., Al-Tisan I., Al-Daili M., Green T.N., Ba-Mardouf K., Al-Qahtani S.A., and Al-Sabai K., 2003, Marine macrofouling: a review of control technology in the context of an on-line experiment in the turbine condenser water box of Al-Jubail Phase-1 power/MSF plants, Desalination, Volume 154, Issue 3, Pages 277-290

B

Baier, R.E. (1980). Adsorption of Micro-organisms to Surface, Wiley-Interscience Publishers, New York, 59-104.

Baier, R.E., DePalma, V.A., Meyer, A.E., King, R.W., Fornalik, M.S., (1981). American Society of Mechanical Engineers, Heat Transfer Division 17, 97-103.

Baier R.E., Meyer A.E., Depalma V.A., King R.W., and Fornalik M.S., 1983, Surface microfouling during the induction period, Journal of Heat Transfer, Volume 105, Issue

3, Pages 619-624

Bambauer R, Jutzler GA (1982), Transcutaneous Insertion of the Shaldon Catheter Through the Internal Jugular Vein as Access for Acute Hemodialysis, *Dial Transplant*, Volume 11, pp.766-771

Bambauer R, Mestres P, Pirrung KH (1994), Side Efffects and Infections Associated with Large-bore Catheters for Extracorporeal Detoxification Methods, *ECC International*, Volume 6, pp.5-19

Bates J (1998), Why Use Electroless Nickel Today?, *Plat Surf Finish*, Volume 85, pp.14-16

Baum, C., Meyer, W., Stelzer, R., Fleischer, L.G., and Siebers, D. (2002). Average Nanorough Skin Surface of the Pilot Whale: consideration on the Self-cleaning abilities based on nanoroughness, Marine Biology, 140(3), 653-657.

Bayoudh S., Othmane A., Mora L., and Ouada H.B., 2009, Assessing bacterial adhesion using DLVO and XDLVO theories and the jet impingement technique, Colloids and Surfaces B: Biointerfaces, Volume 73, Issue 1, Pages 1-9

Beigbeder A, Degee P, Conlan S L, Mutton R J, Clare A S, Pettitt M E, Callow M E, Callow J A, Dubois P. 2008. Preparation and characterisation of silicone-based coatings filled with carbon nanotubes and natural sepiolite and their application as marine fouling-release coatings. Biofouling 24: 291-302.

Bell, R. et al, State of the Art Mechanical Systems for Scale and Biofilm Controls, *Electric Power Research Institute* (*EPRI) CS-4339,* November, 1985

Berger L.R., McCoy W.F., and Berger J.A., 1979, Biofouling assay for O.T.E.C. pipes, in proceedings of the ocean thermal energy conversion (O.T.E.C.) Biofouling, Corrosion And Materials Workshop, Rosslyn, Virginia, USA, pp: 38-56. Argonne National Laboratory, Argonne, Illinois, USA

Bernoulli, C. *et al.* 1977. Danger of accidental person-to-person transmission of Creutzfeldt-Jakob disease by surgery [letter]. . *Lancet,* **1**, 478-479

Bers, A.V. and Wahl, M. (2004). The influence of Natural Surface Microtopographies on Fouling, Biofouling, 20(1), 43-51

Blot F, Nitenberg G, Chachaty E, Raynard B, Germann N, Antoun S, Laplanche A, Brun-Buisson C, Trancrede C (1999), Diagnosis of Catheter-Related Bacteremia: A Prospective Comparison of the Time to Positivity of Hub-Blood Versus Peripheral-Blood Cultures, *Lancet*, Volume 354, No.9184, pp.1071-1077

Bollen C.M.L., Lambrechts P., and Quirynen M., 1997, Comparison of surface roughness of oral hard materials to the threshold surface roughness for bacterial plaque retention: a review of the literature. Dent Mater, Volume13, Pages 258–269

Bornhorst, A., Müller-Steinhagen, H., Zhao, Q. 1999. Reduction of Scale Formation By

Ion-Implantation and Magnetron Sputtering on Heat Transfer Surfaces, Heat Transfer Engineering, Volume 20 (2):.6–14
Borsenko KB, Reavy HJ, Zhao Q and Abel EW. Adhesion of protein residues to substituted (111) diamond surfaces: an insight from density functional theory and classical molecular dynamics simulations. J. Biomedical Materials Research Part A 2008; 86A: 1113-1121

Bos R, van der Mei HC, Busscher HJ. 1999. Physico-chemistry of initial microbial adhesive interactions--its mechanisms and methods for study. FEMS Microbiol Rev. 23(2):179-230

Bosque,P.J. 2002. Bovine spongiform encephalopathy, chronic wasting disease, scrapie, and the threat to humans from prion disease epizootics. *Curr. Neurol. Neurosci. Rep.* **2**, 488-495

Bosetti M, Masse A, Tobin E, Cannas M., 2002. Silver coated materials for external fixation devices: in vitro biocompatibility and genotoxicity. Biomaterials, 23(3):.887-892

Bott T.R., Fouling of heat exchangers, In: Churchill S.W., Editor. Chemical engineering monographs, Volume26. Amsterdam, The Netherlands: Elsevier, 1995

Bott TR. 2001. Potential Physical Methods for the Control of Biofouling in Water Systems. Chemical Engineering Research and Design. 79: 484-490.

Bott T.R. and Miller P.C.,2008, Mechanisms of biofilm formation on aluminium tubes, Journal of Chemical Technology and Biotechnology. Biotechnology, Volume 33, Issue 3, Pages 177-184

Boyer, RME, Malherbe, C, 1979. Experience Of Electricite De France In The Use Of Sea Water For Cooling Thermal Power Stations, *Institution of Mechanical Engineers, Conference Publications,* pp.21-28

Braceras I, Alava JI, O˜nate JI, Brizuela M, Garcia-Luis A, Garagorri N, 2002. Improved osseointegration in ion implantation-treated dental
implants. Surf Coat Technol.158–159:28–32.

Brady R.F. and Singer I.L., 2000, Mechanical factors favoring release from fouling release coatings, Biofouling, Volume 15, No. 1-3, Pages 73-81

Brenner A, Riddell G (1946), Nickel Plating on Steel by Chemical Reduction, *J. Research Nat. Bur. of Standards*, Volume 37, pp.31-34

Breteau P (1911), *Bull. Soc. Chim.,* Volume 9, pp.515-518

Brown, P. *et al.* 1982. Chemical disinfection of Creutzfeldt-Jakob disease virus. *N. Engl. J Med.* **306**, 1279-1282

Brown, P. *et al.* 2000. New studies on the heat resistance of hamster-adapted scrapie agent: Threshold survival after ashing at 600°C suggests an inorganic template of replication. *Proc. Natl. Acad. Sci. USA* **97**, 3418-3421

Bruce, M.E. *et al.* 1997. Transmissions to mice indicate that 'new variant' CJD is caused by the BSE agent. *Nature,* **389**, 498-501

Brun-Buisson C, Abrouk F, Legrand P, Huet Y, Larabi S, Rapin M (1987), Diagnosis of Central Venous Catheter-Related Sepsis, *Arch Intern Med*, Volume 147, No.5, pp.873-877

Brink, L.E.S., Elbers, S.J.G., Robbertsen, T., Both, P., (1993). The anti-fouling action of polymers preadsorbed on ultrafiltration and microfiltration membranes. Journal of Membrane Science 76, 281-291.

Burton, D.T., 1979. Biofouling Control Procedures for Power Plant Cooling Water Systems., EPRI Symp. Proc., pp.251-266, Atlanta

Busscher H.J., Modern Approaches to Wettability, Theory and Applications, Plenum, New York, 1992

Butter RS and Lettington AH (1995), Diamond-like Carbon for Biomedical Application, *J. Chem. Vapor Depos.*, Volume 3, pp.182-192

Butterworth D., 2002, Design of shell-and-tube heat exchangers when the fouling depends on local temperature and velocity, Applied Thermal Engineering, Volume 22, Issue 7, Pages 789-801

C

Callow J.A., Callow M.E., Ista L.K., Lopez G., and Chaudhury M.K., 2005, The influence of surface energy on the wetting behaviour of the spore adhesive of the marine alga Ulva linza (synonym Enteromorpha linza), Journal of the Royal Society, Interface, Volume 2, No. 4, Pages 319-325

Carlos, WC, 1981. Corrosion Control Of An OTEC Platform. *Proceedngs of the Ocean Energy Conference*, Vol.1, pp.127-131

Carmen, M.L., Estes, T.G., Feinberg, A.W., Schumacher, J.F., Wilkerson, W., Wilson, L.H., Callow, M.E., Callow, J.A., and Brennan, A.B.(2006). Engineered Antifouling Microtopographies – Correlating Wettability with Cell Attachment, Biofouling, 22(1), 11-21.

Chambers, L.D., Stokes, K.R., Walsh, F.C., and Wood, R.J.K., (2006). “Modern Approaches to Marine Antifouling Coatings,” Surface & Coatings Technology, 201, 362-3652.

Campbell, I, Hall, K, Searle, NK, 1979. Use of Titanium In Seawater Heat Exchangers. *Institution of Mechanical Engineers, Conference Publications,* pp.123-130

Characklis, W.G. (1983). Mathematics in Microbiology, in Bazin, M. (Eds), Academic Press, London, 171-234.

Chibowski E, Holysz L, Wójcik W. 1994. Changes in zeta potential and surface free energy of calcium carbonate due to exposure to radiofrequency electric field. Colloids and Surfaces A 92:79-85.

Chitty J, Pertuz A, Hintermann H, Staia MH, Puchi ES (1997), Influence of Electroless Ni-P Deposits on the Corrosion-Fatigue Properties of an AISI 1045 Steel, *Thin Solid Films*, Volume 308, pp.430-435

Choong S, Wood S, Fry C, Whitfield H. (2001), Catheter associated urinary tract infection and encrustation, International J of Antimicrobial Agents, 17:305-310

Chow W., 1987, Targeted Chlorination Schedules and Corrosion Evaluations, American Power Conference Chicago

Clasper JC, Cannon LB, Stapley SA, Taylor VM, Watkins PE., 2001. Fluid accumulation and the rapid spread of bacteria in the pathogenesis of external flxator pin track infection, *Injury, Int. J. Care Injured*, **32**: 377-381

Clifford RP, Lyons TJ, Webb JK., 1987. Complications of external fixation of open fractures of the tibia. *Injury*, **18** (3):174-176

Collinge CA, Goll G, Seligson D, Easley KJ., 1994. Pin tract infections: silver vs uncoated pins. *Orthopedics*, 17(5):445-448

Collinge, J., Sidle, K.C.L., Meads, J., Ironside, J. & Hill, A.F. 1996. Molecular analysis of prion strain variation and the aetiology of 'new variant' CJD. *Nature*, **383**, 685-690

Cook G, Costerton JW, Darouiche RO. (2000), Direct confocal microscopy studies of the bacterial colonization in vitro of a silver-coated heart valve. International Journal of Antimicrobial Agents, 13:169-173

Cwikel, D., Zhao, Q., Liu, C., **Su, XJ**, Marmur,A., 2010, Comparing Contact Angle Measurements and Surface Tension Assessments of Solid Surfaces, Langmuir, Volume 26(19):15289–15294

D

Darouiche RO (2001), Device-Associated Infections: A Macroproblem That Starts with Microadherence, *Clin Infect Dis*, Volume 33, pp.1567-1572

Darouiche RO (2003), Antimicrobial Approaches for Preventing Infections Associated with Surgical Implants, *Clin Infect Dis*, Volume 36, pp.1284-1289

Darouiche RO (2004), Treatment of Infections Associated with Surgical Implants, *N. Engl. J. Med.,* Volume 350, pp.1422-1429

Darouiche RO (2007), Preventing Infection in Surgical Implants, *US Surgery 2007*, pp.40-44

Demichelis F, Pirri CF, Tagliaferro A. 1992. Influence of silicon on the physical properties of diamond-like films, Mat. Sci. Eng. B-Solid 11:313-316.

Denyer, S.P., 1990. Mechanism of Action of Biocides. International Biodeterioration. Vol.26, pp.89-100

Deslys, J.-P. *et al.* 1997. New variant Creutzfeldt-Jakob disease in France. *Lancet,* **349**, 30-31

Dexter, S.C., Sullivan, J.D., Williams, J., Watson, S.W., (1975). Influence of substrate wettability on the attachment of marine bacteria to various surfaces. Applied Microbiology 30, 298-308.

Dexter S.C., 1979, Influence of substratum critical surface tension on bacterial adhesion in situ studies, J. Colloid Interface Sci, Volume 70, Pages 346-354

DiCinto, R.A., DeCarolis, G., (1993). Biofouling and corrosion. Corrosion Prevention & Control 40, 104-107.

Duncan RN (1989), Metal Finish, Vol. 9, pp.33

Duncan RN (1995), Electroless Nickel-Past, Present and Future-An Update, in Electroless Nickel'95, Fort Mitchell, KY, November 6-8

E

Ederth, T.; Ekblad, T.; Petitt, M.; Conlan, S.; Du, CX; Callow, M; Callow, J; Mutton, R; Clare, A; D'Souza, F; Donnelly, G; Bruin, A; Willemsen, P; **Su, XJ**; Wang, S; Zhao, Q; Hederos, M; Konradsson, P; Lieberg, B. 2011, Resistance of galactoside-terminated alkanethiol self-assembled monolayers to marine fouling organisms, ACS Applied Materials & Interfaces, 3, 3890–3901.

Eggimann P, Pittet D (2002), Overview of Catheter-Related Infections with Special Emphasis on Prevention Based on Educational Programs, *Clin Microbiol Infect*, Volume 8, pp.295-309

Eguia E, Trueba A, Giron A, Rio-Calonge B, Otero F, Bielva C. 2007. Optimisation of biocide dose as a function of residual biocide in a heat exchanger pilot plant effluent. Biofouling 23:231 – 247.

Eguia E., Trueba A., Río-Calonge B., Girón A., and Bielva C., 2008, Biofilm control in tubular heat exchangers refrigerated by seawater using flow inversion physical treatment, International Biodeterioration and Biodegradation, Volume 62, Issue 2, Pages 79-87

Efird, K.D., Effect of Fluid Dynamics on the Corrosion of Copper Base Alloys in Sea Water, *Corrosion'76, Conference Houston, March 1976*.

Efird and Anderson. "Sea Water Corrosion of 90-10 and 70-30 Cu-Ni C 14 Year Exposures." Materials Performance, November 1975.

Elliott TSJ, Faroqui MH (1992), Infections and Intravascular Devices, *Br J Hosp Med*, Volume 48, pp.496-503

Epstein, N. (1983). Thinking About Heat Transfer Fouling: A 5x5 Matrix, *Heat Transfer Engng.,* Vol.4**,** pp43-56.

Ernst, D.R. & Race, R.E. 1993. Comparative analysis of scrapie agent inactivation methods. *J Virol Methods* **41**, 193-201

F

Fang H.H.P., Xu L.C., and Chan K.Y., 2002, Effects of toxic metals and chemicals on biofilm and biocorrosion, Water Research, Volume 36, Issue 19, Pages 4709-4716

Fattom, A., Shilo, M., (1984). Hydrophobicity as an adhesion mechanism of benthic cyanobacteria, Applied and Environmental Microbiology 47, 135-143.

Feldstein MD (1998), Composite Electroless Nickel Coatings for the Aerospace & Airline Industries, *Plat Surf Finish*, Vol.85, No.11, pp.248-252

Fitzgerald RH (1989), Infections of Hip Prostheses and Artificial Joints, *Infect Dis Clin North Am*, Volume 3, pp.329-338

Flechsig, E. *et al.* 2001. Transmission of scrapie by steel-surface-bound prions. *Mol. Med.* **7**, 679-684

Flemming HC, Schaule G, Griebe T, Schmitt J, Tamachkiarowa A. 1997. Biofouling—the Achilles heel of membrane processes. Desalination. 113:215-225.

Fletcher, M., Marshall, K.C., (1982). Are solid surfaces ecological significance to aquatic bacteria? Advances in Microbial Ecology 47, 135-143.

Fletcher M., and Pringle J.H., 1985, The effect of surface free energy and medium surface tension on bacterial attachment to solid surfaces, Journal of Colloid and Interface Science, Volume 104, Pages 5-14

Forster M., and Bohnet M., 1999, Influence of the interfacial free energy crystal/heat transfer surface on the induction period during fouling, International Journal of Thermal Sciences, Volume 38, No. 11, Pages 944-954

Förster, M., Bohnet, M., (2000). Modification of molecular interactions at the interface crystal/heat transfer surface to minimize heat exchanger fouling. International Journal of Thermal Sciences 39, 697-708.

Fowkes FM (1962), Determination of Interfacial Tensions, Contact Angles, and Dispersion Forces in Surfaces by Assuming Additivity of Intermolecular Interactions in Surfaces, *J. Phys. Chem.,* Volume 66, pp.382.

Fowkes, F.M., (1964). Dispersion force contributions to surface and interfacial tensions, contact angles, and heats of immersion. Advances in Chemistry 43, 99-111

Franceschini, DF, Achete CA, Freire FLJr.1992. Internal stress reduction by nitrogen incorporation in hard amorphous carbon thin films. Applied Physics letters 60:3229-3231.

Frosh A, Joyce R, Johnson A., 2001. Iatrogenic vCJD from surgical instruments, *BMJ*. **322**(7302):1558-1559

Fuller, R, 1976. Plate Heat Exchangers Solve Cooling Problem, *Petroleum Engineers, Oct* , 1976, pp.22-28

Fuller, R, 1979. Plate Heat Exchangers In Sea Water Cooling Systems, *Institution of Mechanical Engineers, Conference Publications*, 1979, pp.29-38

G

Gaffoglio, C.J., (1987). Beating biofouling with copper-nickel alloys offshore, Sea Technology, 28, 43-46.

Gago R, Sánchez-Garrido O, Climent-Font A, Albella JM, Román E, Raisanen J, Raühala E. 1999. Effect of the substrate temperature on the deposition of hydrogenated amorphous carbon by PACVD at 35 kHz. Thin Solid Films 338:88-92.

Gangopadhyay AK, Willermet PA, Tamour MA, Vassell WC. 1997. Amorphous hydrogenated carbon films for tribological application I. Development of moisture insensitive films having reduced compressive stress Tribology International 30:9-18.

Garrett-Price, B. A. et al. (1985) Fouling of heat Exchangers- Characteristics, Costs, Prevention, Control and Removal. Noyes Publications, Park Ridge, New Jersey.

Ger MD, Hwang BJ (2002), Effect of Surfactants on Codeposition of PTFE Particles with Electroless Ni-P Coating, *Mater Chem Phys*, Vol.76, No.1, pp.38-45

Ghanem, N.A., EI-Awady, N.I., EI-Hamouly, W.S. and EI-Awady, M.M., 1982. New Approaches to Non-Toxic Antifouling Coatings for Ship-Hull Protection, *Journal of Coatings Technology*, Vol.54, No.684, pp.83-88

Ghani, A.C., Ferguson, N.M., Donnelly, C.A., Hagenaars, T.J., Anderson, R.M.1999, Epidemiological determinants of the pattern and magnitude of the vCJD epidemic in Great Britain. Proc R Soc Lond B 265, 2443-2452

Ghani, A.C., Ferguson, N.M., Donnelly, C.A., Anderson, R.M. 2000, Predicted vCJD mortality in Great Britain. *Nature,* **406**, 583-584

Gibbs, C.J.Jr. *et al.* 1968. Creutzfeldt-Jakob Disease (Spongiform Encephalopathy): Transmission to the Chimpanzee. *Science,* **161**, 388-389

Gibbs, C.J.Jr. *et al.* 1994. Transmission of Creutzfeldt-Jakob disease to a chimpanzee by electrodes contaminated during neurosurgery. *J. Neurol. Neurosurg. Psychiatry* **57**, 757-758

Gilbert, PT. and North, W., 1972. Copper Alloys in Marine Engineering Applications, *Trans. of The Institute of Marine Eng.*, Vol 84, Part 16, pp.520-525.

Gilbert_PT, 1978. Copper Alloys For Offshore Applications. *Metallurgist and Materials Technologist*, Vol.10, No.6, pp.316-319

Gilbert_PT, 1982. Review Of Recent Work On Corrosion Behavior Of Copper Alloys In Sea Water, *Materials Performance*, Vol.21, No.2, pp.47-53.

Girifalco LA, Good RJ (1957), A Theory for the Estimation of Surface and Interfacial Energies, *J Phys Chem*, Volume 61, pp.904-909

Goldie W., Metallic Coating of Plastics, Electrochemical Publications Ltd., British Isles, 1968

Good, R.J., (1992). Contact-angle, wetting, and adhesion – A critical – review. Journal of Adhesion Science and Technology 6, 1269-1302

Gopal S, Majumder S, Batchelor AG, Knight SL, De Boer P, Smith RM., 2000. Fix and flap: the radical orthopaedic and plastic treatment of severe open fractures of the tibia, *J Bone Joint Surg Br* , **82**(7):959-966

Greenberg T., and Itzhak D., 2005, Marine biofouling of titanium alloys in the coral reef environment, Corrosion Reviews, Volume 23, Issue 4-6, Pages 405-413

Grischke M, Hieke A, Morgenweck F, Dimigen H (1998), Variation of the wettability of DLC-coatings by network modification using silicon and oxygen, Diamond and Related Materials 7:454-458

Giffin, OM, Some Early And Recent Novel OTEC Systems. *American Society of Mechanical Engineers, Ocean Engineering Division (Proceedings) OED*, 1978, Vol.5, pp.1-6

Gregory P, Pevny T, Teague D (1996), Early Complications with External Fixation of Pediatric Femoral Shaft Fractures, *J Orthop Trauma*, Volume 10, pp.191-198

Grill A. 1993. Review of the tribology of diamond-like carbon, Wear. 168:143-153.

Gristina, AG. 1987. Biomaterial-centered infection: microbial adhesion versus tissue integration, Science 237 : 1588-1599

Grosjean A, Eezrazi M, Tachez M (1997), Influence of Nickel Ions on the Surface Charge of Silicon Carbide Particles for Elaboration of Nickel-SiC Electroless Composite Deposits, *Surf. Coat. Technol*. Vol.96, pp. 300-304

Gutzeit G., and Crehan W.J., 1954, U.S. Patent, Volume 2, Page 690

H

Hadley JS, Harland LE (1987), *Metal Finishing*, Vol.85, No.12, pp.51

Hahnel S., Rosentritt M., Handel G., and Bürgers R., 2009, Surface characterization of dental ceramics and initial streptococcal adhesion in vitro, Dental Materials, Volume 25, Issue 8, Pages 969-975

Hamza, A., Pham, V.A., Matsuura, T, Santerre, J.P., (1997). Development of membranes with low surface energy to reduce the fouling in ultrafiltration applications. Journal of Membrane Science 131, 217-227.

Hardy F.G., and Moss B.L., 1979, The effects of the substratum on the morphology of the rhizoids of Fucus germlings, Estuarine and Coastal Marine Science, Volume 9, Issue 5, Pages 577-578

Hasebe, T., Yohena, S., Kamijo, A., Okazaki, Y., Hotta, A., Takahashi, K., Suzuki, T. 2007. Journal of Biomedical Materials Research Part A 83A, 1192.

Hauert R. 2003. A review of modified DLC coatings for biological applications Diamond and Related Materials, 12:583-589.

Hedin H, Hjorth K, Rehnberg L, et al (2003), External Fixation of Displaced Femoral Shaft Fractures in Children: A Consecutive Study of 98 Fractures, *J Orthop Trauma*, Volume 17, pp.250-256

Higashitani K, Yoshba A, Tanise T and Murata H (1993), Dispersion of Coagulated Colloids by Ultrasonication, *Colloids and Surface A: Physicochem. Eng. Aspects*, Vol.81, pp.167-175

Helle K. and Walsh, F. 1997. *Transactions of the Institute of Metal Finishing*, **75** (2), 53

Hill, A.F. *et al.* 1997. The same prion strain causes vCJD and BSE. *Nature*, **389**, 448-450

Hilton,D.A. *et al.* 2002. Accumulation of prion protein in tonsil and appendix: review of tissue samples. *BMJ* , **325**, 633-634

Hilton, D.A., Fathers, E., Edwards, P., Ironside, J.W., Zajicek, J. 1998. Prion immunoreactivity in appendix before clinical onset of variant Creutzfeldt-Jakob disease. *Lancet* **352**, 703-704

Huang Z, Maness P C, Blake DM, Wolfrum EJ, Smolinski SL, Jacoby WA Bactericidal mode of titanium dioxide photocatalysis, Journal of Photochemistry and Photobiology

A: Chemistry. Journal of Photochemistry and Photobiology A: Chemistry. 2000;130:163-170

I

Ilker, M. F.; Schule, H.; Coughlin, E. B. Macromolecules, 2004, 37(3), 694

Illingworth B, Bianco RW, Weisberg S (2000), In Vivo Efficacy of Silver-Coated Fabric Against Staphylococcus Epidermidis, *J Heart Valve Dis*, Volume 9, pp.135-141

Ishihara, M., Kosaka, T., Nakamura, T., Tsugawa, K., Hasegawa, M., Kokai, F. , Koga, Y. 2006. Diamond and Related Materials 15:1011.

Israelachvili, J.N. (1992). Intermolecular and Surface Forces. 2nd Ed., London, Academic Press.

J

Jarvis WR (1996), Selected Aspects of the Socioeconomic Impact of Nosocomial Infections: Morbidity, Mortality, Cost, and Prevention, *Infect Control Hosp Epidemiol*, Volume 17, pp.552-557

Jenner, H.A., Taylor, C.J.L., vanDonk, M., Khalanski, M.,(1997). Chlorination by-products in chlorinated cooling water of some European coastal power stations. Marine Environmental Research 43, 279-293

Johnson EE, Simpson LA, Helfet DL (1990), Delayed Intramedullary Nailing after Failed External Fixation of the Tibia, *Clin Orthop*, Volume 253, pp.251-257

Jones GLI, Russell AD, Caliskan Z, Stickler DJ (2005), A strategy for the control of catheter blockage by crystalline Proteus mirabilis biofilm using the antibacterial agent triclosan, European Urology 48 (5): 838-845

K

Kaiga, N, Seki, T, Iyasu, K, 1989. Ozone treatment in cooling water systems, *Ozone: Science and Engineering,* Vol.11, No.3, pp.325-338.

Katsikogianni M., and Missirlis Y.F., 2004, Concise review of mechanisms of bacterial adhesion to biomaterials and of techniques used in estimating bacteria-material interactions, European Cells & Materials Journal, Volume 8, Pages 37-57

Katsikogianni M., Amanatides E., Mataras D., and Missirlis Y.F., 2008, Staphylococcus epidermidis adhesion to He, He/O_2 plasma treated PET films and aged materials: Contributions of surface free energy and shear rate, Colloids and Surfaces B: Biointerfaces, Volume 65, Issue 2, Pages 257-268

Keating JF, Gardner E, Leach WJ, Macpherson S, Abrami G., 1991. Management of tibial fractures with the orthofix dynamic external fixator, *J R Coll Surg Edinb*, **36** (4): 272-277

Kenausis G.L., Voros J., Elbert D.L., Huang N., Hofer R., Ruiz-Taylor L., Textor M., and Spencer N.D., 2000, Poly(L-lysine)-g-poly(ethylene glycol) layers on metal oxide surfaces: Attachment mechanism and effects of polymer architecture on resistance to protein adsorption, Journal of Physical Chemistry B, Volume 104, No. 14, Pages 3298-3309

Kerr A., Effect of Surface Roughness on the Accumulation of Marine Biofouling, Postgraduate Colloquium, 2000

Kerr C, Barker D, Walsh F, Archer J (2000), The Electrodeposition of Composite Coatings Based on Metal Matrix-Included Particle Deposits, *T I Met Finish*, Vol.78, No. 5, pp.171-178

Kesel, A. and Liedert, R. (2007). "Learning from Nature: Non-toxic Biofouling Control by Shark Skin Effect," Comparative Biochemistry &. Physiology. A, 146, S130.

Kikuchi Y, Sunada K, Iyoda T, Hashimoto K, Fujishima A. Photocatalytic bactericidal effect of TiO_2 thin films: dynamic view of the active oxygen species responsible for the effect. J. Photochem. Photobiol. A: Chem. 1997;106:51–56

Kim J, Chisholm BJ, Bahr J. 2007. Adhesion study of silicone coatings: The interaction of thickness, modulus, and shear rate on adhesion force. Biofouling 23: 113-120.

Kim MG, Lee KR, Eun KY. 1999. Tribological behavior of silicon-incorporated diamond-like carbon films. Surface and Coatings Technology, 112:204-209.

Kinelski_EH, Ocean Thermal Energy Conversion Heat Exchangers: A Review of Research and Development, *Marine Technology*, Jan 1985, Vol.22, No.1, pp.64-73

Kinelski, E.H. (1978). Proc. of the Ocean Thermal Energy Conversation Conference, 5th, Miami Beach Fla, VIII. 1-VIII. 6.

Kingshott P., and Griesser H.J., 1999, Surfaces that resist bioadhesion, Current Opinion in Solid State & Materials Science, Volume 4, No. 4, Pages 403-412

Kite P, Dobbins BM, Wilcox MH, McMahon MJ (1999), Rapid Diagnosis of Central Venous-Catheter-Related Bloodstream Infection Without Catheter Removal, *Lancet*, Volume 354, No.9189, pp.1504-1507

Kjaer, E.B., 1992. Bioactive Materials For Antifouling Coatings, *Progress in Organic Coatings,* Vol.20, pp.339-352

Koh, L.L., Hong, W.K., Lip, L.K., (1991). Ecology of marine fouling organisms at eastern Johore strait. Environmental Monitoring and Assessment 19, 319-333.

Kreutzwiesner, E., Noormofidi, N., Wiesbrock, F., Kern, W., Rametsteiner, K., Stelzer, F., Slugovc, C., 2010, Contact Bactericides and Fungicides on the Basis of Amino-Functionalized Poly(norbornene)s. C. *J. Polym. Sci. Part A: Polym. Chem.* 48, 4504-4514.

Kukulka D.J., and Devgun M., 2007, Fluid Temperature and velocity effect on fouling, Applied Thermal Engineering, Volume 27, Issue 16, Pages 2732-2744

Kumar PS, Nair PK (1996), Studies on Crystallization of Electroless Ni-P Deposits, *J Mater Process Tech*, Vol.56, No.1-4, pp.511-520

Kumon K, Hashimoto H, Nishimura M, Monden K, Ono N (2001), Catheter-associated urinary tract infections: impact of catheter materials on their management, International Journal Of Antimicrobial Agents, 17 (4): 311-316

Kvajic, G, 1978. Electromagnetic Water Treatment And Fouling Of Heat Exchangers, *Proc of the Ocean Therm Energy Convers Conf, 5th, Miami Beach Fla*, Feb 20-22,1978, pp.III. 231-III. 234a

Kwok D.Y., and Neumann A.W., 1999, Contact angle measurements and contact angle interpretation, Colloid Interfac., Volume 81, Pages 167-249

Kwok D.Y., and Neumann A.W., 2000, Contact angle interpretation in terms of solid surface tension, Colloids and Surface A: Physicochem. Eng. Aspects, Volume 161, Pages 31-48

L

La, B., V, Collinge, J., Pocchiari, M. & Piccoli, F. 2002. Variant Creutzfeldt-Jakob disease in an Italian woman. *Lancet,* **360**, 997

Lai KK, Fontecchio SA. (2002), Use of silver-hydrogel urinary catheters on the incidence of catheter-associated urinary tract infections in hospitalized patients. American Journal of Infection Control, 30 (4): 221-225

Lascovich JC, Scaglione S. 1994. Comparison among XAES, PELS and XPS techniques for evaluation of sp^2 percentage in a-C:H, Appl. Surf. Sci. 78:17-23.

Laurenson IF, Whyte AS, Fox C, Babb JR., 1999. Contaminated surgical instruments and variant Creutzfeldt-Jakob disease. *Lancet*, **354**(9192):1823

Lee KR, Kim MG, Cho SJ, Eun KY, Seong TY.1997. Structural dependence of mechanical properties of Si incorporated diamond-like carbon films deposited by RF plasma-assisted chemical vapour deposition. Thin Solid Films 308/309:263-267.

Leone M, Garnier F, Avidan M and Martin C (2004), Catheter-Associated Urinary Tract Infections in Intensive Care Units, *Microbes and Infection*, Volume 6, pp.1026-1032

Li BK, Logan BE. The impact of ultraviolet light on bacterial adhesion to glass and metal oxide-coated surface. Colloids and Surfaces B: Biointerfaces. 2005;41: 153-161

Li D., and Neumann A.W., 1990, A reformulation of the equation of state for interfacial tension, Journal of Colloid and Interface Science, Volume 137, No. 1, Pages 304-307

Lin CR, Wang TJ, Chen KC, Chang CH. 2001. Nano-tip diamond-like carbon fabrication utilizing plasma sheath potential drop technique, Mater. Chem. Phys. 72:126-129.

Lindner, E., 1988. Failure Mechanism of Copper Antifouling Coatings, *International Biodeterioration,* Vol. 24, pp.247-253

Lira, R, Sengupta, S, 1990. Effects of Wall Shear on Biofilm Growth, Heat Transfer and Fluid Resistance in Shell and Tube Heat Exchangers. *American Society of Mechanical Engineers, Heat Transfer Division, (Publication) HTD,* Vol.129, pp.101-109

Lira, R, Poteat, LE, Camerota, L, Sengupta, S, 1985. Marine Biofouling Control With Anodically Polarized Protection In Shell And Tube Heat Exchangers. *American Society of Mechanical Engineers, Heat Transfer Division, (Publication) HTD,* Vol.50, pp.25-32

Little B., and Lavoie D., 1979, Gulf of mexico ocean thermal energy conversion (O.T.E.C.) biofouling and corrosion experiment, in proceedings of the ocean thermal energy conversion (O.T.E.C.) Biofouling, Corrosion And Materials Workshop, Rosslyn, Virginia, USA, pp: 60-61. Argonne National Laboratory, Argonne, Illinois, USA

Liu C., 2011, Influence of Surface Free Energy of Ni-P based Coatings on Biofouling Adhesion, PhD thesis, University of Dundee, UK

Liu, C and Zhao Q. (2011a), The CQ Ratio of Surface Energy Components Influences Adhesion and Removal of Fouling Bacteria, Biofouling, 27 (3):275–285

Liu C. and Zhao Q. (2011b), Influence of Surface-Energy Components of Ni–P–TiO2–PTFE Nanocomposite Coatings on Bacterial Adhesion. Langmuir, 27(15):9512–9519.

Liu Y., 2005, Development and Evaluation of electroless Metal-PTFE composite coatings and their potential applications, PhD thesis, University of Dundee, UK

Liu, Y and Zhao, Q. 2003. "Effects of Surfactants On The PTFE Particle Sizes In Electroless Plating Ni-P-PTFE Coatings", *Transactions of the Institute of Metal Finishing*, Volume 81 (5):168–171

Liu Y, Zhao Q (2005), Influence of surface energy of modified surfaces on bacterial adhesion, Biophysical Chemistry, 117:39-45

Losiewicz B, Stepien A, Gierlotka D, Budniok A (1999), Composite Layers in Ni-P System Containing TiO2 and PTFE, *Thin Solid Films*, Vol. 349, No.1-2, pp.43-50

Lucas, K.E., Bergh, J.O., Christian, D.K., (1996). Dechlorination equipment development for shipboard pollution prevention. Naval Engineers Journal 108, 19-25.

M

Mahan J, Seligson D, Henry SL, Hynes P, Dobbins J (1991), Factors in Pin Tract Infections, *Orthopedics*, Volume 14, pp.305-308

Maki D, Tambyah P (2001), Engineering out the Risk of Infection with Urinary Catheters, *Emerg Infect Dis*, Volume 7, pp.1-13

Mallory G.O., Product Finishing, 1979

Mallory G.O., and Hajdu J.B., Electroless plating: fundamentals and applications, American electroplaters and surface finishers society, New York, 2000

Martyak NM, Wetterer S, Harrison L, Mcneil M, Heu R, Neiderer AA (1993), Structure of Electroless Nickel Coatings, *Plat. Surf. Finish*. Vol. 80, No.6, pp.60-64

Mason WT, Khan SN, James CL, Chesser T, Ward A (2005), Complications of Temporary and Definitive External Fixation of Pelvic Ring Injuries, *Injury*, Volume 36, pp.599-604

Masse A, Bruno A, Bosetti M, Biasibetti A, Cannas M, Gallinaro P (2000), Prevention of Pin Track Infection in External Fixation with Silver Coated Pins: Clinical and Microbiological Results, *J Biomed Mater Res*, Volume 53, pp.600-604

Matsunaga T, Tomoda R, Nakajima T, Wake H, Photoelectrochemical sterilization of microbial cells by semiconductor powders Photoelectrochemical sterilization of microbial cells by semiconductor powders. FEMS Microbiology Letters. 1985; 29:211-214

Mauer D, Merkow RL, Gustilo RB (1989), Infection after Intramedullary Nailing of Severe Open Tibial Fractures Initially Treated with External Fixation, *J Bone Joint Surg Am*, Volume 71A, pp.835-838

Mathiyarasu J., Palaniswamy N., and Muralidharan V.S., 2002, Cyclic voltammetric studies on the electrochemical behaviour of cupronickel in sodium chloride solution, Bulletin of Electrochemistry, Volume 18, No. 11, Pages 489-495

Matsuda H, Nishira M, Kiyono Z, Takano O (1995), Effect of Surfactants Addition on The Suspension Of PTFE Particles In Electroless Plating Solutions, *T I Met Finish*, Vol.73, No.1, pp.16-18

McGowan JE Jr (2001), Economic Impact of Antimicrobial Resistance, *Emerg. Infect. Dis*., Volume 7, pp.286-292

McGraw JW, Lim EVA (1988), Treatment of Open Tibial-Shaft Fractures. External Fixation and Secondary Intramedullary Nailing, *J Bone Joint Surg Am.,* Volume 70A, pp.900-911

McGuire J., and Swartzel K.R., Influence of solid surface energetics on macromolecular adsorption from milk, American Institute of Chemical Engineers, National Meeting, 1987

Medilanski E, Kaufmann K, Wick LY, Wanner O, Harms H. 2002. Influence of the surface topography of stainless steel on bacterial adhesion. Biofouling 18:193 – 203.

Melo L. F., and Bott T. R., 1997, Biofouling in water systems, Experimental Thermal and Fluid Science, Volume 14, Issue 4, Pages 375-381

Mermel LA (2000), Correction: Catheter-Related Blood Stream Infections, *Ann Intern Med*, Volume 5, pp.395

Meyer A., Baier R., Wood C.D., Stein J., Truby K., Holm E., Montemarano J., Kavanagh C., Nedved B., Smith C., Swain G., and Wiebe D., 2006, Contact angle anomalies indicate that surface-active eluates from silicone coatings inhibit the adhesive mechanisms of fouling organisms, Biofouling, Volume 22, Issue 6, Pages 411 – 423

Milne, A., Callow, M.E. (1985). Polymers in Marine Enviroment, in Smith, R. (Eds), The Institute of Marine Engineers, London, 229-233.

Moonir-Vaghefi SM, Saatchi A, Hejazi J (1997), The Effect of Agitation on Electroless Nickel-Phosphorus-Molybdenum Disulfide Composite Plating, *Metal Finish*. Vol. 95, No.6, pp.102-106

Morris NS, Stickler DJ, Winters C (1997). Which indwelling urethral catheters resist encrustation by Proteus mirabilis biofilms? British J. of Urology, 80 (1): 58-63

Mostafavi HR, Tornetta III P (1997), Open Fractures of the Humerus Treated with External Fixation, *Clin Orthop Relat Res*, Volume 337, pp.187-197

Mott I.E.C., Biofouling and studies using simulated cooling water, PhD thesis, University of Birmingham, UK, 1991

Müller-Steinhagen, H., Zhao, Q., (1997). Investigation of low fouling surface alloys made by ion implantation technology. Chemical Engineering Science 52, 3321-3332.

Müller-Steinhagen, H., Zhao, Q., Helali-Zadeh, A., Ren, X. 2000. The Effect of Surface Properties on CaSO4 Scale Formation During Convective Heat Transfer and Subcooled Flow Boiling, Canadian Journal of Chemical Engineering, Volume78 (1):12–20.

Müller-Steinhagen, H. (2013), Heat Exchanger Fouling and Cleaning, http://www.heatexchanger-fouling.com/

Mussalli, Y.G., Tsou, J. (1989). Proc. of the 51st American Power Conference, 1094-1099.

N

Navabpour, P, Teer, D., **Su, XJ**, Liu, C., Wang, S., Zhao, Q., Donik, C., Kocijan, A., Jenko, M., 2010, Optimisation of the properties of siloxane coatings as antibiofouling coatings: Comparison of PACVD and hybrid PACVD-PVD coatings, Surface and Coatings Technology, Volume 204 (20):3188–3195

Nebot E., Casanueva J.F., Casanueva T., and Sales D., 2007, Model for fouling deposition on power plant steam condensers cooled with seawater: Effect of water velocity and tube material, International Journal of Heat and Mass Transfer, Volume 50,

Issues 17-18, Pages 3351-3358

Neumann A.W., Good R.J., and Hope C.J., 1974, An equation-of–state approach to determine surface tensions of low-energy solids from contact angles, Journal of Colloid and Interface Science, Volume 49, Pages 291-304

Nishira M, Takano O (1994), Friction And Wear Characteristics of Electroless Ni-P-PTFE Composite Coatings, *Plat Surf Finish*, Vol.81, No.1, pp.48-50

Nishira M, Yamagishi K, Matsuda H, Suzuki M, Takano O (1996), Uniform Dispersibility of PTFE Particles in Electroless Composite Plating, *T I Met Finish*, Vol.74, No.2, pp.62-64

Nosetani, T, Sato, S, Onda, K, Kashiwada, J, Kawaguchi, K, 1981. Effect of Marine Biofouling on the Heat Transfer Performance of Titanium Condenser Tubes. *Sumitomo Light Metal Technical Reports,* Vol.22, No.1- 2, pp.30-41

Nosetani, T, Hotta, Y, Sato, S, 1987. Improvement Of Surface Condenser Performance By In-Situ Artificial Protective Film Coating, *Sumitomo Keikinzoku Giho/Sumitomo Light Metal Technical Reports,* Vol.28, No.1, pp.29-38

Nosetani, T, Sato, S, Onda, K, Kato, Y, 1988. Biofouling Control of Titanium Condenser Tubes By New-Type Abrasive Sponge Balls, *Sumitomo Keikinzoku Giho/Sumitomo Light Metal Technical Reports,* Vol.29, No.4, pp.40-49

Nosetani, T, Hotta, Y, Sato, S, Onda, K, Nakamura, T, Kato, Y, 1989. Biofouling Control of Titanium Condenser Tubes By New-Type Abrasive Sponge Balls. *American Society of Mechanical Engineers, Heat Transfer Division, (Publication) HTD*, Vol.108, pp.281-288

Novak, L, Comparison Of The Rhine River And The Oresund Sea Water Fouling And Its Removal By Chlorination. *American Society of Mechanical Engineers, Heat Transfer Division, (Publication) HTD*, 1981, Vol.17, pp.61-66.

Novak. L, Comparison Of The Rhine River And The Oresund Sea Water Fouling And Its Removal By Chlorination, *Journal of Heat Transfer, Transactions ASME,* NOV 1982, Vol.104,No.4, pp.663-669

O

O'Connor DJ, Sexton BA, Smart RStC (1992), Surface Analysis Methods in Materials Science, Spring-Verlag, Berlin.

ODonnell, J., Improve Seawater Cooling With Titanium Finned Tubes. *Hydrocarbon Processing*, Oct 1992, Vol.71, No.10, pp.61-63, 65

O'Grady NP *et al.* (2002), Guidelines for the Prevention of Intracscular Catheter-Related Infections, *MMWR*, Volume 51, pp.1-29

Okpalugo T, Ogwu A, Maguire P, McLaughlin J. (2001). Technology and Healthcare 9:81.

Oliverira, R., (1997). Understanding adhesion: a means for preventing fouling. Experimental Thermal and Fluid Science 14, 316-322.

Öncü S, Sakarya S (2003), Central Venous Catheter-Related Infections: An Overview with Special Emphasis on Diagnosis, Prevention and Management, *The Internet Journal of Anesthesiology*, Volume 7, Number 1

Owens D.K., and Wendt R.C., 1969, Estimation of the surface free energy of polymers, Journal of Colloid and Interface Science, Volume 13, Pages 1714-1747

P

Paal C., and Frederici L., 1931, Berichte der Deutschen Chemischen Gesellschaft, Volume 64, , Issue 9, Page 2561-2569

Paley D (1990), Problems, Obstacles and Complications of Limb Lengthening by the Ilizarov Technique, *Clin Orthop*, Volume 250, pp.81-104

Palraj S., and Venkatachari G., 2008, Effect of biofouling on corrosion behaviour of grade 2 titanium in mandapam seawaters, Desalination, Volume 230, Issues 1-3, Pages 92-99

Parameswaran AD, Roberts CS, Seligson D, et al. (2003), Pin Tract Infection with Contemporary External Fixation: How Much of A Problem? *J Orthop Trauma*, Volume 17, pp.503-507

Park JH, Cho YW, Kwon IC, Jeong SY, Bae YH (2002), Assessment of PEO/PTMO multiblock copolymer/segmented polyurethane blends as coating materials for urinary catheters: in vitro bacterial adhesion and encrustation behavior, Biomaterials 23 (19): 3991-4000

Pasmore M., Todd P., Smith S., Baker D., Silverstein J., Coons D., and Bowman C.N., 2001, Effects of ultrafiltration membrane surface properties on Pseudomonas aeruginosa biofilm initiation for the purpose of reducing biofouling, Journal of Membrane Science, Volume 194, Issue 1, Pages 15-32

Patterson MM (2005), Multicenter Pin Care Study, *Orthop Nurs*, Volume 24, pp.349-360

Patent US4 419 248 The Removal Of Microbial Fouling By Ice Nucleation

Pearson ML (1996), Guideline for Prevention of Intravascular Device-Related Infections. Part I. Practices Advisory Committee, *Am J Infect Control*, Volume 24, pp.262-277

Pereni, CI, Zhao, Q., Liu, Y. , Abel, E., 2006, Surface Free Energy Effect On Bacterial Adhesion, Colloids and Surfaces B: Biointerfaces 48:143-147

Ploof L.,2008. Electroless Nickel Composite Coatings, Advanced Material and Processes, VOL 166; NUMB 5, pages 36-38

Plowman R, Graves N, Griffin M, Roberts JA, Swan AV, Cookson B, Taylor L (1999), Socio-economic Burden of Hospital Acquired Infection, PHLS, London

Plowman R, Graves N, Esquivel J, Roberts JA (2001), An economic model to assess the cost and benefits of the routine use of silver alloy coated urinary catheters to reduce the risk of urinary tract infections in catheterized patients, Journal of Hospital Infection, 48:33-42

Powell, CA, Preventing Biofouling With Copper-Nickel Alloys, *Materials World*, Apr 1994, Vol.2, No.4, pp.181-183

Preiser H.S., Ticker A., Bohlander G.S., Taylor D.W., Costlow J.D., and Tipper R.C., 1984, Marine Biodeterioration: An Interdisciplinary Study, Naval Institute Press, MD, USA, London E. and F. N. SPON, Page 223

Prescott LM, Harley JP, Klein DA (2005), Microbiology, New York, McGraw-Hill

Pritchard A.M., 1987, The Economics of fouling. in fouling science and technology, Edts. Melo, L.F, Bott, T.R. and Bernardo, C.A. NATO ASl Series E, Vol. 145, KIuwer Academic Publishers

Prusiner, S.B. *et al.* 1990. Transgenetic studies implicate interactions between homologous PrP isoforms in scrapie prion replication. *Cell,* **63**, 673-686
Quirynen M., and Bollen C.M.L., 1995, The influence of surface-roughness and surface-free energy on supragingival and subgingival plaque-formation in man -A review of the literature, Journal of Clinical Periodontology, Volume 22 , Pages 1-14

R

Raad I, Hanna H (2002), Intravascualr Catheter-Related Infection, *Arch Intern Med*, Volume 162, pp.871-878

Raad I, Darouiche RO (1996), Catheter Related Septicaemia: A Risk Reduction, *Infect Med*, Volume 13, pp.807-812; 815-816; 823

Rajagopal, S., Venugopalan, V.P., Van der Velde, G., Jenner, H.A., (2003). Comparative chlorine and temperature tolerance of the oyster Crassostrea madrasensis: Implications for cooling system fouling, 19, 115-124

Ralston, E. and Swain, G. (2009). “Bioinspiration – the Solution for Biofouling Control,” Bioinspiration and Biomimetics, 4, 015007.

Rankin, B. H. and Adamson, W. L. (1973) Scale formation as related to evaporation surface conditions. Desalination 13, 63-87.

Richards MJ, Edwards JR, Culver DH, Gaynes RP (1999), Nosocomial Infections in Medical Intensive Care Units in the United States. National Nosocomial Infections Surveillance System, *Crit. Care Med*., Volume 27, pp.887-892

Robertson J. 2002. Diamond-like amorphous carbon. Materials Science and Engineering: R: Reports, 37:129-281.

Rosmaninho R, Santos O, Nylander T, Paulsson M, Beuf M, Benezech T, Yiantsios S, Andritson S, Karabelas A, Rizzo G, Mu¨ ller-Steinhagen H, Melo LF. 2006. Modified stainless steel surfaces targeted to reduce fouling – evaluation of fouling by milk components. J Food Eng 80:1176 – 1187.

Ritter_RB, Suitor_JM, Handling and Disposal of Solid Wastes from Steam Power Plants, Proc of the Natl Conf on Complete Watereuse, 2nd: Water's Interface with Energy, Air and Solids, Chicago, Ill,, 1975, pp.604-609

Ritter, R.B. and Suitor, J.W., Fouling Research on Copper and its Alloys-Seawater Studies, Heat Transfer Research,Inc,June 1976(Rev.1).pp137.

Roosjen A., van Der Mei H.C., Busscher H.J., and Norde W., 2004, Microbial adhesion to poly(ethylene oxide) brushes: Influence of polymer chain length and temperature, Langmuir, Volume 20, Issue 25, Pages 10949-10955

Rosmaninho R, Santos O, Nylander T, Paulsson M, Beuf M, Benezech T, et al.2007. Modified stainless steel surfaces targeted to reduce fouling—evaluation of fouling by milk components. J Food Eng. 80:1176–87.

Roux F.G., 1916, U.S. Patent No. 119612870

S

Saikhwan P., Geddert T., Augustin W., Scholl S., Paterson W.R., and Wilson D.I., 2006, Effect of surface treatment on cleaning of a model food soil, Surface and Coatings Technology, Volume 201, Issues 3-4, Pages 943-951

Saint S (2000), Clinical and Economic Consequences of Nosocomial Catheter-Related Bacteriuria, *Am J Infect Control*, Volume 28, pp.68-75

Samano EC, Soto G, Olivas A, Cota L. 2002. DLC thin films characterized by AES, XPS and EELS. Applied Surface Science, 202:1-7

Santos O., Nylander T., Rosmaninho R., Rizzo G., Yiantsios S., Andritsos N., Karabelas A., Müller-Steinhagen H., Melo L., Boulangé-Petermann L., Gabet C., Braem A., Trägårdh C., and Paulsson M., 2004, Modified stainless steel surfaces targeted to reduce fouling–surface characterization, Journal of Food Engineering, Volume 64, Issue 1, Pages 63-79

Scardino, A.J., Hudleston, D., Peng, Z., Paul, N.A., and De Nys, R. (2009). "Biomimetic Characterisation ooofff Key Surface Parametersfor te Development of Fouling Resistant Materials," Biofouling, 25(1), 83-93.

Schierholz JM, Lucas LJ, Rump A, Pulverer G. (1998), Efficacy of sliver-coated medical devices. Journal of Hospital Infection, 40:257-262

Schierholz JM, Beuth J (2002), Implant Infections: a Haven for Opportunistic Bacteria, *J. Hosp. Infect.,* Volume 49, pp.87-93

Scholder R., and Haken H.I., 1931, Berichte der Deutschen Chemischen Gesellschaft, Volume 64B, Pages 2870

Scholder R., and Heckal H., 1931, Zeitschrift für anorganische und allgemeine Chemie, Volume 198, Page 329

Seki, A, Auker, B, Fujioka, R, Ono, P, Takahashi, P, 1985. Ultraviolet Irradiation For Controlling Biofouling In OTEC Heat Exchangers: A Preliminary Report. *Oceans (*New York), pp.1273-1278

Seki, A, Auker, B, Fujioka, R, Ono, P, Takahashi, P, 1986. OTEC Heat Exchangers Biofouling Control By Ultraviolet Irradiation, *Oceans* (New York), No.1986., pp.232-237

Shao, W., Zhao, Q., Abel, E.W., Bendavid, A. 2010. Influence of interaction energy between Si-doped diamond-like carbon films and bacteria on bacterial adhesion under flow conditions, J. Biomedical Materials Research Part A Volume 93 (1): 133–139.

Sharma PK, Rao KH. 2002. Analysis of different approaches for evaluation of surface energy of microbial cells by contact angle goniometry. Adv. Colloid Interface Sci. 98:341-463.

Sharma PK, Rao KH (2003), Adhesion of *Paenibacillus Polymyxa* on Chalcopyrite and Pyrite: Surface Thermodynamics and Extended DLVO Theory, *Colloids Surface B: Biointerfaces*, Volume 29, pp.21-38

Sheng S, Sacher E, Yelon A. 2001. Structural changes in amorphous silicon studied by X-ray photoemission spectroscopy: a phenomenon independent of the Staebler–Wronski effect?. J. Non-Cryst Solids 282:165-172.

Sherertz RJ, Ely EW, Westbrook DM, Gledhill KS, Streed SA, Kiger B, Flynn L, Hayes S, Strong S, Cruz J, Bowton DL, Hulgan T (2000), Education of Physicians-in-Training can Decrease the Risk for Vascular Catheter Infection, *Am Intern Med*, Volume 132, No.8, pp.641-648

Shone, EB, Grim, GC, 1974. Problems in Seawater Circulating Systems. *British Corrosion Journal, ,* No.1, pp.32-38

Shone, EB, Grim, GC, 1986. Experience With Seawater-Cooled Heat Transfer Equipment. *Marine Engineers Review,* Mar 1986, No.Mar 1986, pp.20-23

Shuji Y, Chiba N (1996), Patent No.EP 0 737 759 A1, Oct.

Sims M, Saleh M (2000), External Fixation - the Incidence of Pin Site Infection: A Prospective Audit, *J Orthop Res*, Volume 4, pp.59-63

Singh A, Ehteshami G, Massia S, He J, Storer RG and Raupp G (2003), Glial Cell and Fibroblast Cytotoxicity Study on Plasma-deposited Diamond-like Carbon Coatings, *Biomaterials,* Volume 24, pp.5083-5089

Sipahi C., Anil N., and Bayramlib E., 2001, The effect of acquired salivary pellicle on the surface free energy and wettability of different denture base materials, Journal Of Dentistry, Volume 29, Issue 3, Pages 197-204

Sleigh M.A., Microbes in the sea, Chichester Ellis Horwood, 1987

Sriyutha Murthy P., Venkatesan R., Nair K.V.K., and Ravindran M., 2004, Biofilm control for plate heat exchangers using surface seawater from the open ocean for the OTEC power plant, International Biodeterioration and Biodegradation, Volume 53, Pages 133–140

Staia MH, Castillo EJ, Puchi ES, Lewis B, Hintermann HE (1996), Wear Performance and Mechanism of Electroless Ni-P Coating, *Surf. Coat. Technol.,* Volume 86-87, pp.598-602

Steinhagen R., Müller-Steinhagen H.M., and Maani K., 1990, Heat Exchanger Applications, Fouling Problems and Fouling Costs in New Zealand Industries, Ministry of Commerce Report RD8829

Straight M.R., Sudarshan T.S., and Wilson J.H., 1988, Significance of defects in fatigue of Cu-Ni/steel welds, Engineering Fracture Mechanics, Volume 31, Issue 4, Pages 673-681

Strauss S.D., 1989, New methods: chemical improve control of biological fouling, Power , Pages 51-52

Su, X.J., Zhao, Q., Wang, S., Bendavid, A. 2010, Modification of diamond-like carbon coatings with fluorine to reduce biofouling adhesion, Surface and Coatings Technology, Volume 204 (5):2454–2458

Su, **X.J**., Zhao, Q., Wang, S., Zhang, S., Noormofidi N., Kreutzwiesner, E., Slugovc, C. 2011. Antimicrobial Efficiency of Metal-Polymer Nanocomposite Coatings. Euro-Therm Heat Exchanger Fouling and Cleaning - June 05-10, 2011, Fodele Beach & Water Park Holiday Resort, Crete, Greece

Su, **X.J**. Zhao, Q., Wang, S., Kienberger, J., Slugovc, C., 2012. Coating reducing the attachment of bacteria. EU Patent Application. 1st June 2012.

Swain G., Proceedings of the International Symosium on Sea Water Drag Reduction, The Naval Undersea Warfare Center, Newport, 1998, Pages 155-161

T

Tachev D, Georgieva J, Armyanov S (2001), Magnetothermal Study of Nanocrystalline Particle Formation in Amorphous Electroless Ni-P And Ni-Me-P Alloys, *Electrochim Acta*, Volume 47, pp.359-369

Takahoshi, P., 1986. Study of the Non-Chemical Methods of Biofouling Control in OTEC Heat Exchangers, *Solar Energy Research Institute,* April, 1986

Taylor R.L., Verran J., Lees G.C., and Ward A.J.P., 1998, The influence of substratum topography on bacterial adhesion to polymethyl methacrylate, Journal of Materials Science: Materials in Medicine, Volume 9, Pages 17-22

Taylor, D.M. *et al.* 1994. Decontamination studies with the agents of bovine spongiform encephalopathy and scrapie. *Arch. Virol.* **139**, 313-326

Taylor, D.M., McConnell, I., Fernie, K. 1996. The effect of dry heat on the ME7 strain of mouse-passaged scrapie agent. *J. Gen. Virol.* **77**, 3161-3164

Thibon P, Le Coutour X, Leroyer R, Fabry J. (2000), Randomized multi-centre trial of the effects of a catheter coated with hydrogel and silver salts on the incidence of hospital-acquired urinary tract infections. J. Of Hospital Infection; 45 (2):117-124

Tomozeiu N, van Faassen EE, Palmero A, Arnoldbik WM, Vredenberg AM, Habraken FHPM. 2004. Study of the a-Si/a-SiO_2 interface deposited by r.f. magnetron sputtering. Thin Solid Films 447-448:306-310.

Torbin, RN and Mussalli, Y.G., The Cost Effectiveness of Alternative Condenser Biofouling Control Methods, EPRI Symp. Proc., pp. 497-517, Atlanta, 1979.

Tozzi P, Al-Darweesh A, Vogt P, Stumpe F. (2001), Silver-coated prosthetic heart valve: a double-bladed weapon. European J of Cardio-Thoracic Surgery, 19:729-731

Tsai Y.P., 2005, Impact of flow velocity on the dynamic behaviour of biofilm bacteria, Biofouling, Volume 21, Issue 5-6, Pages 267–277

Tsibouklis J., Stone M., Thorpe A.A., Graham P., Peters V., Heerlien R., Smith J.R., Green K.L., and Nevell T.G., 1999, Preventing bacterial adhesion onto surfaces: The low-surface-energy approach, Biomaterials, Volume 20, Issue 13, Pages 1229-1235

Tsibouklis J., Stone M., Thorpe A.A., Graham P., Nevell T.G., Ewen R.J., 2000, Inhibiting bacterial adhesion onto surfaces: the non-stick coating approach, International Journal of Adhesion and Adhesives, Volume 20, Issue 2, Pages 91-96

Tsou, J., Mussalli, Y.G., (1988). American Society of Mechanical Engineers, Heat Transfer Division, 1, 231-237.

Tulsi SS, Ebdon P (1982), Electroless Nickle-PTFE Composite Coatings, UK National Corrosion Conference, London

Tulsi SS (1983), Electroless Nickel-PTFE Composite Coatings, Trans. Inst. Metal Finish. Vol. 61, pp. 142-149.

Tulsi, S.S., (1983). Composite PTFE-nickel coatings for low friction applications. Finishing 7, 14-18.

Tunney MM, Gorman SP (2002), Evaluation of a poly(vinyl pyrollidone)-coated biomaterial for urological use, Biomaterials 23 (23): 4601-4608

Tuthill, A.H., Guidelines for the Use of Cooper Alloys in Sea Water, *Materials Performance*, Vol. 26, No 9, 1987. pp 12-22.

V

van Dijk J., Herkstroter F., Busscher H., Weerkamp A., Jansen H. and Arends J., 1987, Surface-free energy and bacterial adhesion: An in vivo study in beagle dogs, Journal of Clinical Periodontology, Volume 14, Issue 5, Pages 300–304

van Oss, C.J. (1994). Interfacial Forces in Aqueous Media. Marcel Dekker, New York.

van Oss, C.J., Good, R.J., Chaundhury, M.K., (1988). Additive and nonadditive surface-tension components and the interpretation of contact angles. Langmuir 4, 884-891.

van Oss C.J., Good R.J., and Chaudhury M.K., 1986, The role of van der waals forces and hydrogen bonds in 'hydrophobic interactions' between biopolymers and low energy surfaces, Journal of Colloid and Interface Science, Volume 111, No. 2, Pages 378-390

Veenstra DL, Saint S, Saha S, Lumley T, Sullivan SD (1999), Efficacy of Antiseptic-Impregnated Central Venous Catheters in Preventing Catheter-Related Bloodstream Infection: A Meta-Analysis, *JAMA*, Volume 281, pp.261-267

Venugopalan, V.P., Thyagarajan, V. and Nair, K.V.K., 1997, Marine growth in large seawater intake systems: Problems and their control, Proc. 2nd Indian Nat. Conf. Harb. and Ocean eng., Thiruvananthapuram (India), Voloume 1, Pages 640-647

Verwey EJW, Overbeek JTG (1955), Theory of the Stability of Lyophobic Colloids, Journal of Colloid Science, Volume 10, Issue 2, April 1955, Pages 224-225.

Videla H.A., 1994, Biofilms and corrosion interactions on stainless steel in seawater, International Biodeterioration & Biodegradation, Volume 34, Issues 3-4, Pages 245-257

Vishwakarma V., and Josephine J., and George R.P., 2009, Antibacterial copper-nickel bilayers and multilayer coatings by pulsed laser deposition on titanium, Biofouling, Volume 25, Issue 8, Pages 705-710

Visser H., 1998, The role of surface forces in fouling of stainless steel in the dairy industry, Journal Of Dispersion Science And Technology, Volume 19, No. 6-7, Pages 1127-1150

Vladkova T., 2007, surface engineering for non-toxic biofouling control review, Journal of the University of Chemical Technology and Metallurgy, Volume 42, No. 3, Pages 239-256

von Eiff, C, Jansen B, Kohnen W, Becker K (2005), Infections Associated with Medical Devices: Pathogenesis, Management and Prophylaxis, *Drugs*, Volume 65, pp.179-214

W

Wang, C., 2008, Development and Evaluation of Anti-Bacterial Nano-Biomaterials for Medical Devices and Implants, PhD thesis, University of Dundee.

Wang XP, Yu Y, Hu XF, Gao L. Hydrophilicity of TiO_2 films prepared by liquid phase deposition Hydrophilicity of TiO_2 films prepared by liquid phase deposition Thin Solid Films. 2000; 371:148-152

Waite, T.D. and Fagan, J.R.,1979. Summary of Biofouling Control Alternatives, EPRI Symp. Proc., pp.441-462, Atlanta

Wassall MA, Santin M, Isalberti C, Cannas M, Denyer SP. (1997), Adhesion of bacteria to stainless steel and silver-coated orthopedic external fixation pins. Journal of Biomedical Materials Research, 36:325-330

Wheelwright EF, Court-Brown CM (1992), Primary External Fixation and Secondary Intramedullary Nailing in the Treatment of Tibial Fractures, *Injury*, Volume 23, pp.373-376

Will,R.G. *et al.* 1996. A new variant of Creutzfeldt-Jakob disease in the UK. *Lancet*, **347**, 921-925.

Wu S., 1971, The work of adhesion tool determines an index of wetting ability of a liquid for a solid, Journal of Polymer Science, Volume C34, Page 19

Wu WJ, Hon MH. 1999. Thermal stability of diamond-like carbon films with added silicon. Surface and Coatings Technology, 111:134-140.

Xu Z.M., Zhang Z.B., and Yang S.R., Costs Due to Utility Fouling in China, ECI Symposium Series, Volume RP5: Proceedings of 7th International Conference on Heat Exchanger Fouling and Cleaning - Challenges and Opportunities, Engineering Conferences International, Tomar, Portugal, July 1 - 6, 2007

Y

Yebra D.M., Kiil S., and Dam-Johansen K., 2004, Antifouling technology-past, present and future steps towards efficient and environmentally friendly antifouling coatings, Progress in Organic Coating, Volume 50, Issue 2, Pages 75-104

Yokoyama K, Itoman M, Tanaka K, et al. (1988), Secondary Undreamed Intramedullary Nailing Following External Fixation and Acute Flap Coverage for Type IIIB Open

Tibia Fractures: A Report of Three Successful Cases, *J Orthop Surg*, Volume 6, pp.71-77

Yoon J., and Lund D.B., 1994, Magnetic treatment of milk and surface treatment of plate heat exchangers: Effects on milk fouling, Journal of Food Science, Volume 59, Issue 5, Pages 964 – 969

Yoshinari M, Oda Y, Kato T, Okuda K. 2001. Influence of surface modifications to titanium on antibacterial activity in vitro. Biomaterials. 22:2043–8.

Young, T., (1805). An essay on the cohesion of fluids. Phylosophical Transactions of the Royal Society London 95, 65-87.

Z

Zajíčková L, Veltruská K, Tsud N, Franta D. 2001, XPS and ellipsometric study of DLC/silicon interface. Vacuum 61:269-273.

Zettler, HU., Weiß, M., Zhao, Q., H. Müller-Steinhagen, H., 2005. Influence of Surface Properties and Characteristics on Fouling in Plate Heat Exchangers, Heat Transfer Engineering, Volume 26 (2):3–17

Zhao, Q., Liu, Y., Müller-Steinhagen, H., Liu, G., 2002. "Graded Ni-P-PTFE Coatings and Their Potential Applications", Surface & Coatings Technology, Volume 155 (2-3):279–284

Zhao, Q., Müller-Steinhagen, H., 2002. Intermolecular and adhesion forces of deposits on modified heat transfer surfaces. in Heat exchanger fouling – Fundamental Approches and Technical Solutions, eds. H. Müller-Steinhagen et.al., Publico Publ., Essen, pp. 41-46.

Zhao, Q., Wang S. and Müller-Steinhagen, H. 2004a. Tailored Surface Free Energy of Membrane Diffusers to Minimize Microbial Adhesion, Applied Surface Science, 230 (1-4):371–378.

Zhao Q., 2004b, Effect of surface free energy of graded Ni–P–PTFE coatings on bacterial adhesion, Surface and Coatings Technology, Volume 185, Issues 2-3, Pages 199-204

Zhao Q, Liu Y, Abel EW. 2004c. Effect of temperature on the surface free energy of amorphous carbon films. Journal of Colloid and Interface Science, 280:174-183.

Zhao, Q., Liu, Y., Wang, S., Müller-Steinhagen, H. 2005a. Effect of surface free energy on the adhesion of biofouling and crystalline fouling. Chemical Engineering Science, 60 (17):4858–4865

Zhao Q, Wang X. 2005b. Heat transfer surfaces coated with fluorinated diamond-like carbon films to minimize scale formation. Surface and Coatings Technology, 192:77-80.

Zhao Q, and Liu Y., 2005c, Electroless Ni–Cu–P–PTFE composite coatings and their anticorrosion properties, Surface and Coatings Technology, Volume 200, Pages 2510-2514

Zhao Q, Liu Y, Wang C. 2005d, Development and evaluation of electroless Ag-PTFE composite coatings with anti-microbial and anti-corrosion properties Applied Surface Science, 252(5):1620-1627

Zhao Q, Liu Y (2006), Modification of stainless steel surfaces by electroless Ni-P and small amount of PTFE to minimize bacterial adhesion, Journal of Food Engineering, 72 (3):266-272

Zhao Q., Liu Y., Wang C., Wang S., Peng N., and Jeynes C., 2007a, Bacterial adhesion on ion-implanted stainless steel surfaces, Applied Surface Science, Volume 253, Issue 21, 31, Pages 8674-8681

Zhao Q, Liu Y, Wang C, Wang S 2007b. Evaluation of bacterial adhesion on Si-doped diamond-like carbon films. Applied Surface Science, 253:7254-7259

Zhao, Q., Wang, C., Liu Y., Wang, S. 2007c. Bacterial Adhesion on the Metal-Polymer Composite Coatings, International Journal of Adhesion and Adhesives 27 (2):85–91.

Zhao Q, Liu Y, Wang C, Wang S, Peng N, Jeynes C. 2008. Reduction of bacterial adhesion on ion implanted stainless steel surfaces, Medical Engineering & Physics, Volume 30 (3):341–349

Zhao, Q., **Su, XJ**., Wang, W., Zhang, X., Navabpour, P., Teer, D. 2009, Bacterial removal properties of Si-and N-doped diamond-like carbon coatings, Biofouling 25 (5):377 – 385

Zobeley, E., Flechsig, E., Cozzio, A., Masato, E., Weissmann, C. 1999. Infectivity of scrapie prions bound to a stainless steel surface. *Molecular Medicine* **5**, 240-243

Su XJ' PUBLICATIONS

Su, X.J., Zhao, Q., Wang, S., Bendavid, A. 2010, Modification of diamond-like carbon coatings with fluorine to reduce biofouling adhesion, Surface and Coatings Technology, Volume 204 (5):2454–2458

Su, **X.J**., Zhao, Q., Wang, S., Zhang, S., Noormofidi N., Kreutzwiesner, E., Slugovc, C. 2011. Antimicrobial Efficiency of Metal-Polymer Nanocomposite Coatings. Euro-Therm Heat Exchanger Fouling and Cleaning - June 05-10, 2011, Fodele Beach & Water Park Holiday Resort, Crete, Greece

Su, **X.J**. Zhao, Q., Wang, S., Kienberger, J., Slugovc, C., 2012. Coating reducing the attachment of bacteria. EU Patent Application. 1st June 2012.

Akesso, L., Navabpour, P, Teer, D., Pettitt, ME., Callow, ME., Liu, C., **Su, XJ**., Wang, S., Zhao, Q., Donik, C., Kocijan, A., Jenko, M., Callow, JA., 2009a, Deposition

parameters to improve the fouling-release properties of thin siloxane coatings prepared by PACVD. Applied Surface Science, Volume 255 (13-14):6508–6514

Cwikel, D., Zhao, Q., Liu, C., **Su, XJ**, Marmur,A., 2010, Comparing Contact Angle Measurements and Surface Tension Assessments of Solid Surfaces, Langmuir, Volume 26(19):15289–15294

Ederth, T.; Ekblad, T.; Petitt, M.; Conlan, S.; Du, CX; Callow, M; Callow, J; Mutton, R; Clare, A; D'Souza, F; Donnelly, G; Bruin, A; Willemsen, P; **Su, XJ**; Wang, S; Zhao, Q; Hederos, M; Konradsson, P; Lieberg, B. 2011, Resistance of galactoside-terminated alkanethiol self-assembled monolayers to marine fouling organisms, ACS Applied Materials & Interfaces, 3, 3890–3901.

Navabpour, P, Teer, D., **Su, XJ**, Liu, C., Wang, S., Zhao, Q., Donik, C., Kocijan, A., Jenko, M., 2010, Optimisation of the properties of siloxane coatings as antibiofouling coatings: Comparison of PACVD and hybrid PACVD-PVD coatings, Surface and Coatings Technology, Volume 204 (20):3188–3195

Zhao, Q., **Su, XJ**., Wang, W., Zhang, X., Navabpour, P., Teer, D. 2009, Bacterial removal properties of Si-and N-doped diamond-like carbon coatings, Biofouling 25 (5):377 – 385

Q. Zhao, **XJ Su**, S Wang, Development and evaluation of modified DLC coatings to minimize bacterial adhesion. International Conference on Heat Exchanger Fouling and Cleaning, 14-19 June 2009, Schladming, 8973, AUSTRIA

Q. Zhao, **XJ Su**, S Wang, X Zhang, P. Navabpour, D Teer, Development of nano-structured diamond-like carbon coatings with biofouling-resistant property. Proceedings of European and International Forum on Nanotechnology, 2-5 June, 2009, Prague, Czech Republic, Page 70.

}